

**Oromucosal drug delivery:
Implementation of standardized and
physiologically relevant
ex vivo permeation studies
in preclinical drug development**

INAUGURAL - DISSERTATION

zur Erlangung des Doktorgrades
der Mathematisch-Naturwissenschaftlichen Fakultät
der Heinrich-Heine-Universität Düsseldorf

vorgelegt von

Haidara Majid

aus Damaskus

Düsseldorf, September 2021

aus dem Institut für Klinische Pharmazie und Pharmakotherapie
der Heinrich-Heine-Universität Düsseldorf

Gedruckt mit der Genehmigung der
Mathematisch-Naturwissenschaftlichen Fakultät der
Heinrich-Heine-Universität Düsseldorf

Berichtersteller:

1. Prof. Dr. Stephanie Lärer

2. Prof. Dr. Dr. Norbert Kübler

Tag der mündlichen Prüfung: 14. Dezember 2021

“The highest peaks are not attained but by those who embrace discipline and hard work.”

– Ali ibn Abi Talib

To my beloved father,
Walid Majid Ibrahim

I. Erklärung zur Dissertation

Hiermit versichere ich an Eides statt, dass die vorgelegte Dissertation mit dem Titel:

“Oromucosal drug delivery:

Implementation of standardized and physiologically relevant ex vivo permeation studies in preclinical drug development”

von mir selbstständig und ohne unzulässige fremde Hilfe unter Beachtung der Grundsätze zur Sicherung guter wissenschaftlicher Praxis an der Heinrich-Heine-Universität Düsseldorf erstellt worden ist. Die Dissertation wurde in der vorgelegten oder in ähnlicher Form noch bei keiner anderen Institution eingereicht. Ich habe bisher keinen erfolglosen Promotionsversuch unternommen.

Düsseldorf, den 30.09.2021

Haidara Majid

II. Danksagung

Die vorliegende Arbeit wurde in der Zeit von Januar 2018 bis September 2021 am Institut für Klinische Pharmazie und Pharmakotherapie der Heinrich-Heine-Universität Düsseldorf angefertigt. Für jede damit verbundene erfahrene Unterstützung möchte ich mich herzlich bedanken.

An erster Stelle möchte ich mich bei Prof. Dr. Stephanie Lärer für die Betreuung und die Möglichkeit bedanken meine Dissertation am Institut für Klinische Pharmazie und Pharmakotherapie anzufertigen.

Ich bedanke mich herzlich bei Prof. Dr. Dr. Norbert Kübler für die konstruktiven Gespräche und die Übernahme der Mentorenschaft sowie des Korreferats meiner Arbeit.

Mein besonderer Dank gilt Dr. Björn Burckhardt für seine lehrreiche und engagierte Betreuung im Rahmen meiner Promotion. Weiterhin bedanke ich mich für die zahlreichen wissenschaftlichen Diskussionen, die gemeinsamen Publikationen, die Durchsicht meiner Arbeit und den sowohl intellektuellen als auch persönlichen Beistand. Für seine weitere Laufbahn wünsche ich ihm den größtmöglichen Erfolg.

Ich danke meinen Koautoren für die gemeinsamen Veröffentlichungen und ihren wissenschaftlichen Beitrag im Rahmen der behandelten Forschungsfragestellungen. Meinen ehemaligen Kolleginnen und Kollegen danke ich für die gemeinsame Zeit, die vielseitigen Anregungen und die gegenseitigen Zusprüche. Anke Bartel danke ich für die Hilfestellung in der Entwicklung und Durchführung der experimentellen Studien.

Für den bedingungslosen und kontinuierlichen Beistand der letzten Jahre möchte ich mich bei meinen engsten Freunden herzlichst bedanken. Danke für die nötige Ablenkung, die Motivation und eine einzigartige Freundschaft die maßgeblich zu meinem Werdegang beitrug. Rabia Ben Makhlof danke ich besonders für die stetige Ermutigung, moralische Unterstützung und Teilhabe an all meinen bisherigen Lebenslagen.

Ein besonderer Dank gilt meiner gesamten Familie, vor allem meinen Geschwistern für den Antrieb, die Unterstützung und den Rückhalt.

Zu guter Letzt danke ich meinen Eltern Iman Al Bawab und Walid Majid Ibrahim, ohne deren Liebe, Geduld, Aufopferung und Edukation diese Arbeit nicht zustande gekommen wäre.

III. Zusammenfassung

Die oromukosale Applikation von Arzneimitteln ist dadurch gekennzeichnet, dass der Wirkstoff in der Mundhöhle freigesetzt und über die Mundschleimhaut in den Blutkreislauf aufgenommen wird. Dabei nimmt sie bei der Behandlung spezieller Patientenpopulationen und akuter Beschwerden eine hohe Bedeutung ein und stellt eine Alternative zu herkömmlichen Applikationsrouten dar. Da die Bioverfügbarkeit von der oromukosalen Permeation der Arzneimittel abhängt, ist die Permeabilität bereits in der frühen präklinischen Entwicklung zu berücksichtigen, um die Entwicklungsschritte zwischen physikochemischer Charakterisierung, Formulierungsentwicklung und pharmakokinetischer *in vivo* Studien auszurichten. Dazu fehlt es jedoch an Permeationsstudien mit ausreichender Reliabilität, Prädiktivität und physiologischer Relevanz. Infolgedessen wird die Entwicklung und Zulassung klinisch vorteilhafter oromukosaler Arzneimittel erschwert und der übermäßige Bedarf an ethisch bedenklichen und kostspieligen Tierversuchen aufrechterhalten.

Im Rahmen dieser Arbeit wurde daher ein innovatives *ex vivo* Permeationsmodell erfolgreich entwickelt, validiert und standardisiert, um die präklinische Entwicklung oromukosaler Arzneimittel zu unterstützen. Das Modell kombiniert die Kerski-Diffusionszelle, Prozessautomatisierung, neuartige Assays zur Gewebsintegrität und Lebensfähigkeit sowie empfindliche LC-MS/MS-Analytik, welche in ein umfassendes analytisches Kontrollsystem eingebunden sind. Dadurch konnten physiologisch-klinische Bedingungen berücksichtigt werden, wie die Umgebung der oralen Mukosa, therapeutische Dosen und die kurze Verweildauer von intraoralen Arzneimitteln. Die Anwendbarkeit des Modells wurde in der Präformulierung zur oromukosalen Applikation von Cyclobenzaprinhydrochlorid nachgewiesen. Dabei wurde eine erhebliche Verbesserung der Permeabilität durch Anpassung und Kontrolle des pH-Werts der Mikroumgebung erreicht. Aufbauend auf diesen Erkenntnissen konnte in der anschließenden sublingualen Formulierungsentwicklung eine 4,68-fach verbesserte Permeation anhand des Modells erreicht werden. Darüber hinaus war es möglich das Modell in der Hilfsstoffauswahl sowie zur Bewertung der Stabilität der Darreichungsformen einzusetzen. Anschließend zur nachgewiesenen Anwendbarkeit in den Stadien der präklinischen Entwicklung in Zusammenarbeit mit der pharmazeutischen Industrie, wurde die *in vivo* Prädiktivität des Modells untersucht. Aussagekräftige multiple Level-C sowie Level-A Punkt-zu-Punkt-Korrelationen ($R^2 \geq 0,860$) zwischen der ermittelten Permeation und pharmakokinetischen Tierdaten wurden für verschiedene sublinguale Formulierungen erzielt.

Demnach erlaubt das oromukosale Permeationsmodell die zuverlässige Durchführung in qualitätskontrollierten Umgebungen und unterstützt dabei die Entwicklung intraoraler Arzneimittel. Die Integration der kohärenten Prozesse des Zerfalls, der Dissolution, der Permeation und der mukosalen Metabolisierung in ein physiologisches Design ermöglichte die Anwendung in verschiedenen Phasen der präklinischen Entwicklung und führte zu erfolgreichen *in vivo* Korrelationen. Dies bestätigte das Modell als vorteilhafte Alternative zu Tierversuchen in der Bewertung der Absorption oromukosaler Pharmazeutika und fördert klinisch angepasste und patientenorientierte Therapiestrategien.

IV. Summary

The oromucosal application of drugs is characterized by the release of the active ingredient in the oral cavity and its absorption into the blood circulation via the oral mucosa. Thereby, it is of great importance in the treatment of special patient populations and acute complaints while providing an alternative to conventional routes of administration. Since bioavailability depends on oromucosal permeation of drugs, permeability needs to be considered from the early stages of preclinical development to enable targeted development steps between physicochemical characterization, formulation development, and pharmacokinetic *in vivo* studies. However, permeation studies with sufficient reliability, predictivity, and physiological relevance are lacking for this purpose. As a result, the development and approval of clinically beneficial oromucosal drugs is hampered and the excessive need for ethically questionable and costly animal studies is perpetuated.

Therefore, as part of this thesis, an innovative *ex vivo* permeation model was successfully developed, validated, and standardized to overcome the limitations of current studies and support the preclinical development of oromucosal drugs. This model combines the Kerski diffusion cell, process automation, novel assays for tissue integrity and viability, as well as sensitive LC-MS/MS analysis embedded in a comprehensive analytical control system. In this manner, it facilitates the representation of physiological-clinical conditions including the oromucosal environment, therapeutic doses, and the short residence time of intraoral drugs. The applicability of the model was proven in preformulation studies of the oromucosal delivery of cyclobenzaprine hydrochloride, resulting in the substantial enhancement of permeability via the adaptation and control of microenvironmental pH. Based on these findings, a 4.68-fold improvement in permeation was achieved in the following formulation development of sublingual cyclobenzaprine guided by the permeation model. Additionally, it was feasible to characterize the transmucosal permeation of cyclobenzaprine for the first time, choose the disintegrant during excipient selection, and assess the clinical impact of dosage form alterations based on permeation results. According to demonstrated applicability in the stages of preclinical development—and in collaboration with the pharmaceutical industry—the *in vivo* predictivity of the model was addressed. Explorative multiple level C as well as level A point-to-point correlations ($R^2 \geq 0.860$) between obtained permeability results and pharmacokinetic animal data were revealed for several sublingual formulations.

Thus, the oromucosal permeation model allows the implementation of reliable studies within quality-controlled environments and supports the intraoral drug development. Integration of the coherent processes of disintegration, dissolution, permeation, and metabolism within a physiological design enabled its application at different stages of preclinical development and resulted in successful *in vivo* correlations. This confirmed the model as an advantageous alternative to animal studies for assessing the absorption of oromucosal pharmaceuticals and encourages clinically adapted and patient-oriented therapeutic strategies.

V. Table of Contents

I. Erklärung zur Dissertation	IV
II. Danksagung	V
III. Zusammenfassung	VI
IV. Summary	VII
V. Table of Contents	VIII
VI. Abbreviations	XI
VII. Tables	XIV
VIII. Figures	XV
IX. Equations	XVII
1. Introduction	1
1.1. Oromucosal drug delivery	1
1.1.1. Oral cavity: Anatomy, physiology, and drug absorption	2
1.1.2. Advantages and disadvantages of oromucosal administration	5
1.1.3. Recent status of oromucosal drugs	7
1.2. Cyclobenzaprine hydrochloride: New therapeutic options by administration via the oral mucosa	8
1.3. Studies on oromucosal permeation and absorption	12
1.3.1. Overview	12
1.3.2. Applicability in preclinical drug development.....	12
1.3.3. Classification and current state.....	15
1.3.4. Challenges and limitations of <i>in vitro</i> and <i>ex vivo</i> permeation approaches	19
1.3.5. Clinical, ethical, and social relevance	22
2. Aim of the thesis.....	24
3. Development, validation and standardization of oromucosal <i>ex vivo</i> permeation studies for implementation in quality-controlled environments	25
3.1. Introduction.....	25
3.2. Materials and Methods.....	28
3.2.1. Chemicals and materials	28
3.2.2. Preparation of solutions, standards and quality control samples.....	28
3.2.3. Permeation study set-up.....	29
3.2.4. Quality assurance.....	33
3.2.5. Selected challenges during method development	33
3.2.6. Analytical validation.....	34
3.2.7. Membrane integrity.....	36
3.2.8. Membrane viability	36
3.2.9. Application.....	37
3.3. Results and Discussion.....	39
3.3.1. Selected challenges during method development	39
3.3.2. Analytical validation.....	43

3.3.3. Membrane integrity.....	46
3.3.4. Membrane viability	47
3.3.5. Application.....	48
3.4. Conclusion.....	52
4. Exploring the transmucosal permeability of cyclobenzaprine: A comparative preformulation by standardized and controlled <i>ex vivo</i> and <i>in vitro</i> permeation studies.....	53
4.1. Introduction.....	53
4.2. Material and Methods	55
4.2.1. Chemicals and material.....	55
4.2.2. Standardized <i>ex vivo</i> permeation study set-up	55
4.2.3. Quality control and monitoring system.....	56
4.2.4. Investigation and characterization of the transmucosal permeability of cyclobenzaprine	57
4.3. Results and Discussion.....	62
4.3.1. Effects of pH, phosphate salt type, and quantity on permeability	62
4.3.2. Effects of membrane thickness and storage conditions on permeability	67
4.3.3. Scaling the dose to the sublingual surface area	71
4.3.4. Effects of simultaneous permeation and potential marker compounds on permeability.....	71
4.4. Conclusion.....	75
5. Formulation development of sublingual cyclobenzaprine tablets empowered by standardized and physiologically relevant <i>ex vivo</i> permeation studies.....	76
5.1. Introduction.....	76
5.2. Material and Methods	78
5.2.1. Simultaneous quantification of cyclobenzaprine and its related compounds.....	78
5.2.2. Sublingual formulation development guided by permeation studies.....	79
5.2.3. Standardized and physiologically relevant permeation model.....	81
5.2.4. Dissolution studies	83
5.3. Results and Discussion.....	84
5.3.1. Simultaneous quantification of cyclobenzaprine and its related compounds.....	84
5.3.2. Sublingual formulation development guided by permeation studies.....	86
5.3.3. Metabolism of cyclobenzaprine during mucosal administration.....	89
5.3.4. Impact of alteration in dosage forms on drug liberation and absorption	92
5.4. Conclusion.....	96
6. Predictivity of Standardized and Controlled Permeation Studies: <i>Ex vivo</i> – <i>In vitro</i> – <i>In vivo</i> Correlation for Sublingual Absorption of Propranolol.....	97
6.1. Introduction.....	97
6.2. Materials and Methods.....	99
6.2.1. Analytical method validation	99
6.2.2. pH-dependent thermodynamic solubility	100
6.2.3. <i>Ex vivo</i> and <i>in vitro</i> permeability	101
6.2.4. <i>Ex vivo</i> – <i>in vitro</i> – <i>in vivo</i> correlation.....	102
6.3. Results and Discussion.....	104

6.3.1. Analytical method validation	104
6.3.2. pH-dependent thermodynamic solubility	106
6.3.3. Impact of formulation pH on oromucosal permeability	108
6.3.4. <i>Ex vivo</i> – <i>in vitro</i> – <i>in vivo</i> correlation	112
6.4. Conclusion	116
7. Overall conclusion and perspective.....	117
8. Funding	122
9. References	123
10. Appendix	141
11. Publications of Haidara Majid.....	160
12. Curriculum vitae	162

VI. Abbreviations

ACN:	Acetonitrile
ADME:	Absorption-distribution-metabolism-excretion
ANOVA:	Analysis of variance
API:	Active pharmaceutical ingredient
AUC:	Area under the curve
AUC_{est}:	Estimated area under the curve
BCS:	Biopharmaceutical classification system
BM:	Basal membrane
CAF:	Caffeine
CalConc.:	Calculated concentration
CBP:	Cyclobenzaprine
CBP-d3:	Cyclobenzaprine-d3
CBP HCl:	Cyclobenzaprine hydrochloride
CCK-8:	Cell counting kit-8
C_{max}:	Maximum plasma concentration
COVID-19:	Coronavirus disease 2019
Cps:	Counts per second
CT:	Connective tissue
CV:	Coefficient of variation
CYP:	Cytochrome P450
Da:	Dalton
DAPI:	4',6-Diamidino-2-phenylindole
DBA:	Dolichos Biflorus Agglutinin
DMSO:	Dimethyl sulfoxide
EDTA:	Ethylenediaminetetraacetic acid
EF:	Enhancement factor
EMA:	European Medicines Agency
ET:	Epithelial tissue
FA:	Formic acid
FDA:	United States Food and Drug Administration
FEP:	Fluorinated ethylene propylene
FITC:	Fluorescein isothiocyanate
FITC-DBA:	Fluorescein isothiocyanate-conjugated Dolichos Biflorus Agglutinin
HE:	Hematoxylin-eosin
HLM:	Human liver microsomes
HPLC:	High performance liquid chromatography
HQC:	High quality control
ICH:	International Council for Harmonisation
IS:	Internal standard
IVIVC:	<i>In vitro</i> – <i>in vivo</i> correlation
J_{ss}:	Steady-state flux
LB:	Protein low binding
LC:	Liquid chromatography
LC-MS/MS:	Liquid chromatography with tandem mass spectrometry
LLOQ:	Lower limit of quantification
Log D:	Logarithm of distribution coefficient

Log P_{ow}:	Logarithm of partition coefficient
LQC:	Low quality control
m/z:	mass-to-charge ratio
MCG:	Membrane-coating granules
MEL:	Melatonin
MET:	Metronidazole
MeOH:	Methanol
MQC:	Middle quality control
MRM:	Multiple reaction monitoring
MS:	Mass spectrometry
MTT:	3-(4, 5-Dimethylthiazol-2-yl)-2, 5-diphenyltetrazolium bromide
n.a.:	Not applicable
NCE:	New chemical entity
NomConc.:	Nominal concentration
OCT:	Optimal cutting temperature
OD:	Optical density
PAMPA:	Parallel artificial membrane permeation assay
P_{app}:	Apparent permeability coefficient
PAT:	1,10-phenanthroline
PBS:	Phosphate-buffered isotonic saline solution
PEEK:	Polyether ether ketone
pH_{max}:	pH of maximum solubility
PFA:	Perfluoroalkoxy alkane
PFP:	Pentafluorophenyl
pK_a:	Negative decimal logarithm of the acid dissociation constant
PP:	Polypropylene
PQ:	Performance qualification
PR:	Permeability ratio
PS:	Polystyrene
Psi:	Pound per square inch
PTFE:	Polytetrafluoroethylene
PTSD:	Posttraumatic stress disorder
PVPA:	Phospholipid vesicle-based permeation assay
QC:	Quality control
Q_t:	Cumulative amount of permeated drug per area at time t
r:	Coefficient of correlation
R²:	Coefficient of determination
RE:	Relative error
rpm:	Rotations per minute
RSE:	Relative standard error
S/N:	Signal-to-noise ratio
SARS-CoV-2:	Severe acute respiratory syndrome coronavirus 2
SB:	Stratum basale
SD:	Standard deviation
SF:	Saliva factor
SEM:	Standard error of the mean
SLT:	Sublingual tablet
SSRI:	Selective serotonin reuptake inhibitor
SST:	System suitability test

STD:	Standard
TEER:	Transepithelial electrical resistance
THF:	Tetrahydrofuran
TOF-MS:	Time-of-flight mass spectrometry
ULOQ:	Upper limit of quantification
USP:	United States Pharmacopeia
UV:	Ultraviolet
UV/Vis:	Ultraviolet-visible

VII. Tables

Table 1:	Advantages and disadvantages of oromucosal drug delivery	5
Table 2:	Physicochemical and pharmaceutical properties of cyclobenzaprine hydrochloride.....	8
Table 3:	Mass spectrometric conditions for the active ingredient cyclobenzaprine and the internal standard cyclobenzaprine-d3	31
Table 4:	Summary of accuracy and precision results of cyclobenzaprine hydrochloride..	44
Table 5:	Summary of dilution integrity results of cyclobenzaprine hydrochloride	45
Table 6:	Composition of the investigated drug solutions within preformulation	59
Table 7:	Mass spectrometric conditions for cyclobenzaprine and the respective marker compounds	61
Table 8:	Mass spectrometric conditions for cyclobenzaprine and its related compounds	79
Table 9:	Compositions of the sublingual tablets within formulation development.....	80
Table 10:	Summary of accuracy and precision results for simultaneous quantification of cyclobenzaprine hydrochloride and its related compounds.....	85
Table 11:	Physicochemical and pharmaceutical properties of propranolol hydrochloride ..	99
Table 12:	Summary of accuracy, precision, and dilution integrity of propranolol hydrochloride.....	106
Table 13:	Summary of permeability results for each sublingual formulation from <i>ex vivo</i> and <i>in vitro</i> studies	111

VIII. Figures

Figure 1: Anatomy of the oral cavity	2
Figure 2: Differences in tissue types and organization between intestinal (a) and oral mucosa (b)	3
Figure 3: Schematic illustration of the paracellular and transcellular permeation pathway for drugs through the oral mucosa.....	4
Figure 4: Symptoms of posttraumatic stress disorder in relation with sleep disturbances	10
Figure 5: Role of preclinical studies in the drug development process.....	13
Figure 6: Simultaneous processes between oromucosal administration and systemic absorption	15
Figure 7: Schematic illustration of the Franz diffusion cell	18
Figure 8: Schematic workflow of the standardized ex vivo permeation model	38
Figure 9: Percentage recovery rates of cyclobenzaprine hydrochloride in relation to the used tubing material, sampling method and buffer medium.....	40
Figure 10: Linearity (logarithmic scaled) by different sample preparation conditions	41
Figure 11: Optical densities measured after incubation of mucosa with different incubation media and after extraction of post-incubated mucosa with different solvents.....	42
Figure 12: Chromatogram of standard solution with inlets of the Q1 scans in multi-channel analyses for cyclobenzaprine and cyclobenzaprine-d3	43
Figure 13: Relative error of cyclobenzaprine hydrochloride recovery using three different concentrations.....	45
Figure 14: Blank-normalized optical densities for integrity verification using blue dextran 20.....	47
Figure 15: Cumulative amounts of permeated cyclobenzaprine hydrochloride from different sublingual dosage forms (2.80 mg drug load).....	49
Figure 16: Effect of pH and phosphate salts on cyclobenzaprine permeability by ex vivo studies.....	64
Figure 17: Effect of pH and phosphate salts on cyclobenzaprine permeability by in vitro studies.....	66
Figure 18: Correlation of the obtained cyclobenzaprine permeability by ex vivo and in vitro studies with the calculated unionized fraction of the drug	67
Figure 19: Effect of membrane thickness, storage condition and dose on cyclobenzaprine permeability.....	69
Figure 20: Hematoxylin-eosin and FITC-DBA stained cryosections of esophageal mucosal tissue	70
Figure 21: Product-ion scan with structural formula of the respective analytes in multi-channel-analysis	72
Figure 22: Permeability coefficients of cyclobenzaprine, cyclobenzaprine + marker compound and of the marker compound itself.....	73
Figure 23: LC-MS/MS chromatogram of desmethyl cyclobenzaprine, cyclobenzaprine, cyclobenzaprine-d3 and cyclobenzaprine N-oxide with the respective structural formula	84

Figure 24: Impact of excipient addition in preformulation and formulation development of cyclobenzaprine	87
Figure 25: Disintegration of cyclobenzaprine sublingual tablets after addition of 150 μ L freshly collected human saliva in dependence on time	88
Figure 26: Cytochrome P450 metabolism of cyclobenzaprine	91
Figure 27: Alteration of cyclobenzaprine sublingual tablets under ambient and stress conditions.....	95
Figure 28: LC-MS/MS chromatograms of propranolol and propranolol-d7 including the respective mass transition and fragmentation.....	105
Figure 29: Impact of pH on the relationship between the thermodynamic solubility and the unionized fraction of propranolol in the liquid formulations.....	107
Figure 30: Impact of pH on ex vivo permeability of propranolol as cumulative amount of permeated drug per cm^2 for the respective formulation	109
Figure 31: Impact of pH on in vitro permeability of propranolol as cumulative amount of permeated drug per cm^2 for the respective formulation	110
Figure 32: Multiple ex vivo/in vitro – in vivo correlation of obtained propranolol permeability with pharmacokinetic animal data.....	113
Figure 33: Ex vivo – in vivo point-to-point correlation for the respective propranolol formulations	114
Figure 34: Overview of the conducted development steps and purposive applications.....	121

IX. Equations

Equation 1:	Cumulative amount of permeated drug per area at time t (Q_t).	37
Equation 2:	Steady-state flux (J_{ss}).	37
Equation 3:	Apparent permeability coefficient (P_{app}).	37
Equation 4:	Fraction of unionized drug ($F_{unionized}$).	58
Equation 5:	Permeability ratio (PR).	58
Equation 6:	Estimated area under the curve (AUC_{est}).	60
Equation 7:	Enhancement factor (EF).	82

1. Introduction

1.1. Oromucosal drug delivery

Oromucosal drug delivery is defined as the administration of drugs through the oral mucosa to achieve a local or systemic pharmacological effect. It must be differentiated from drugs that release in the oral cavity but are absorbed through the intestinal tract after swallowing. As an alternative to oral and invasive conventional routes of administration, oromucosal administration is beneficial for special patient populations, such as patients with swallowing difficulties or fear of injections (dysphagia or trypanophobia). Moreover, it enables increased bioavailability by avoiding degradation and metabolism by the digestive tract and enterohepatic circulation [Pinto et al., 2020]. Oromucosal drug administration occurs either sublingually (under the tongue) or buccally (in the cheek pouch).

In the 1910s and 1920s, oromucosal administration received increasing attention from medical researchers. Studies of drug uptake from the oral cavity were conducted entirely *in vivo* and based on either the direct detection of clinical effects or the amount of drug remaining in the mouth [Davis and Ayman D., 1928]. Studies on numerous oromucosally administered drugs have been carried out (i.e., organic nitrates, opioids, alkaloids, and hormones) [Katz and Barr, 1955]. Approval of the widely known sublingual nitroglycerine was accompanied by a substantial research commitment over the last two decades. From a clinical perspective, pharmaceutical scientists are primarily motivated by the advantages of treating acute complaints and diseases (e.g., pain, insomnia, but also erectile dysfunction) through the rapid drug onset after oromucosal administration as well as the feasibility of rendering chemically/metabolically labile substances non-invasively bioavailable. In addition to investigating the developability of chemical molecules for oromucosal use, innovative approaches to patient- and complaint-centered dosage forms have emerged [Krampe et al., 2016]. Especially the application of biological substances such as therapeutic peptides, peptidomimetics, and vaccines benefiting from oromucosal drug delivery, since invasive administration represents the standard in these cases [Goyal et al., 2018; Morales and Brayden, 2017]. To achieve the appropriate absorption of drugs by the oral cavity and take advantage of these benefits, several innovative dosage forms were developed, e.g., oromucosal liquid formulations, gels, films, sprays, patches, sublingual and buccal (mucoadhesive) tablets, etc. [Hua, 2019]. Nonetheless, despite the popularity of research in this field, relatively few drugs are approved for oromucosal application. The main reasons include the complex absorption mechanism with low permeability for certain drugs, lack of adequate studies in the preclinical stage, and sophisticated formulation development [Pather et al., 2008; Rathbone et al., 2015b; Sattar et al., 2014; Wang and Chow, 2014].

1.1.1. Oral cavity: Anatomy, physiology, and drug absorption

The human oral cavity represents the first stage of the digestive tract and is divided into the oral vestibule and oral cavity proper [Çelebi and Yörükan, 1999]. The oral vestibule is defined as the region between the teeth and the lips or buccal cheeks, respectively. Medial to the teeth, the oral cavity proper is bounded superiorly by the palate, inferiorly by the floor of the mouth, laterally by the cheeks, and posteriorly by the fauces (Figure 1) [Goel and Long, 2019].

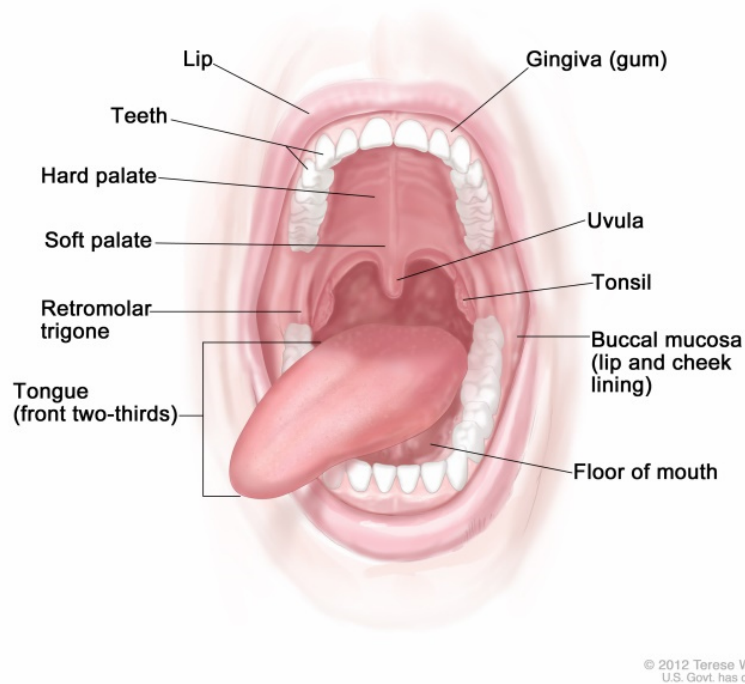


Figure 1: Anatomy of the oral cavity. *Used by permission from Terese Winslow. (Copyright © (2012) Terese Winslow LLC, U.S. Govt. has certain rights).*

The oral cavity is lined with stratified squamous epithelium, which is structurally subdivided into resistant keratinized (gingiva and hard palate), elastic non-keratinized (soft palate, cheeks, and mouth floor), and specialized mucosa (dorsal tongue) [Johnston, 2015]. The oral cavity has a total surface area of 214.7 cm², with approximately 30% of non-keratinized epithelium [Collins and Dawes, 1987]. The epithelium varies in thicknesses depending on its localization and separates the mucosal surface from the highly vascularized lamina propria. Due to the characteristics and thicknesses of the tissues, the sublingual mucosa is the most permeable and is thus particularly suitable for the treatment of acute complaints. In contrast, the buccal mucosa offers a larger absorption surface and longer residence time of the dosage form [Wertz, 2021]. The systemic uptake of xenobiotics through the internal jugular vein into the superior vena cava is enabled via the blood vessels in the lamina propria directly parallel to the basal membrane [Naumova et al., 2013]. In contrast to the single-layered columnar epithelium of the intestine, the oral mucosa resembles the skin and consists of multiple cell layers of varying differentiation (Figure 2) [Squier and Kremer, 2001]. Additionally, the oral

cavity lacks the surface-enlarging microvilli that increase the absorption area of the intestinal mucosa, thereby rendering it more permeable and absorbent overall (intestinal mucosa > oral mucosa > skin). For the oromucosal permeation of applied drugs, the epithelium forms the main barrier—specifically the superficial apical third [Wertz, 2021]. In this region, membrane-coating granules (MCG) fuse with the cell membrane of the upper epithelial cells and release their lipids, which accumulate intercellularly and contribute to the formation of the permeation barrier [Johnston, 2015; Squier and Kremer, 2001].

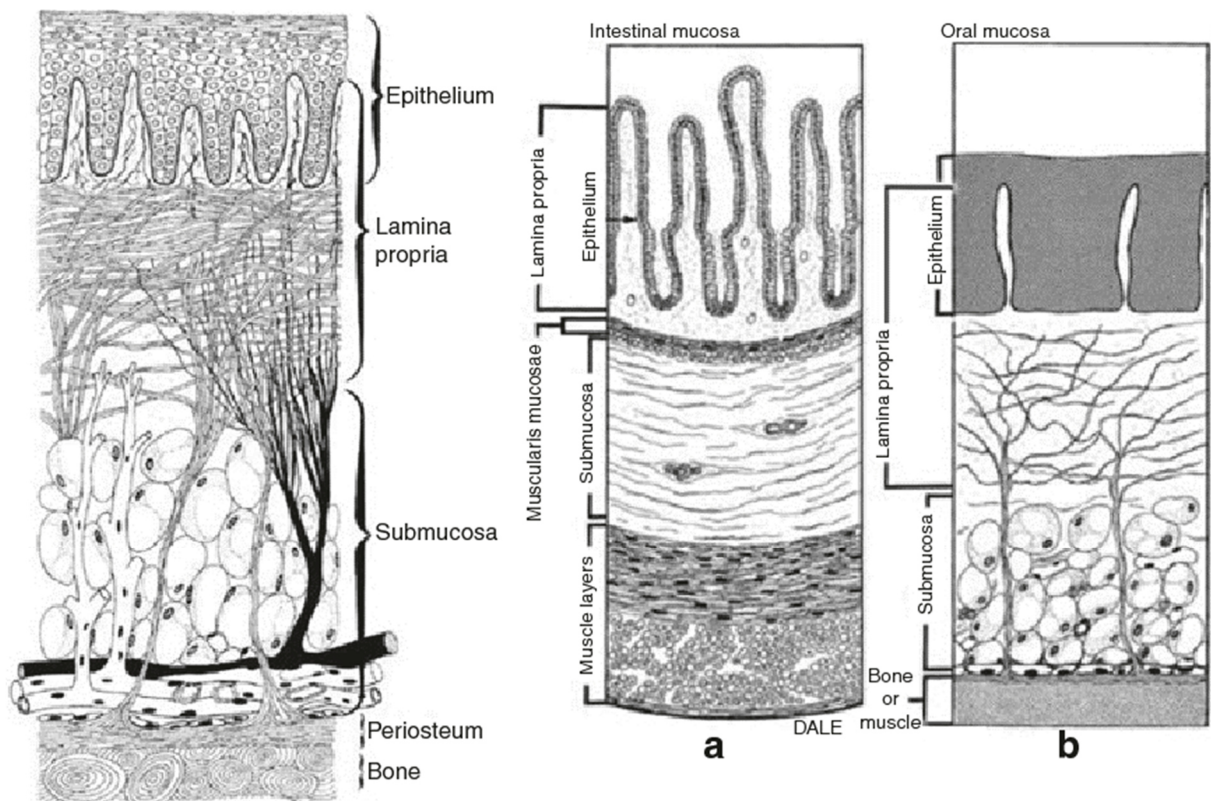


Figure 2: Differences in tissue types and organization between intestinal (a) and oral mucosa (b). Adapted by permission from Springer Nature: [Cruchley and Bergmeier, 2018], Copyright © Springer Nature (2018).

For the passive transmucosal diffusion of drugs, two routes are given: paracellular (between epithelial cells via intercellular spaces) and transcellular (through epithelial cells) (Figure 3). Hydrophilic and small molecules preferentially permeate through the relatively hydrophilic intercellular spaces of the paracellular pathway. In contrast, the transcellular pathway is characterized by the lipophilic cell membrane of epithelial cells and is thus preferred by lipophilic substances. Furthermore, the available area for transcellular permeation is larger and the permeation path shorter compared to the paracellular route [Johnston, 2015].

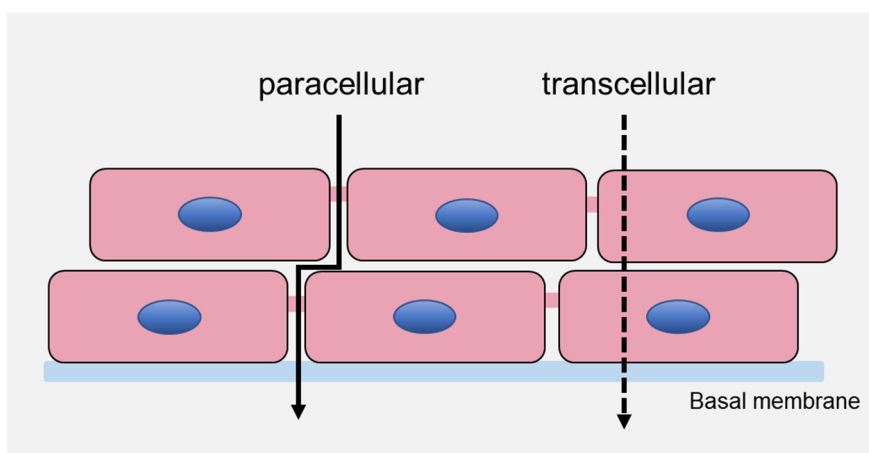


Figure 3: Schematic illustration of the paracellular and transcellular permeation pathway for drugs through the oral mucosa.

In general, drug absorption is based on Fick's laws of diffusion. The diffusion rate is directly proportional to the concentration gradient between the oral cavity and the bloodstream and additionally depends on the diffusion coefficient, the contact area available for absorption, the distribution coefficient of the substance between the site of administration and the mucosa, and the thickness of the diffusion layer [Rane and Moe, 2015]. Thus, in addition to the biological barrier function of the mucosa and the physicochemical properties of the drug, the physiology-based microenvironmental conditions at the oral site of administration essentially influence drug permeation. Here, a major factor is the daily secretion of 1.0 to 1.5 L of saliva, a hypotonic biological fluid containing low molecular weight components such as electrolytes and high molecular weight components including enzymes (e.g., α -amylase, lysozymes, esterase, peroxidase, protease, etc.) and glycoproteins (e.g., mucin). Carbonates and phosphates contribute to the modulation of the pH range, which is between 5.3 and 7.8, depending on the salivary flow [Humphrey and Williamson, 2001]. The composition, volume, formation of a mucus layer, and the potential metabolism of the drugs influences the solubility, release, concentration, residence time, and degree of ionization, which collectively affect the permeation capacity of the drug [Humphrey and Williamson, 2001; Obradovic and Hidalgo, 2008]. Along with the presented microenvironmental conditions, their evaluation of their impacts on permeability by pharmaceutical scientists is required to achieve clinically adequate and controlled drug absorption following oromucosal administration.

1.1.2. Advantages and disadvantages of oromucosal administration

Administration via the oral mucosa provides a number of pharmacokinetic and clinical advantages that can positively contribute to the patient's pharmacotherapy. There are also certain limitations associated with this route of drug administration. An overview of the advantages and disadvantages of oromucosal administration is provided in Table 1.

Table 1: Advantages and disadvantages of oromucosal drug delivery.

Advantages	
Ease of (self)-administration and accessibility	Improvement of patient adherence via high acceptance rate
Avoidance of gastrointestinal degradation	Avoidance of gastrointestinal and hepatic metabolism
Reduction of dose and associated side effects	Applicable in pediatrics and geriatrics
Non-invasive administration of drugs that are primarily injected	Rapid systemic onset
Therapy of local complaints	Short cellular turnover time
Increased of bioavailability	Affectable microenvironment by formulation
Beneficial for several patient populations (i.e., those with dysphagia, trypanophobia, nausea, intestinal insufficiency, etc.)	Treatment of specific disorders (i.e., pain, insomnia, erectile dysfunction, status-epilepticus, opioid dependence, etc.)
Disadvantages	
Risk of aspiration	Necessary drug potency and permeability
Discomfort while speaking, drinking and eating	Impact of nutritional and disease conditions (xerostomia, ptyalism, fasting, food, etc.) on the oromucosal microenvironment
Salivary clearance	Mucosal irritation
Limited surface area and residence time	Organoleptic properties

Overall, the advantages of oromucosal delivery outweigh the disadvantages and render it an attractive alternative to conventional routes of administration, especially for special patient groups (i.e., dysphagia, trypanophobia, nausea, intestinal insufficiency, etc.) and acute complaints [Hua, 2019; Rathbone et al., 2015b]. Additionally, indications requiring rapid

systemic availability as well as the treatment of local oral diseases are also targeted. Most importantly, the aforementioned limitations related to adequate drug availability and absorption, as well as the factors influencing patient comfort, represent challenges currently being addressed in pharmaceutical development of oromucosal drugs.

1.1.3. Recent status of oromucosal drugs

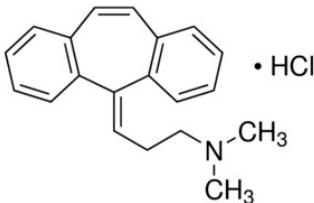
Currently, several drugs have been approved for sublingual and buccal administration. These include small molecules, which are predominantly used systemically for example for pain, smoking cessation, insomnia, angina pectoris, nocturnal enuresis, epilepsy and schizophrenia, and for the treatment of local microbial and inflammatory complaints [Hua, 2019]. In addition, biological compounds are marketed, such as allergen extracts for sublingual immunotherapy [Hua, 2019]. The majority of approved pharmaceuticals for systemic use are solid dosage forms (tablets) or semisolid and liquid dosage forms (gels, pastes, liquids) for local therapy. Many other drugs for oromucosal application are in clinical phases. The majority of these are already approved active ingredients, but for a different indication and/or route of administration. Tablets, solutions, and oral films represent the popular dosage forms in studies of neurological and mental disorders as the most common indications. Although biological agents such as insulin and vaccines are even in the early stages of development [Hua, 2019], they present a particular challenge. Due to their lower transmucosal availability, effective strategies for absorption enhancement as well as enzymatic protection are required. To overcome the limitations and disadvantages of oromucosal administration, innovative and complex dosage forms were developed. Thus, various formulations (i.e., polymeric films, nanoparticles, microneedle patches, 3D printing, mucoadhesion, etc.), strategies to increase permeation were explored and tested, and taste masking methods were investigated to face them. In addition to the development of chemical agents, interest in oromucosally available biological macromolecules is increasing considerably, including peptide drugs, vaccines, and polynucleotides [Jacob et al., 2021; Rane and Moe, 2015; Rathbone et al., 2015a; Sandri et al., 2020; Şenel et al., 2012].

However, there is an incongruity between the scientific advances in drug delivery and promising clinical benefits compared to the relatively low number of oromucosal drugs that are approved or undergoing late-stage clinical trials [Hua, 2019; Rathbone et al., 2015b]. Besides the comprehensive development of the optimal formulation of each drug, additional reasons for this include anatomical-physiological based permeability of the route and the poor transferability between laboratory experiments and clinical studies [Kolli and Pather, 2015]. From a regulatory perspective, evidence and advantage in terms of efficacy, drug safety, and pharmacokinetics are required, depending on the objective (public health benefit, reformulation, new indication, or new agent) [Hughes and Ghosh, 2015]. Moreover, sophisticated formulation development and novel strategies are often carried out in academic environments or by relatively small companies. These issues complicate the transfer into clinical phases, meeting regulatory standards and implementing a manufacturable scale-up [Hua, 2019; Rathbone et al., 2015b; Wang and Chow, 2014].

1.2. Cyclobenzaprine hydrochloride: New therapeutic options by administration via the oral mucosa

Cyclobenzaprine hydrochloride is a centrally acting skeletal muscle relaxant approved by the United States Food and Drug Administration (FDA) since 1977 for the short-term oral treatment of muscle pain and spasms [Chou et al., 2004]. Chemically, cyclobenzaprine is a tricyclic compound with a dibenzocycloheptene ring system (Table 2). It is structurally similar to amitriptyline with an additional C9-C10 double bond. Cyclobenzaprine is pharmacologically characterized by its antagonistic effects in the serotonergic, histaminergic, and adrenergic systems as well as minor inhibition of serotonin and norepinephrine reuptake [Daugherty et al., 2015; Mestres et al., 2011; Moniri et al., 2021]. Known life-threatening cases (e.g., ventricular arrhythmias) caused by tricyclic antidepressants occurred rarely in cyclobenzaprine overdose intoxications, highlighting their differences [Bebarta et al., 2011]. Due to its profile of action and new options of administration, cyclobenzaprine is currently being investigated and discussed with regard to several indications.

Table 2: Physicochemical and pharmaceutical properties of cyclobenzaprine hydrochloride [National Center for Biotechnology Information, 2021b].

Drug	Cyclobenzaprine hydrochloride
Molecular formula	C ₂₀ H ₂₂ ClN
Structural formula	
Molecular weight [g/mol]	311.8 g/mol
Solubility	Freely soluble in water
pK _a	8.5
Log P _{ow}	5.2 (free base)
Bioavailability (oral)	33 – 55%
Pharmacological class	Skeletal muscle relaxant

Log P_{ow}: logarithm of partition coefficient, *pK_a*: negative decimal logarithm of the acid dissociation constant

Specifically, cyclobenzaprine has been intensively studied and used off-label for the treatment of fibromyalgia in recent decades [Moldofsky et al., 2011]. Fibromyalgia is a chronic musculoskeletal pain syndrome with spreading muscle pain, stiffness, sleep disturbance, fatigue, and exhaustion as core symptoms. Pathophysiologically, a disorder of pain perception with involvement of the autonomic and neuroendocrine systems is assumed [Bradley, 2009]. In a meta-analysis of five randomized placebo-controlled trials, Tofferi et al. reported a short-term benefit in fibromyalgia with daily doses of 10 to 40 mg of oral cyclobenzaprine. Hereby, global functioning and modest improvement in pain and sleep quality were registered, while no effect was noted on fatigue. However, an 85% occurrence of side effects (i.e., dry mouth, somnolence, and dizziness) was detected in combination with high rates of study-drop out, indicating low patient adherence in practice [Tofferi et al., 2004]. In contrast, a double-blind randomized placebo-controlled study from 2011 concluded that treatment with bedtime-administrated low-dose cyclobenzaprine hydrochloride (≤ 4 mg/d orally) improved pain relief, sleep quality, fatigue and mood while reducing side such as like somnolence in patients with fibromyalgia [Moldofsky et al., 2011]. Nevertheless, despite improvements from dose reduction, approval has not yet been granted for its use in fibromyalgia. On the other hand, the broad pharmacological profile of cyclobenzaprine and the reported therapeutic effects regarding sleep disturbances offer a potential psychopharmacotherapeutic use (i.e., in affective and anxiety-related insomnia).

Posttraumatic stress disorder (PTSD) is a mental disorder caused by exposure to previous trauma. PTSD is characterized by four symptom criteria, which are intrusion with involuntary re-experiences, avoidance behavior concerning internal and external reminders, cognitive impairment with partial amnesia and apathetic behavior as well as hyperarousal symptoms such as hypervigilance, anxiety, and irritability [American Psychiatric Association, 2013]. Figure 4 demonstrates the symptom categories of PTSD and their relationship with sleep disturbances as part of hyperarousal symptoms. These are defined as difficulty falling asleep, nocturnal wake-up, and trauma-associated nightmares, which may lead to the maintenance or exacerbation of the overall symptomatology and again result in sleep disturbances through confrontation [Brownlow et al., 2020].

The cross-national prevalence of PTSD in adults was reported as 3.9% [Koenen et al., 2017], with 80 to 90% of patients suffering from sleep disturbances [Spoormaker and Montgomery, 2008]. Moreover, the common traumas associated with PTSD include experiences from military deployment, sexual violence, or the death of loved ones [Guina et al., 2018]. In context of current global events, a substantial increase in PTSD prevalence is assumed due to the impacts of the severe acute respiratory syndrome coronavirus 2 (SARS-CoV-2) pandemic on populations and health care workers. Notably, high rates of PTSD following recovery from coronavirus disease 2019 (COVID-19) were reported for patients and health care workers

(30.2 and 21.5%, respectively) [Janiri et al., 2021; Li et al., 2021]. On the other hand, the prevalence of PTSD among internationally fled and displaced populations from conflict zones is enormous and may be increasing considering underreporting, the impact on affected children and youth, and ongoing wars and conflicts [Acarturk et al., 2021; Blackmore et al., 2020; Close et al., 2016].

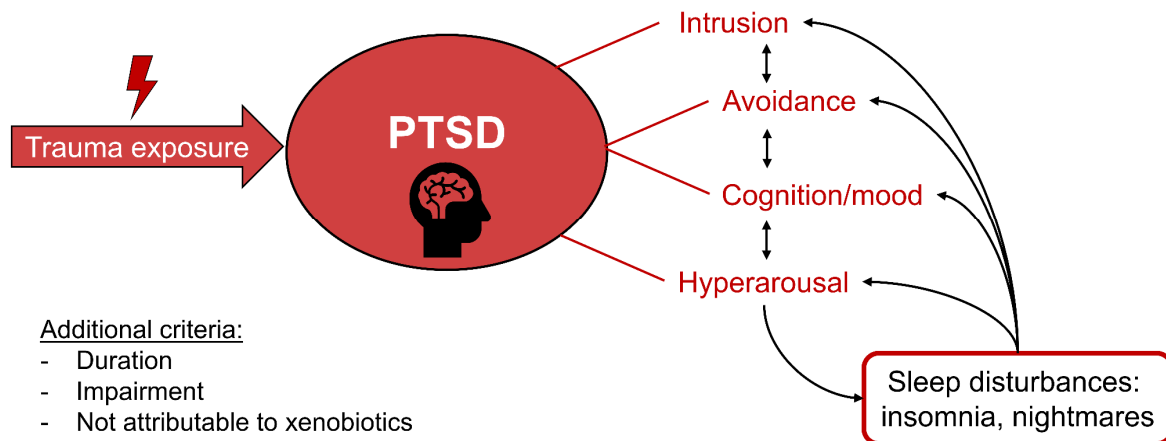


Figure 4: Symptoms of posttraumatic stress disorder in relation with sleep disturbances. *PTSD: posttraumatic stress disorder.*

For therapy of PTSD, only the selective serotonin reuptake inhibitors (SSRIs) sertraline and paroxetine are currently approved for use in Europe and the United States [National Institute for Health and Care Excellence, 2018; Sartori and Singewald, 2019]. Thus, both have a similar profile of action and do not form viable alternatives. Their potential side effects (e.g., emotional dullness, gastrointestinal issues, insomnia, and suicidality), combined with the latency period of 2 to 3 weeks, restrict their use for acute therapy to address sleep disturbances in PTSD [Sartori and Singewald, 2019]. Notably, this led to an increase of off-label therapies. Indeed, high rates of sedative medications such as quetiapine, mirtazapine, and benzodiazepines have been reported in PTSD inpatients [Reinhard et al., 2021]. Therefore, there is a consistent and explicit demand for studies on the effectiveness of medications that are already widely prescribed for the treatment of PTSD as well as novel therapeutic options [Krystal et al., 2017]. In the search for alternatives, well-known and pharmacologically broad-acting tricyclic drugs are also being considered, with a particular focus on low-dose cyclobenzaprine administered via the sublingual route due to increased patient safety and efficacy in sleep disorders. [Davidson, 2015].

Sublingual low-dose cyclobenzaprine decreased hyperarousal symptoms through improved sleep quality by reducing trauma-related complaints and nightmares in several clinical studies on military-related PTSD [Bestha et al., 2018; Sartori and Singewald, 2019; Sullivan et al., 2021]. Therapy of PTSD-related sleep disturbances via the bedtime administration of low-dose

sublingual cyclobenzaprine exploit the clinical advantages of sublingual administration. The rapid systemic uptake ensures an indication-appropriate and immediate effect. Simultaneously, the higher bioavailability compared to peroral administration (bioavailability of 33 to 55%) allows dose reduction and thus increased patient safety. In particular, it provides the reduction of daytime side effects (e.g., somnolence), by avoiding the first-pass effect with the formation of the active and long-lived metabolite desmethyl cyclobenzaprine (norcyclobenzaprine) [Sullivan et al., 2021]. Desmethyl cyclobenzaprine has a similar broad pharmacologic profile of action to cyclobenzaprine, which, when used regularly, is associated with the aforementioned frequent side effects due to accumulation of the active metabolite by the long elimination time. In this case, the commonly reported side effects of somnolence, dry mouth and dizziness can be connected to histamine, serotonin, adrenergic and muscarinic receptor antagonism and are assumed to affect patient adherence.

Oromucosal administration of cyclobenzaprine contributes to an overall improvement in patient adherence, forms a novel therapeutic option for sleep disorders of different origins, and may interrupt the cycle of PTSD symptoms presented in Figure 4. Further potential application areas for cyclobenzaprine have also been discussed, such as Alzheimer's disease, alcoholism, affective disorders, and long-COVID syndrome. The evaluation and realization of this potential starts with the absorption of the drug. Initial comprehensive characterization and exploration of the transmucosal permeation of cyclobenzaprine are necessary to ensure appropriate bioavailability and patient-oriented accessibility for PTSD and other disorders.

1.3. Studies on oromucosal permeation and absorption

1.3.1. Overview

Studies of oral mucosal drug permeability can be used in phases of preclinical drug development, ranging from screening the permeability of new chemical entities (NCEs) to assessing permeation impacting factors and formulations. In this manner, they allow researchers to decide on the developability of novel substance as well as to lead formulation development for ensuring an appropriate drug absorption [Cabrera-Pérez et al., 2016]. Oromucosal permeation studies are classified into *in vitro* (in glass), *ex vivo* (outside the living organism) and *in vivo* (within the living organism). For *in vitro* studies, cell-based and artificial membranes are applied as permeation barriers, while dissected biological tissue is used for *ex vivo* studies. *In vivo* studies comprise experiments on animal or human subjects. To apply the individual studies as decisive elements during drug development, advantages and disadvantages regarding reliability, predictivity, practicability, and ethics must be considered.

1.3.2. Applicability in preclinical drug development

It is estimated that the time between drug discovery and approval takes approximately 15 years and costs 800 million US dollars. Among 5,000 to 10,000 compounds involved in drug discovery, 250 may reach the preclinical stage and only 5 enter clinical studies [Shah et al., 2014]. The role of preclinical development and its investigations are presented in Figure 5. During preclinical development, information is collected on pharmacodynamics, pharmacokinetics, and safety of the compounds, which provides a feedback mechanism back toward drug discovery and the requisite knowledge for initial studies on humans. For drug absorption, the initial phases in pharmacokinetics, permeability, together with solubility, are the most important factors [Ajavon and Taft, 2010].

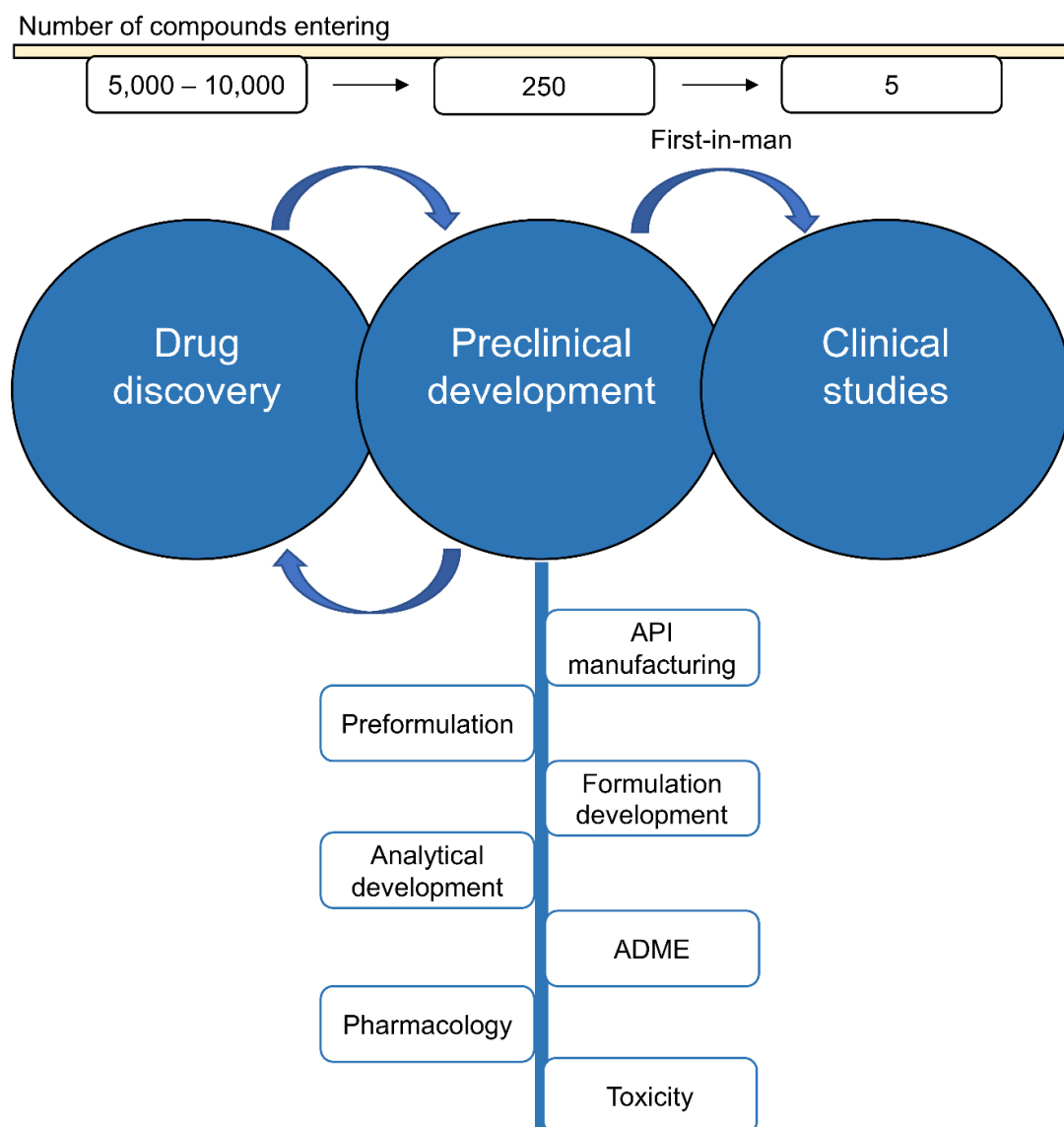


Figure 5: Role of preclinical studies in the drug development process. *ADME: absorption-distribution-metabolism-excretion, API: active pharmaceutical ingredient.*

The permeability of the oral mucosa depends on the physicochemical properties of the drug in relation to the conditions of the environment and the added ingredients of the formulation. Studies on drug permeability are promising tools that can be effectively used in the phases of preclinical drug development (i.e., within preformulation and formulation development). Even during drug discovery, the permeability of NCEs represents an essential selection criterion for their further development before they enter the preclinical phase.

Preformulation studies include the comprehensive characterization of the physicochemical properties of a compound. These studies assess acid/base properties, solubility, lipophilicity, morphology, and permeation behavior, which initially require the purpose-oriented development and validation of appropriate analytical methods [Lundqvist and Bredenberg,

2013; Shah et al., 2014]. Common parameters determined for this purpose include the negative logarithm of the acid dissociation constant (pK_a), the logarithm of the partition coefficient ($\log P_{ow}$), melting point, aqueous solubility, apparent permeability coefficient (P_{app}), and the selection of an appropriate salt form [Shah et al., 2014]. Since most NCEs and drugs are acidic or basic compounds, the given pH value not only influences solubility and partition but also the extent and mechanism of permeation. Thus, pH-dependent solubility including the pH of maximum solubility (pH_{max}), logarithm of the distribution coefficient ($\log D$), and pH-dependent permeability profiles are required at least considering physiologically relevant ranges (route of administration, biological fluids, targeted disease or population). Drug permeability studies serve as an essential screening tool for various active derivatives, additives, and microenvironment conditions at this stage, thereby assisting the medicinal chemist in advancing their studies, while also providing the formulation scientist with aspects to consider in subsequent formulation development.

Based on the preformulation results, the design of the dosage form is then developed. This includes the selection and evaluation of appropriate excipients based on known characteristics of the drug. To improve oromucosal absorption, solubilizers, enhancers, pH modulation, and the related adjustment of the microenvironment are assessed. In addition to conventional disintegration and dissolution tests, permeation studies can be applied for this purpose. Since these processes are directly related to each other (Figure 6), well-regulated studies on disintegration and dissolution are not sufficient to generate a reliable statement on the effects on oromucosal absorption and may result in unsuccessful animal pharmacokinetic studies. Thus, considering the interplay between solubility and permeability is required in the formulation procedure [Dahan and Miller, 2012]. Permeation studies can fill this gap and—through the possibility of applying the final formulation—assess the impact on simultaneous disintegration-dissolution-permeation processes. This enables a formulation development guided by the resulting permeability, in which broad approaches can be investigated and only the most suitable dosage forms proceed to the *in vivo* phase. In this context, Freedman et al. reported on the increasing irreproducibility in preclinical studies due to errors in design and analysis as well as non-standardized conduct [Freedman and Gibson, 2015]. Thus, to successfully implement resource-efficient and animal-test-reducing preclinical development, the standardization, control, and predictivity of the permeation studies are mandatory. This would improve their reliability and—in combination with an automatable and routine-suitable study design, which is in accordance with transposed regular recommendations—their broad application in academic, pharmaceutical, and cosmetic environments can be established.

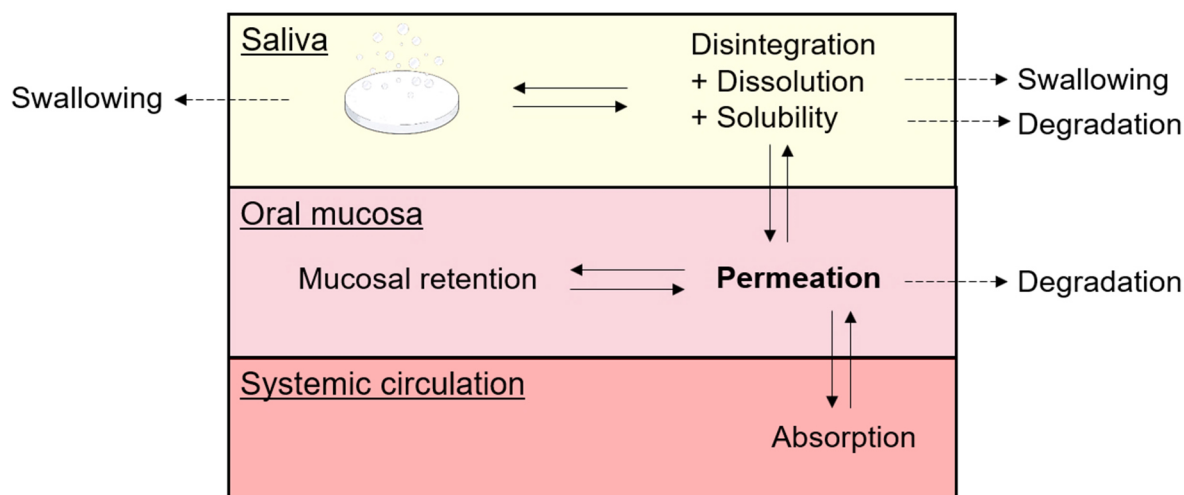


Figure 6: Simultaneous processes between oromucosal administration and systemic absorption. While recent pharmacopeia considers only single steps (i. disintegration, ii. dissolution, iii. solubility), in preclinical evaluation a meaningful permeation model encompasses the entire absorption procedure (disintegration-dissolution-permeation-absorption).

1.3.3. Classification and current state

1.3.3.1. *In vivo* absorption studies

In vivo studies were the first type of experiments for oromucosal absorption, started with absorption test in human. Buccal absorption tests describe the swirling of drug solutions in the oral cavity for a specified time and the subsequent determination of the drug remaining and rinsed out [Pinto et al., 2020]. This test does not provide information on the site of absorption or resulting bioavailability. Likewise, the test is susceptible to accidental drug loss, dilution by saliva secretion, limitation to the initial absorption of the drug, and does not provide absorption time profiles. Therefore, various optimizations (marker compounds (with unknown effect on drug permeation), correction factors, aliquot sampling, etc.) were implemented. Nevertheless, the buccal absorption test does not present the current state of the art and ethical principles.

Ideally, the properties in humans should be fully considered. However, *in vitro* as well as *ex vivo* studies have not succeeded in reflecting the entire *in vivo* situation and its physiological interaction. Thus, animal experiments constitute the most popular *in vivo* studies to investigate drug absorption, primarily with anesthetized minipigs, rabbits, and rats, which serve as pharmacokinetic models for the evaluation of drugs and dosage forms [Dali et al., 2006; Gayrard et al., 2013; Itin et al., 2020; Meng-Lund et al., 2014; Song et al., 2018; Tsagogiorgas et al., 2013]. The obvious disadvantages of *in vivo* studies include the high cost and effort, as well as the ethical constraints associated with animal experimentation. At this point, novel *in vitro* or *ex vivo* studies adapted to preclinical applications can lead to the replacement of disproportionate animal testing and the reduction and targeting of their conduct.

1.3.3.2. *In vitro* permeation studies

For *in vitro* permeation studies, different cell line approaches can be used, e.g. primary cell lines from hamster cheek [Tavakoli-Saberi and Audus, 1989]. Since the buccal mucosa of hamsters is normally keratinized, this is absent due to the lack of differentiation, thus mimicking human epithelial conditions. However, primary cell cultures are permanently dependent on isolation of new cells due to the limited lifespan, resulting in increased variability, which limited their present usage [Shrestha et al., 2016].

More commonly and widely used is the TR146 cell line, a continuous human cell line from neck node metastasis of buccal carcinoma. After cultivation and filter growth (23 days), they form an epithelium of multiple cell layers with similar properties to human non-keratinized buccal mucosa [Jacobsen et al., 1999; Jacobsen et al., 1995]. TR146-based permeation studies have been previously used for assessment of drug permeability and the effects of enhancing substances [Brayden and Stuetgen, 2021; Nielsen and Rassing, 2002]. However, an up to tenfold higher permeability of the TR146 cell line was reported due to lower barrier function compared to the human mucosa [Nielsen and Rassing, 2000]. This is attributed to the carcinogenic origin and the total thickness of 100 μm (four to seven cell layers) instead of a total thickness of around 500 μm (40 to 50 cell layers) in human [Patel et al., 2012; Shrestha et al., 2016; Smart, 2004]. Furthermore, permeability depends on their cultivation conditions such as growth rate, number of cell layers and cultivation time. In sum, this complicates the reliable broad use of the TR146 cell line within drug development beyond the initial relative ranking of compounds [Wang et al., 2020].

These drawbacks were addressed by a commercially available 3D human cell culture model derived from oral biopsies of healthy subjects (EpiOralTM) [Boateng and Okeke, 2019; Pinto et al., 2020]. This model closely reproduce the morphology, MCG's, differentiation, and lipid composition of human oral mucosa and allow for interdisciplinary investigations concerning mucosal irritation, pathology, permeability, metabolism and toxicity [Klausner et al., 2021; Shrestha et al., 2016]. In particular, for the study of special drug absorption mechanisms and metabolic degradation, the 3D human cell model offers substantial advantages. Nevertheless, only few studies on its applicability in oromucosal drug absorption as well as on its *in vivo* predictivity are known. Due to the reduced number of epithelial layers, higher permeability was determined compared to animal tissue models. Despite the aforementioned advantages, 3D tissue models are inflexible (prescribed use within 24 hours), complex and costly processes that may be used in isolated research questions, but are limited as a predictive routine tool in oromucosal formulation development [Klausner et al., 2021; Sohi et al., 2010; Wang et al., 2020].

Non-cellular artificial membranes provide an *in vitro* alternative to cell-based models. Starting with filter membranes, artificial membranes have evolved in order to mimic the biological condition of mucosal tissue. The artificial approaches aim for simpler execution, lower effort, high throughput and reproducibility compared to the introduced cellular models. Thereby, polymeric filter membranes were impregnated with different lipid solutions (parallel artificial membrane permeation assays (PAMPA)) or combined with liposomal vesicles (phospholipid vesicle-based permeation assay (PVPA)). Although, PAMPA and PVPA were initially applied for studying intestinal drug permeability, different variants regarding the composition of supporting filter and lipid membrane/liposome depending on the intended use (PAMPA skin, PAMPA blood-brain-barrier) are available [Berben et al., 2018]. However, no composition specifically for the oral mucosa is known to date. In addition, the limited number of comparability studies on oromucosal permeation, short shelf life, elaborate preparation and potential substance accumulation in the material, are known difficulties [Wang et al., 2020]. With Permeapad®, a commercially, phospholipid-based (biomimetic) artificial membrane, consisting of phosphatidylcholine S-100 between two cellulose support layers is available [Di Cagno et al., 2015]. As a ready-to-use membrane, it simplifies the application compared to PAMPA and PVPA and offers high shelf life and pH stability. After contact to water, the dry lipid membrane swells and form densely packed phospholipid double layers. Applying Permeapad® as permeation barrier achieved correlations to well-established *in vitro* assays of intestinal absorption (PAMPA, Caco-2) [Di Cagno et al., 2015]. Regarding oromucosal permeability, Bibi et al. reported an *in vitro* – *in vivo* correlation (IVIVC) regarding pH-dependent permeability using metoprolol [Bibi et al., 2016]. As this is the only known study on the oromucosal transferability of Permeapad®, further studies of drugs with different physiochemical properties are needed to reliably evaluate the potential of the artificial barriers [Wang et al., 2020].

1.3.3.3. *Ex vivo* permeation studies

Due to the difficulty of obtaining excised human mucosa and its limited tissue area, it is seldom used in research. Thus, animal mucosal tissue mainly serves as an *ex vivo* model instead. Therefore, species selection should be made based on having the closest properties to human oral mucosa. However, the oromucosal tissue of rodents is considered inappropriate due to keratinization. Although the tissues of monkeys and canines are composed of non-keratinized epithelium, they prove to be more permeable and are impractical in terms of expense and accessibility [Nielsen and Rassing, 2000; Siegel and Gordon, 1985]. Porcine mucosa has close anatomical, morphological, and metabolic similarities to humans, is readily available in local slaughterhouses, and crucially shows comparable permeability properties [Kulkarni et al., 2010; Nielsen and Rassing, 2000]. Despite the wide use of porcine oral mucosa, high variations often occur due to biological interindividual and intraindividual variability as well as

destruction by the self-biting of animals during the slaughter process. This results in the loss of tissue integrity and reduces the limited amount of usable mucosa. Animal tissue-based studies are generally error-prone and heterogeneous due to the multiple processes required in their conduct, which result in low comparability [Kolli and Pather, 2015; Kulkarni et al., 2010; Sarmiento, 2016].

1.3.3.4. Diffusion methodologies

The Franz diffusion cell as the conventional diffusion apparatus is basically divided into two chambers (donor and acceptor chamber), with the permeation membrane between them (Figure 7). The open donor chamber is filled with a drug solution and the acceptor chamber with 6 to 8 mL acceptor medium. Samples are taken through the side sampling port and the amount of drug permeated is measured. To mimic physiological conditions, the diffusion cell is placed in a 37 °C water bath [Wang et al., 2020].

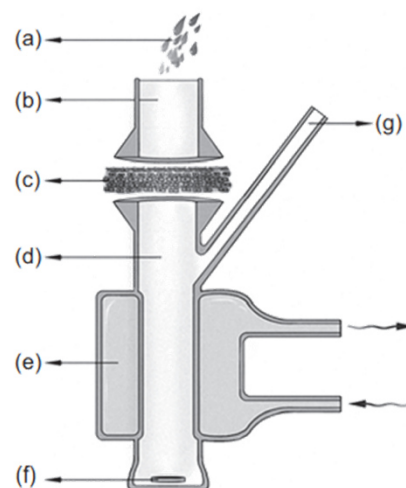


Figure 7: Schematic illustration of the Franz diffusion cell. (a): drug solution, (b): donor chamber, (c): membrane, (d): acceptor chamber, (e): water jacket, (f): stirrer, (g): sampling port. Used by permission from Elsevier Ltd: [Castro et al., 2016], Copyright © Elsevier Ltd (2016).

Based on the Franz cell, further modifications were developed, such as the flow-through diffusion cell and the Ussing chamber. In contrast to the vertical static setup, these mimic *in vivo* blood circulation with a continuous flow of donor and acceptor medium, provide an alternative for poorly soluble drugs, and prevent the accumulation of air at the membrane. The Ussing chamber consists of two half-chambers perfused throughout and connected by a U-shaped tubing system with gas for sufficient convection [Nicolazzo and Finnin, 2008; Pinto et al., 2020].

1.3.4. Challenges and limitations of *in vitro* and *ex vivo* permeation approaches

Despite having the physiologically closest representation of human conditions for *in vivo* animal studies, these are increasingly being attempted to be reduced. The high cost, effort, and moral appeal for the reduction of animal experiments are the primary motivators for this trend [Pinto et al., 2020; Sarmiento, 2016]. Moreover, *in vitro* and *ex vivo* studies offer more flexible and adaptable experimental conditions to serve as a systematic screening for testing candidates and formulations prior to entry into *in vivo* studies [Cabrera-Pérez et al., 2016]. However, this theoretical objective is hindered by numerous limitations of the available studies on oromucosal drug permeability.

Firstly, the heterogeneity of studies directly affects the permeation results, such as the cultivation conditions in the case of *in vitro* cell studies [Wang et al., 2020]. The additional time and expense, the vulnerability of cell lines to excipients, and the lack of ability to evaluate dosage forms challenge the widespread application of cell-based approaches and create an increasing trend toward *ex vivo* experiments [Wang et al., 2020]. However, heterogeneity issues arise also in *ex vivo* studies in terms of species selection, mucosa thickness (full-thickness or separated epithelium), region of excision (localization of mucosal region), self-destruction of the mucosa during slaughter, use of fresh or frozen tissue, composition of applied media, study duration, sampling time, quantification methods until diffusion cell methodologies, and their individual modifications [Kolli and Pather, 2015; Pather et al., 2008; Sarmiento, 2016]. During the preparation of the excised mucosa, the epithelium as the main diffusion barrier is usually be separated chemically (i.e., by ethylenediaminetetraacetic acid (EDTA)), surgically or by heat (at 60 °C for 1 minute) from the underlying connective tissue [Sarmiento, 2016]. These methods result in different permeation properties due to different mucosal thicknesses, while the effects of the treatments on barrier properties remains unclear.

Second, the study design is neither clinically nor physiologically representative regarding oromucosal drug administration. The use of analytical quantification methods with low analytical specificity and sensitivity results in inadequate drug doses, sampling times and durations, regarding the intended short-term application of intraoral drugs by the patient [Esim et al., 2018; Koradia and Chaudhari, 2018]. Drug permeation measurements taken over several hours impede the detection of clinically relevant effects related to the active pharmaceutical ingredient (API) or dosage form used. There are also challenges to be assigned to the diffusion cells. For example, drug accumulation occurs in static Franz-type cells, which leads to the required use of solubilizing compounds on the acceptor side while failing to comply with physiological properties (e.g., sink conditions). Ultimately, this results in the distortion of the concentration gradients and consequent permeation [Sarmiento, 2016]. Although the Ussing chamber circumvents this problem by providing constant circulation, it does not offer any possibilities for the examination of oromucosal formulations. Thus, only a

few *ex vivo* studies achieved a successful correlation with oromucosal *in vivo* data [Holm et al., 2013; Itin et al., 2020; Nicolazzo and Finnin, 2008; Sattar et al., 2014; Wang et al., 2020].

Thirdly, a sophisticated quality control (QC) and a monitoring system based on common regulatory recommendations to ensure reliability is missing. This includes the validation of quantification methods, an appropriate quality management of the studies as well as standardized and practicable examinations for mucosal integrity (physical intactness) and the viability of the used membrane. Marker compounds are usually applied to test tissue integrity and include substances with high (e.g., mannitol) or low (e.g., dextran, polyethylene glycol) permeability. In this case, the added marker compounds could affect the permeability of the API or, conversely, could be influenced in their permeation by the different environmental conditions (e.g., during formulation development). Low sensitivity combined with the use of low-permeability markers leads to lengthy post-study permeation testing that fails to represent the time frame of the actual permeability study and delays subsequent viability testing. Transepithelial electrical resistance (TEER) assays, derived from cell culture and skin tissue studies, measure the alternating current resistance between two separated media as an integrity characteristic. However, this limits the compatibility of TEER assays to specific diffusion cells with low throughput and complicates studies with varying media and formulations. So far, TEER tests for the oral mucosa have barely been tested [Araújo et al., 2021]. For mucosal viability, modified cell activity test determining the mitochondrial dehydrogenase activity using 3-(4, 5-dimethylthiazol-2-yl)-2,5-diphenyltetrazolium bromide (MTT) are applied. MTT test were previously considered for evaluation of storage conditions of mucosal membranes and were not applied as post-study controls. The number of practical steps, the long duration (> 4 hours), and low assay sensitivity resulted in MTT tests being deemed inappropriate for standardized routine application [Nicolazzo and Finnin, 2008].

The fourth problem is the lack of automation. The design of current diffusion cells leaves few options for study automation. Thus, sampling and sample preparation are manually conducted, which presents an additional source for accidental error. Moreover, manual sampling often leads to the accumulation of air under the mucosal membrane and negatively affects permeability. Even the use of commercially available autosamplers requires prior verification and the consideration of drug-tubing interaction as well as of the necessary volume exchange for accurate sampling, which has not been considered in previous studies with sample draw volumes of around ≤ 1 mL.

No specific regulatory guidance has been provided for the conduct of oromucosal permeation studies (*in vitro* and *ex vivo*). However, the guidelines of the European Medicine Agency (EMA) on transdermal patches and topical products address the design of skin permeability studies in Annex 1 and Annex II, respectively [European Medicines Agency, 2018a, 2014]. Herein, the following recommendations are defined to provide sufficient evidence of suitability and to

conduct them in compliance with quality assurance principles: Permeation studies should be able to distinguish and characterize permeation profiles while also being applicable within product life cycle management. Other areas of application include pharmaceutical development, preliminary bioequivalence, and stability studies [European Medicines Agency, 2018a, 2014; International Council for Harmonisation of Technical Requirements for Pharmaceuticals for Human Use, 2009, 2008]. It is recommended that human or animal tissues be applied as a permeation barrier, with standardized tissue types, processing, and storage. The integrity of the inserted membranes serves as a validity parameter for the studies. Diffusion cells should be inert with simple sampling procedures. The acceptor medium should mimic physiological *in vivo* conditions, not affect the integrity of the tissue, and maintain sink conditions. Full contact between the membrane and the acceptor volume, appropriate agitation, and the maintenance of physiological temperature should be ensured. Validated quantification methods in accordance with the guideline of the International Council for Harmonisation (ICH) Q2(R1) should be applied for the measurements of collected samples with a clinically adjusted study duration [International Council for Harmonisation of Technical Requirements for Pharmaceuticals for Human Use, 2005].

Since oromucosal application represents a form of topical application where the resulting absorption depends on the permeability through the respective tissue, the aforementioned guidelines seem to be the most appropriate reference. To achieve a reliable and meaningful implementation of permeation studies in preclinical drug development, the EMA recommendations should be considered in the study design. The discrepancy between the set-up of known oromucosal permeability studies and the range of recommendations and requirements has restricted the use of these studies to scholarly questions or unregulated preliminary studies in the past. For the majority of other applications, laborious, expensive, and ethically sensitive *in vivo* studies remain the method of choice. Even the use of highly standardized dissolution studies as a standard method for formulation evaluation appears inappropriate when it comes to accounting for oromucosal physiology and its effects on absorption [Ali et al., 2021; Song et al., 2018]. Therefore, standardized, extensively controlled, routine-suitable, physiologically relevant, and predictive studies are required for the characterization and evaluation of intraoral drugs and their dosage forms. In this manner, the potential of these studies can be fully realized by using them as an integral and guiding part of galenic development and preclinical investigation [Cabrera-Pérez et al., 2016; Itin et al., 2020; Kolli and Pather, 2015; Patel et al., 2012; Sarmiento, 2016; Volpe, 2010].

1.3.5. Clinical, ethical, and social relevance

Suitable and predictive oromucosal permeability studies can fill the existing gap in preclinical studies of intraoral drugs. Thus, exploitation of the clinical benefits of this administration route can be supported to enable the accessibility of patient-friendly therapy options, complaint- and indication-appropriate dosage forms, and increased patient safety, which would result in improved patient adherence. For instance, 20 to 50% of adolescent and adult patients have a fear of needles, with an even higher prevalence expected in children [McLenon and Rogers, 2019]. Moreover, about one-third of people between the ages of 19 and 66 years have difficulty swallowing medications [Radhakrishnan et al., 2021], which can increase with age or with certain drugs or diseases. The consequences on adherence and jeopardizing therapeutic success resulting from these two complaints are addressed by oromucosal administration. Furthermore, this type of administration still facilitates the rapid but non-invasive treatment of acute cases. Its reliable applicability in controlled environments will induce widespread use of the studies and attract both academic and commercial pharmaceutical interest. From a scientific perspective, the development of innovative oromucosal dosage forms, the assessment of novel enhancing compounds, and the establishment of the oral cavity as an alternative route for the increasingly focused biopharmaceutical drugs would be promoted and supported by a uniform permeation platform.

It is estimated that approximately 190 million animal experiments are conducted for scientific purposes each year, which represents a growing trend [Taylor and Alvarez, 2019]. Currently, approximately half of animal testing is performed in the field of medical research and development, where it is still used as an assessment and decision-making tool in preclinical stages [Sántha, 2020; Zane et al., 2019]. In 1959, William Russel and Rex Burch published "*The Principles of Humane Experimental Technique*", where they defined the 3R principle (Replacement, Reduction, Refinement) with the aim of replacing and reducing experiments on animals and refining their conditions within the studies [Russell W. M. S., Burch R. L., 1959]. Since then, the 3Rs principle has formed the basis for animal welfare within science and has been incorporated into pharmaceutical guidelines of regulatory agencies. Herein, it is demanded that a scientifically satisfactory alternative method to animal testing should be applied whenever possible while reducing animal testing to a minimum [European Medicines Agency, 2018b, 2016]. Specifically, regarding pharmacokinetic studies such as those on intestinal absorption, the Caco-2 method is mentioned as an implemented 3R option. During preclinical drug development, permeation studies can assist the decision-making process in the early stages in terms of compound selection and characterization. In further stages, the impact of excipients, microenvironments, and the developed dosage forms can be evaluated to guide the preformulation and formulation development. A good IVIVC would provide the estimation and transfer of effects to the *in vivo* situation, thereby facilitating more targeted and

reduced animal studies. Equivalent to the Caco-2 method, standardized *ex vivo* processes for oromucosal permeation can be established as a predictive and implemented 3R option to advance the ethically desired reduction and replacement of animal testing while minimizing costs and effort in selected preclinical phases. Looking forward, expanded application with different drugs can enhance the optimization of *in silico* models using reliable experimental data for future pharmacokinetic *in human* prediction.

The oromucosal administration of low-dose cyclobenzaprine offers a viable approach to targeting the pharmacotherapeutic crisis of PTSD [Krystal et al., 2017], especially in light of the predicted increase in PTSD within the global population due to the COVID-19 pandemic and its aftermath as well as for the high prevalence of mental disorders in populations from conflict areas [Acarturk et al., 2021; Blackmore et al., 2020; Dutheil et al., 2021]. Moreover, increasing attention to the oromucosal route also facilitates a promising approach to the treatment of psychological disorders by reconsideration and repurposing known substances and providing higher patient acceptance [Davidson, 2015; Sartori and Singewald, 2019; Tricklebank et al., 2021]. As a needle-free alternative to invasive administration, transmucosal administration is also gaining traction in end-of-life care (e.g., in severe COVID-19 and pediatric palliative cases) [Lam et al., 2020]. In the case of cyclobenzaprine, there has been no comprehensive characterization of its oromucosal permeation behavior to date. Detailed impressions on this promote the mucosal development of the drug with regard to prospective additional indications.

2. Aim of the thesis

The advantages offered by drug delivery via the oral cavity (i.e., avoidance of gastrointestinal drug degradation and first-pass metabolism, rapid systemic availability, patient adherence, and safety, etc.) increased its pharmaceutical attractiveness as a beneficial patient- and indication-centered alternative route of administration. Nonetheless, despite of their scientific popularity, only a few drugs are approved for oromucosal application. To support their progressive development, reliable and meaningful studies predicting pharmacokinetic properties are essential in preclinical drug development. However, current studies on oromucosal permeability are insufficiently adapted to physiological-clinical conditions and show several conceptual limitations (i.e., heterogeneous study designs, deficiency of standardization and monitoring, lack of routine suitability, barely correlations to *in vivo* data), which restrict their broad use in pharmaceutical environments and translation into preclinic.

Thus, the present work aimed to develop and establish an innovative and physiologically adapted *ex vivo* model for oromucosal permeability, and to comprehensively assess its usefulness and predictivity in stages of preclinical drug development.

To accomplish this, the following four main objectives were pursued:

1. The development, validation, and standardization of an entire tissue-based *ex vivo* model to reliably explore oromucosal drug permeability and its integration in a sophisticated analytical control system. The model was intended to incorporate physiologically relevant conditions and enable implementation in pharmaceutical environments.
2. The application of the model in preformulation studies as an early stage of preclinical drug development to evaluate its sensitivity and meaningfulness. This included the comprehensive characterization of transmucosal permeability of cyclobenzaprine hydrochloride and affecting factors such as the type and quantity of excipients as well as environmental/experimental conditions (i.e., pH, membrane thickness, dosage).
3. The demonstration of model applicability and suitability in sublingual formulation development as a later stage of preclinical drug development. In addition to its ability to detect and classify the impact of dosage form alteration, the relevance of drug metabolism during transmucosal permeation was to be monitored and assessed, since data on metabolic activity in the oral cavity is limited.
4. Verification of the model concerning its *in vivo* predictivity and comparison with biomimetic artificial barriers as an alternative approach (*in vitro*). For this purpose, *ex vivo* – *in vitro* – *in vivo* correlations between permeability and sublingual *in vivo* plasma concentrations of the model drug propranolol hydrochloride were performed.

3. Development, validation and standardization of oromucosal ex vivo permeation studies for implementation in quality-controlled environments

3.1. Introduction

The intraoral route is becoming an increasingly popular alternative to the conventional routes of drug administration, such as the peroral and parenteral routes [Brandl and Bauer-Brandl, 2019]. Improved patient adherence to intraoral administration is due to the combination of pharmacokinetic and clinical benefits, such as avoidance of the first-pass effect and gastrointestinal metabolism, simple and painless administration, and a rapid, systemic onset [Brandl and Bauer-Brandl, 2019; Rossi et al., 2005]. Oromucosal drug administration is particularly beneficial for patients who suffer from nausea, intestinal insufficiency, dysphagia, and various neurodegenerative diseases [Zhang et al., 2002]. These advantages initiated research on novel dosage forms and drugs with potentially useful intraoral administration [Kottke et al., 2020; Montero-Padilla et al., 2017]. The oromucosal permeation of pharmaceuticals depends on their physicochemical properties as well as on their applied formulation. To characterize potentially oromucosal available substances and to assess novel intraoral dosage forms, reliable studies with insights on release and mucosal permeability are required.

Current permeation studies progressively concentrate on *in vitro/ex vivo* studies rather than *in vivo* studies due to their lower cost, easier sampling procedures, adjustable experimental conditions and the need for fewer experiments on animals [Pinto et al., 2020]. By bridging the gap between typical *in vitro* characterization and *in vivo* trials, *ex vivo* studies offer information on planned dose-finding, first-in-man or bioavailability studies [Holm et al., 2013; Patel et al., 2012; Pinto et al., 2020]. *Ex vivo* permeation studies enable the prediction of the oromucosal permeation capability of certain drugs and can enable cost-intensive *in vivo* experiments to be performed in a more targeted and therefore reduced manner [Kottke et al., 2020]. Nevertheless, the systematic and widespread use of *ex vivo* studies in academic and regulatory pharmaceutical environments is still restricted by several conceptual limitations. The modest number of approved oromucosal drugs is repeatedly attributed to the lack of suitable studies as a specific challenge [Pather et al., 2008; Rossi et al., 2005].

Conventional *ex vivo* permeation experiments consist of different diffusion cells and isolated biological barriers with manual sampling procedures, often in combination with ultraviolet-visible (UV/Vis) spectroscopy or high performance liquid chromatography (HPLC) used as quantification methods [Kokate et al., 2008]. However, using quantification methods with

This work was published in an international peer-reviewed journal [Majid et al., 2021a]:

Majid, H., Bartel, A., Burckhardt, B.B., 2021a. Development, validation and standardization of oromucosal ex-vivo permeation studies for implementation in quality-controlled environments. *Journal of Pharmaceutical and Biomedical Analysis* 194, 113769. <https://doi.org/10.1016/j.jpba.2020.113769>.

The author of this thesis was responsible for conceptualization, methodology, validation, writing-original draft, and visualization.

limited analytical specificity and sensitivity result in a clinically non-representative setting for the pharmaceutical dose, measurement time and duration with regard to the relatively short residence time of intraoral drugs in the oral cavity [Sattar et al., 2014]. This is reflected in the *ex vivo* determination of the permeated drug over several hours, although an application time of a few minutes is intended by patients. Even in more recent *ex vivo* studies, the first measurement times are at least 30 min after administration. Due to the design of the common diffusion cells, there are fewer possibilities for automation and standardization of sampling when considering the required sink conditions [Kolli and Pather, 2015; Obradovic and Hidalgo, 2008]. Furthermore, various mucosal membranes are applied as a diffusion barrier. Porcine oral mucosa, which is the most commonly used barrier, has certain disadvantages in resection and preparation, such as yielding a limited amount of useful mucosa from the cheek pouch due to its size, structure and its tendency to self-destruct as a result of the stress experienced by the animals before slaughter [Sarmiento, 2016]. The heterogeneous experimental set-ups which include differences in the selection of diffusion cells and sampling procedures, different species, mucosal regions, thicknesses, media compositions and permeation duration in addition to the aforementioned limitations—impede the establishment of comparable and standardized *ex vivo* permeation studies in regulatory environments [Pather et al., 2008].

This is accompanied by missing incorporation of the processes in a sophisticated QC and monitoring system according to common regulatory guidelines [International Council for Harmonisation of Technical Requirements for Pharmaceuticals for Human Use, 2008]. Besides guideline-compliant quality and documentation management, there are no standardized controls for cell viability or for ensuring the integrity of inserted mucosal tissues in order to ensure reproducible results. Previously known modified MTT tests are mainly concerned with the storage conditions of mucosal membranes and are not standardized as post-experimental controls of inserted membranes [Obradovic and Hidalgo, 2008]. Due to limited analytical sensitivity and the low permeability of used integrity markers (dextran or polyethylene glycols), a relatively long post-study permeation test is required (four hours), which in turn leads to a delay in the above-mentioned viability tests making it unsuitable as a regular control within the studies and impractical for incorporation into a usual working day [Kulkarni et al., 2010]. Thus, current permeation studies are often carried out without monitoring mucosal integrity and viability.

Accordingly, the scientific literature calls for process standardization, since each individual step in the experimental procedure can represent a possible source of error [Cabrera-Pérez et al., 2016; Obradovic and Hidalgo, 2008; Pather et al., 2008; Sarmiento, 2016]. Hence, the demand is uniform, comprehensively controlled as well as a routine-suitable study design for the characterization and evaluation of intraoral drugs and their dosage forms. In this way, the potential of the studies can be fully exploited by applying them as an established element in

galenic development and preclinical research, while facilitating the replacement and reduction of animal experiments according to the three R's principle [Cabrera-Pérez et al., 2016].

Therefore, the aim of this study was to develop, validate and standardize an entire process of tissue-based *ex vivo* studies to reliably assess oromucosal drug permeability. In addition, an approach to quality-controlled implementation will be pursued by combining new components for viability, integrity and quality assurance. Cyclobenzaprine hydrochloride, a centrally acting muscle relaxant with a dibenzocycloheptene structure served as a model drug. Due to its structural similarities to tricyclic antidepressants, the drug is associated with sedative, anxiolytic and antidepressant effects. This offers potential benefits by its oromucosal application regarding its fast onset in the treatment of PTSD and insomnia [Krystal et al., 2017].

3.2. Materials and Methods

3.2.1. Chemicals and materials

Cyclobenzaprine hydrochloride ($\geq 98\%$) was used as API (Hetero drugs Ltd, Hyderabad, India) and cyclobenzaprine-d3 (98%) as internal standard (IS) (Sigma-Aldrich, Taufkirchen, Germany). Sodium chloride ($\geq 99.5\%$, p.a.) and potassium dihydrogen phosphate ($\geq 99\%$, p.a.) were purchased from Roth GmbH (Karlsruhe, Germany). Potassium chloride ($\geq 99.5\%$, p.a.) and ortho phosphoric acid (85%, p.a.) were obtained from AppliChem GmbH (Darmstadt, Germany). Disodium hydrogen phosphate ($\geq 99\%$, p.a.) was supplied by Riedel-de-Haen (Seelze, Germany) and sodium hydroxide ($\geq 99\%$, p.a.) as well as dipotassium hydrogen phosphate (99%, Ph. Eur.) from VWR Chemicals (Langenfeld, Germany).

Formic acid (FA) ($\geq 98\%$, p.a.), tetrahydrofuran ($\geq 99.9\%$, p.a.), alizarin yellow (dye content 50%), fluorescein isothiocyanate-conjugated dextran (FITC)-dextran (average molecular weight 20,000 Da), blue dextran 20 (average molecular weight 20,000 Da), 1,10-phenantroline monohydrate ($\geq 99.9\%$) and cell counting kit-8 (CCK-8 assay kit) were obtained from Sigma-Aldrich (Taufkirchen, Germany). Water (liquid chromatography (LC)-grade), acetonitrile (ACN) (LC-grade), propan-2-ol (LC-grade), methanol (LC-grade), and dimethyl sulfoxide (DMSO) ($\geq 99.9\%$, p.a.) were purchased from Fisher Scientific (Schwerte, Germany). 1.5 mL protein low binding micro tubes were provided by Sarstedt AG & Co. KG (Nümbrecht, Germany). Saliva was donated by healthy volunteers and collected in salivettes (Sarstedt AG & Co. KG, Nümbrecht, Germany). Porcine esophagi were obtained from the slaughterhouses Naturverbund Thönes (Wachtendonk, Germany) and Frank Prill (Bergheim, Germany).

3.2.2. Preparation of solutions, standards and quality control samples

Phosphate-buffered isotonic saline solution (PBS buffer) was prepared by dissolving 8.00 g sodium chloride, 0.20 g potassium chloride, 1.44 g disodium hydrogen phosphate, and 0.24 g potassium dihydrogen phosphate in 1 L of water, while the pH value was subsequently adjusted to 7.4 using orthophosphoric acid. A 1:10 dilution of PBS buffer with water served as the sample solvent for standard and QC samples.

The stock solution of cyclobenzaprine hydrochloride (prepared by dissolving approximately 5 mg of accurately weighted substance in 250 mL methanol) was diluted 1:10 with sample solvent to obtain a fresh working solution (2.00 $\mu\text{g}/\text{mL}$). Standards and QCs were prepared by serial dilution from their respective working solutions. All standards as well as QCs were spiked with IS. Spiking and agitation were performed automatically by HTS PAL (CTC Analytics AG, Zwingen, Germany).

3.2.3. Permeation study set-up

The core elements within the permeation process presented here are based on a combination of the novel Kerski diffusion cell (Appendix 1) [Kerski et al., 2020] coupled to Hanson Research AutoPlus™ (Teledyne Hanson, Los Angeles, USA) and HTS PAL with the following quantification via liquid chromatography with tandem mass spectrometry (LC-MS/MS). Fresh esophageal porcine mucosa was applied as a biological barrier. Within three hours after slaughter, the esophagus was opened longitudinally, rinsed with PBS buffer and stretched onto a dissection device. The mucosal membranes were uniformly separated into thicknesses of 500 µm using an electric dermatome (Integra® Dermal, Ratingen, Germany), punched to a diameter of 20 mm and adapted to the surface of the Kerski diffusion cell. After visual inspection, the mucosal membrane was clamped between both chambers of the diffusion cell. In order to equilibrate the inserted membranes, the acceptor chamber was filled with 10 mL PBS buffer (acceptor medium) and the donor chamber was filled with 50 µL freshly collected and purified human saliva.

The formulation to be tested was placed in the donor chamber and 100 µL human saliva (donor medium) was added on top (Appendix 2). The studies were performed in constant conditions of 37 °C, 20% relative humidity and continuous stirring at 750 rpm. Within the 60-minute permeation period, Hanson Research AutoPlus™ performed nine fully automated samplings after 1, 5, 10, 15, 20, 30, 40, 50 and 60 minutes, and transferred the samples through MultiFill™ into LC vials. Before each sampling, a rinsing volume of 2 x 2 mL was discarded from the Kerski diffusion cells. Next, 0.5 mL of the sample was automatically transferred into an LC vial and the acceptor chamber of the diffusion cell was refilled with 4.5 mL of PBS buffer. The sample preparation was performed automatically by the HTS PAL autosampler using Chronos XT software (Axel Semrau GmbH, Sprockhoevel, Germany). For this purpose, the samples were spiked with 25 µL of a cyclobenzaprine-d3 hydrochloride solution, diluted with water (1:10) and agitated.

3.2.3.1. Quantification method

Concentrations of cyclobenzaprine and the IS were determined by utilizing high performance liquid chromatography coupled with electrospray ionization tandem mass spectrometry (HPLC-ESI-MS/MS). A HPLC Prominence system (Shimadzu Deutschland GmbH, Duisburg, Germany) consisting of a controller CBM-20A Lite, two binary pumps (LC-20AD), an online degasser DGU-20A3, an autosampler SIL-20A HT, a column oven (CTO-20A) with a column valve (FCV-12AH) was used. For chromatography, a pentafluorophenyl column (PFP) Luna PFP (2) (100.0 x 2.0 mm; 3 μ m) equipped with SecurityGuard PFP (2) (4.0 x 2.0 mm) as guard column was utilized. The mobile phases consisted of 0.1 % FA in water and 0.1 % FA in ACN with an optimized flow rate of 450 μ L/min and a maintained column temperature of 55 °C. The injection volume was set to 5 μ L and the total run time per sample was set to 3.9 minutes. The retention time for cyclobenzaprine and IS was 3.06 minutes, by applying linear gradient elution.

For MS detection an API 2000 LC/MS/MS system (AB Sciex, Darmstadt, Germany) equipped with an electrospray ionization source was used in positive ion mode. For quantification in multiple reaction monitoring mode (MRM), the mass transitions of 276.2 to 215.0 mass-to-charge ratio (m/z) for cyclobenzaprine and 279.2 to 215.0 m/z for cyclobenzaprine-d3 were selected. The analyte-specific parameters and the conditions of the ion source were optimized by flow injection analysis, considering signal intensity, reproducibility and peak shape (Table 3). Data acquisition and evaluation were carried out with Analyst® 1.5.1 (AB Sciex, Darmstadt, Germany).

Table 3: Mass spectrometric conditions for the active ingredient cyclobenzaprine and the internal standard cyclobenzaprine-d3.

<u>Analyte-specific parameters</u>	<u>Cyclobenzaprine</u>	<u>Cyclobenzaprine-d3</u>
Mass transition [m/z]	276.2 → 215.0	279.2 → 215.0
Declustering potential	30 V	30 V
Focusing potential	380 V	380 V
Entrance potential	9 V	9 V
Cell Entrance potential	20 V	24 V
Collision energy	61 V	61 V
Cell Exit potential	25 V	25 V
<u>Mass spectrometric parameters</u>		
Source	Electrospray ionization	
Mode	Positive ion mode	
Detection	Multiple reaction monitoring mode	
Dwell time	100 msec	
Ion spray voltage	2000 V	
Temperature	550 °C	
Curtain gas (nitrogen)	20 psi	
Nebulizer gas (zero air)	36 psi	
Heater gas (zero air)	75 psi	
Collision gas (nitrogen)	7 psi	

3.2.3.2. Membrane integrity

Within the permeation studies, a tailored post-experimental examination for determining the integrity of applied mucosal membranes was developed. After the final sampling, a solution of the labeled marker compound was injected into the donor chamber and overpressure was built up by Hanson Research AutoPlus™. After five minutes, samples were drawn from the acceptor site of each diffusion cell. Reactive Blue 2 (blue)-dextran 20 (3 mg/mL), a photo-actively

labeled biopolysaccharide with a molecular mass of 20 kDa, was used for this purpose. The optical density (OD) of blue dextran 20 was measured at 620 nm by Tecan infinite f50 absorbance microplate reader (Crailsheim, Germany). If the integrity of the mucosal membrane was insufficient, diffusion of the dextran molecules occurred leading to an increase in OD. For analysis, the OD was normalized to the OD of the blank (PBS buffer), specifying a blank-normalized OD of ≤ 2 for integrity.

3.2.3.3. Membrane viability

Following the integrity examination, the post-experimental viability of the used mucosal membranes was studied by semi-quantitatively determining the metabolic activity of the epithelial cells. The membranes were removed from the diffusion cells, washed with PBS buffer and punched to a uniform area of 1.13 cm². The punched membranes were transferred into a 96-well microplate containing 250 μ L DMSO as well as 10 μ L CCK-8 reagent before being incubated for two hours at 37 °C, 20% relative humidity and shaken at 500 rpm on a microplate shaker (Grant Instruments Ltd, Shepreth, UK). After incubation, the OD of the supernatant was measured at 450 nm. Membranes treated with 1% FA in methanol for at least three hours were used as the negative control and fresh saliva as the positive control. In reference to [Imbert and Cullander, 1999], the positive viability result was defined as having a relative viability of $\geq 50\%$ compared to the earliest possible control.

3.2.4. Quality assurance

Besides post-experimental integrity and viability examinations, a quality assurance system was implemented to control and verify the processes during the permeation studies. This included tests for system suitability of LC-MS/MS and the absorbance reader, and QCs within the analytical runs as well as comprehensive quality documentation.

3.2.4.1. System suitability tests

LC-MS/MS

A fresh standard solution of cyclobenzaprine hydrochloride was prepared by diluting the stock solution and spiking it with 25 μ L of IS (190.48 ng/mL). The six-fold injection of the standard was then evaluated regarding signal intensity, retention time ($\pm 10\%$), and repeatability (coefficient of variation (CV) of analyte/IS area ratios $\leq 15\%$).

Absorbance reader

A serial dilution of alizarin yellow GG in water (with a concentration range from 28.13 to 900.00 μ g/mL) was performed and measured at a wavelength of 450 nm in quintuplicate. The six concentration levels represented the span of ODs from approximately 0.1 to 3.0. The maximum deviations of the resulted ODs had to be $\pm 10\%$ compared to reference values to fulfill the performance qualification.

3.2.4.2. Quality controls in analytical runs

Three QCs at concentrations of 476.19, 29.76 and 3.72 ng/mL were used in duplicate to check the quantification of the permeated drug by LC-MS/MS. As the aforementioned QCs did not undergo additional sample treatment by the HTS system, an additional QC at a concentration of 190.48 ng/mL ($n = 4$) was used to monitor the entire automated sample preparation procedure by HTS system prior to LC-MS/MS. The maximum deviation of the determined IS-normalized concentrations per QC level from the nominal concentration had to be $\pm 15\%$.

3.2.4.3. Documentation

The studies were conducted according to approved in-house forms/standard operating procedures and in line with the principle of dual control within a regulatory-compliant design.

3.2.5. Selected challenges during method development

The extent of method development included the automation of sampling practice and preparation, reliable drug quantification as well as the establishment of a standardized tissue viability and integrity examination. Specific challenges that were encountered during development are described in the following sections.

3.2.5.1. Automated sampling procedure

The recovery rates using the automated sampling with Hanson Research AutoPlus™ were determined and optimized. The manufacturer's recommendations were compared to in-house optimization by applying different sampling methods, sample solvents and tubing material. For the tubing material, different fluoropolymers (polytetrafluoroethylene (PTFE), perfluoroalkoxy alkane (PFA), fluorinated ethylene propylene (FEP)), polyether ether ketone (PEEK) and stainless steel were used. Also, 10 mM dipotassium hydrogen phosphate at pH 7.4 (phosphate buffer) and PBS buffer were used as sample solvents with cyclobenzaprine hydrochloride concentrations of 40 ng/mL.

3.2.5.2. Linearity and calibration curve

Calibration standards were prepared equivalent to section 3.2.2, using different sample solvents and tube material. Water, acidified water (0.1% FA), phosphate buffer, PBS buffer and methanol were used as sample solvents. The dilution steps were carried out in conventional polypropylene tubes, protein low binding tubes, polystyrene 96-well plates and various glass vials. Linearity were assed in duplicate on Kinetex XB-C18 (1.7 µm; 100.0 x 2 mm) and Luna PFP (2) (100.0 x 2.0 mm; 3 µm) with SecurityGuard PFP (2) (4.0 x 2.0 mm) (Phenomenex Ltd, Aschaffenburg, Germany) using gradient and isocratic elution, respectively.

3.2.6. Analytical validation

The quantification method for cyclobenzaprine from *ex vivo* permeation studies was validated by considering the ICH guideline Q2, the EMA guideline on bioanalytical method validation and FDA guideline "Bioanalytical Method Validation - Guidance for Industry" [European Medicines Agency, 2012; International Council for Harmonisation of Technical Requirements for Pharmaceuticals for Human Use, 2005; U.S. Department of Health and Human Services Food and Drug Administration, 2018].

3.2.6.1. Selectivity and specificity

The blank, the lower limit of quantification (LLOQ) (0.93 ng/mL) and the cyclobenzaprine hydrochloride standard solution (190.48 ng/mL) were applied in order to check the selectivity and specificity of the LC-MS/MS method (n = 6). Additionally, six matrix samples were prepared to check for cross-link by eluted matrix compounds from the biological membrane. Therefore, 1 mL of water was added to the donor chamber and sampling was performed after 60 minutes followed by IS-spiking (defined as a zero-matrix sample). A suitable selectivity and specificity were given if (1) the difference between the retention time of the analyte, the IS peak and all matrix components was ≥ 0.2 min; (2) the analyte peak areas in the blank and the zero-matrix sample were $\leq 20\%$ of the peak areas in the LLOQ and (3) the IS peak areas in the blank was $\leq 5\%$ of the IS peak areas in the zero-matrix, the LLOQ and the standard solution.

3.2.6.2. Linearity and calibration curve

Eleven non-zero calibration standards were examined in duplicate in the range of 0.93 to 952.38 ng/mL. The slope, intercept, coefficient of correlation (r) and CV were determined for eight calibration curves. For at least 75% of the standards per calibration curve, the relative error (RE) of the measured IS-normalized to the nominal concentration had to be within $\pm 15\%$ and within $\pm 20\%$ for the LLOQ).

3.2.6.3. Accuracy, precision and lower limit of quantification

Five replicates of four QCs at 0.93 (LLOQ), 1.86 (low quality control, LQC), 29.76 (middle quality control, MQC) and 714.29 ng/mL (high quality control, HQC) were independently prepared and examined for accuracy and precision. Three different runs on three different days were evaluated against fresh calibration curves. The RE, as deviation of the mean values of the determined IS-normalized concentrations per QC level to the nominal concentration had to be within $\pm 15\%$ and for LLOQ within $\pm 20\%$. The assessment of within-run (repeatability) and between-run precision (day-different intermediate precision) was carried out using one-way analysis of variance (ANOVA). The CV had to be $\leq 15\%$ and for LLOQ $\leq 20\%$.

3.2.6.4. Dilution integrity

Five replicates each with concentrations at 1500 and 3000 ng/mL were prepared using stock solution and diluted by two dilution factors (1:5 and 1:10) into the calibration range of the method to simulate the procedure for study samples with concentrations above the upper limit of quantification (ULOQ). For integrity of each dilution factor, RE had to be within $\pm 15\%$ and the CV $\leq 15\%$. Spiking with IS, dilution and agitation were performed automatically by HTS PAL system.

3.2.6.5. Recovery of automated sampling procedure

The sampling procedure within the permeation studies was performed automatically using a modified stainless steel-tubed Hanson Research AutoPlus™. Three model solutions were prepared in PBS buffer and were then sampled and diluted by 1:10, corresponding to the concentrations of HQC, MQC and LQC at 714.29, 29.71 and 1.87 ng/mL. Spiking with IS, dilution and agitation were performed automatically by the HTS PAL system to mimic the permeation study workflow with both the sampling and sample preparation. For reference, samples were drawn manually from the respective model solutions and prepared equivalently. The deviation of the analyte/IS area ratio per channel to the corresponding reference solution had to be within $\pm 15\%$. Acceptance criteria were set in line with accuracy and precision to ensure adequate recovery.

3.2.7. Membrane integrity

Five diffusion cells were prepared for verification of the integrity examination. Therefore, the resulting OD of intact and impaired membranes were compared (n = 5). The physical damage was performed using a thin needle, while for the chemical damage, the membranes were treated for 30 minutes with 350 μ L of 0.1 M 1,10-phenanthroline in DMSO. As a two-way examination, a visual inspection of the increasing liquid level in the donor chamber and the OD were both used to assess membrane integrity. Between the measurement of the intact and damaged membranes, the donor chamber was washed out and the membranes were re-equilibrated for 15 minutes. For evaluation with blue dextran, the measured OD was normalized to the OD of the blank (PBS buffer) and the threshold value was set at a blank-normalized OD ≤ 2 (defined as twice the OD of the blank).

3.2.8. Membrane viability

A novel method for analyzing tissue viability within *ex vivo* permeation studies was developed using a cell proliferation and cytotoxicity kit (CCK-8). The choice and composition of the incubation media was also evaluated. Organic solvents (DMSO, methanol, tetrahydrofuran) were added to the prescribed incubation medium (PBS buffer) and the resulting OD was evaluated. Simultaneously, a complete incubation cycle in PBS buffer was performed and the membranes were subsequently extracted by different solvents (water, DMSO, methanol). Furthermore, fresh membranes from five different animals were examined on three different days to verify the earliest reference value for the viability assessment and additionally the period of epithelial cell viability at four timepoints. The examinations were carried out as described above (section 3.2.3.3) with an applicable threshold of $\geq 50\%$ relative viability compared to the earliest measurable viability value.

3.2.9. Application

A pharmaceutical industry-related topic regarding galenic development was addressed by investigating oromucosal dosage forms of cyclobenzaprine hydrochloride in order to demonstrate the applicability of the entire permeation process (Figure 8). Therefore, sublingual tablets (SLT) of 2.80 mg cyclobenzaprine hydrochloride with different excipients were studied. SLT A contained crosslinked polyvinylpyrrolidone, while SLT B contained sodium croscarmellose in equal amounts instead. The other tablet ingredients remained unchanged. Permeation studies with seven tablets per dosage form were performed as described, including post-experimental investigation of membrane integrity and viability (section 3.2.3). The concentrations of permeated drug were quantified by LC-MS/MS, cumulated per area and were plotted against the time. In order to compare and evaluate the dosage forms, the cumulative amount of permeated drug per area at time t (Q_t), the steady-state flux (J_{SS}) and the apparent permeability coefficient were calculated using Equations 1 – 3.

Equation 1: Cumulative amount of permeated drug per area at time t (Q_t).

$$Q_t = \frac{C_t \cdot V_A + (\sum_{t=1}^t C_{t-1}) \cdot V_R}{A} \quad [\mu\text{g}/\text{cm}^2]$$

C_t : Drug concentration at time point n
 C_{t-1} : Drug concentration at time point $n-1$
 V_A : Volume of acceptor chamber
 V_R : Removed volume
 A : Available area for permeation

Equation 2: Steady-state flux (J_{SS}).

$$J_{SS} = \frac{\Delta Q_t}{(\Delta t \cdot A)} \quad [\mu\text{g}/\text{cm}^2/\text{h}]$$

ΔQ_t : Difference of Q_t between time points
 Δt : Difference of time
 A : Available area for permeation

Equation 3: Apparent permeability coefficient (P_{app}).

$$P_{app} = \frac{J_{SS}}{CD} \quad [\text{cm} \cdot \text{s}^{-1}]$$

J_{SS} : Steady-state flux
 CD : Initial drug concentration

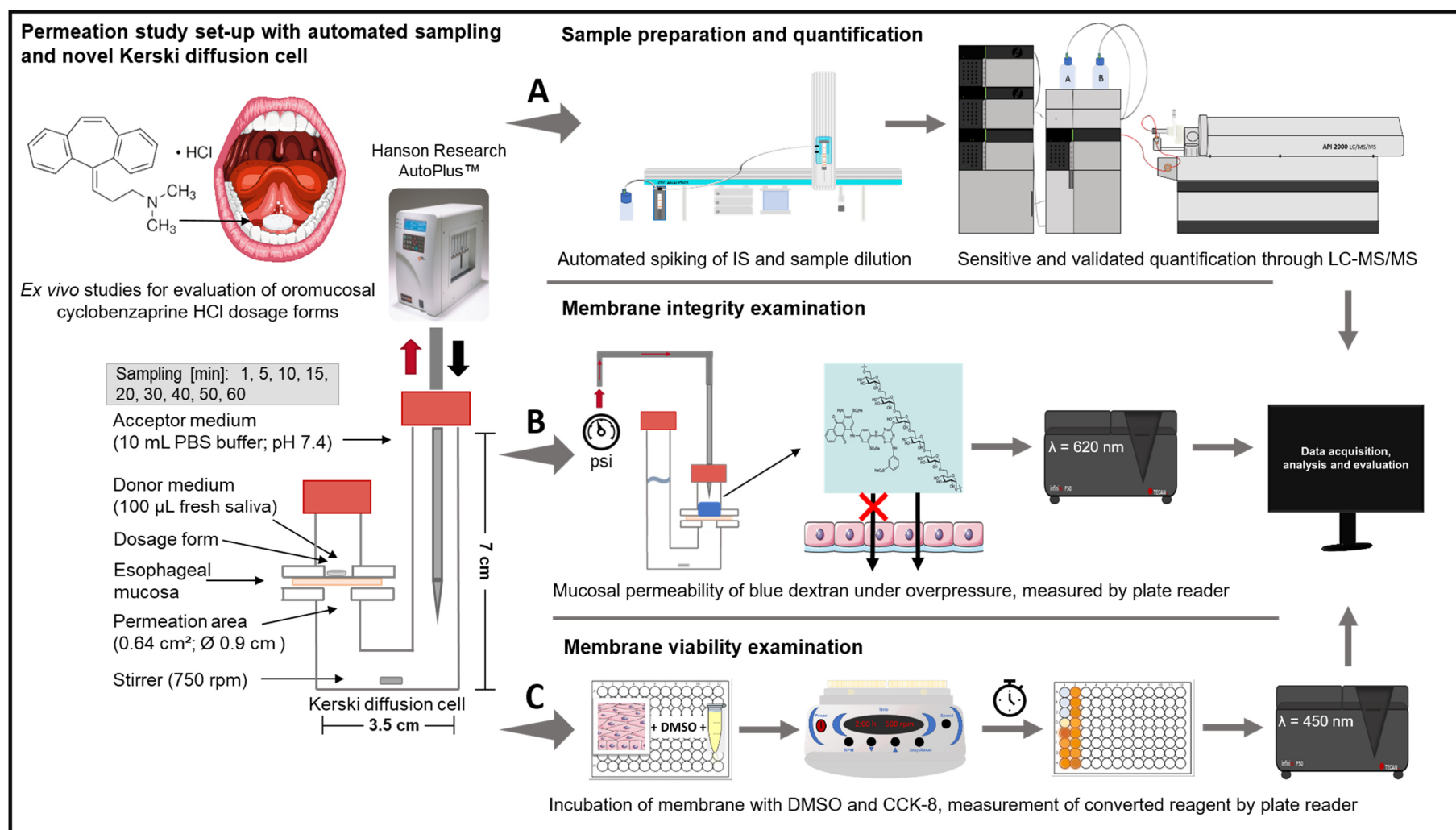


Figure 8: Schematic workflow of the standardized *ex vivo* permeation model. After the permeation experiment, three further processes followed: In A, study samples were automatically spiked with IS, diluted and agitated. After completion of automated sample preparation, the permeated drug amount was quantified by LC-MS/MS. In parallel (B), blue dextran 20 as marker compound was applied in the donor chamber to examine the integrity of the used mucosal membranes. The membranes were subsequently rinsed and punched to an area of 1.13 for viability examination (C).

3.3. Results and Discussion

3.3.1. Selected challenges during method development

3.3.1.1. Automated sampling procedure

Insufficient recovery rates of the API were obtained by automated sampling under standard conditions. The recommended total sampling volume of 4.5 mL, consisting of 3.0 mL rinse, 1.5 mL sample volume with full refill resulted in a recovery of only 52% using PTFE-tubed Hanson Research AutoPlus™. The recovery rate improved material-independently by 22% under the same sampling conditions by exchanging phosphate against physiological PBS buffer. In the final developed method, the tubing system between the plungers of the Hanson Research AutoPlus™ and MultiFill™ were blown out automatically by air before every sampling. Followed by rinsing with 4.0 mL sample solution, actual sampling of 0.5 mL and refilling the acceptor chamber with 4.5 mL. Consequently, remaining medium was reduced, unintentional dilutions were avoided and the tubing were sufficiently rinsed with sample solution, which led consistently to an improvement of +11%. So, by combining the finalized method and PBS as sample solvent, recovery rates of 85% (+33% compared to initial conditions) were achieved with PTFE. Following a comprehensive investigation of diverse alternative tubing material, a further improvement with recovery rates up to 97% was only reached by applying stainless steel tubing. Thus, the PTFE tubing of the autosampler were largely replaced by stainless steel tubing and PBS were set as acceptor buffer under application of the developed sampling method. Figure 9 summarized the recovery rates under two sampling methods, two sample solvents and five different tubing material.

In several published studies, a total sampling volume of ≤ 1 mL were reported, conditioned due to the structure of the used Franz type diffusion cells [Kokate et al., 2008]. Based on our findings, the low volume impedes automation through dilution and intermixture of the permeated drug by remaining solvent in the tubing. Moreover, the volume exchange for maintaining sink conditions in the diffusion cell might not be ensured and leads to a constant accumulation of the drug in the acceptor medium. Due to the resulting higher recovery rates by using steel tubes instead of fluoropolymers (+31% and +12% in phosphate buffer and PBS buffer respectively), a substance-specific adsorption of the API on fluoropolymers surfaces seemed to occur. Studies of Assmus et al. showed a relation between the coplanar structure of hydrophobic organic bases and the adsorption on PTFE surfaces [Assmus, 2015]. For example, an aqueous buffer solution with chlorpromazine, which has a comparable molecular geometry to cyclobenzaprine, led to a drug loss of $12 \pm 7\%$ (mean \pm SD) after contact with a PTFE well plate. Although this would result in an adsorption of the drug on the fluoropolymer surfaces, it would still not sufficiently explain the increased recovery in PBS instead of phosphate buffer. The study of Yasuhara et al. offers an explanatory approach, describing a

reduction of the surface tension of salt solutions in the presence of tricyclic antidepressants by up to 54% by chlorimipramine [Yasuhara et al., 1979]. The resulting concentration-dependent reduction of surface tension may lead largely to interactions between the drug molecules and the polymer surfaces. So, it can be assumed that the high salt content of PBS compared to the 10 mM phosphate buffer, reduced the adsorption effect.

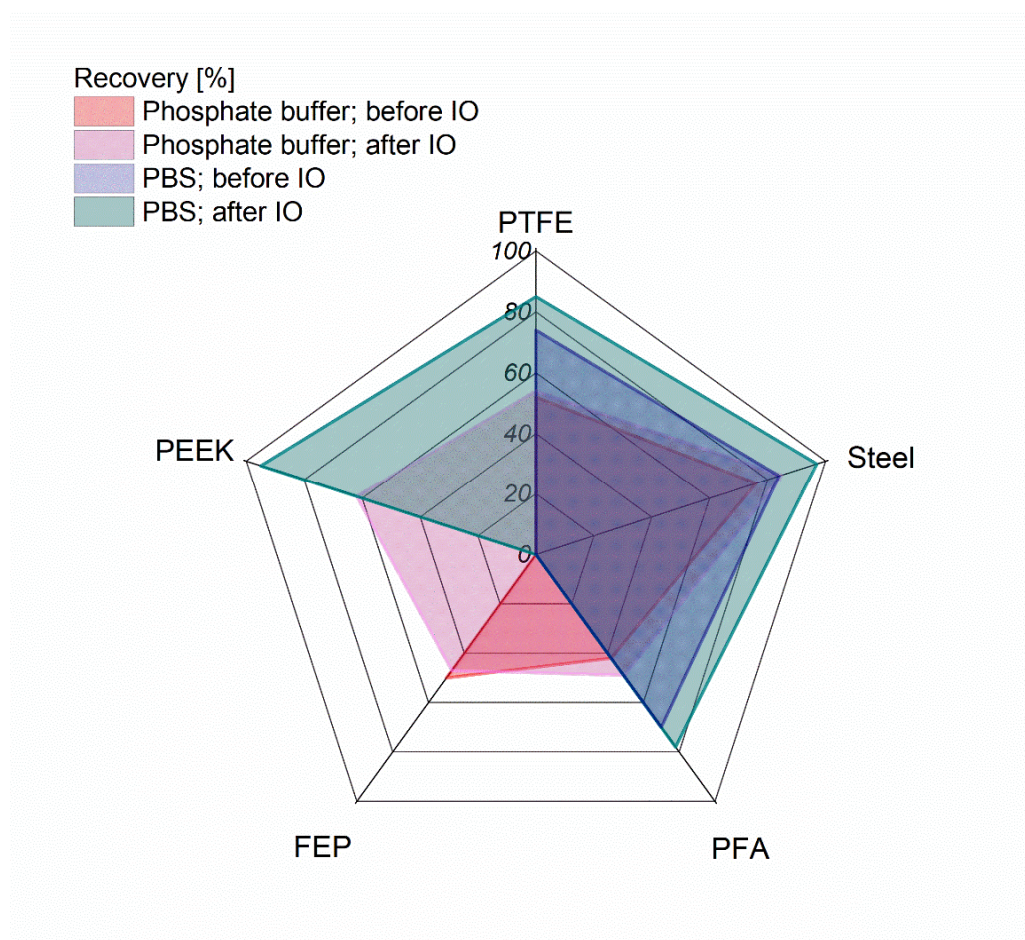


Figure 9: Percentage recovery rates of cyclobenzaprine hydrochloride in relation to the used tubing material, sampling method and buffer medium. The sample size ranged from 1 to 7 experiments. *IO*: instrument optimization, *PTFE*: polytetrafluoroethylene, *PFA*: perfluoroalkoxy alkane, *FEP*: fluorinated ethylene propylene, *PEEK*: polyether ether ketone.

3.3.1.2. Linearity and calibration curve

Linearity tests revealed a lack of proportionality between signal response and concentration levels. The sample solvent and the used tube material were investigated as a potential cause for this. Inadequate linearity was achieved when using aqueous media in conventional polypropylene tubes and polystyrene well plates. Hereby, the discrimination of the lower calibration standards was uniformly insufficient (Figure 10A, C). Although replacement by methanol led to a substantial improvement in linearity ($r = 0.976$), it did not provide an optional sample solvent regarding the development of a physiological permeation model (Figure 10D).

Improved correlations were obtained with direct dilution in glass vials instead of polypropylene tubes. The dilution in low-binding tubes, using PBS buffer as the sample solvent, proved to be optimal in terms of practicability and linearity ($r = 0.996$) and were adapted for permeation studies (Figure 10B).

For cyclobenzaprine, an adsorption behavior on polypropylene and polystyrene was observed, similar to fluoropolymer surfaces (section 3.3.1). The abrupt decrease of signal-concentration proportionality below concentrations of 100 ng/mL indicated a dependence on concentration and successive transfer steps. The interactions with the polyolefin surface could be minimized by organic solvents and by acidification with FA (data not shown) to a more limited extent. The implementation of sensitive analytical methods to determine clinically relevant concentrations within permeation studies relies upon the management of analyte-specific challenges. Less sensitive analytical methods might mask these effects.

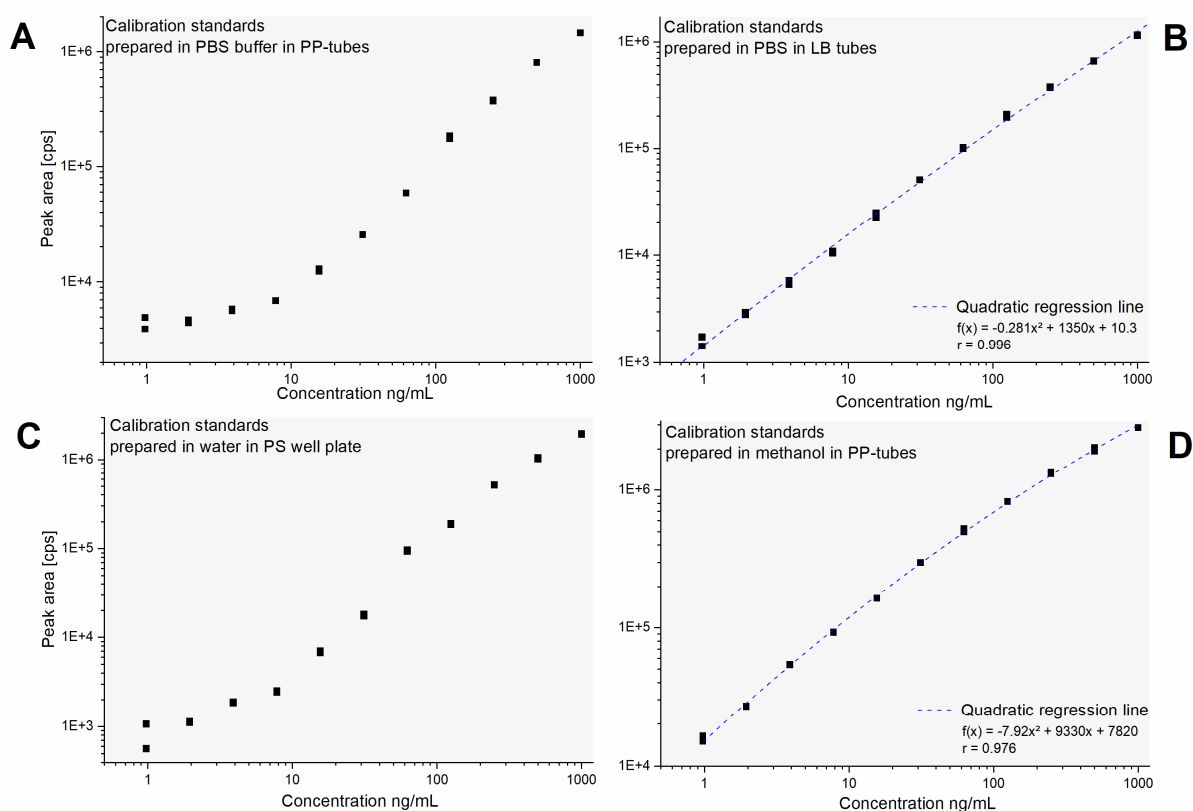


Figure 10: Linearity (logarithmic scaled) by different sample preparation conditions. A: Preparation in PBS buffer using PP tubes. B: Preparation in PBS buffer using LB tubes with quadratic regression line (no weighting). C: Preparation in water using PS tubes. D: Preparation in methanol using PP tubes with quadratic regression line (no weighting). Cps: counts per second, LB: low binding, PBS buffer: phosphate-buffered isotonic saline solution, PP: polypropylene, PS: polystyrene, r = coefficient of correlation.

3.3.1.3. Membrane viability

The CCK-8 assay was not previously applied for epithelial viability. As a result, the assay has been modified in order to overcome the low reproducibility and insufficient sensitivity when performed according to the test protocol. By using different organic solvents, forced cell lysis with repeatable and increased bioreduction of the assay reagent via dehydrogenase activity was achieved. In addition, the enrichment of the converted reagent in the membrane was reduced by the organic medium. Figure 11 shows that the amount of converted reagent and the associated OD increased to the organic proportion in the incubation medium. With the same organic proportions of 7:3 (v/v), DMSO achieved an increase in OD of +103%, compared to methanol. A seven-fold signal increase was obtained by replacing the PBS buffer with pure DMSO as the incubation medium. Additionally, the incubation in PBS buffer with the following extraction of the converted reagent was investigated as a sparing alternative. Although extraction with DMSO after incubation in PBS buffer led to an OD twice as high as the prescribed incubation (PBS buffer), it was still below the signal after incubation in pure DMSO. Due to sensitivity and time restrictions, incubation in DMSO was chosen. This led to higher and more reproducible signals which were necessary for obtaining reliable viability data.

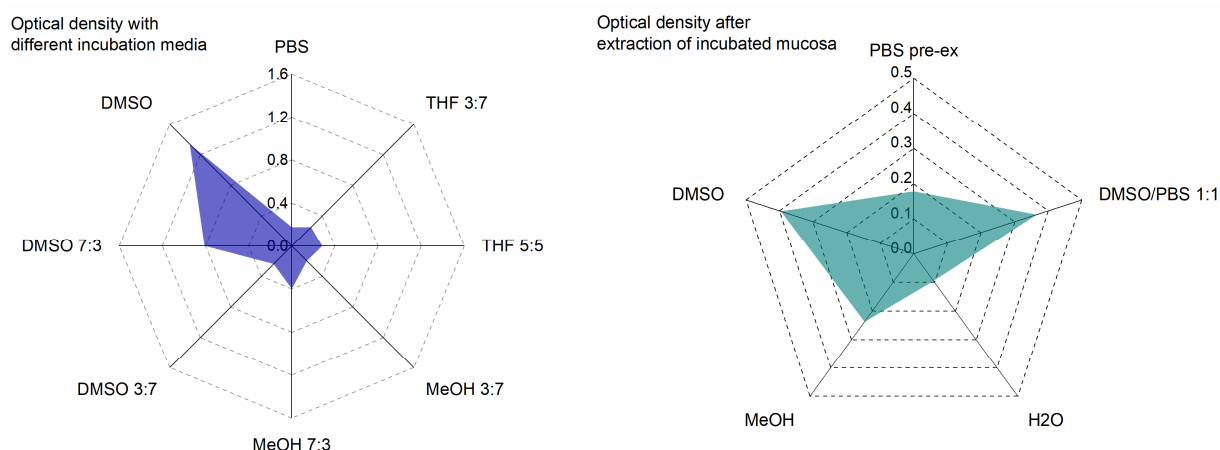


Figure 11: Optical densities measured after incubation of mucosa with different incubation media and after extraction of post-incubated mucosa with different solvents (single values or mean: DMSO 7:3 (n = 8), PBS (n = 5), PBS pre-ex (n = 5)). *DMSO: dimethyl sulfoxide, MeOH: methanol, PBS: phosphate-buffered isotonic saline solution, pre-ex: pre-extraction, THF: tetrahydrofuran.*

3.3.2. Analytical validation

3.3.2.1. Selectivity and sensitivity

Analyte and IS peaks were sufficiently separated from all matrix compounds in the four different solutions (Figure 12). The analyte peak area in the blank and the zero-matrix samples made up 6.4% and 8.5% of the area at the LLOQ, respectively. For IS, a peak area of 0.01% in the blank relative to the zero-matrix, the LLOQ and the standard solution were determined.

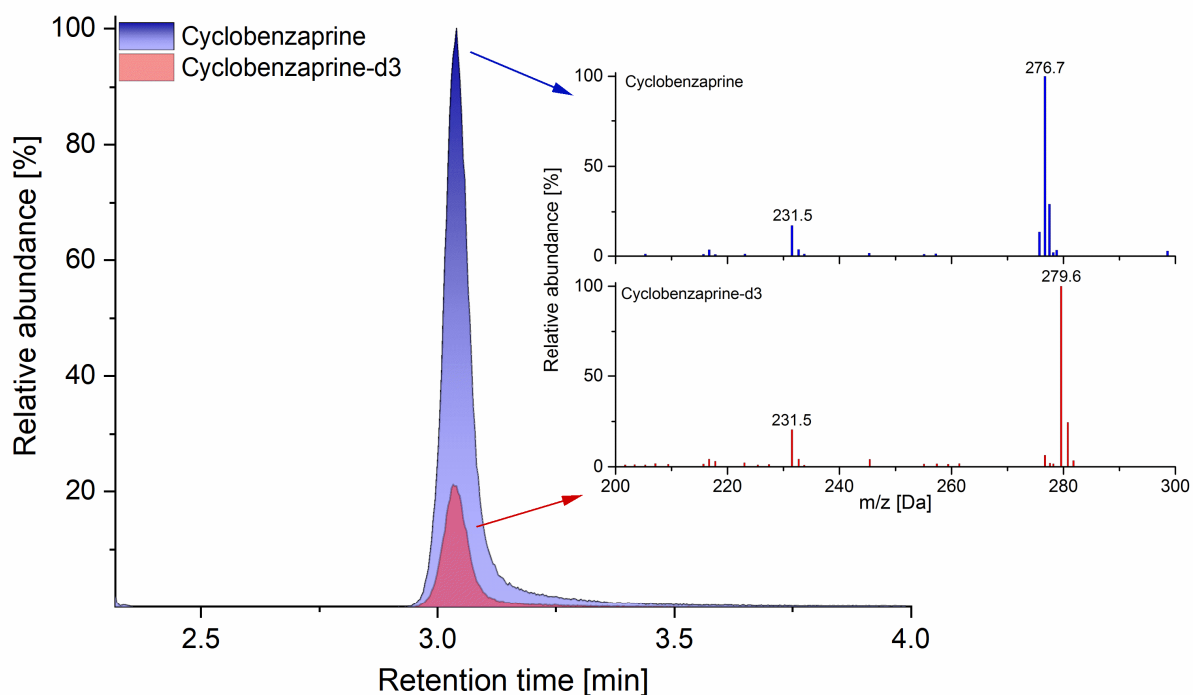


Figure 12: Chromatogram of standard solution with inlets of the Q1 scans in multi-channel analyses for cyclobenzaprine and cyclobenzaprine-d3 (100 cycles with 1000.0 ng/mL respectively).

3.3.2.2. Linearity and calibration curve

Calibration curves, including eleven standards in the range of 0.93 to 952.38 ng/mL, were measured in duplicate. The best fit was achieved with quadratic regression and a weighting of $1/x^2$. The evaluation of eight measured calibration curves resulted in a mean function of $f(x) = (0.0064 \pm 0.0024)x^2 + (1.0324 \pm 0.2159)x + (-0.0010 \pm 0.0051)$ with $r \geq 0.995$. At least 75% of the standards fulfilled the acceptance criteria of $\pm 15\%$ ($\pm 20\%$ for LLOQ) for the deviation of the measured to the nominal concentrations per calibration level.

3.3.2.3. Accuracy, precision and lower limit of quantification

The obtained accuracy values fulfilled the acceptance criteria for within-run and between-run accuracy by evaluating the RE of the IS-normalized mean concentration per QC level to the nominal concentration. The RE for between-run accuracy ranged from -3.6% to 6.3%.

The precision of the method was determined by utilizing an ANOVA test, resulting in 2.1% to 9.2% for within-run (repeatability) as well as between-run precision (day-different intermediate precision). Nearly equal values for within- and between-run precision can be explained by substantially reduced between-day variabilities due to the successful standardization and automation of the previous working steps. Therefore, method precision is primarily restricted to instrument precision. The accuracy and precision results are summarized in Table 4.

For between-run evaluation at the LLOQ (0.93 ng/mL), a RE of 12.4% and a CV of 10.6% were determined. Additionally, signal-to-noise ratios (S/N) of at least 1:46 were obtained in the three analytical runs.

Table 4: Summary of accuracy and precision results of cyclobenzaprine hydrochloride (accuracy as mean relative error and precision as coefficient of variation by analysis of variance).

Quality control [ng/mL]		Accuracy [%]				Precision [%]	
		Run 1	Run 2	Run 3	Between-run	Within-run	Between-run
HQC	714.29	-0.12	1.54	1.40	0.94	2.13	2.13
MQC	29.76	5.05	4.50	9.26	6.27	4.25	4.52
LQC	1.86	-2.28	-0.70	-7.87	-3.62	9.18	9.18
LLOQ	0.93	6.30	15.19	15.76	12.41	10.55	10.55

HQC: high quality control, LLOQ: lower limit of quantification, LQC: low quality control, MQC: middle quality control

3.3.2.4. Dilution integrity

The integrity within the various automated dilution steps of 1:5 and 1:10 was successfully validated. The results for dilution integrity are summarized in Table 5 showing a RE of -12.2% to 12.4%, allowing for accurate quantification of the drug after the automated spiking, dilution and agitation of samples by HTS PAL.

Table 5: Summary of dilution integrity results of cyclobenzaprine hydrochloride (relative error as mean ($n = 5$) \pm standard deviation and within-run precision as coefficient of variation).

Dilution factor	Nominal concentration [ng/mL]	Relative error [%]	Within-run precision [%]
1:5	1500	-10.33	13.81
1:10	3000	-12.23	3.38
1:20	6000	6.98	4.17

3.3.2.5. Recovery of automated sampling procedure

The recovery rates met the specified acceptance criteria with each model solution. A mean RE ($n = 8$) between 2.2% to 5.9% and a CV ranging from 3.6% to 7.1% were determined for three different concentrations (Figure 13). Therefore, the sampling method was considered to be reliable and accurate for use in permeation studies.

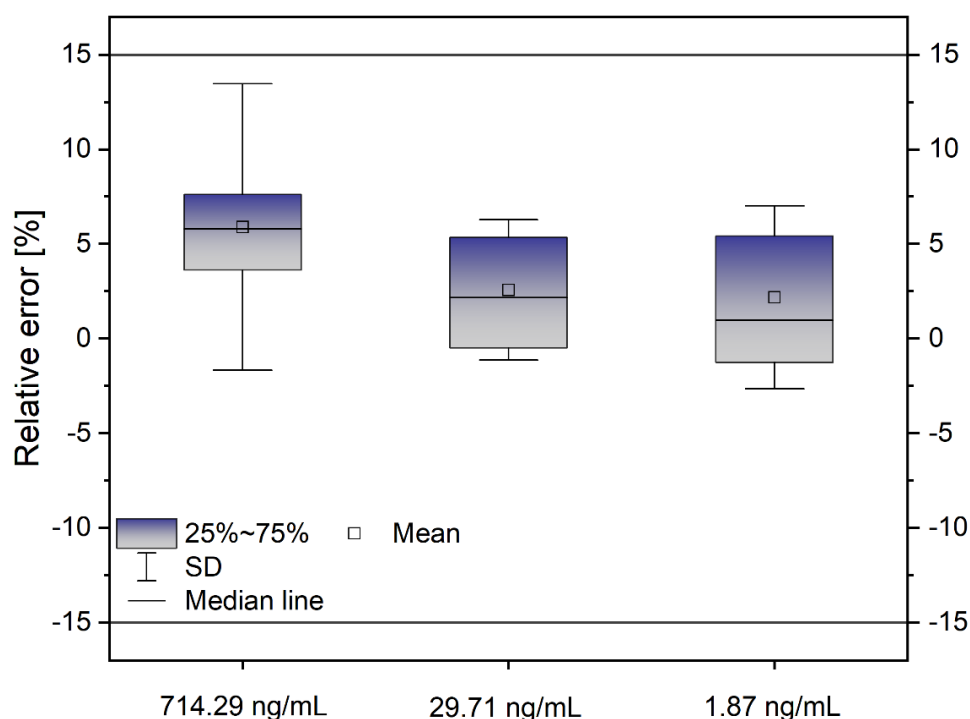


Figure 13: Relative error of cyclobenzaprine hydrochloride recovery using three different concentrations. *SD*: standard deviation.

3.3.3. Membrane integrity

Through the U-shaped construction of the Kerski diffusion cell, the liquid level of the donor chamber increases when damaged and allows for visual inspection of integrity. In contrast, microscopic fissures already present in the mucosa can lead to a loss of molecular integrity and can give a false-positive permeability. The visual detection of such damage is both time-dependent and difficult. Therefore, the integrity of the used membranes was assessed in a two-way examination consisting of a visual inspection and ultraviolet (UV)-spectroscopy, where the membranes were treated chemically or were perforated manually.

In Figure 14, the results are summarized as blank (PBS buffer)-normalized OD. Examination of the untreated membranes revealed a blank-normalized OD of 1, which indicated their integrity. After 30 minutes of treatment with 1,10-phenanthroline, the OD tripled due to increased dextran diffusion levels. This significant (paired t-test; $p < 0.01$) increase can be explained by the chelation of divalent cations in the biomembrane by 1,10-phenanthroline, which is comparable to EDTA treatment [Roblegg et al., 2012]. 1,10-phenanthroline complexes calcium, which is necessary for forming cell-cell connections with proteins such as cadherins. The damage caused by 1,10-phenanthroline enables the diffusion of dextran molecules, which are unable to pass through an intact mucosal epithelium owing to having a molecular weight of 20 kDa [Junginger et al., 1999]. Despite dextran diffusion after treatment with 1,10-phenanthroline, no increase in liquid levels could be registered. However, by artificially perforating the membranes with a thin needle, an increase in both the liquid level and OD was achieved when using blue dextran 20.

Visually imperceptible microscopic damage to the membrane was detected by blue dextran 20, while larger perforations could be ascertained visually. Thus, sensitive and time-effective evaluations (five minutes instead of four hours) of mucosal membrane integrity were verified and can be further enhanced by overpressure in the donor chamber. The combination of a visual inspection of liquid levels and UV-detection of blue dextran as a useful two-way integrity examination was implemented in the permeation studies as a control system for routine purposes.

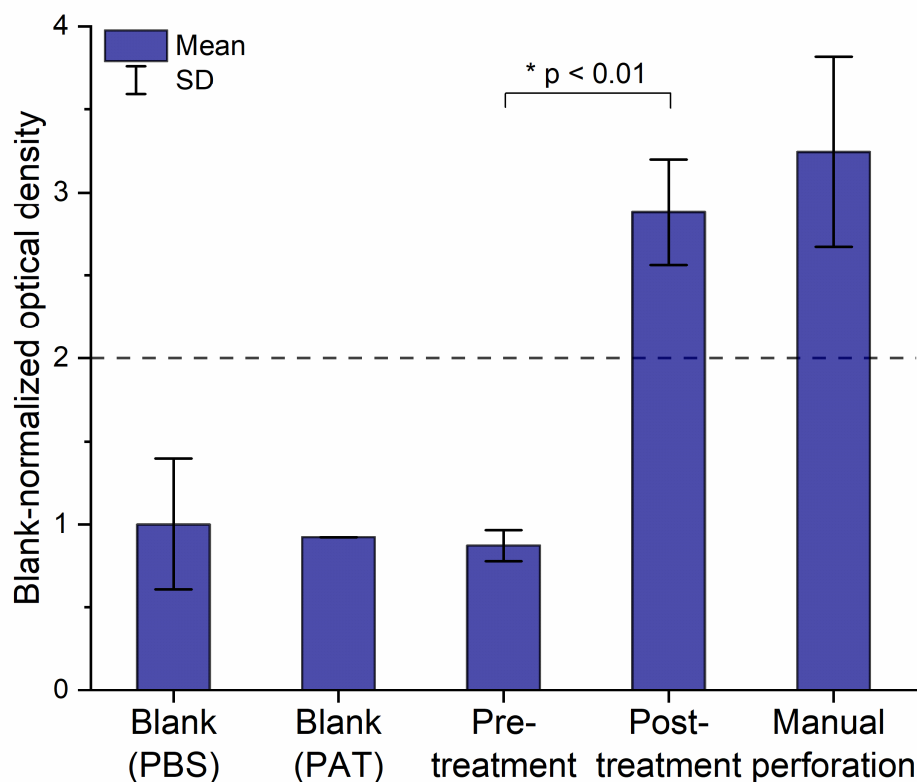


Figure 14: Blank-normalized optical densities for integrity verification using blue dextran 20. Presented as single value (blank (PAT)) or mean \pm SD: blank (PBS), manual perforation ($n = 3$); pre-treatment, post-treatment ($n = 5$). *Straight line: acceptance criterion of membrane integrity, PBS: phosphate-buffered isotonic saline solution, PAT: 1,10-phenanthroline, SD: standard deviation, *: $p < 0.01$ (paired t-test).*

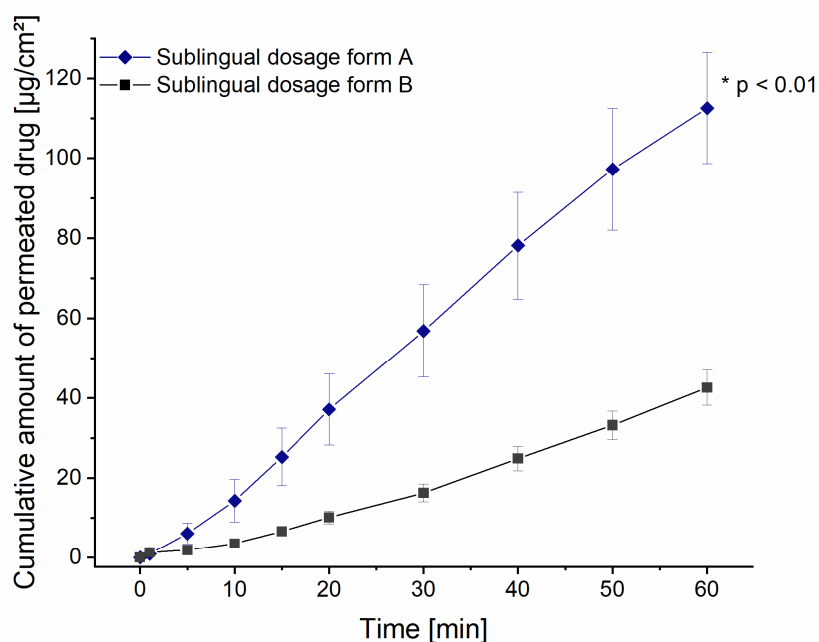
3.3.4. Membrane viability

An inter-individual and inter-day determination of the t_0 value was essential verification as 100% benchmark. This resulted in a mean OD ($n = 40$) of 1.8, normalized to an area of 1.13 cm² and with a CV of 15.4%. The reproducible acquisition of the t_0 value on three days with five different animals was applied in order to assess the post-experimental relative viability of used membranes. Viability was ensured for a period of at least nine hours (post mortem) with $64.7 \pm 2.5\%$ (mean \pm SD, $n = 4$), which corresponds with previous studies [Imbert and Cullander, 1999] and ensures the viability of mucosal membranes during the required duration of the permeation studies. The optimized CCK-8 test was used for the first time for viability studies of mucosal tissue and provides a shorter and simpler application compared to current assays, thus facilitating routine use. The viability studies were suitable as a post-experimental control system within the permeation studies.

3.3.5. Application

Two different sublingual formulations were investigated in which exclusively the disintegrant was replaced in the same amount, representing a typical scenario of excipient selection within formulation development. The permeation studies were performed as described, including automated sampling and sample preparation, LC-MS/MS quantitation, quality assurance, integrity and viability examination. Figure 15 shows the resulting permeation profiles of the two finished dosage forms presented as Q_t . A substantially higher amount of the drug permeated during the first five minutes when using dosage form A, and increased by up to a factor of 2.6 after 60 minutes. By comparing the permeability coefficients, the superiority of dosage form A, with a permeability coefficient of $1.25 \cdot 10^{-6}$ cm/s, was confirmed (unpaired t-test; $p < 0.01$). Moreover, a steeper slope with a shorter lag time can be observed, suggesting a faster release and a faster corresponding permeation of the API by using crosslinked polyvinylpyrrolidone compared to the same amount of sodium croscarmellose. To the best of our knowledge, the oromucosal *ex vivo* permeability of cyclobenzaprine has been shown the first time in clinically relevant time periods that considered the short residence time of SLTs.

Through standardization and comprehensive control of the studies, relative standard errors for the permeability coefficient below 10.8% (< 24.1% CV) were achieved regardless of biological variability and the sequence of multiple processes. Since known permeation studies are conducted over a non-clinical period of hours, a comparison of the obtained variation was hardly possible. Nevertheless, due to heterogeneous experimental settings, noticeably high differences in permeability coefficients of a factor of 20 and CVs of up to 82% were previously reported [Kulkarni et al., 2010]. Besides standardization and automation, sophisticated and practicable quality monitoring system contributed towards higher data quality by reducing variations despite close-meshed clinically adapted measurements. Core elements of this in-house monitoring system were formed by novel integrity and viability examinations, overcoming former limitations (duration, sensitivity, routine application). The reevaluation was carried out on integrity and viability assessment and excluded non-compliant diffusion cells (final valid set of $n = 5$ per study). The studies were valid in terms of system suitability, with a repeatability of 0.6% and 1.4% and QCs within the analytical runs had a RE of -0.4% to 12% and 1.2% to 13% respectively. The entire permeation process was improved to be handled in one working day and emphasizes implementation into academic and regulatory-industrial environments.



Dosage form	Cumulative amount of drug after 60 min		Drug flux		Permeability coefficient	
	Mean	RSE	Mean	RSE	Mean	RSE
	[µg/cm²]	[%]	[µg/cm²/h]	[%]	[cm/s]	[%]
A	112.58	12.39	129.40	10.00	1.21×10^{-6}	10.76
B	42.62	10.35	56.47	10.72	0.53×10^{-6}	8.50

Figure 15: Cumulative amounts of permeated cyclobenzaprine hydrochloride from different sublingual dosage forms (2.80 mg drug load) per cm^2 (mean \pm SEM; $n = 5$). The calculated permeation results were summarized in table form. *RSE*: relative standard error ($n = 5$), *SEM*: standard error of the mean, *: $p < 0.01$ (unpaired *t*-test).

The here presented *ex vivo* permeation studies are a promising tool for bridging *in vitro* and following *in vivo* studies by permitting a physiologically and clinically adapted assessment of drug permeability. Due to the limitations of previous *ex vivo* permeation studies, especially in the field of oromucosal application, *in vitro* dissolution studies are conventionally performed to characterize and evaluate formulations. So far, no regulatory requirements for dissolution tests of oromucosal drugs are known. Therefore, adaptation of the requirements given for orally administered formulations were applied but seems artificial and non-representative. For example, the large dissolution volumes (800 to 1000 mL) combined with rapidly soluble intraoral dosage forms mean that distinguishing impacts between diverse formulations is difficult. Furthermore, no insights into the permeation capacity with regard to the drug transport through the specific oromucosal barrier are provided. On the other hand, *in vivo* studies are expensive, impractical and associated with excessive animal testing. By applying *ex vivo* studies in a validated and standardized scope as a decisive tool, formulation development and following *in vivo* studies can be carried out targeted as well as time, cost and resource efficient.

Potential of correlation between *ex vivo* and *in vivo* permeation studies was already reported by Holm et al. on the buccal administration of metoprolol [Holm et al., 2013]. Furthermore, the presented *ex vivo* studies offer high potential for future IVIVC due to the improved consideration of physiological-clinical conditions.

Central to the permeation model was the novel Kerski diffusion cell. Due to the total volume (12 mL), the pressure conditions and the possibility of monitoring the environmental conditions, the design of the vertical diffusion cell allows for closely automated sampling by imitating the sink conditions through a volume replacement rate of 45% at each sampling. The horizontal part of the acceptor chamber allows a permanent moistening of the membranes and prevents the accumulation of air under the membrane. Saliva influences permeability through pH, electrolytes, mucus as well as enzymes (e.g. phosphatase, carbonic anhydrase) and therefore fresh human saliva was applied as donor medium to imitate physiologically conditions in contrast to the typical use of artificial saliva (buffer solutions). The volume of 100 µL was based on saliva films with a volume of between 70 and 100 µL typically found in the human oral cavity [Collins and Dawes, 1987]. Previous studies have shown that the porcine buccal but also esophageal mucosa is similar to the human mucosa [Lesch et al., 1989]. In contrast to buccal mucosa, the esophageal mucosa is characterized by a uniform membrane thickness, a relatively simple preparation, a high yield of insertable and intact tissue as well as a lower biological variability and correspondingly precise permeability [Diaz Del Consuelo et al., 2005c]. One esophagus is generally enough for a whole permeation experiment (n = 8) thereby reducing the number of animals required by applying buccal tissue or *in vivo* studies. Additionally, it offers the possibility of obtaining esophagi via local slaughterhouses, which would otherwise be wasted (reduction and refinement).

In order to cover the therapeutic short-term application and dose of intraoral dosage forms, the total study time was set at 60 minutes, with the first measurement taken after one minute. This necessitated the sensitive determination by LC-MS/MS meaning that *ex vivo* studies were achieved at clinically relevant time intervals and allowed an accurate evaluation of oromucosal permeability for drugs and dosage forms.

For the integration in quality-controlled environments, it is essential to address regulatory aspects in the best possible way in addition to the optimized experimental setup and conduct. Since no guideline for permeation tests of oromucosal medicinal products is known, the EMA guideline on quality for transdermal patches (EMA/CHMP/QWP/608924/2014) appears most suitable [European Medicines Agency, 2014]. This requires e.g. the validation of analytical methods, sink conditions, integrity tests and quality assurance system in order to obtain meaningful permeation results. Moreover, it encourages the application of *in vitro/ex vivo* studies to characterize and assess drug formulations within their development. Hence, aspects

of the guideline have been successfully considered and addressed in order to advance the regulatory compliant implementation of tissue-based *ex vivo* permeation studies in pharmaceutical research and development.

3.4. Conclusion

It was achievable to develop, validate and standardize an entire distinctive process of tissue-based *ex vivo* studies for oromucosal permeability. Automated sampling and sample preparation coupled to LC-MS/MS quantification and optimization in the experimental set-up enabled a clinically adapted study design, with the first measurements being taken after just one minute. Embedding the coupled processes into a quality assurance system, including a verified test for integrity and viability, facilitated a precise routine application. The entire model is an innovative tool for investigating academic and industry-related aspects of oromucosal permeability in a standardized and controlled manner, thereby supporting drug development and exploiting the advantages of the oromucosal route of administration, while avoiding high costs and animal testing.

4. Exploring the transmucosal permeability of cyclobenzaprine: A comparative preformulation by standardized and controlled *ex vivo* and *in vitro* permeation studies

4.1. Introduction

Advantages such as the ability to achieve higher bioavailability, reduced dosages, and improved patient adherence render the oral mucosa a beneficial alternative to the oral and intravascular routes of drug administration. However, transmucosal diffusion primarily depends on the physicochemical properties of the APIs and the given environmental conditions at the site of administration. Since the environment of a drug can be substantially affected by the drug formulation, which subsequently affects drug permeability, knowledge of influencing factors and additives are essential to support and customize galenical development. The latter aspect can be of particular importance when developing dosage forms for alternative sites of application, such as the oral cavity. Therefore, permeation studies are considered helpful for drug preformulation and oromucosal drug delivery [Kottke et al., 2020; Wang et al., 2020].

However, current permeation studies often have limited predictivity stemming from insufficient adaptation to clinical conditions, lack of monitoring, and inhomogeneous designs [Kolli and Pather, 2015; Patel et al., 2012]. These mandatory aspects for decisive insights into drug permeability were considered in the standardization of an innovative *ex vivo* permeation process incorporating the Kerski diffusion cell [Kerski et al., 2020] coupled to fully automated sampling and sample preparation with validated drug quantification via LC-MS/MS [Majid et al., 2021a]. The Kerski diffusion cell is a vertically oriented U-shaped diffusion cell consisting of an acceptor, isofill and donor chamber (Appendix 1). Unlike the common Franz cell, this model allows for automation of the sampling process, standardized throughput, and high-volume exchange on the acceptor side to maintain sink conditions. Despite the exchange of 45 % of the acceptor volume per sampling, the isofill chamber prevents air bubbles from collecting under the membrane, which remains continuously wetted with medium, thus reducing the risk of a negative influence on permeation. An occurring hydrodynamic gradient is immediately compensated by refilling the acceptor chamber to initial condition after sampling. Additionally, this allowed the adaption of the experimental study design on clinical conditions (i.e., first sampling point after ≤ 5 minutes, human saliva collection, therapeutic doses, sink conditions). Furthermore, routine monitoring via innovative tissue integrity and viability tests were integrated into a comprehensive analytical control system. Nevertheless, due to the need for time-effective preparation, the reduction of biological variability, and high reliability, *in vitro* studies using artificial membranes based on phospholipids offer a valid

This work was published in an international peer-reviewed journal [Majid et al., 2021c]:

Majid, H., Puzik, A., Maier, T., Eberhard, D., Bartel, A., Mueller, H.-C., Burckhardt, B.B., 2021c. Exploring the transmucosal permeability of cyclobenzaprine: A comparative preformulation by standardized and controlled *ex vivo* and *in vitro* permeation studies. *International Journal of Pharmaceutics* 601, 120574. <https://doi.org/10.1016/j.ijpharm.2021.120574>.

The author of this thesis was responsible for conceptualization, methodology, investigation, formal analysis, writing-original draft, and visualization.

alternative to mucosal tissue-based *ex vivo* studies [Brandl and Bauer-Brandl, 2019]. However, artificial membranes are generally adapted to simulate the passive transcellular diffusion of the intestine; thus, their broad applicability for oromucosal permeability is presently restricted to certain drugs. Therefore, the beneficial and suitable applications in drug development must be explored for both models, starting at the preformulation stage.

Cyclobenzaprine hydrochloride is a centrally-acting skeletal muscle relaxant used as an oral formulation for the treatment of pain-associated muscle spasms [Chou et al., 2004]. Recent studies concluded that cyclobenzaprine offers therapeutic potential for the treatment of PTSD, which is characterized by hyperarousal symptoms such as sleep disturbances [Bestha et al., 2018; Sartori and Singewald, 2019]. The use of a sublingual cyclobenzaprine hydrochloride tablet appears beneficial due to its indication-appropriate rapid onset and discussed safety improvements such as fewer daytime side effects [Davidson, 2015]. This has been correlated to decreased formation of the active metabolite norcyclobenzaprine by avoiding first-pass metabolism [Daugherty et al., 2016]. However, to the best of our knowledge, no work has yet been published that provides a detailed investigation of the transmucosal permeability of cyclobenzaprine via either *ex vivo* or *in vitro* studies.

Hence, this work aimed to comprehensively characterize the permeability of cyclobenzaprine in a preformulation study to obtain valuable insights for targeted, lean, and time-efficient formulation development. This work included an investigation of the transmucosal diffusion pathway and affecting factors such as the type and quantity of excipients as well as environmental/experimental conditions (i.e., pH, membrane thickness, storage condition, and dose). Moreover, a direct comparison between tissue-based *ex vivo* studies versus artificial *in vitro* studies was conducted to assess their respective predictivity for preformulation.

4.2. Material and Methods

4.2.1. Chemicals and material

Cyclobenzaprine hydrochloride ($\geq 98\%$) (Hetero drugs Ltd, Hyderabad, India), melatonin (100%) and metronidazole (101%) (Caesar & Loretz GmbH, Hilden, Germany) were used as APIs. Caffeine anhydride (99.9%) was supplied from Siegfried AG (Zofingen, Switzerland). Cyclobenzaprine-d3 (98%, IS), FA ($\geq 98\%$, p.a.), alizarin yellow (dye content 50%), FITC-dextran (average molecular weight 20000 Da), blue dextran 20 (average molecular weight 20000 Da) and CCK-8 were obtained from Sigma-Aldrich (Taufkirchen, Germany). Potassium chloride ($\geq 99.5\%$, p.a.) and ortho phosphoric acid (85%, p.a.) were purchased from AppliChem GmbH (Darmstadt, Germany). Sodium chloride ($\geq 99.5\%$, p.a.) and potassium dihydrogen phosphate ($\geq 99\%$, p.a.) were obtained from Roth GmbH (Karlsruhe, Germany). Disodium hydrogen phosphate ($\geq 99\%$, p.a.) was purchased from Riedel-de-Haen (Seelze, Germany) and dipotassium hydrogen phosphate (99%, Ph. Eur.) as well as sodium hydroxide ($\geq 99\%$, p.a.) from VWR Chemicals (Langenfeld, Germany).

Water, ACN, propan-2-ol and methanol (LC-grade), DMSO (p.a.) as well as 4% paraformaldehyde PBS solution were received from Fisher Scientific (Schwerte, Germany). Optimal cutting temperature (OCT) medium was supplied by Tissue-Tek (Sakura, Japan). FITC-conjugated Dolichos Biflorus Agglutinin (DBA) was purchased from Vector Laboratories (Burlingame, USA) and 4',6-diamidino-2-phenylindole (DAPI) delivered by Thermo Fisher Scientific (Waltham, USA). 1.5 mL protein low binding micro tubes were obtained from Sarstedt AG & Co. KG (Nümbrecht, Germany). Human saliva was provided by healthy volunteers and collected in salivettes (Sarstedt AG & Co. KG, Nümbrecht, Germany) without pooling. The collection was obtained under fasting conditions in the morning of the respective run. Therefore, the swab was chewed for 60 seconds and centrifugated for two minutes (20 °C, 616 x g).

Porcine esophagi were provided by the slaughterhouses Frank Prill (Bergheim, Germany) and Naturverbund Thönes (Wachtendonk, Germany), with a maximum of three hours from slaughter, bleeding, steaming, dissection, transport in PBS buffer to usage. Permeapad® Barrier were received from InnoMe GmbH, Espelkamp, Germany.

4.2.2. Standardized ex vivo permeation study set-up

The experimental set-up was based on a published standardized permeation process [Majid et al., 2021a]. This setting included the coupling of the novel Kerski diffusion cell [Kerski et al., 2020] to automated sampling using a Hanson Research AutoPlus™ (Teledyne Hanson, Los Angeles, USA) and sample preparation using HTS PAL autosampler (CTC Analytics AG, Zwingen, Germany) following quantification via HPLC-ESI-MS/MS (Shimadzu Prominence,

Shimadzu Europe, Duisburg, Germany; AB Sciex API 2000, Darmstadt, Germany). Fresh esophageal porcine mucosa was used as a biological barrier after being dermatomed to a thickness of 500 μm (Integra® Dermal, Ratingen, Germany). Based on previous studies by Diaz et al. [Diaz Del Consuelo et al., 2005b; Diaz Del Consuelo et al., 2005c; Diaz Del Consuelo et al., 2005a] who presented the comparability of esophageal and oral mucosa, esophageal tissue was used as a surrogate for oral mucosa in these studies due to its experimental advantages (simple preparation, uniform, thickness, less destruction during slaughter and high yield of usable membranes).

To equilibrate the inserted membranes, the acceptor chamber of the Kerski cell was filled with 10 mL PBS buffer (pH 7.4), and 50 μL of freshly collected human saliva was added to the donor chamber to mimic physiological conditions of the oral cavity. Thereafter, 2 mL of the drug solution to be tested was pipetted onto the saliva-moistened membrane. The studies were performed at constant conditions of 37 °C, 20% relative humidity (BINDER KBF 115 Constant Climate Chamber, BINDER GmbH, Tuttlingen, Germany), and continuous stirring at 750 rpm (2mag Mixcontrol20, Muenchen, Germany). Within the 60-minute permeation period, fully automated sampling was set at 5, 10, 15, 20, 25, 30, 40, 50, and 60 minutes. This included discarding 4 mL rinsing volume, followed by 0.5 mL of sampling and full replenishment. The samples were spiked with cyclobenzaprine-d3, diluted with water into the validated calibration range, and agitated as part of the automated sample preparation using HTS PAL controlled by Chronos 5.0 software (Axel Semrau GmbH, Sprockhoevel, Germany).

4.2.3. Quality control and monitoring system

The bioanalytical method used for quantification was successfully validated according to the relevant EMA and FDA guidelines [European Medicines Agency, 2012; U.S. Department of Health and Human Services Food and Drug Administration, 2018]. Furthermore, the experiments were performed according to the principles of Good Clinical Laboratory Practice and included a customized five-step analytical control system. This encompassed classical bioanalytical elements (i.e., LC-MS/MS monitoring via system suitability tests and analytical run evaluations), but also the assessment of the automated sample preparation by HTS PAL as well as mucosal tissue integrity and viability verification of the applied membranes within the permeation experiment.

Membrane intactness was determined using an in-house integrity test based on photo-actively labeled dextrans (20 kDa) and served as a complement to visual detection of the donor chamber liquid levels. Membrane integrity was defined as a blank-normalized OD of ≤ 2 . The mucosal viability assay was based on a modified CCK-8 assay in which membranes were punched after integrity testing and incubated with DMSO and CCK reagent. Viability was

confirmed at 450 nm with a threshold of $\geq 50\%$ compared to the earliest activity measurement [Majid et al., 2021a].

The system suitability test included the assessment of a six-fold standard injection regarding signal intensity, retention time ($\leq 10\%$), and reliability ($CV \leq 15\%$) concerning the LC-MS/MS and a five-fold determination of alizarin dilution series for the verification of absorbance reader suitability (deviation of OD from reference values: $\leq 10\%$). For a valid calibration within the range of 0.93 to 953.38 ng/mL, the maximum deviation of the IS-normalized concentrations per calibration standard had to be $\pm 15\%$ ($\pm 20\%$ at the LLOQ) from the nominal concentration with r above 0.99. Seven QCs per run were used to monitor the quantification and automated sample preparation processes. The acceptance criterion was set at a maximum IS-normalized RE of $\pm 15\%$. Based on the aforementioned point, the reevaluation of permeability data was performed while excluding non-compliant measurements and diffusion cells, when applicable.

4.2.4. Investigation and characterization of the oromucosal permeability of cyclobenzaprine

The permeation studies aimed to comprehensively investigate the oromucosal permeability of cyclobenzaprine utilizing esophageal mucosa and biomimetic membranes. This involved determining and evaluating influential factors and conditions (e.g., altering the pH value of the environment) to apply these findings predictively to formulation development. On the other hand, these studies also intended to provide a supportive understanding of the diffusion mechanisms of the API under the new administration route.

4.2.4.1. Effects of pH, phosphate salt type and quantity on permeability

For the physiological pH value of saliva, a range between 5.3 and 7.8 was specified [Humphrey and Williamson, 2001]. These shifts in the oral cavity impact the ionization status of acidic and basic drugs more greatly than for orally administered and systemically absorbed drugs. Therefore, the degree of ionization and subsequent drug permeability must be known and controlled during formulation development.

Ex vivo assessment

For this purpose, physiologically available and commonly used phosphate salts were assessed within an expanded pH range of 5 to 9. Thus, cyclobenzaprine solutions were prepared (at least $n = 5$ per solution) with varying amounts of dipotassium hydrogen phosphate (dibasic) as a basifying excipient or potassium dihydrogen phosphate (monobasic) as an acidifying excipient (Table 6). The resulting pH of each solution was measured before pipetting into the donor chambers of the diffusion cells. The impacts of pH and the amount of utilized salts on cyclobenzaprine permeability were determined and evaluated based on their physicochemical

properties. Therefore, the fraction of unionized drug at presented pH was calculated by Equation 4.

Equation 4: Fraction of unionized drug ($F_{\text{unionized}}$).

$$F_{\text{unionized}} = \frac{100\%}{1 + \text{antilog}(pK_a - pH)} [\%]$$

The J_{SS} represented the mean value of the respective visually defined steady-state plateau, which was formed from the last three measurement time points (40 to 60 min) and corresponded to the slope of this linear section of the cumulative plot. To assess the permeability of cyclobenzaprine, the J_{SS} and the P_{app} were used (Equation 2 – 3) where ΔQ_t is the difference in permeated drug amount between the time points (Δt), A is the permeation area, and CD is the initial drug concentration in the donor chamber. The determined impact on permeability (Equation 5) compared to that with no excipients (drug in pure water) was defined as the permeability ratio (PR).

Equation 5: Permeability ratio (PR).

$$PR = \frac{P_{\text{app}} (\text{examined})}{P_{\text{app}} (\text{in water})} \quad P_{\text{app}}: \text{ Apparent permeability coefficient}$$

Additionally, the used membranes were extracted after the permeation study to assess the pH-dependent tissue retention of cyclobenzaprine and subsequently allow for the determination of its distribution in the donor side, acceptor side, and the membrane itself. Hereby, the membranes were extracted in methanol/water/FA (80:19:1; v/v/v) for three hours at 37 °C and 1050 rpm. Thereafter, the extraction media were centrifugated (10 minutes, 4 °C, 616 x g) and the supernatant was diluted and quantified via LC-MS/MS.

In vitro assessment

Moreover, the suitability of artificial biomimetic membranes for assessing the impact of pH and phosphate salts in the standardized permeation set-up was evaluated against dermatomed porcine esophageal tissue. For this *ex vivo/in vitro* correlation, Permeapad® Barriers were applied at least in triplicate under similar experimental conditions as described for the porcine *ex vivo* approach above.

Table 6: Composition of the investigated drug solutions within preformulation.

Solution	Phosphate salt	Salt conc. [mg/2 mL]	Cyclobenzaprine HCl [mg/2 mL]
A	None	0	2.8
B	Dipotassium hydrogen phosphate	0.5	2.8
C	Dipotassium hydrogen phosphate	1.1	2.8
D	Dipotassium hydrogen phosphate	2.1	2.8
E	Potassium dihydrogen phosphate	1.1	2.8

4.2.4.2. Effects of membrane thickness and storage conditions on permeability

From an anatomical perspective, the oral mucosa can generally be divided into three layers i.e., the epithelium, basal membrane, and connective tissue, whereby each layer has a specific structure and barrier function [Johnston, 2015]. Therefore, the extent of the effect of the layers on permeability provides information regarding the diffusion type of a substance. To analyze the effect of membrane thickness and composition, permeation studies were performed (at least $n = 3$) using fresh mucosa with dermatomed thicknesses of 350, 500, and 750 μm .

To characterize the mucosa layer histologically, dermatomed specimens were fixed in 4% paraformaldehyde solution in PBS, embedded in OCT medium and frozen using dry ice. Standard hematoxylin-eosin (HE) staining was subsequently performed on 12 μm thick cryosections. Moreover, cryosections were stained with FITC-DBA to visualize the squamous epithelial cell layer and finally nuclei were counterstained using DAPI. Stained sections were analyzed using an Eclipse Ti-S microscope (Nikon, Tokyo, Japan). Images were taken using a DS-2Mv camera operated by NIS-Elements software (Nikon, Tokyo, Japan). Additionally, the impact of membrane storage conditions (tissue freezing) on their permeability was compared between 500 μm -thick *ex vivo* membranes stored at either $-80\text{ }^{\circ}\text{C}$ (one freeze/thaw cycle) or freshly prepared (at least $n = 3$). To avoid tissue destruction, membranes were frozen and thawed in a controlled manner (at approximately $1\text{ }^{\circ}\text{C}/\text{min}$ in PBS buffer) using CellCamper® (neoLab, GmbH, Heidelberg, Germany).

4.2.4.3. Scaling the dose to the sublingual surface area

As part of adapting permeation studies to physiological conditions, the dose of the applied solution was scaled to the average available sublingual surface area of 26.5 cm^2 that would be effectively covered by the cyclobenzaprine solution [Collins and Dawes, 1987]. In the actual experimental setup of the present studies, a therapeutic dose of 2.8 mg was applied to a limited

area of 0.64 cm² (the permeation area of the Kerski diffusion cell) instead of 26.5 cm². Thus, the drug and salt amount in solution C was reduced by a factor of 41.18 (cyclobenzaprine hydrochloride from 2.8 mg/0.64 cm² to 0.068 mg/0.64 cm²; drug per permeation area) to reflect the ratio of the dose to sublingual area in the experimental permeation setting (n = 4). Considering the physiological diffusion area, the aim of this study was to investigate whether non-steady-state conditions occur by adapting the dose according to the available area and how they affect dose-permeation proportionality.

To estimate clinical concentrations such as the area under the curve (AUC) after sublingual administration, the J_{SS} per one hour was used and adapted to the physiological area (A_{phy}) of 26.5 cm².

Equation 6: Estimated area under the curve (AUC_{est}).

$$AUC_{est} = \frac{\text{Drug exposure}(J_{SS} \cdot A_{phy} \cdot \text{duration} \cdot SF)}{CL} \text{ [ng} \cdot \text{h/mL]}$$

J_{SS}: Steady-state flux
A_{phy}: Physiological area
SF: Saliva factor
CL: Plasma clearance

In light of the bedtime administration of cyclobenzaprine in PTSD, an unstimulated/nocturnal salivary flow was considered for the calculation. Concerning the entire oral cavity, a lower unstimulated salivary flow of 0.1 mL/min and a mean residual volume of 0.92 mL were reported [Collins and Dawes, 1987; Humphrey and Williamson, 2001]. These values amount in a flow of approximately 0.74 mL/h and a remaining volume of 0.11 mL if scaled to the sublingual area of 26.5 cm² rather than the total oral cavity area of 214.7 cm² [Collins and Dawes, 1987]. The applied saliva factor of 0.7 was intended to estimate the dilution of the drug solution by the calculated saliva volume within one hour (total experimental time). It is based on 0.74 mL of newly secreted saliva within one hour plus 0.11 mL of residual volume (0.85 mL) relative to the 2 mL of drug solution administered. Assuming transmucosal systemic uptake of the drug, a mean plasma clearance (CL) of 689 mL/min was included into AUC_{est} calculation [Winchell et al., 2002].

4.2.4.4. Effects of simultaneous permeation and potential marker compounds on permeability

Caffeine, melatonin and metronidazole were chosen as specific markers in simultaneous permeation studies of cyclobenzaprine due to their physicochemical properties, complying with the requirements as potential candidates for continuous peri-experimental monitoring based on their neutral character and thus pH-independent permeability. Their influence on cyclobenzaprine permeability was analyzed (at least n = 3). Therefore, 2.6 mg caffeine, 2.0 mg

melatonin, or 7.0 mg metronidazole were each prepared in solution C (Table 7), based on preliminary tests regarding their permeation capacity and consistent with their water solubility (22 g/L, 2 g/L and 11 g/L, respectively) [National Center for Biotechnology Information, 2021b, 2021c, 2021d]. For the simultaneous quantification of cyclobenzaprine and the respective marker compound, the chromatographic and mass spectrometric conditions were further optimized and adapted (Table 7).

Table 7: Mass spectrometric conditions for cyclobenzaprine and the respective marker compounds.

Analyte parameters	CBP	CBP-d3	CAF	MEL	MET
Mass transition [m/z]	276.2 → 215.0	279.2 → 215.0	195.2 → 138.2	233.3 → 174.3	172.2 → 127.9
Declustering potential	30 V	30 V	81 V	75 V	25 V
Focusing potential	380 V	380 V	400 V	280 V	400 V
Entrance potential	9 V	9 V	12 V	7 V	5 V
Cell entrance potential	20 V	24 V	18 V	10 V	20 V
Collision energy	61 V	61 V	31 V	15 V	23 V
Cell exit potential	25 V	25 V	18 V	14 V	22 V
Mass spectrometric parameters					
Source	Electrospray ionization				
Mode	Positive ion mode				
Detection	Multiple reaction monitoring mode				
Dwell time	100 msec				

CAF: caffeine, CBP: cyclobenzaprine, CBP-d3: cyclobenzaprine-d3, m/z: mass-to-charge ratio, MEL: melatonin, MET: metronidazole

4.3. Results and Discussion

4.3.1. Effects of pH, phosphate salt type, and quantity on permeability

As an essential part of the preformulation study, the effect of pH alteration on the transmucosal permeability of cyclobenzaprine hydrochloride was investigated and evaluated using two approaches (*ex vivo/in vitro correlation*). Within this study, six different solutions of cyclobenzaprine—representing various phosphate compositions and their subsequent pH values—were used. The changes in pH due to different phosphate salts (from pH 5.5 to 8.9) influenced the protolysis equilibrium of the API, resulting in a wide range of percentages (0.11 to 72.91%) of the unionized free base (Equation 4).

Ex vivo assessment

Figure 16 shows the obtained permeation profiles as Q_t and the calculated permeation parameters for the *ex vivo* approach. The permeated amount was positively correlated with increasing pH due to the stepwise addition of dibasic phosphate. In parallel, permeability improved with the amount of basifying excipient up to the addition of 1.1 mg (unpaired t-test; $p < 0.05$). However, nearly doubling the amount to 2.1 mg dibasic phosphate (solution D) showed a negligible change in pH (8.8 vs. 8.9) and only minor improvements in permeability (PR = 2.00 vs. 2.19). By replacing 1.1 mg dibasic with monobasic phosphate as an acidifying excipient, a substantial drop in permeated cyclobenzaprine was observed. The effect of the monobasic phosphate solution was non-significant when compared to the amounts measured in the pure aqueous drug solution. The sigmoidal curve of unionized drug proportion as a function of pH was plotted, whereby pH-dependent permeability increased proportionally to the aforementioned curve (Figure 16B).

The twofold higher permeability between adding dibasic and monobasic phosphate was in line with the increase in membrane-retained drug content. Post-experimental extraction also revealed an approximately twofold higher mean relative drug content in the mucosal membrane of 8.87% (solution C, $n = 8$) compared to 4.44% (solution E, $n = 8$). Following the pH partition theory [Shore et al., 1959], membrane permeability is directly related to the amount of unionized drug. In the case of cyclobenzaprine (a weak aromatic base with a pK_a value of 8.47), an increase in the unionized portion and permeation was expected with higher pH values. Based on the reported pH value variation in the oral cavity, the applied solutions within these *ex vivo* studies covered a physiologically tolerable range. The lipophilic unionized portion ($\log P_{OW} = 5.2$) of the API was assumed to permeate transcellularly through the epithelial cells. However, with the acidification of the solution to a unionized proportion of only 0.11% (pH 5.5), a J_{SS} of $48.13 \pm 5.46 \mu\text{g}/\text{cm}^2/\text{h}$ was still measured. This finding indicates that even the protonated drug can permeate through the oral mucosa, suggesting a simultaneous

paracellular and transcellular mechanism. Consistent to the higher amount of unionized drug on the donor side in the presence of higher pH, a higher J_{ss} through the membrane was formed according to Fick's law of diffusion. After reaching the steady-state, a diffusion equilibrium was formed between the donor side, the membrane and the acceptor side so that the increase in permeation observed between the unionized form and the hydrochloride is accompanied by higher drug amount in the membrane [Sattar et al., 2015]. Considering both, the improvement achieved by the addition of dibasic phosphate and ease of solubility of the API at the given pH, the amount of 1.1 mg achieved the optimum.

Thus, the successful preformulation offered insights into the need to add a basic excipient to the subsequent formulation development of sublingual cyclobenzaprine. In clinical practice, the pH-sensitive permeability combined with the varying pH range of the oral cavity would impede the attainment of constant therapeutic levels, especially depending on each patient's nutritional and disease state. The results of this study showed that the amount of permeated cyclobenzaprine varied by approximately twofold within the physiological pH range. By controlling the microenvironmental pH and corresponding permeability, optimized formulation development facilitates API reduction, which offers subsequent economic advantages and also supports sufficient and rapid transmucosal bioavailability.

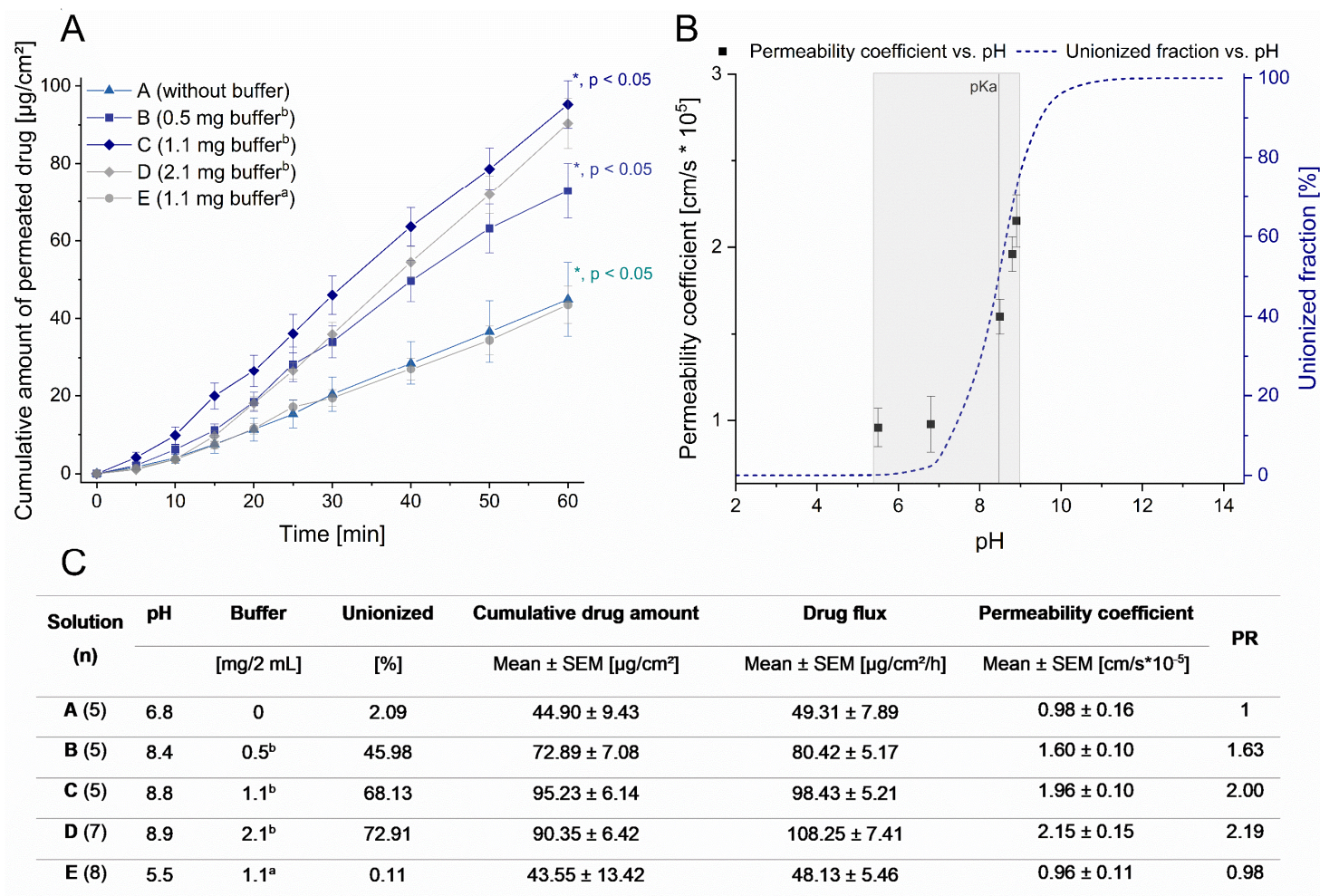


Figure 16: Effect of pH and phosphate salts on cyclobenzaprine permeability by *ex vivo* studies. A: Cumulative amount of permeated drug per cm² of the respective solution (mean ± SEM). B: Relation between obtained permeability (mean ± SEM), pH, and the unionized fraction of drug. The pK_a of cyclobenzaprine (line) and the investigated physiologically tolerable range (gray background) are highlighted. C: Summary of the study conditions and obtained permeation results. ^a: *potassium dihydrogen phosphate*, ^b: *dipotassium hydrogen phosphate*, PR: *permeability ratio*, SEM: *standard error of the mean*, *: *p < 0.05 (unpaired t-test)*.

In vitro assessment

By applying Permeapad® Barriers as artificial membranes instead of the esophageal mucosa, similar permeabilities of 1.27×10^{-5} vs. 0.98×10^{-5} cm/s were measured for purely aqueous cyclobenzaprine solutions. Nevertheless, the highest permeability was obtained with the addition of 0.5 mg dibasic phosphate (solution B), which was superior to the twofold amount of phosphate salt that performed best in the *ex vivo* model (Mann-Whitney U-test, $p < 0.05$). However, neither acidified nor basified solutions were detected as significantly different from the permeability of the aqueous solution (Figure 17A). Contrary to existing *ex vivo* studies, the present results showed a decrease in permeability when over 0.5 mg dibasic phosphate was added. Thus, there was no proportionality between determined permeability and presented pH value, which deviates from the ionization degree trend (Figure 17B). Considering the amount of drug retained led to comparable findings, with 3.78 and 3.03% of cyclobenzaprine being extracted after permeation studies of solutions C ($n = 8$) and E ($n = 4$), respectively.

Accordingly, the applied *ex vivo* model confirmed the linear correlation between the unionized API and its permeability with a coefficient of determination (R^2) of 0.995, whereby no linear relationship ($R^2 = 0.322$) could be observed for the artificial *in vitro* approach (Figure 18).

Permeapad® Barriers are artificial biomimetic phospholipid-based membranes that were initially developed for intestinal passive drug diffusion. However, the predictive determination of oromucosal permeability has been performed in relatively few studies. Perhaps due to the recent use of Permeapad® for this route of administration, the data is limited once it exceeds the classification of substances (e.g., by additionally considering other elements such as environmental conditions and additives). Bibi et al. reported the determination of pH-dependent increase of metoprolol permeability using Permeapad® [Bibi et al., 2016]. However, the results of metoprolol ($\log P_{OW} = 1.8$; topological polar surface area = 50.7 \AA^2) may not be transferable to cyclobenzaprine with respect to their different physicochemical properties, particularly regarding their lipophilicity ($\log P_{OW} = 5.2$; topological polar surface area = 3.2 \AA^2). While Permeapad® was unsuitable for sophisticated preformulation studies of cyclobenzaprine, the artificial barrier remains a useful alternative for screening and ranking compounds regarding their permeation behavior [Di Cagno et al., 2015].

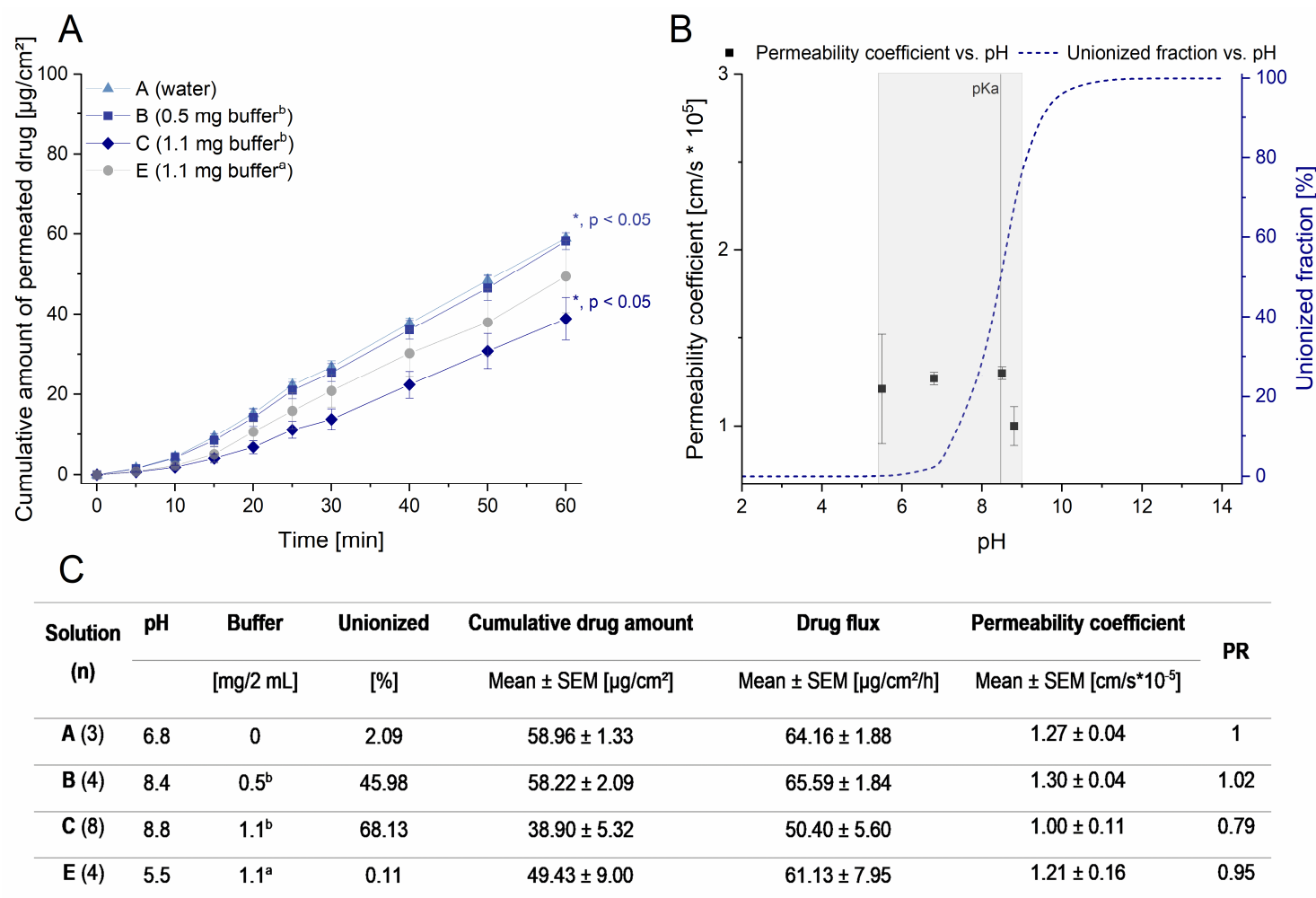


Figure 17: Effect of pH and phosphate salts on cyclobenzaprine permeability by *in vitro* studies. A: Cumulative amount of permeated drug per cm² of the respective solution (mean ± SEM). B: Relation between obtained permeability (mean ± SEM), pH and the unionized fraction of drug. The pK_a of cyclobenzaprine (line) and the investigated physiologically tolerable range (grey background) are highlighted. C: Summary of the study conditions and obtained permeation results. ^a: potassium dihydrogen phosphate, ^b: dipotassium hydrogen phosphate, PR: permeability ratio, SEM: standard error of the mean, *: *p* < 0.05 (unpaired *t*-test).

In summary, the here investigated *ex vivo/in vitro* correlation approach highlighted the superiority of the assessed *ex vivo* model in terms of the environment-dependent permeability of cyclobenzaprine. Therefore, its suitability and sensitivity for prediction in preformulation as part of early drug development were demonstrated within the standardized and automated permeation process.

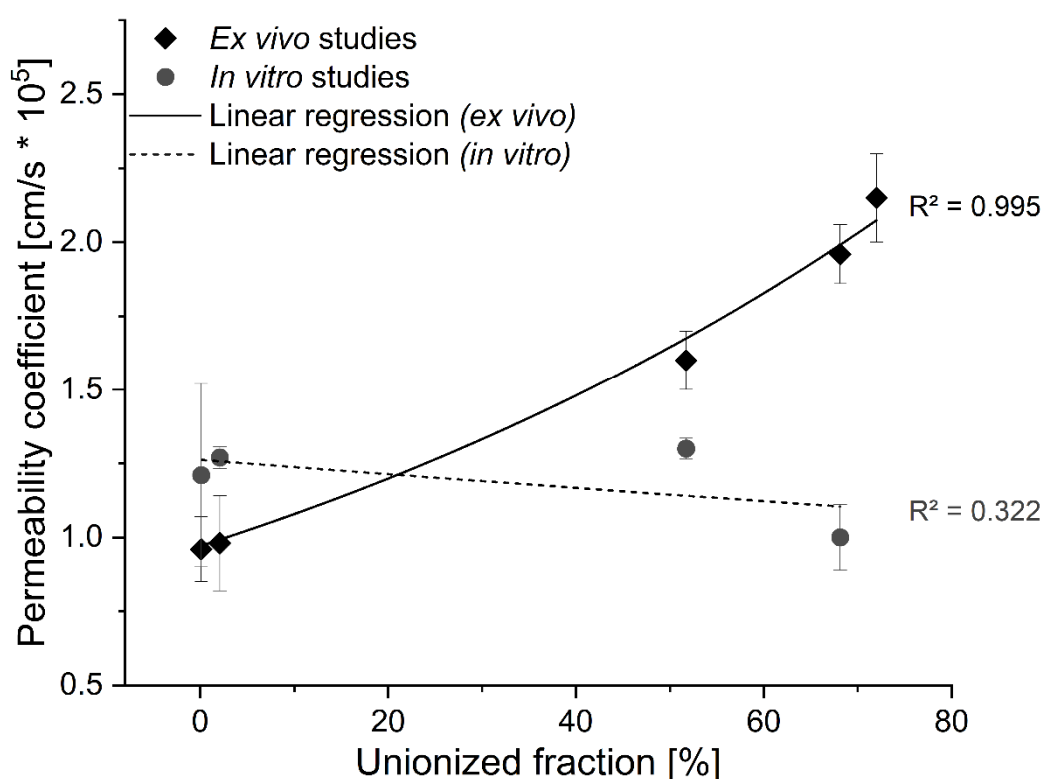


Figure 18: Correlation of the obtained cyclobenzaprine permeability by *ex vivo* and *in vitro* studies with the calculated unionized fraction of the drug (mean \pm SEM). R^2 : coefficient of determination, SEM: standard error of the mean.

4.3.2. Effects of membrane thickness and storage conditions on permeability

An inverse proportional relationship between cyclobenzaprine permeability and mucosa thickness was obtained (Figure 19A, C). Accordingly, calculated permeability significantly decreased with increasing membrane thickness from 350 to 500 μm (-21.29%) and from 500 to 750 μm (-56.6%) (unpaired t-test; $p < 0.05$). This was also accompanied by a substantial decrease in the slope of cumulated drug over time between the thicknesses. Hence, the influence of membrane thickness on the permeability of the API was summarized by the correlation between the determined permeability coefficient and reciprocal membrane thickness (linear regression with $r = 0.963$), which is in accordance with Fick's law of diffusion. HE staining of the mucosal tissues (Figure 20) showed that all membranes contained the outer stratified epithelium, whereas 500 and 750 μm thick membranes additionally included the

stratum spinosum (purple stained layer in 500 and 750 μm preparations, Figure 20C, E), respectively. Moreover, membranes with 750 μm thickness included the basal membrane with parts of the underlying lamina propria (Figure 20E). Consistently, a distinctive DBA staining of the stratified epithelium (Sato et al., 1991) was observed throughout the cell layers in 350 μm membranes, whereas staining decreases progressively in the subsequent layers of 500 and 750 μm preparations as these also included additional DBA negative epithelial cell layers (Figure 20B, D, F). While the decrease in permeability from 350 to 500 μm may represent the effect of the longer diffusion distance of the epithelium, the larger decrease between 500 and 750 μm suggests that the more hydrophilic properties of connective tissue compared to epithelium provide an additional diffusion barrier for cyclobenzaprine. This finding is in line with results published by Kulkarni et al., who showed that lipophilic drugs were more strongly affected by mucosal thickness than hydrophilic drugs [Kulkarni et al., 2009]. Presumably, this can be explained by the preferential transcellular pathway, which also applies to cyclobenzaprine.

Furthermore, differences in permeability were analyzed with regard to the storage of prepared membranes at $-80\text{ }^{\circ}\text{C}$ in PBS buffer (Figure 19B). No difference was detected between frozen or fresh mucosa (2.01×10^{-5} vs. 1.96×10^{-5} cm/s). Since post-experimental integrity tests of the thawed membranes were positive, the negative impact could be excluded by controlled freezing of the mucosal tissue. In contrast, membrane viability was under the predefined threshold, with a mean of 36.3% for the frozen tissue. These results support the assumption of a passive diffusion pathway of cyclobenzaprine, which was not affected by freezing and decreased membrane viability. Heterogenous outcomes of investigations on the impact of freezing underline that the specific assessment depends on the drug, its diffusion mechanism, and the freezing and thawing techniques [Caon and Simões, 2011; van Eyk and van der Biijl, 2006]. After all, tissue storage offers the prospective procurement of tissue material, reduction of experimental time, and increased independence from slaughterhouses. However, the authors suggest that fresh mucosa with proven viability should preferably be used to ensure physiological conditions during permeation experiments.

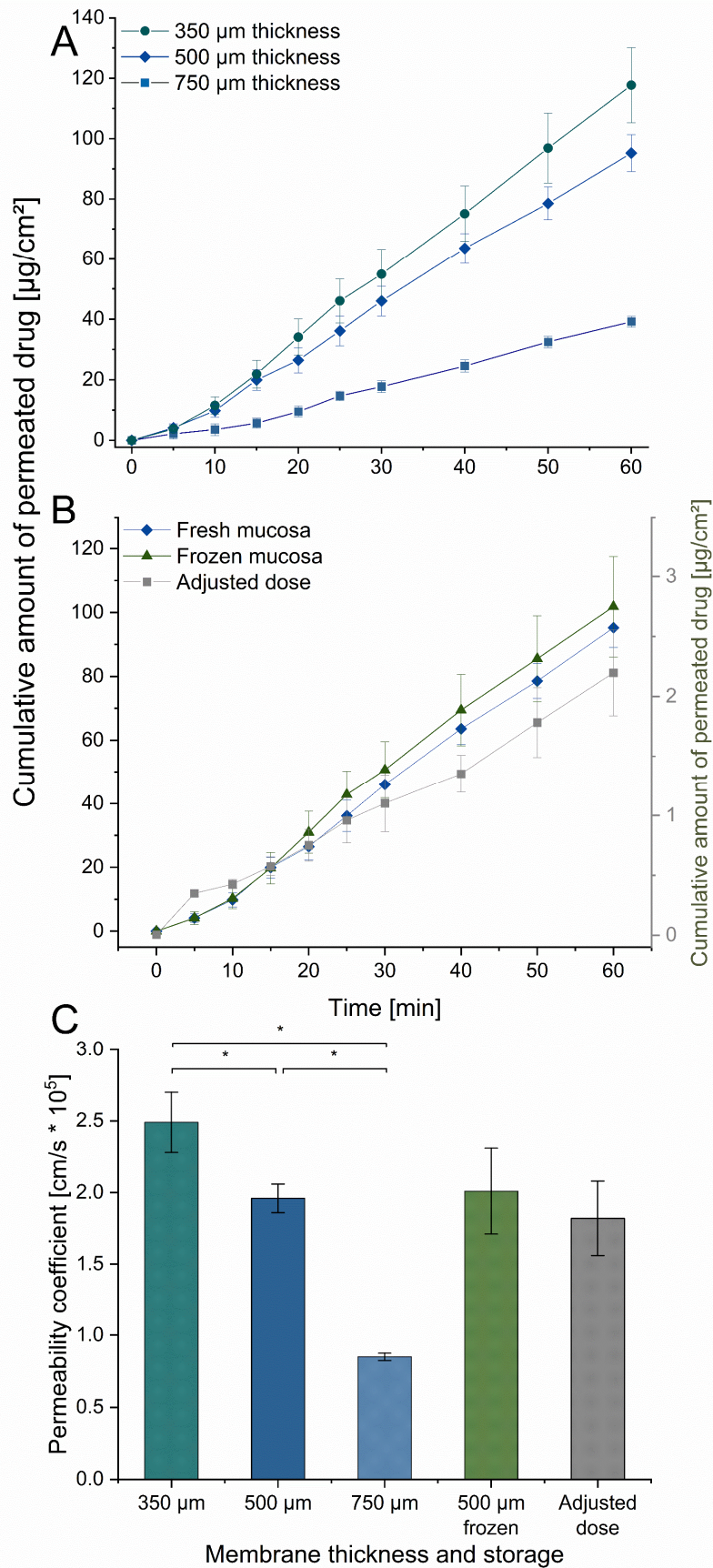


Figure 19: Effect of membrane thickness, storage condition and dose on cyclobenzaprine permeability. A: Cumulative amount of permeated drug per cm² through the respective thickness (mean \pm SEM: 350 μm (n = 6), 500 μm (n = 5), and 750 μm (n = 3)). B: Cumulative

amount of permeated drug per cm^2 (mean \pm SEM: freshly prepared mucosa ($n = 5$), frozen mucosa ($n = 3$), and adjusted dose with freshly prepared mucosa ($n = 4$)). C: Comparison of the obtained permeability regarding membrane thickness, storage condition and dose adjustment (mean \pm SEM). SEM: standard error of the mean, *: $p < 0.05$ (unpaired t -test).

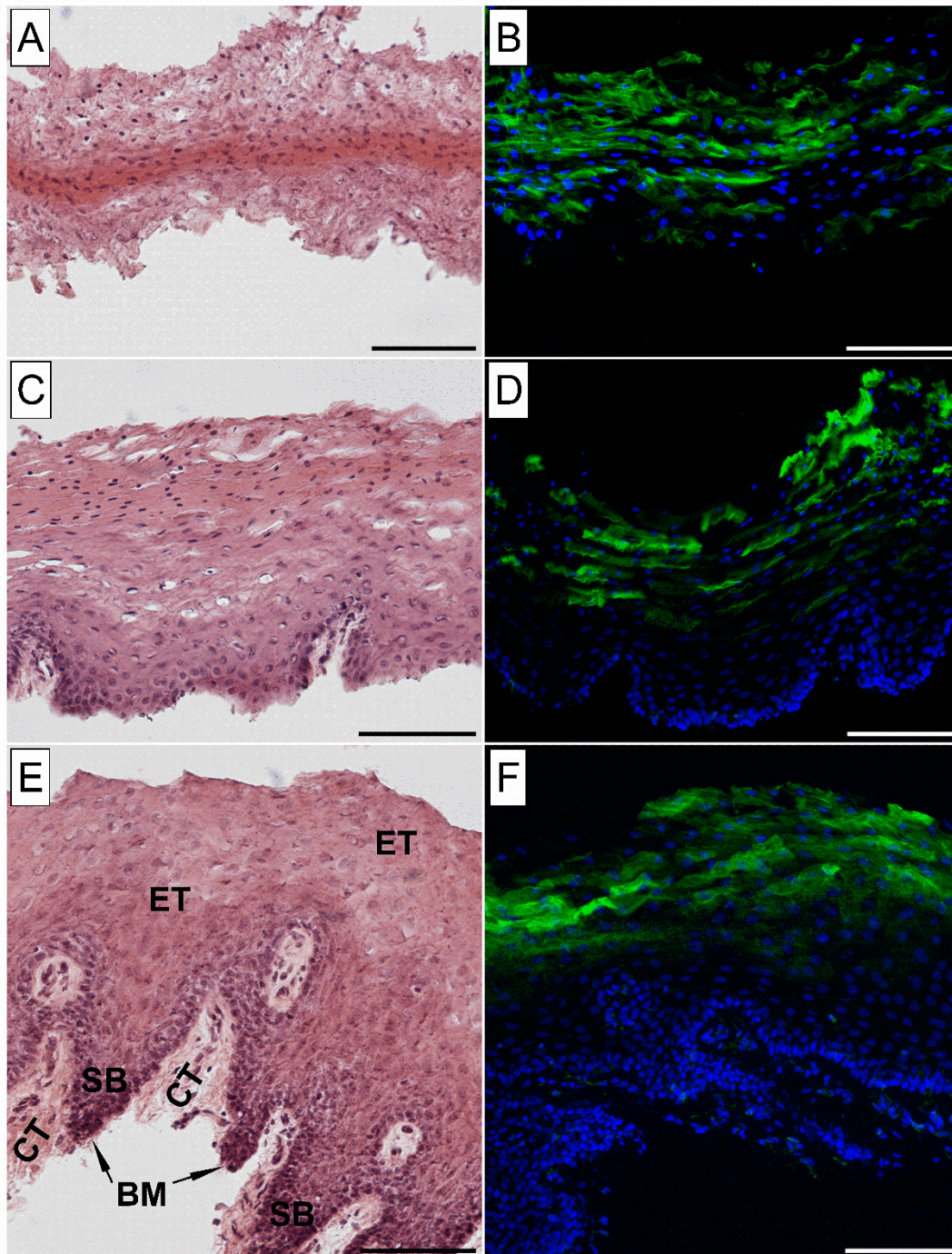


Figure 20: Hematoxylin-eosin and FITC-DBA stained cryosections of esophageal mucosal tissue at thicknesses of 350 (A, B), 500 (C, D), and 750 μm (E, F). Scale bar, 100 μm . BM: basal membrane, CT: connective tissue, ET: epithelial tissue, FITC-DB: Fluorescein isothiocyanate-conjugated Dolichos Biflorus Agglutinin, SB: stratum basale.

4.3.3. Scaling the dose to the sublingual surface area

Permeation studies were performed with an adjusted drug amount regarding the distribution of the dose over the mouth floor in clinical applications. Figure 19B shows similar permeation profiles despite the reduced dosage. Moreover, no difference in permeability was detected between the previous experimental set-up and adjustment to the sublingual area (unpaired t-test; $p < 0.05$), which demonstrates dose-permeation proportionality (Figure 19C).

Since proportionality was highlighted as a precondition for scaling, the J_{SS} was calculated using the permeability coefficient and the initial concentration in the oral cavity corrected by the SF. Thereby, relevant to the indication of cyclobenzaprine in PTSD, an unstimulated nocturnal salivary flow of 0.1 mL /min was aligned to the sublingual area (estimated total saliva volume of 0.85 mL). This provides a physiologically adjusted flux of 68.90 $\mu\text{g}/\text{cm}^2/\text{h}$, which by considering the actual dose of 2.8 mg and the intraorally available area (26.5 cm^2) results to a total exposure of 1.83 mg. Derived from a previous study [Gimeno et al., 2014], using the total drug exposure and knowledge about the plasma clearance (41.34 L/h), an AUC of 44.17 $\text{ng}\cdot\text{h}/\text{mL}$ was estimated for the sublingual administration of cyclobenzaprine using the presented model.

According to pharmacokinetic investigations by Winchell et al., a mean AUC of 45.9 $\text{ng}\cdot\text{h}/\text{mL}$ was determined after a single oral administration of 10 mg cyclobenzaprine [Winchell et al., 2002]. Considering the bioavailability of 33 to 55% for oral administration and scaling to sublingual administration (in which a first-pass effect is lacking), comparable exposure after a dose of 2.8 mg is reasonable. This strengthens the aforementioned indication-related advantages of a higher oromucosal bioavailability by avoiding the first-pass effect, the possibility of dose reduction, and the rapid systemic absorption of the drug. The successful estimation into clinical ranges reflected the physiological adaption of the *ex vivo* permeation model and confidently suggested that its *in vivo* predictivity, at least allows screening for the potential of novel intraoral drugs. However, further studies concerning *ex vivo* – *in vivo* correlation are required for more purposes.

4.3.4. Effects of simultaneous permeation and potential marker compounds on permeability

Permeation studies in the presence of specific marker compounds were performed to evaluate their potential use in continuous peri-experimental monitoring. Figure 21 presents the structural formulas of the marker compounds and their specific product-ion mass spectra, while Appendix 3 shows an exemplary LC-MS/MS chromatogram of simultaneous analysis. Additionally, the diffusion-relevant physicochemical properties of the compounds were comparatively summarized. According to their pK_a values, the markers remain unionized in the physiological

pH range of the oral cavity in contrast to cyclobenzaprine. This aspect is considered advantageous for environment-independent monitoring since it allows a medium-universal definition of specific permeability coefficients as a validity criterion. Therewith, permeation capability was primarily related to the structural properties of the markers. They were also selected *a priori* with deviation in the properties of the API (e.g., $\log P_{OW}$ and topological polar surface area) to allow the unaffected monitoring of cyclobenzaprine permeation.

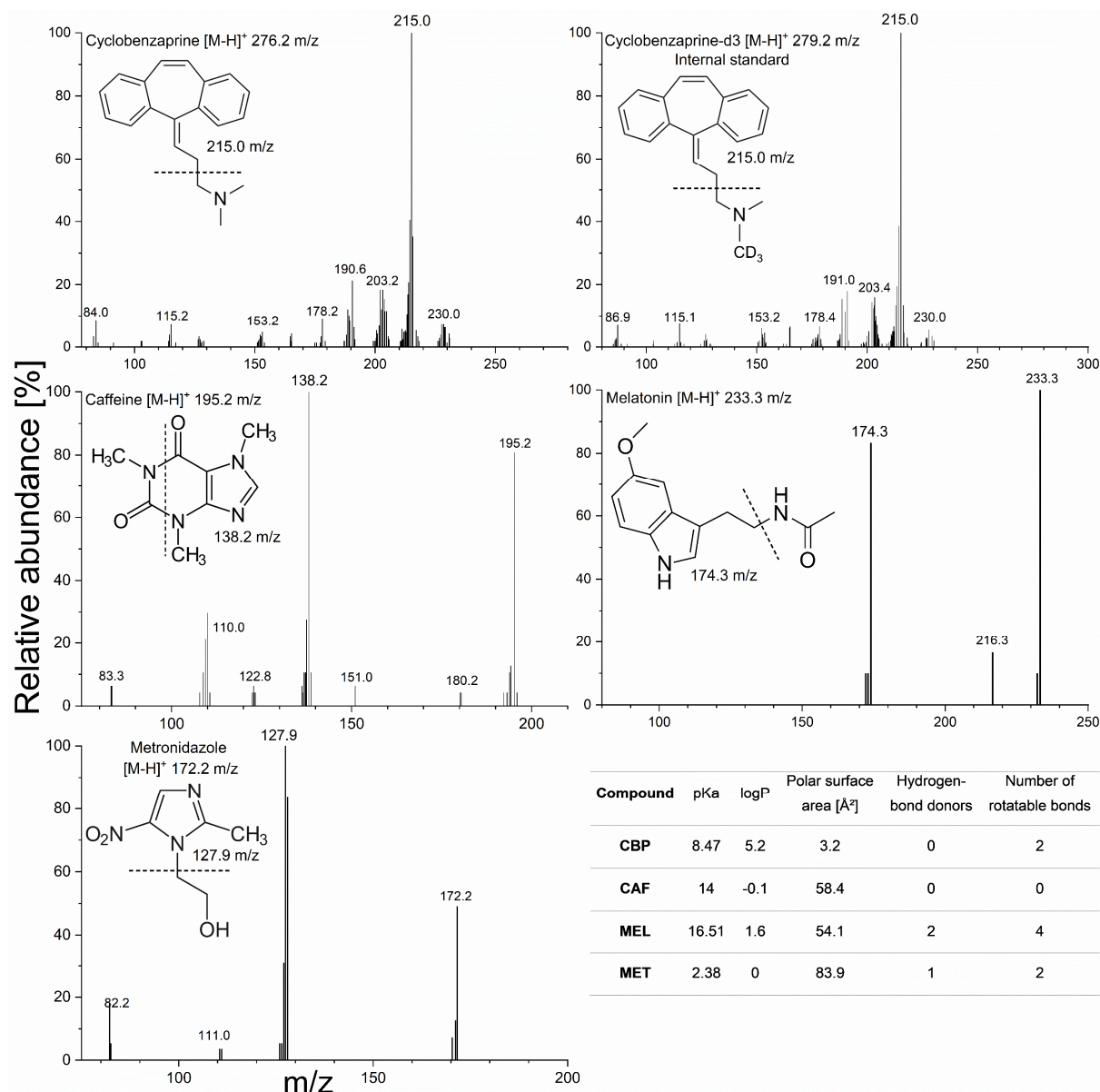


Figure 21: Product-ion scan with structural formula of the respective analytes in multi-channel-analysis (100 cycles with 1000.0 ng/mL). The fragments used for simultaneous quantification are highlighted with the expected fragmentation mechanism (dotted line). The physicochemical properties are summarized tabularly [National Center for Biotechnology Information, 2021a, 2021b, 2021c, 2021d]. CAF: caffeine, CBP: cyclobenzaprine, CBP-d3: cyclobenzaprine-d3, m/z: mass-to-charge ratio, MEL: melatonin, MET: metronidazole.

Conventional integrity markers (e.g., mannitol or lucifer yellow) are of limited suitability due to their primarily hydrophilic or lipophilic properties, challenging analytical determination, and the long post-study duration following the actual permeation experiments [Kulkarni et al., 2010; Lee et al., 2002; Marxen et al., 2017; Sarmento, 2016]. Furthermore, the influence of these substances on drug permeation has not been clearly defined to date.

The impacts of caffeine, melatonin, and metronidazole on the permeability of cyclobenzaprine are presented in Figure 22. Compared to the single permeation of cyclobenzaprine without additional compounds, its permeability decreased significantly (unpaired t-test; $p < 0.05$). From a permeability of 1.96×10^{-5} cm/s, the largest reduction to $1.10 \pm 0.07 \times 10^{-5}$ cm/s was measured with the addition of melatonin (-43.88%), followed by caffeine (-29.08%) to $1.39 \pm 0.09 \times 10^{-5}$ cm/s and metronidazole (-15.82%) to $1.65 \pm 0.05 \times 10^{-5}$ cm/s. Thus, inter-variability between the impacted cyclobenzaprine permeability by the three marker compounds were detected (unpaired t-test; $p < 0.05$). The decreased permeability of cyclobenzaprine in the presence of the marker compounds may be related to competition for the respective diffusion pathway.

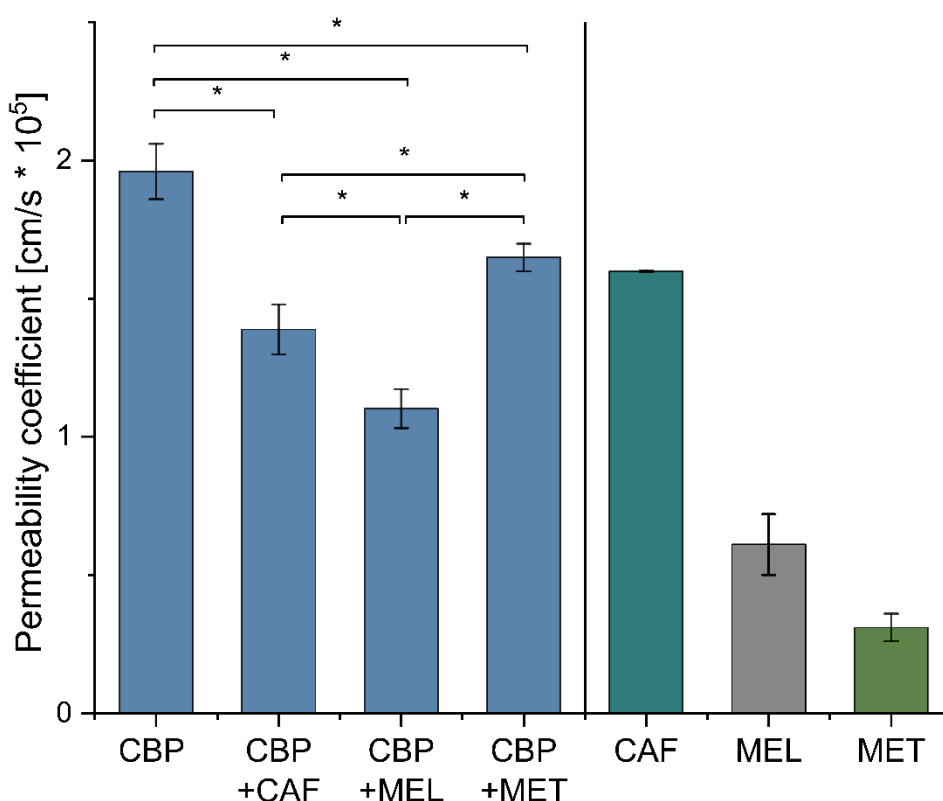


Figure 22: Permeability coefficients of cyclobenzaprine, cyclobenzaprine + marker compound and of the marker compound itself, (mean \pm SEM): CBP ($n = 5$), CBP + CAF ($n = 3$), CBP + MEL ($n = 4$), CBP + MET ($n = 10$). CAF: caffeine, CBP: cyclobenzaprine, MEL: melatonin, MET: metronidazole, SEM: standard error of the mean, *: $p < 0.05$ (unpaired t-test).

Thus, caffeine, melatonin, and metronidazole were not appropriate markers for the peri-experimental monitoring of permeation studies. Overall, a remarkable phenomenon of the mutual influence of the mucosal permeability of drugs was observed. These results inspired the question of whether conventional marker substances also show such effects. Since low concentrations of these three markers negatively affected the permeability of the analyte of interest, the role and influence of commonly used marker substances should be reconsidered. For example, Nielsen and Rassing reported a decrease in nicotine and mannitol permeability with an increase in nicotine concentration, which may be also related their decreased paracellular permeability [Nielsen and Rassing, 2002].

4.4. Conclusion

The oromucosal permeability of cyclobenzaprine was comprehensively investigated and characterized for the first time in terms of impacting factors and various study conditions using esophageal mucosa as surrogate membrane. The standardized and controlled *ex vivo* permeation process proved to be suitable for predictive evaluations during preformulation studies and was purposefully superior to the cell-free artificial *in vitro* approach. Thus, successful permeation enhancement was achieved by adjusting microenvironmental conditions at the site of administration, thereby enabling the further targeted development of sublingual cyclobenzaprine dosage forms. Combined with the adaption of the study design to physiological and clinical conditions, an estimation of plasma AUC from determined permeability in proper reported windows was facilitated and emphasized the effective application in preformulation.

5. Formulation development of sublingual cyclobenzaprine tablets empowered by standardized and physiologically relevant *ex vivo* permeation studies

5.1. Introduction

For certain special patient populations (e.g. children, the elderly, or patients with dysphagia, intestinal insufficiency, nausea, or trypanophobia), the common routes of drug administration (oral and parenteral) appear to be inappropriate and are often accompanied by poor adherence [Schiele et al., 2013]. Administration via the oral mucosa as a patient- and indication-centered treatment offers a beneficial alternative. In addition to easier application, rapid and high systemic availability is achieved for the therapy of acute cases. Bypassing the digestive tract and first-pass metabolism allows for dose reduction [Pinto et al., 2020], which facilitates patient safety and adherence by reducing the risk of side effects [Gilhotra et al., 2014].

In order to support the progressive development and approval of oromucosal drugs, meaningful studies predicting pharmacokinetic properties are already essential at the preclinical stage [Cabrera-Pérez et al., 2016]. During the preclinical stage, formulation development represents a useful tool to influence pharmacokinetic properties, with consideration given to the intended site of administration as well as the targeted patient population and indication. Decisive criteria include solubility, compatibility, stability, taste, and in particular drug release and absorption rate [Kalia et al., 2016]. Conventionally, dissolution studies provide information on the drug release achieved, e.g. in QC and stability studies, as well as on formulation development. However, *in vitro/ex vivo* permeation studies are useful for the investigation of the impact of the formulation on drug absorption, and allow for an extensive screening to guide formulation development and support transfer to *in vivo* studies [Cabrera-Pérez et al., 2016]. Unlike dissolution studies, particularly for administration via the oral mucosa, drug permeation studies are not clearly regulated and the associated heterogeneity hinders their broad application. On the one hand, their use as continuous, decisive elements embedded into formulation development requires sensitivity and adaptation to physiological conditions in order to detect the pharmacokinetically/clinically relevant impacts of the formulations developed. On the other hand, a standardized, comparable and regulatory implementable design with controlled processes is required to ensure efficient and reliable application [Cabrera-Pérez et al., 2016; Castro et al., 2016; Kolli and Pather, 2015; Patel et al., 2012]. These unmet requirements restrict the current application of *ex vivo* absorption studies to academic research and unregulated preliminary studies. For most other applications elaborate, expensive, and ethically sensitive *in vivo* studies are the method of choice for

This work was published in an international peer-reviewed journal [Majid et al., 2021d]:

Majid, H., Puzik, A., Maier, T., Merk, R., Bartel, A., Mueller, H.-C., Burckhardt, B., 2021. Formulation development of sublingual cyclobenzaprine tablets empowered by standardized and physiologically relevant *ex vivo* permeation studies. *Pharmaceutics* 13, 1409. <https://doi.org/10.3390/pharmaceutics13091409>.

The author of this thesis was responsible for conceptualization, methodology, validation, formal analysis, investigation, writing-original draft, writing-review and editing, and visualization.

evaluation formulation of candidates [AlAli et al., 2021; Pather et al., 2008]. In order to address this imbalance, an oromucosal *ex vivo* permeation model was successfully developed, standardized and validated [Majid et al., 2021a]. Processes were automated and incorporated into a sophisticated control system which consisted of analytical QC and verification of tissue viability and integrity. The model was applied in comprehensive preformulation studies of oromucosal drug delivery [Majid et al., 2021c]. Nonetheless, the expansion of the model from preformulation to formulation development for predicting the pharmacokinetically relevant impacts of developed dosage forms on absorption, especially under a physiology-based design and within clinically relevant application periods, has not yet been studied.

Cyclobenzaprine hydrochloride is a tricyclic dibenzocycloheptene muscle relaxant approved for the oral treatment of muscle pain and spasms [Chou et al., 2004]. Due to its antagonistic effects in the serotonergic, histaminergic, and adrenergic systems, cyclobenzaprine is currently being investigated and discussed with regard to various additional indications, most notably for sleep disturbances in PTSD and fibromyalgia [Lawson, 2020; Moldofsky et al., 2011]. PTSD is characterized by involuntary re-experiences and hyperarousal symptoms, for example sleep disturbances with nightmares, hypervigilance, and anxiety. The cross-national prevalence of PTSD in adults has been found to be 3.9% [Koenen et al., 2017], and within this cohort 80-90% of the patients suffer from sleep disturbances [Spoormaker and Montgomery, 2008]. Further potential application for cyclobenzaprine include Alzheimer's disease and long-COVID syndrome. Besides these new potential indications, sublingual administration is also intended to reduce daytime side effects [Sartori and Singewald, 2019], such as somnolence, by providing a lower dose and avoiding the first-pass effect with the formation of the active and long-lived metabolite desmethyl cyclobenzaprine (norcyclobenzaprine) [Sullivan et al., 2021].

The aim of this study was to verify the power of the model to lead sublingual formulation development and thereby facilitate the targeted development of patient-centered oromucosal drugs. Moreover, an enhancement of oromucosal cyclobenzaprine permeation through optimized compositions was intended to exploit its therapeutic benefits and improve patient safety. Furthermore, the relevance of drug metabolism during transmucosal permeation was to be monitored and assessed, since data about metabolic activity in the oral cavity is limited. Finally, in this proof of concept, the sensitivity of the *ex vivo* permeation model for the purpose of detection and classification of the impact of alteration on dosage forms was investigated.

5.2. Material and Methods

5.2.1. Simultaneous quantification of cyclobenzaprine and its related compounds

The simultaneous quantification of cyclobenzaprine hydrochloride ($\geq 98\%$, Hetero drugs Ltd, Hyderabad, India), its main metabolite desmethyl cyclobenzaprine hydrochloride (99.8%, Toronto Research Chemicals, Toronto, Canada) and cyclobenzaprine N-oxide (96%, Toronto Research Chemicals, Toronto, Canada) as its major degradation product was performed by HPLC-ESI-MS/MS (Shimadzu Prominence, Shimadzu Europe, Duisburg, Germany; AB Sciex API 2000, Darmstadt, Germany). Chromatography was carried out on a Luna PFP (2) column (100.0 \times 2.0 mm; 3 μ m) with SecurityGuard PFP (2) pre-column (4.0 \times 2.0 mm) (Phenomenex Ltd, Aschaffenburg, Germany) using cyclobenzaprine-d3 (98%, Sigma-Aldrich, Taufkirchen, Germany) as deuterated IS. At a maintained column temperature of 55 °C, 0.1% FA ($\geq 98\%$, p.a., Sigma-Aldrich, Taufkirchen, Germany) in water (LC-grade, Fisher Scientific, Schwerte, Germany) and 0.1% FA in ACN (LC-grade, Fisher Scientific, Schwerte, Germany) served as mobile phases A and B at a flow rate of 450 μ L/min. Gradient elution went from 7% to 72% of mobile phase B with a total run time of 5.3 min and an injection volume of 5 μ L. The mass transitions and analyte specific parameters for detection in MRM mode are summarized in Table 8. Mass spectrometric source parameters were set as follows: curtain gas (nitrogen): 20 psi, ion spray voltage: 2000 V, nebulizer gas (zero air): 42 psi, heater gas (zero air): 75 psi, collision gas (nitrogen): 7 psi and source temperature: 550 °C. Control of instrument and data acquisition were performed using Analyst®1.5.1 (AB Sciex, Darmstadt, Germany).

Validation of the simultaneous quantification method for cyclobenzaprine, desmethyl cyclobenzaprine and cyclobenzaprine N-oxide was performed according to international guidelines (EMA, FDA, and ICH Q2 guidelines) [European Medicines Agency, 2012; International Council for Harmonisation of Technical Requirements for Pharmaceuticals for Human Use, 2005; U.S. Department of Health and Human Services Food and Drug Administration, 2018] for the parameters linearity, accuracy, precision, sensitivity, dilution integrity, and recovery. In addition to method validation, each LC-MS/MS conducted run was monitored by system suitability tests, intra-run QCs and QCs regarding automated sample preparation. For this purpose, intra-run specifications were defined as a maximum RE of $\pm 15\%$ ($\pm 20\%$ at the LLOQ) and $r \geq 0.995$ for freshly prepared calibration curves.

Table 8: Mass spectrometric conditions for cyclobenzaprine and its related compounds desmethyl cyclobenzaprine and cyclobenzaprine N-oxide.

Analyte-specific parameters	CBP	CBP N-oxide	Desmethyl CBP	CBP-d3
Mass transition [m/z]	276.2 → 215.0	292.4 → 231.2	262.4 → 231.2	279.2 → 215.0
Declustering potential	55 V	55 V	55 V	55 V
Focusing potential	380 V	380 V	380 V	380 V
Entrance potential	10 V	9 V	9 V	10 V
Cell entrance potential	21 V	10 V	10 V	21 V
Collision energy	61 V	25 V	25 V	61 V
Cell exit potential	10 V	10 V	10 V	10 V
Mode	ESI (+)			
Dwell time	80 msec			

ESI: electrospray ionization, m/z: mass-to-charge ratio

5.2.2. Sublingual formulation development guided by permeation studies

Preliminary preformulation studies [Majid et al., 2021c] on the impact of pH and utilized excipients on transmucosal cyclobenzaprine permeability demonstrated a significant dependence on the addition of dipotassium hydrogen phosphate (dibasic phosphate) and also on environmental pH. These findings were transferred into formulation development by manufacturing SLT of three different compositions with varying amounts of dibasic phosphate (0.0 to 1.4%). All SLTs were manufactured by direct compression using a rotary tablet press (Kilian RTS21, Romaco, Karlsruhe, Germany) and had a diameter and a weight of 0.6 cm and 76 mg, respectively. The ingredients of the SLTs are compiled in Table 9.

With consideration given to optimized physiological and clinical conditions (e.g. low saliva volume of 150 μ L for disintegration, short-term application due to indication and site of administration, sink conditions, etc.), the sensitivity of the model to variations in the sublingual formulation was investigated and compared with the outcomes from preformulation studies, as well as from dissolution studies as a conventional reference method (section 5.2.2 and 5.2.4). The disintegration behavior of the developed SLTs was visually assessed within a low-volume benchtop approach to mimic the physiological environment of the oral cavity. Therefore, 150 μ L of fresh human saliva was added to the tablets and disintegration was monitored. The

potential of the permeation model to lead formulation development was classified. Subsequently, the drug release, Q_t , J_{SS} and P_{app} were assessed.

Table 9: Compositions of the sublingual tablets within formulation development.

Ingredients	Amount [%]
Cyclobenzaprine hydrochloride (API) (Hetero drugs Ltd, Hyderabad, India)	3.7
Crospovidone (Kollidon CL, BASF, Ludwigshafen, Germany)	5.3
Peppermint aroma (Symrise, Holzminden, Germany)	3.7
Sodium stearyl fumarate (Pruv, JRS Pharma, Rosenberg, Germany)	2.6
Dipotassium hydrogen phosphate (Merck KGaA, Darmstadt, Germany)	0.0 (SLT-A); 0.7 (SLT-B); 1.4 (SLT-C)
Silicon dioxide (Syloid 244 FP, Grace, Worms, Germany)	1.3
Sucralose (Merck KGaA, Darmstadt, Germany)	0.3
Levomenthol (L-Menthol, BASF, Ludwigshafen, Germany)	0.03
Mannitol (Pearlitol 100 SD, Frankfurt, Germany)	ad 100
Physical attributes	
Shape	White round sublingual tablet
Diameter and height	0.60 and 0.27 cm
Weight	76.0 mg

API: active pharmaceutical ingredient, SLT: sublingual tablet

5.2.3. Standardized and physiologically relevant permeation model

5.2.3.1. Model set-up

An innovative, widely standardized and controlled *ex vivo* model, which has been described elsewhere [Majid et al., 2021a], was used to study oromucosal permeability of cyclobenzaprine SLTs (section 5.2.2). The model consists of the combination of the following elements.

Fresh porcine esophageal mucosa, obtained by Naturverbund Thönes (Wachtendonk, Germany), separated and dermatomed to a thickness of 500 μm (Integra® Dermal, Ratingen, Germany) was applied as a surrogate for oral mucosa [Diaz Del Consuelo et al., 2005b; Diaz Del Consuelo et al., 2005c; Diaz Del Consuelo et al., 2005a; Telò et al., 2016]. The biological membrane was inserted in the Kerski diffusion cell and moistened with human saliva freshly collected under fasting conditions. After application of the formulation to be investigated, 100 μL of human saliva was pipetted on top of the SLT. The Kerski diffusion cell [Kerski et al., 2020] allows for automated sampling with modified Hanson Research AutoPlus™ (Teledyne Hanson, Los Angeles, CA, USA), scheduled from 5 to 60 minutes after drug administration. In order to mimic physiological conditions, PBS buffer at pH 7.4 was used as an acceptor medium with environmental conditions of 37 °C temperature and 20% relative humidity (KBF 115 Constant Climate Chamber, Binder GmbH, Tuttlingen, Germany), and continuous stirring at 750 rpm (2mag Mixcontrol20, Munich, Germany) was maintained during the study period. The automation of sample preparation involved spiking cyclobenzaprine-d3 to the samples, dilution into the analytical calibration range, and agitation using an HTS PAL autosampler (CTC Analytics AG, Zwingen, Germany) and Chronos 5.0 software (Axel Semrau GmbH, Sprockhoevel, Germany). Coupling with sensitive quantification by validated LC-MS/MS method (section 5.2.1.) enabled a clinically representative study design (in terms of duration, measurement points, and therapeutic dose). Novel post-study tissue integrity and viability assays were incorporated to monitor and reevaluate the permeation results by excluding non-compliant measurements and diffusion cells, where applicable [Majid et al., 2021a].

The Q_t , J_{SS} , and P_{app} were calculated using Equation 1 – 3 to assess permeability. Statistical differences were analyzed using an unpaired Student's t-test with $\alpha = 0.05$. The P_{app} values from varying amounts of dibasic phosphate of the SLTs and those from the preformulation were correlated. The enhancement factor (EF) was used to rate the impact of formulation and excipient addition on cyclobenzaprine permeability (Equation 7).

Equation 7: Enhancement factor (EF).

$$EF = \frac{P_{app} \text{ (with dibasic phosphate)}}{P_{app} \text{ (without dibasic phosphate)}} \quad P_{app}: \text{ Apparent permeability coefficient}$$

5.2.3.2. Metabolization of cyclobenzaprine during mucosal permeation

The permeation model was extended by mucosal metabolic activity examination as an additional physiological model property. Therefore, the focus was on the formation of desmethyl cyclobenzaprine – the main active metabolite, which is responsible for clinically relevant daytime side effects – by mucosal administration. The cytochrome P450 isoenzymes 1A2, 3A4, and 2D6 are implicated in the catalysis of cyclobenzaprine demethylation [Wang et al., 1996; Yu, 2014]. To determine the extent of mucosal cyclobenzaprine metabolism, solutions containing 2.8 mg cyclobenzaprine and 1.1 mg dibasic phosphate were prepared. In this setup, esophageal mucosa, buccal (500 µm thickness) and sublingual mucosa (300 µm thickness) were examined to determine potential differences between metabolic activities of the esophagus and oral mucosa. Thus, permeation studies followed by extraction of the used mucosal membranes by 10 mL of methanol/water/FA (80:19:1 v/v/v) at 37 °C and 1000 rpm were conducted to detect the metabolized amount in the tissues. The relative mass balance of desmethyl cyclobenzaprine, as a relevant active metabolite, was calculated from the permeated amount, the membrane-extracted amount, and the amount in the applied donor solution. The different mucosa membranes were also incubated with solutions of 14 mg/mL cyclobenzaprine for 4 hours at 37 °C to detect minor metabolite formation. As a negative control, served membranes were treated for at least 3 hours with 1% FA in methanol to eliminate metabolic activity. In order to investigate metabolic activity in saliva, 2.8 mg cyclobenzaprine was added to fresh human saliva, incubated under the aforementioned conditions, and measured by LC-MS/MS.

Additionally, human liver microsomes (HLM) (UltraPool™ HLM 150 Mixed Gender, Corning Inc., Amsterdam, The Netherlands) were used to study hepatic formation of desmethyl cyclobenzaprine, which is representative for first-pass metabolism. Microsomal metabolism studies were performed using a final concentration of 5 µM cyclobenzaprine at 37 °C. For this purpose, the substrate was added to an assay medium consisting of an NADPH regeneration system (NADPH Regenerating System Solution A and B, Corning Inc., Amsterdam, The Netherlands), 0.1 M potassium phosphate buffer and 0.25 mg HLM. Propranolol hydrochloride (100%, API, Caesar & Loretz GmbH, Hilden, Germany), verapamil hydrochloride (≥ 99, Sigma-Aldrich, Taufkirchen, Germany) and negative controls (drugs without HLM) served as assay

controls. Samples were drawn at 0, 5, 15, 30, 45 and 60 minutes, according to sampling time points during the permeation experiments. The reaction was stopped by the addition of ice-cold ACN.

5.2.3.3. Impact of alteration in dosage forms on drug liberation and absorption

In this context, the permeation model was intended to detect dosage form alteration and assess its effect on drug absorption in order to estimate the implications on *in vivo* application. Therefore, the SLTs were stored under stress conditions of 40 °C and 75% relative humidity for six months and subjected to the permeation model. Dissolution studies were conducted as reference method (section 5.2.4). SLTs stored at ambient conditions of 25 °C with 60% relative humidity were used as a control.

In addition to dissolution and permeation behavior, surface analysis was performed using visual examination as well as light microscopy (Leica DM LM, Leica Microsystems, Heerbrugg, Switzerland) of the tablets and the aluminum-aluminum primary packaging material (Patz 38/ALU-H 20, Constantia Patz, Loipersbach, Austria). Further analysis and identification of residual compounds was performed by high resolution time-of-flight mass spectrometry (TOF-MS) (AB Sciex TripleTOF 6600, Darmstadt, Germany), equipped with an IonDrive TurboV® electrospray ionization source (AB Sciex, Darmstadt, Germany) in positive ion mode under the following conditions: curtain gas (nitrogen) at 25 psi, ion spray voltage at 5500 V, nebulizer gas (zero air) at 20 psi, heater gas (zero air) at 20 psi, source temperature at 100 °C, declustering potential at 30 V and collision energy at 10 V. The aluminum-aluminum primary packing materials foiled with Pentapack BP 540 (Kinrooi, Belgium) were rinsed with 2 mL tetrahydrofuran ($\geq 99\%$, p.a., Sigma-Aldrich, Taufkirchen, Germany), evaporated under nitrogen stream at 40 °C with 300 rpm, and resuspended in methanol/water/FA (80:19:1 v/v/v).

5.2.4. Dissolution studies

Dissolution studies, as a conventional pharmaceutical evaluation procedure in formulation development, were performed for the SLTs to compare the power of dissolution studies versus the permeation model. Dissolution studies were conducted using baskets (United States Pharmacopeia (USP) apparatus 1) at 37 °C with a rotation speed of 50 rpm (Sotax AT7 smart, Sotax GmbH, Loerrach, Germany). The tablets were placed in 900 mL each of pH 6.8 phosphate buffer, and the released drug amount was quantified by LC with UV detection after sampling of 5 mL and filtering through 0.45 μm regenerated cellulose filter (Whatman GmbH, Dassel, Germany).

5.3. Results and Discussion

5.3.1. Simultaneous quantification of cyclobenzaprine and its related compounds

A LC-MS/MS method for simultaneous quantification of cyclobenzaprine, desmethyl cyclobenzaprine and cyclobenzaprine N-oxide has been successfully validated. Figure 23 shows the chromatogram of the three analytes and the IS with the respective structural formula. Linearity of the method ranging from 0.93 to 952.38 ng/mL for each analyte was achieved by using 11 non-zero calibration levels. The best fit was revealed by quadratic regression (weighted $1/x^2$) with $r \geq 0.997$.

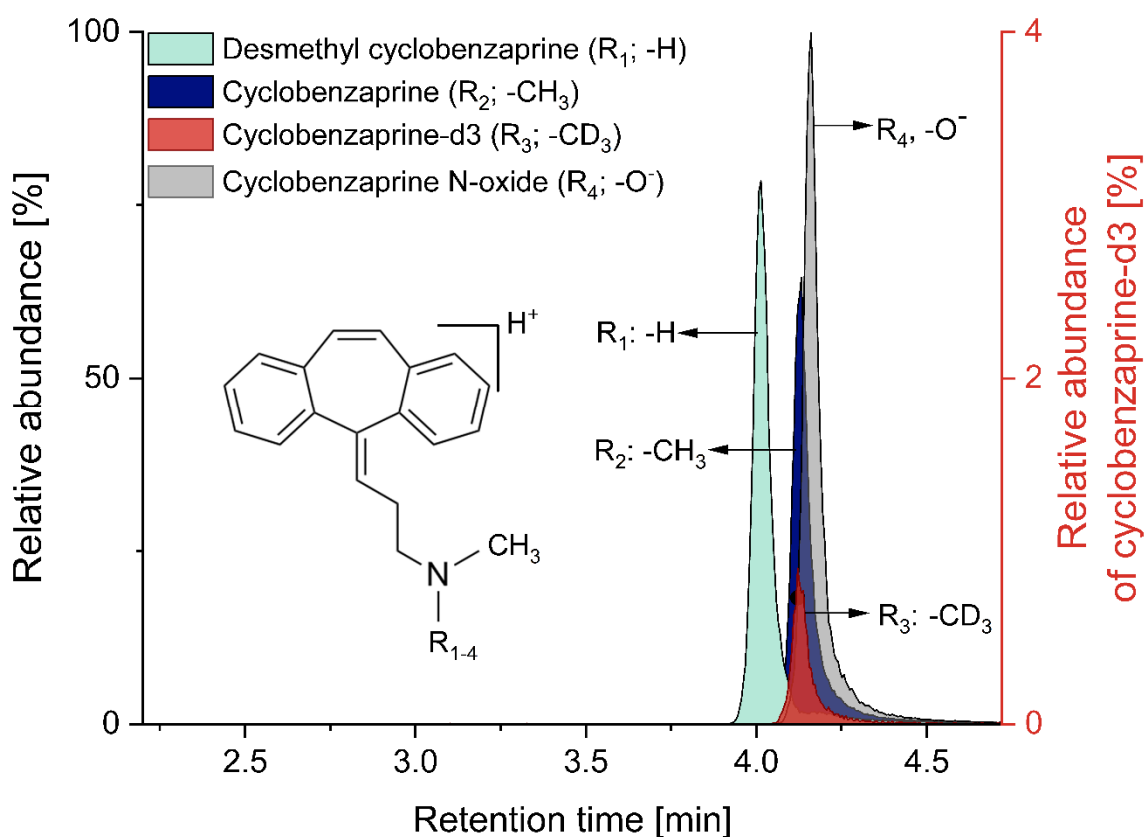


Figure 23: LC-MS/MS chromatogram of desmethyl cyclobenzaprine, cyclobenzaprine, cyclobenzaprine-d₃ and cyclobenzaprine N-oxide with the respective structural formula.

The results for accuracy and precision (within-run and between-run) complied with the acceptance criteria of the international guidelines and are summarized in Table 10. Sensitivity was achieved by analyte responses at the LLOQ of ≥ 7 compared to zero standard and S/N of $\geq 127:1$. Dilution integrity (1:5, 1:10, 1:20) of cyclobenzaprine was confirmed using concentrations between 1500 and 12000 ng/mL with RE ranging from -6.16 to 14.31% and CVs of 0.82 to 3.75%. Automated sampling by modified Hanson Research AutoPlus™ was verified for all analytes, resulting in a RE of -13.50 to 11.24%.

Thus, a sensitive LC-MS/MS quantification method including automated sampling and sample preparation for cyclobenzaprine, desmethyl cyclobenzaprine, and cyclobenzaprine N-oxide was reported for the first time and used within the studies presented here (Appendix 4 – 6).

Table 10: Summary of accuracy and precision results for simultaneous quantification of cyclobenzaprine hydrochloride and its related compounds, desmethyl cyclobenzaprine hydrochloride and cyclobenzaprine N-oxide (accuracy presented as mean relative error and precision as CV, n = 5 per run).

Analyte	Quality control [ng/mL]		Relative error [%]				CV [%]	
			Within-run			Between- run	Within-run	Between- run
			Run 1	Run 2	Run 3			
CBP HCl	HQC	476.19	4.50	-0.24	1.97	2.08	3.46	3.87
	MQC	59.52	1.04	3.27	3.71	2.67	2.73	2.81
	LQC	3.72	-6.06	-6.74	-5.03	-5.94	4.08	4.08
	LLOQ	0.93	13.33	8.68	16.63	12.82	4.28	5.21
Desmethyl CBP HCl	HQC	476.19	4.15	-3.98	-5.18	-0.66	3.57	6.07
	MQC	59.52	1.30	1.95	1.76	2.27	2.25	2.25
	LQC	3.72	-2.21	-5.04	-4.70	-3.41	4.25	4.25
	LLOQ	0.93	1.73	8.19	0.35	3.99	3.54	5.14
CBP N-oxide	HQC	476.19	-0.74	-8.36	-2.30	-3.21	3.77	5.37
	MQC	59.52	-5.49	-3.61	-1.34	-2.91	2.20	2.92
	LQC	3.72	-0.47	-3.99	0.57	-0.71	4.92	5.02
	LLOQ	0.93	0.25	-2.41	-3.18	-1.24	2.83	3.13

CBP HCl: cyclobenzaprine hydrochloride, CV: coefficient of variation, HQC: high quality control, LLOQ: lower limit of quantification, LQC: low quality control, MQC: middle quality control

5.3.2. Sublingual formulation development guided by permeation studies

In order to assess the usefulness of the permeation model in leading formulation development, cyclobenzaprine permeation from the differently composed SLTs was studied. In Figure 24 the impacts of dibasic phosphate on cyclobenzaprine permeation using SLTs are shown with calculated permeation lag times between 4.1 and 6.4 minutes. Q_t was improved significantly from 46.91 to 232.53 $\mu\text{g}/\text{cm}^2$ by increasing the amount of dibasic phosphate to 1.4% per tablet (EF of 2.89 and 4.68 for SLT-B and SLT-C, compared to SLT-A). Consequently, SLT-C improved cyclobenzaprine permeation most effectively. Increasing the permeation of cyclobenzaprine (pK_a of 8.47) by increasing pH values as a result of phosphate addition is in line with the pH-partition theory.

This trend is also consistent with results from preformulation studies (Figure 24B) using cyclobenzaprine solutions [Majid et al., 2021c], in that further increase of dibasic phosphate did not contribute to improvement of permeation. According to a direct comparison of results from cyclobenzaprine solutions versus those from tablets, an absolute increase in permeation as well as in the EF (4.68 vs. 2.00) was superior for the tablets. This could be attributable to the different concentration gradients during disintegration of the tablets in a volume of 100 μL , compared to the drug solution which was normalized to the donor volume of 2 mL. In the studies presented here, the physiological conditions for permeation were predetermined, so the formulation had to both increase and maintain pH in the microenvironment by its excipients to achieve the predicted improvement in permeation. Therefore, the permeation profiles of solution A and SLT-A without excipient addition were comparable. Due to the resulting pH in solution A as well as after administration of SLT-A, cyclobenzaprine was present almost completely ionized. This indicates that the paracellular pathway is the most likely for diffusion. As its capacity is limited, a less sensitive response to concentration changes can be expected [Nielsen and Rassing, 2002].

Moreover, based on the previous study of solutions consisting only of the two components cyclobenzaprine and varying proportions of dibasic phosphate, the permeation-enhancing effect can be attributed to the addition of dibasic phosphate acting by controlling the pH at the site of administration. Accordingly, only the phosphate portion was changed in the SLT compositions to selectively determine its effect on drug permeation. Analogously, the addition of dibasic phosphate to the tablets increased the permeability of cyclobenzaprine, which highlighted the effect of phosphate on permeability, while permeation between the SLT-A and solution A (both without dibasic phosphate) was comparable. Thus, the relationship between the obtained permeability coefficients and the amount of dibasic phosphate added showed a linear correlation in the preformulation study ($R^2 = 0.977$) as well as for the manufactured SLTs ($R^2 = 0.999$).

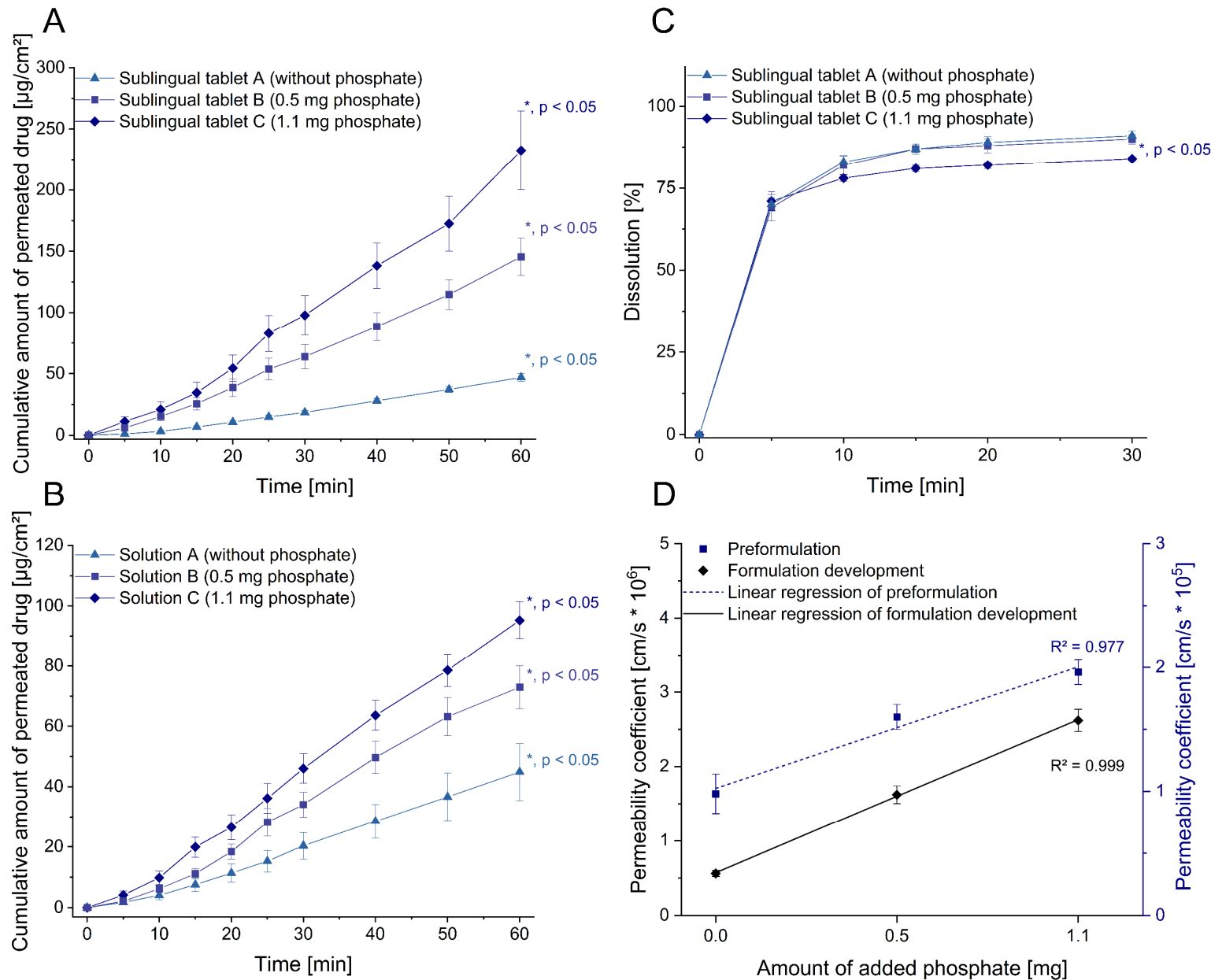


Figure 24: Impact of excipient addition in preformulation and formulation development of cyclobenzaprine.

A: Cumulative amount of permeated drug per cm^2 of the respective sublingual tablet (mean \pm SEM; $n \geq 5$).

B: Cumulative amount of permeated drug per cm^2 of the respective solution (mean \pm SEM; $n \geq 5$) [Majid et al., 2021c].

C: Dissolution of the respective sublingual tablet (mean \pm SEM; $n = 3$).

D: Correlation of obtained cyclobenzaprine permeability with the added amount of dibasic phosphate (mean \pm SEM).

R^2 : coefficient of determination, SEM: standard error of the mean, *: $p < 0.05$ (unpaired t-test).

Dissolution studies for evaluation of the new formulations showed no significant difference in the profiles of SLT-A and SLT-B, with 91% and 90% drug release respectively (Figure 24C). In contrast, a significantly lower drug release was measured with SLT-C (84%). Thus, an inconsistent rank order was observed compared to the preformulation and formulation development. Despite the use of a phosphate buffer medium, dissolution studies were not able to discriminate between the effects of formulation ingredients. For ionizable drugs such as cyclobenzaprine, the preferred properties for solubility or release are partially opposite to those for permeability, limiting the exclusive use of dissolution to assess the developed oromucosal formulations regarding absorption-affecting parameters and underlining the requirement for standardized permeation studies. During the permeation studies, a rapid disintegration of the tablets was observed, which was further investigated in a benchtop approach. The visually detected disintegration time of SLT-A, SLT-B and SLT-C after addition of saliva was uniform within 30 seconds. The records of the time course of the disintegration are shown in Figure 25. The oromucosal model presented combines absorption under physiological conditions, taking parallel processes such as disintegration, dissolution and permeation into consideration. In addition, it provides information on the amount of drug at the application site as well as its absorption capacity, so that technological outcomes can be linked to clinical significance.

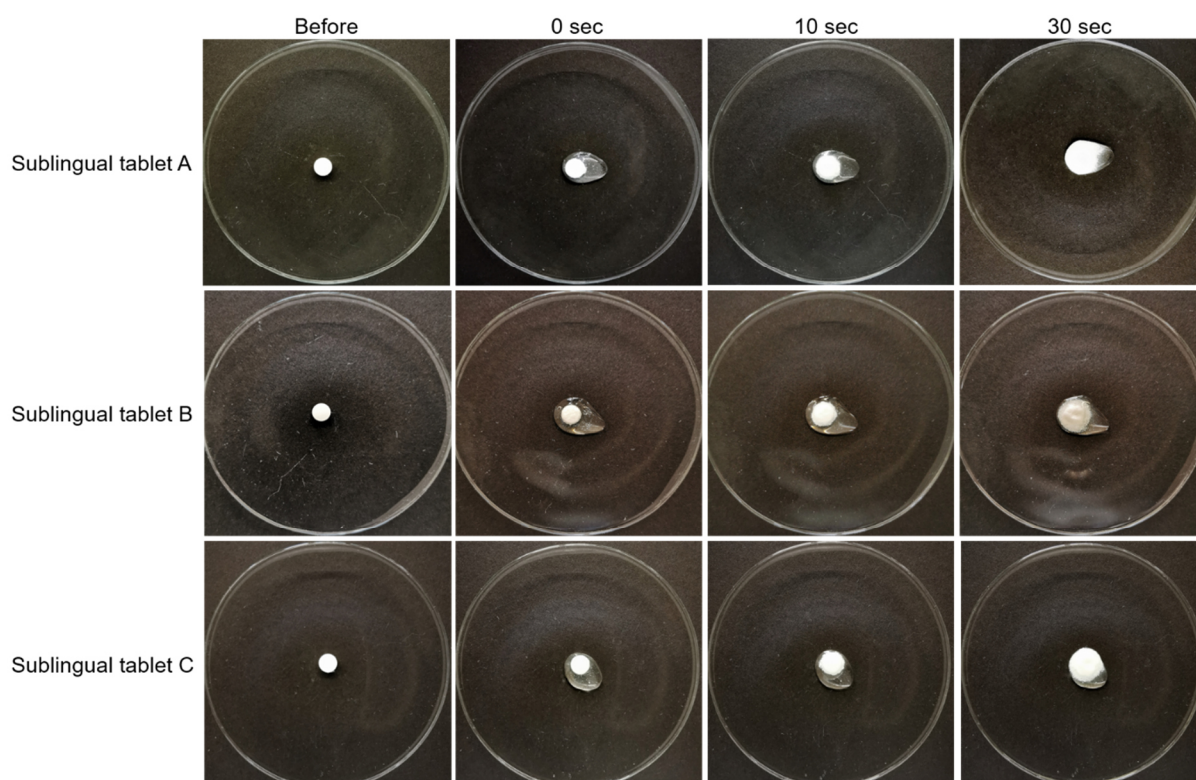


Figure 25: Disintegration of cyclobenzaprine sublingual tablets after addition of 150 μL freshly collected human saliva in dependence on time.

In summary, the SLTs were successfully evaluated in terms of resulting permeation as part of the formulation development for cyclobenzaprine. Furthermore, transferability between

preformulation and the final dosage forms allows in contrast to dissolution, the screening and grading of compositions and specific additives even before the dosage forms are manufactured. Under physiological conditions and standardized procedures, the selection of the final composition (SLT-C) was feasible and enables the targeted transfer into the following *in vivo* processes. As a result, a reliable and representative screening of the formulation candidates supports their development and optimization, and enables a reduction in the number of animal experiments required as well as a reduction of the resource expenditure associated with such experiments.

5.3.3. Metabolism of cyclobenzaprine during mucosal administration

In order to monitor the drug metabolism during transmucosal permeation, the formation of desmethyl cyclobenzaprine was analyzed (Figure 26). A remarkably low Q_t of $0.39 \mu\text{g}/\text{cm}^2$ was determined for desmethyl cyclobenzaprine, compared to a cyclobenzaprine permeation of $95.23 \mu\text{g}/\text{cm}^2$ after 60 minutes (Figure 26B). The relative mass balance of desmethyl cyclobenzaprine resulted in low values (from 0.04 to 0.11%) for the esophageal, buccal, and sublingual mucosa (Figure 26C). Concentrations of desmethyl cyclobenzaprine around and below the LLOQ were measured even when incubated with high cyclobenzaprine solutions of 14 mg/mL. In conclusion, no substantial formation by the mucosal tissues was detected as comparable amounts of desmethyl cyclobenzaprine were also found in the negative controls.

Thus, the overall percentages of less than 0.15% in each metabolization approach were in line with the degree of desmethyl cyclobenzaprine impurity and might be derived from drug synthesis. The USP defines desmethyl cyclobenzaprine as a compound related impurity B with an acceptable level of $\leq 0.15\%$ [The United States Pharmacopeia, 2019]. In contrast to mucosal tissue, HLM studies demonstrated continuous formation of desmethyl cyclobenzaprine of up to 2.5% relative to the applied amount of cyclobenzaprine (Figure 26D). In the negative control, the amount of desmethyl cyclobenzaprine was below the LLOQ. Intrinsic clearance of propranolol and verapamil as assay controls was consistent with reported data. In the literature, cyclobenzaprine is defined as an extensively metabolized drug with enterohepatic circulation [Cimolai, 2009]. The ratio of urinary desmethyl cyclobenzaprine to cyclobenzaprine was at least fivefold lower in clinical trials when administered intravenously, therefore bypassing the first-pass effect, compared to oral administration [Hucker et al., 1977]. A decreased formation of desmethyl cyclobenzaprine is linked to a reduction in daytime side effects. Since no mucosal formation of desmethyl cyclobenzaprine was detected by the oral mucosa and this route of administration circumvents the first-pass effect as well, sublingual delivery seems to compare favorably with approved oral administration.

The activity of the cytochrome P450 (CYP) system in the mucosa of the oral cavity has been studied to only a limited extent thus far. Determination of oromucosal CYP3A4 expression in comparable dimensions to the intestinal performed by Gao et al. indicated the potential presence of an absorption-related drug metabolism [Gao et al., 2014]. However, further studies showed limited catalytic activity by cytochrome P450, in which the use of CYP-inhibitors had no significant effect on permeation in human cell cultures [Obradovic and Hidalgo, 2008]. The studies presented here support this finding with respect to the demethylation of cyclobenzaprine, which resulted in the absence of substantial metabolization despite quantitatively monitored tissue viability. Similarly, after incubation of cyclobenzaprine in fresh human saliva desmethyl cyclobenzaprine levels were not detectable, although the expression of CYP1A2 and CYP3A4 in human salivary glands was reported [Kragelund et al., 2008]. In the case of cyclobenzaprine, beneficial sublingual administration was confirmed by a lack of absorption-related as well as avoided enterohepatic formation of desmethyl cyclobenzaprine when administered orally. The study of oromucosal metabolism was successfully implemented and applied to the permeation model and a further step in refinement to clinical conditions was achieved. When it comes to the assessment of metabolically susceptible peptides, the integration of metabolism studies in parallel to permeation appears especially necessary, and should also be further amended by non-CYP-based metabolism, e.g. by esterases and peptidases.

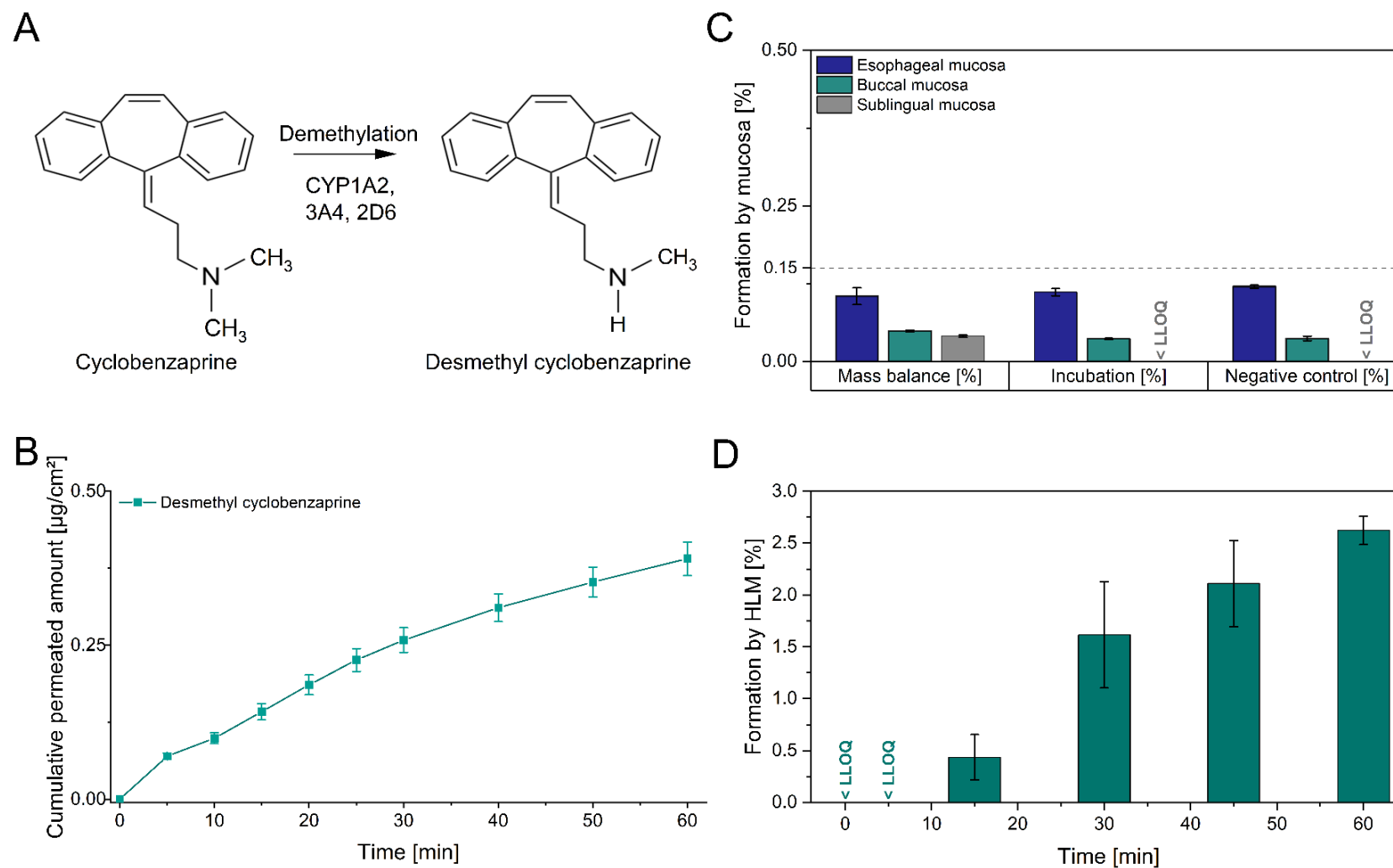


Figure 26: Cytochrome P450 metabolism of cyclobenzaprine. A: Scheme of cyclobenzaprine demethylation by CYP isoenzymes. B: Cumulative amount of permeated desmethyl cyclobenzaprine per cm^2 (mean \pm SEM; $n = 8$). C: Formation of desmethyl cyclobenzaprine by different mucosae and approaches (mean \pm SEM; $n \geq 2$). D: Formation of desmethyl cyclobenzaprine by human liver microsomes per time (mean \pm SEM; $n = 3$). CYP: cytochrome P450, HLM: human liver microsomes, LLOQ: lower limit of quantification, SEM: standard error of the mean.

5.3.4. Impact of alteration in dosage forms on drug liberation and absorption

Within formulation development, SLT-C proved to be the most promising candidate and was chosen as the final composition. Accordingly, stability studies of the SLTs under stress conditions (40 °C and 75% relative humidity for six months) were conducted in order to detect and compare formulation-related alterations using dissolution studies and the permeation model, while also estimating their clinical impact. Figure 27A and B illustrate the influence of stress storage conditions on dissolution and permeation. The permeated amount decreased significantly by 33.85% while dissolution decreased by 10.71% (based on the respective last measurement time) compared with storage under ambient conditions. In addition to the measurable decrease in release and permeation, a yellow oily coloration was observed in the aluminum-aluminum primary packaging material of the stressed SLTs (Figure 27C, D), which was not visible after ambient storage. Light microscopy images of the SLTs showed a uniform flat surface after ambient storage; however, under stress conditions the surface appeared much more porous with yellowish crystals on the tablet surface as well as in more pronounced form in the primary packaging material. TOF-MS spectra of the rinsed primary packaging material showed an approximately tenfold higher intensity for cyclobenzaprine under stress compared to ambient conditions, and no substantial signals for cyclobenzaprine N-oxide (Appendix 7 – 8)—which is described as the main degradation product of oxidation [Liu et al., 2014]—for either storage (Figure 27E, F).

Liu et al. reported a total of 15 degradation products for cyclobenzaprine based on three degradation pathways (exocyclic, endocyclic as well as oxidation of the tertiary amino group) by forced degradation studies [Liu et al., 2014]. None of the reported degradation products were detected in our studies. Salt disproportionation, rather than degradation, provided an explanation for the significantly higher cyclobenzaprine signal in the stressed primary packing material of the final composition SLT-C. Salt disproportionation is a process where the microenvironmental pH exceeds the pH_{max} of a basic drug and results in the conversion of the salt to the free base [Stephenson et al., 2011]. In solid dosage forms, salt disproportionation is both solution and excipient-mediated. The increased humidity of 75% and the use of hygroscopic excipients (crospovidone) may have led to initial moistening of the tablet surface with the formation of an aqueous diffusion layer and its internal migration [Koranne et al., 2017], resulting in a basic microenvironmental pH due to the use of dibasic phosphate. This may have exceeded the pH_{max} of cyclobenzaprine as a weak base with a pK_a of 8.47 and gradually induced the thermodynamically driven crystallization and accumulation of the lipophilic compound ($\log P_{ow} = 5.2$) on the primary packaging material through the tablet surface. Further factors affecting the extent of disproportionation are the ratio of API to basic excipient,

the temperature (40 °C rather than 25 °C), and the amorphization of compressed tablets [Patel et al., 2018].

Different results in dissolution and permeation according to alteration of the dosage forms underline the effectiveness of the permeation model from section 5.3.2., whereas the discrepancy between the effects can be explained as follows. The sole adoption of dissolution studies for SLTs does not consider the physiological situation, hence the storage effects are only defined by the drug loss to the primary packaging material, which was not accessible for dissolution. In addition, the precipitated drug amount on the tablet surface might be resolved due to the pH of 6.8 in dissolution studies. During the disproportionation reaction, the dibasic phosphate dissolved in the aqueous layer and contributed to the assumed alkalization of the medium, which caused its migration out of the tablet. In section 5.3.2 the substantial influence of reduced phosphate amount on the permeation capacity of cyclobenzaprine was presented. Besides the steps of disintegration and dissolution, the model also considers the drug permeation interaction in physiological approximation instead of using the artificial vessel approach. Thus, the influence of the tablet texture, the reduced phosphate content, the solubility of the precipitated drug, the concentration gradient, the composition, and the available volume of the biological medium on the multiple processes were all considered, whereas these influences are suppressed in the dissolution approach. Therefore, a loss measurement of 10.71% in dissolution might underestimate the actual clinical impact of lower drug exposure. Using the permeation model enabled a clinically representative description of the potential impact on patients. This emphasizes the suitability and sensitivity of the physiologically relevant permeation model for the detection and classification of alterations and the instability of solid oromucosal dosage forms, and thus also for estimation of their clinical relevance.

Within this proof of concept approach, the performance of the model in several stages of formulation development was demonstrated by the clinically representative assessment of optimizations in the sublingual dosage form. The permeation of cyclobenzaprine was thereby enhanced by a factor of 4.68 in the final composition, enabling dose reduction and consequently contributing to patient safety. The metabolization of cyclobenzaprine to desmethyl cyclobenzaprine during mucosal permeation was successfully integrated into the permeation model. It has been shown that no desmethyl cyclobenzaprine was formed by the permeation of various mucosal membranes, thus supporting the improvement of patient adherence by reducing side effects associated with the active metabolite [Sullivan et al., 2021].

In addition to previously reported model suitability in preformulation, an advancement to sublingual formulation development was achieved within this study. The parallel processes of disintegration, dissolution, permeation and metabolization were integrated in a physiological

study design and a standardized controlled environment, allowing efficient and targeted drug development. In comparison with conventional dissolution studies, the model obtained more sensitive and distinct outcomes by its adaptation to sublingual administration, with regard to the optimization of composition in formulation development as well as the impact of dosage form stability. Therefore, the model proves its usefulness as a bridging element between conventional *in vitro* characterization and pharmacokinetic *in vivo* studies. Oromucosal administration contributes to patient adherence through broad patient acceptance, ease of administration, and therapeutic safety [Tian et al., 2019] and also allows for patient- and symptom-tailored drug delivery. However, for the evaluation of patient-oriented dosage forms in early development stages, appropriate *ex vivo* studies are limited. For these development-intensive formulations in particular, the model presented here enables a reliable and physiologically/clinically relevant screening mechanism to support the advancement of patient-oriented drugs under resource-efficient conditions.

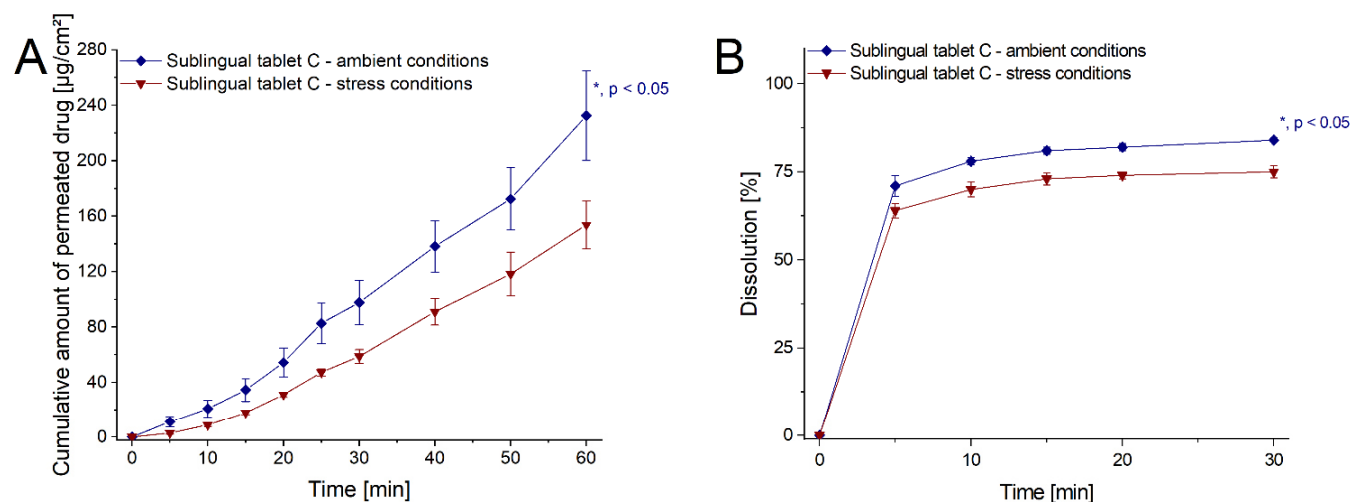


Figure 27: Alteration of cyclobenzaprine sublingual tablets under ambient and stress conditions.

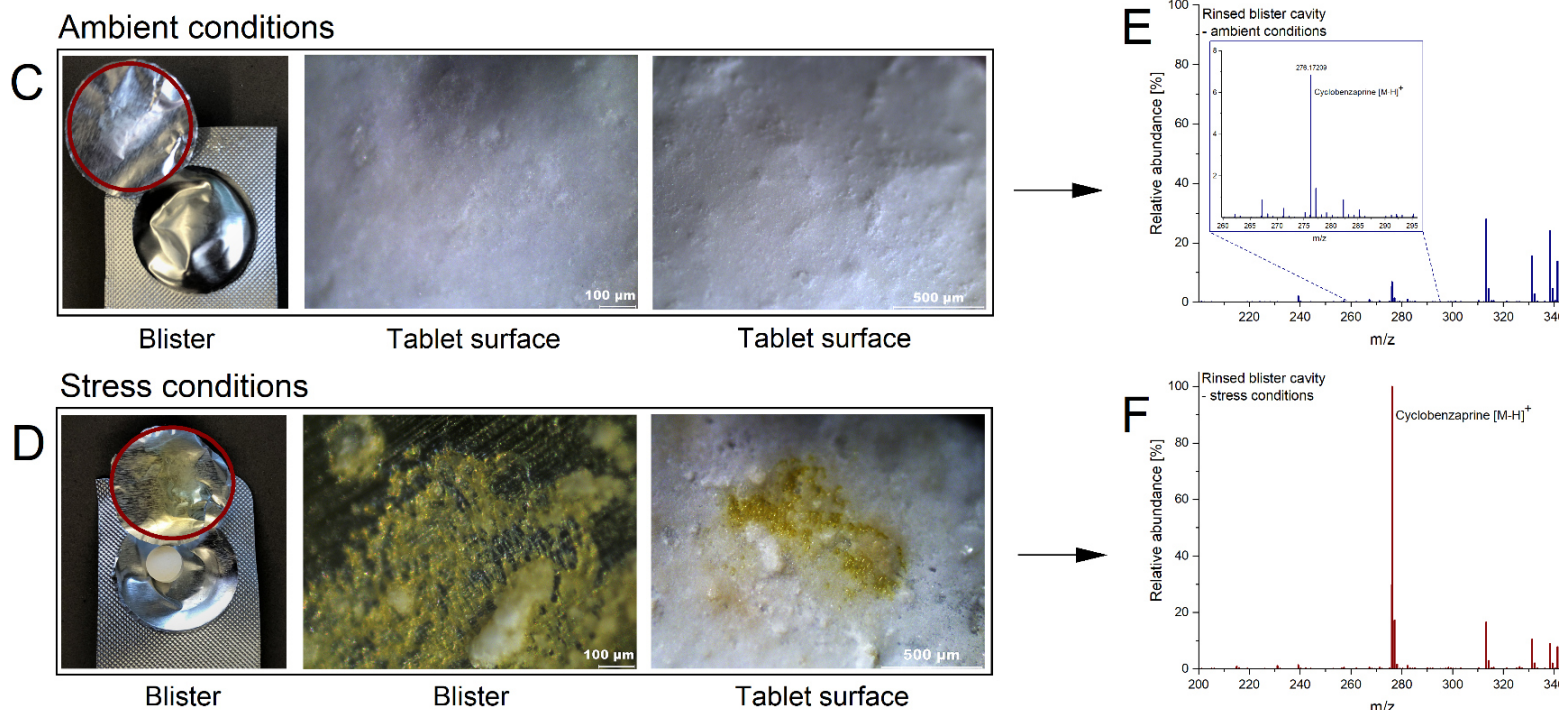
A: Cumulative amount of permeated drug per cm² of the respective sublingual tablet stored (mean ± SEM; n ≥ 4).

B: Dissolution of the respective sublingual tablet stored (mean ± SEM; n = 3).

C, D: Visual and microscopic inspection of the primary packaging material and the tablet surface after storage under ambient and stress conditions, respectively.

E, F: TOF-MS scan of the rinsed residuals from packaging material after storage under ambient and stress conditions, respectively.

m/z: mass-to-charge ratio, *SEM*: standard error of the mean, *: *p* < 0.05 (unpaired *t*-test).



5.4. Conclusion

A standardized and physiologically relevant *ex vivo* model on oromucosal permeability was successfully applied to lead sublingual formulation development of cyclobenzaprine, with more than fourfold enhancement in permeation achieved by optimizing the formulation. Advanced optimization of the model facilitated the decisive assessment of oromucosal formulations combining the simultaneous impact on disintegration, dissolution, permeation and metabolization. In addition, the suitability of the method of detection and evaluation of dosage form alteration and its impact on drug absorption was demonstrated. The effectiveness and predictivity of the presented model thus enable its application for the purposive development of patient-centered intraoral dosage forms.

6. Predictivity of Standardized and Controlled Permeation Studies: Ex vivo – In vitro – In vivo Correlation for Sublingual Absorption of Propranolol

6.1. Introduction

The advantages offered by drug administration via the oral cavity (avoidance of gastrointestinal drug degradation and first-pass metabolism, rapid systemic availability, patient adherence, etc.) increased its pharmaceutical attractiveness as an alternative route of administration and concomitantly the development of novel oromucosal dosage forms [Sattar et al., 2014]. In this regard, studies on drug permeability are a widely applied biopharmaceutical prediction tool at the preclinical stage. They facilitate the characterization of compounds and NCEs for their absorption potential through this new route of administration. Thereby, the pH of the microenvironment plays an ambivalent role between solubility and permeability for ionizable drugs. Besides their fundamental application in substance classification, applicability has been demonstrated in subsequent galenic phases, particularly in preformulation, excipient screening, and formulation development [Kottke et al., 2020; Majid et al., 2021c; Majid et al., 2021d].

Permeation studies are generally classified accordingly to their design and the type of barrier used, into *in vitro* (cell lines or artificial membranes), *ex vivo* (dissected tissue) and *in vivo* (living organism). The effort and cost associated with *in vivo* experiments lead to an increasing focus on *ex vivo* and *in vitro* studies [Pinto et al., 2020; Wang et al., 2020]. However, it is estimated that approximately 190 million animal experiments are conducted annually [Taylor and Alvarez, 2019], with a substantial proportion attributed to pharmaceutical development. However, in the specific case of oromucosal permeability, the experimental limitations of *ex vivo* and *in vitro* approaches (e.g., clinically non-representative and diverse study designs or a deficiency of standardization and control combined with few reliable correlations to *in vivo* data) [Delvadia et al., 2012; Holm et al., 2013; Palem et al., 2016; Patel et al., 2012; Sattar et al., 2014] often confine their application to academic research and impede broad regulatory use [Pather et al., 2008; Sarmiento, 2016; Sattar et al., 2014]. Oromucosal permeability studies using *in vitro* models mainly consist of primary (e.g. hamster cheek pouch) or continuous cell lines (e.g. TR146) with incomplete differentiation or carcinogenic origin. Human keratinocytes or available tissue models (e.g. EpiOral™) simulate the oral cavity more accurately but are less suitable for wide routine implementation [Shrestha et al., 2016]. Therefore, there is growing interest in the use of biomimetic artificial membranes (Permeapad® Barrier) as an alternative

This work was published in an international peer-reviewed journal [Majid et al., 2021b]:

Majid, H., Bartel, A., Burckhardt, B.B., 2021. Predictivity of Standardized and Controlled Permeation Studies: Ex vivo – In vitro – In vivo Correlation for Sublingual Absorption of Propranolol. *European Journal of Pharmaceutics and Biopharmaceutics* 169, 12–19. <https://doi.org/10.1016/j.ejpb.2021.09.002>.

The author of this thesis was responsible for conceptualization, methodology, validation, formal analysis, investigation, writing-original draft, and visualization.

barrier to study oromucosal permeability without the use of animal tissue or cell models [Brandl and Bauer-Brandl, 2019]. While artificial barriers were primarily investigated for the peroral administration, such studies remain limited to single drugs regarding their oromucosal *in vivo* predictivity [Bibi et al., 2016]. However, cell-free membranes are a promising alternative due to their rapid and easy application as well as high reproducibility by avoiding biological variability.

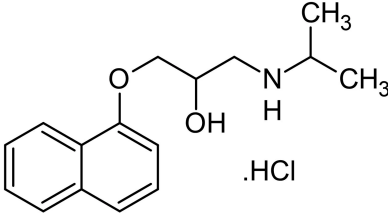
On the one hand, reliable and predictive *ex vivo* and *in vitro* models are a prerequisite for reducing the amount of future animal testing during preclinical drug development according to the principle of the 3Rs (replacement, reduction, refinement) [Russell and Burch, 1992]. On the other hand, the choice between heterogeneous and inadequate *ex vivo/in vitro* permeability studies or costly and disproportionate animal experiments hinders the progressive development of further intraoral drugs [Wang et al., 2020]. To address the aforementioned experimental limitations (e.g., lacking reliability through insufficient standardization), an *ex vivo* permeation model considering experimental, analytical, and physiological optimizations was validated [Majid et al., 2021a]. Accurate correlation renders this *ex vivo* model suitable for oromucosal preformulation and excipient selection for SLTs [Majid et al., 2021c; Majid et al., 2021d]. However, within its proof of concept approach, *in vivo* correlation has not yet been investigated.

Accordingly, the objective of this study was to evaluate the predictivity of the developed model using porcine mucosa (*ex vivo*) in comparison to available animal data (*in vivo*). In addition, the usefulness of biomimetic barrier (*in vitro*) as an alternative for porcine mucosa was investigated. For this purpose, a multiple level C *ex vivo* – *in vitro* – *in vivo* correlation was applied based on the pH-dependent permeability of the model drug propranolol hydrochloride and reported *in vivo* plasma concentrations after sublingual administration.

6.2. Materials and Methods

With reference to the published animal studies on propranolol from Dali et al. [Dali et al., 2006], an IVIVC was conducted to evaluate the *in vitro* and *ex vivo* models regarding their respective *in vivo* predictions. Therefore, the *in vitro* and *ex vivo* models were initially adapted (e.g. analytical method validation) for sublingual liquid formulations of propranolol being reported by Dali et al. Followed by corresponding investigation of drug solubility, *ex vivo* and *in vitro* permeability, as well as IVIVC. The physicochemical properties of the model drug propranolol hydrochloride are presented in Table 11.

Table 11: Physicochemical and pharmaceutical properties of propranolol hydrochloride.

Drug	Propranolol hydrochloride
Molecular formula	C ₁₆ H ₂₂ ClNO ₂
Structural formula	
Molecular weight [g/mol]	295.8
pK _a	9.23
Log P _{ow}	3.21 (free base)
BCS class	1 (high solubility; high permeability)
Pharmacological class	Nonselective beta receptor blocker

BCS: biopharmaceutical classification system, log P_{ow}: Logarithm of partition coefficient, pK_a: negative decimal logarithm of the acid dissociation constant

6.2.1. Analytical method validation

Propranolol quantification was performed via LC-ESI-MS/MS (Shimadzu Prominence, Shimadzu Europe, Duisburg, Germany; AB Sciex API 2000, Darmstadt, Germany). Chromatographic separation occurred on a Luna PFP (2) (100.0 × 2.0 mm; 3 μm) column equipped with SecurityGuard PFP (2) (4.0 × 2.0 mm) (Phenomenex Ltd. Aschaffenburg, Germany). Then, 0.1% FA (≥ 98%, p.a., Sigma-Aldrich, Taufkirchen, Germany) in water (LC-grade, Fisher Scientific, Schwerte, Germany) and 0.1% FA in ACN (LC-grade, Fisher Scientific, Schwerte, Germany) were used as mobile phases at a flow rate of 450 μL/min and

a maintained column temperature of 50 °C. The retention time of propranolol and propranolol-d7 (99%, Cayman Chemical, Ann Arbor, MI, USA) as a deuterated IS was 2.68 minutes after an injection of 5 µL and linear gradient elution with a total run time of 3.9 minutes. For determination in MRM mode, the mass transitions of 260.2 to 116.0 m/z for propranolol and 267.4 to 116.0 m/z for propranolol-d7 were used with the following compound-specific conditions: declustering potential of 25 V/61 V, focusing potential of 290 V/380 V, entrance potential of 5 V/11 V, cell entrance potential of 10 V/22 V, cell exit potential of 14 V/12 V, and collision energy of 28 V for both. Analyst®1.5.1 (AB Sciex, Darmstadt, Germany) software was used for data acquisition and evaluation.

The quantification method was validated considering EMA, FDA, and ICH Q2 guidelines for linearity, accuracy, precision, dilution integrity, and recovery [European Medicines Agency, 2012; International Council for Harmonisation of Technical Requirements for Pharmaceuticals for Human Use, 2005; U.S. Department of Health and Human Services Food and Drug Administration, 2018]. Moreover, the conducted studies were monitored by an aligned QC system, comprising LC-MS/MS run evaluation through system suitability and QCs as well as verification of automated sample preparation. The corresponding specifications were defined as a maximum RE of ±15% (±20% at the LLOQ), r above 0.99 for the freshly prepared calibration curve, and an acceptance criterion for the seven QCs with a maximum RE of ±15%.

6.2.2. pH-dependent thermodynamic solubility

By applying a modified shake-flask method, the impact of various pH, buffer systems, and solubilizing agents on the solubility of propranolol in the referred liquid formulations were determined [Baka et al., 2008; Dali et al., 2006]. Therefore, solubility was investigated in 0.15 M citrate-phosphate buffer using citric acid (100%, Caesar & Loretz GmbH, Hilden, Germany) and disodium hydrogen phosphate, adjusted at pH 5.0, 6.4, 7.4 and 8.0 as well as in 0.05 M glycine (≥ 99.7%, p.a., Sigma-Aldrich, Taufkirchen, Germany), adjusted to pH 9.0 with sodium hydroxide (≥ 99%, p.a., VWR Chemicals, Langenfeld, Germany). The aforementioned solutions additionally consisted of 10% propylene glycol (Ph. Eur., Caesar & Loretz GmbH, Hilden, Germany) and 5% ethanol (≥ 99.8%, GC-grade, Sigma-Aldrich, Taufkirchen, Germany). An excess quantity of propranolol hydrochloride (100%, API, Caesar & Loretz GmbH, Hilden, Germany) was added to the solutions and the pH was readjusted using 0.1 M citric acid or 1.0 M sodium hydroxide. Equilibration of the drug solution occurred under a constant temperature of 37 °C and 360° agitation using a rotary shaker for 6 hours (Intelli Mixer RM-2S, Elmi, Riga, Latvia) followed by sedimentation of 18 hours at 37 °C. Thereafter, the pH was readjusted and the tubes were centrifugated for 30 minutes at 37 °C and 2000 x g (Centrifuge 5810 R, Eppendorf AG, Hamburg, Germany). Finally, the supernatant was filtered

through 0.2 µm pore size cellulose filter, diluted into the calibration range, spiked with IS, and measured by LC-MS/MS.

6.2.3. Ex vivo and in vitro permeability

6.2.3.1. Permeation study design

A standardized *ex vivo* permeation process [Majid et al., 2021a] was used to investigate the permeability of propranolol. The single components comprised the Kerski diffusion cell [Kerski et al., 2020] with fully automated sampling and sample preparation performed using a modified Hanson Research AutoPlus™ (Teledyne Hanson, Los Angeles, USA) and HTS PAL autosampler (CTC Analytics AG, Zwingen, Germany), respectively. Drug quantification was carried out by coupling to LC-MS/MS. PBS buffer was used as acceptor medium prepared by dissolving sodium chloride (≥ 99.5%, p.a.), potassium dihydrogen phosphate (≥ 99%, p.a., Roth GmbH, Karlsruhe, Germany), disodium hydrogen phosphate (≥ 99%, p.a., Riedel-de-Haen, Seelze, Germany) as well as potassium chloride (≥ 99.5%, p.a.) and adjusting the pH to 7.4 using orthophosphoric acid (85%, p.a., AppliChem, Darmstadt, Germany). To mimic the physiological conditions of the oral cavity, the membrane was equilibrated through the donor chamber using freshly collected human saliva under fasting conditions. Thereafter, the formulation to be tested was placed onto the saliva-moistened barrier. Constant environmental conditions of 37 °C and 20% relative humidity (KBF 115 Constant Climate Chamber, Binder GmbH, Tuttingen, Germany), as well as continuous stirring at 750 rpm (2mag Mixcontrol20, Muenchen, Germany), were maintained throughout the study period. Fully automated sampling was scheduled from 5 to 60 minutes. The sampling procedure included 4 mL of rinsing followed by 0.5 mL of sampling and full refilling to 10 mL. This was followed by spiking with propranolol-d7, dilution with water (1:10) into the analytical calibration range, and agitation using HTS PAL with Chronos 5.0 software (Axel Semrau GmbH, Sprockhoevel, Germany). Novel post-study tissue integrity and viability assays were implemented to monitor the permeation process [Majid et al., 2021a]. A reevaluation of the permeability data was conducted and excluded non-compliant measurements and diffusion cells, where applicable.

For the standardized *ex vivo* model, fresh porcine esophagi were provided by the slaughterhouse Naturverbund Thönes (Wachtendonk, Germany) as a waste product and were dermatomed to a thickness of 500 µm (Integra® Dermal, Ratingen, Germany). Several studies [Diaz Del Consuelo et al., 2005b; Diaz Del Consuelo et al., 2005c; Diaz Del Consuelo et al., 2005a; Telò et al., 2016] proved the comparability of esophageal mucosa to oral mucosa. Accordingly, esophageal tissue was used as a surrogate for oral mucosa due to its experimental advantages (i.e., ease of preparation, consistent thickness, less destruction during slaughter, and high yield of usable membranes in line with 3Rs). As a sub-investigation (*in vitro*), an artificial biomimetic Permeapad® Barrier (25 mm diameter, InnoMe GmbH,

Espekamp, Germany) was applied in the permeation process instead of the usual porcine mucosa.

6.2.3.2. Impact of formulation pH on oromucosal permeability

In addition to studying the impact of the formulation on drug solubility, its impact on oromucosal permeability was comparatively examined utilizing the standardized *ex vivo* model and the alternative *in vitro* studies. In this context, five different liquid formulations in line with Dali et al. were investigated [Dali et al., 2006]. Therefore, 12.1 mg/mL propranolol hydrochloride solutions were prepared with different pH values. For pH 5.0, 6.4, 7.4, and 8.0, 0.15 M citrate-phosphate buffer was adjusted to the respective pH and 10% propylene glycol as well as 5% ethanol were added. For the formulation at pH 9.0, 0.05 M glycine solution was adjusted with sodium hydroxide, while 10% propylene glycol and 5% ethanol were also added. The freshly prepared solutions were vortexed for 5 minutes and 500 μ L was applied in the donor chamber of the diffusion cell.

In the *ex vivo* model, the different formulations of propranolol were investigated using excised mucosal membranes. To examine the suitability of the alternative biomimetic membranes, the effect of the formulation on permeability was investigated using Permeapad® and compared to the *ex vivo* approach (*ex vivo* vs. *in vitro*). For this purpose, biomimetic Permeapad® Barriers were used instead of porcine mucosa under equal experimental conditions.

For the analysis of propranolol permeability, the Q_t , J_{SS} , and P_{app} were calculated using Equation 1 – 3. Statistical differences were evaluated using unpaired Student's t-test or Mann-Whitney U test with $\alpha = 0.05$.

6.2.4. Ex vivo – in vitro – in vivo correlation

In the interest of animal welfare, we refrained from conducting our own animal experiments and instead used published *in vivo* data on sublingual absorption. Dali et al. investigated the impact of various parameters (e.g., the pH of liquid formulations) in oromucosal drug delivery using a rabbit model. For this purpose, four different liquid formulations containing 41 mM (\pm 12.1 mg/mL) propranolol hydrochloride in citrate-phosphate buffer (pH 5.0, 6.4, and 7.4) or glycine-sodium hydroxide (pH 9.0), respectively with 10% propylene glycol and 5% ethanol were prepared and applied sublingually to New Zealand rabbits (weight approx. 3 kg). The plasma concentration profile with the AUC, including the maximum plasma concentration (C_{max}) and the corresponding time (T_{max}), were determined for each formulation to characterize the effect of formulation pH on systemic availability of propranolol after oromucosal administration [Dali et al., 2006].

A multiple level C correlation compares several experimental parameters with the appropriate pharmacokinetic parameters to predict the effects of individual factors on drug exposure [Lu et

al., 2011]. Therefore, the mean \pm standard deviation of the reported AUC and C_{max} values were cross-correlated with the obtained P_{app} , Q_t , and J_{SS} from *ex vivo* and *in vitro* studies (multiple level C correlation) to verify their predictive power regarding pH-dependent oromucosal absorption. Additionally, a point-to-point correlation of the *in vivo* AUC_{0-t} with the corresponding Q_{0-t} data was conducted. The single plasma concentration values were extracted (mean of $n = 3$ using WebPlotDigitizer Version 4.4 [Rohatgi, Pacifica, California, USA]) from Dali et al. [Dali et al., 2006].

6.3. Results and Discussion

6.3.1. Analytical method validation

The analytical method for the quantification of propranolol within permeation studies was successfully validated. Chromatograms after the injection of the zero sample, the LLOQ, and the ULOQ are shown in Figure 28. During validation, the intra-run and inter-run CVs for system suitability ($n = 6$) were ≤ 2.16 and 7.07%, respectively. Method linearity was verified in the range of 1.86 to 1904.76 ng/mL using 11 non-zero calibration standards. Quadratic regression and a weighting of $1/x^2$ provided the best fit with $r \geq 0.995$.

The RE for LQC, MQC, and HQC ranged from -7.40 to 0.82%. Moreover, at the LLOQ, the within-run accuracy ranged from -18.98 to -7.87%. The between-run accuracy obtained on two different days resulted in a RE between -12.53 and -0.54%. Method precision was assessed by one-way ANOVA and resulted in a CV of 1.29 to 14.74% for within-run and between-run precision. Additionally, S/N at the LLOQ of at least 123:1 were achieved in three analytical runs. The automated 1:10 dilution step for the appropriate dilution of samples into the calibration range met the acceptance criteria. The accuracy, precision, and dilution integrity results are summarized in Table 12. The recovery rates were in line with the specified acceptance criteria. A mean RE ($n = 8$) of between -3.78 and -0.50%, as well as a CV ranging from 2.21 to 3.34%, were determined for the concentrations of 200 and 20 ng/mL.

Thus, a sensitive and validated LC-MS/MS quantification method incorporating automated sampling and sample preparation for propranolol was applied for subsequent *in vitro* and *ex vivo* permeation studies.

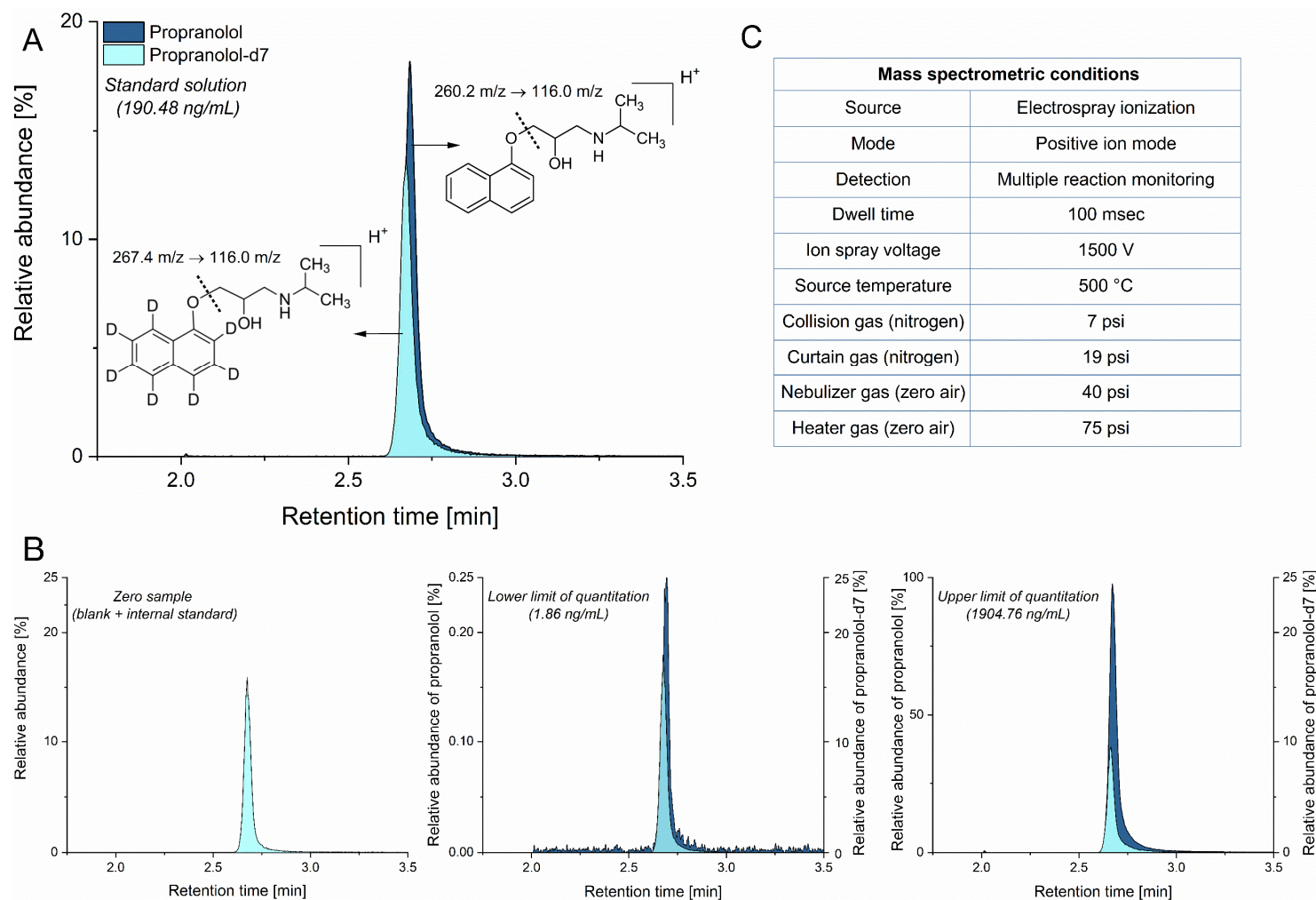


Figure 28: LC-MS/MS chromatograms of propranolol and propranolol-d7 including the respective mass transition and fragmentation (A), at different concentrations (B) with a tabular summary of mass spectrometric conditions (C). *m/z*: mass-to-charge ratio.

Table 12: Summary of accuracy, precision, and dilution integrity of propranolol hydrochloride (accuracy as mean relative error and precision as CV).

Parameter	Level	NomConc. [ng/mL]	Relative error [%]				CV [%]		
			Run 1	Run 2	Run 3	Between -run	Within -run	Between -run	
Accuracy + precision	HQC	1904.76	-2.07	-3.88	-0.92	-2.29	1.35	1.94	
	MQC	119.05	-2.47	0.03	0.82	-0.54	1.29	2.08	
	LQC	7.44	-0.87	-7.40	-5.70	-4.66	2.87	4.38	
	LLOQ	1.86	-7.87	-18.98	-10.73	-12.53	14.74	14.74	
Dilution integrity	1:10	3200				-11.35	2.97		

CV: coefficient of variation, HQC: high quality control, LLOQ: lower limit of quantification, LQC: low quality control, MQC: middle quality control, NomConc.: nominal concentration

6.3.2. pH-dependent thermodynamic solubility

The thermodynamic solubility of the API was studied in the specific formulation medium reported by Dali et al. [Dali et al., 2006]. The pH examination of the saturated solutions resulted in the following effective pH values: 5.0, 6.4, 7.4, 7.8, and 8.9. The solubility in acidified mediums of pH 5.0 and 6.4 were 175.0 and 178.5 mg/mL, respectively and decreased substantially from pH values above 6.4. By increasing the pH of the medium from 7.4 to 7.8, the solubility halved from 159.2 mg/mL and reached the lowest solubility at pH 8.9 (1.9 mg/mL). Figure 29 shows the influence of pH on the solubility profile compared to the degree of ionization of propranolol. An inverse proportional relation between the percentage of unionized fraction of the drug and its total solubility was observed. Within the pH range of 5.0 to 9.0, the proportion of unionized propranolol ranged from 0.01 to 37.06%.

The total solubility of a basic drug is composed of the solubility of the ionized and free base form. This fact was addressed by two individual pH-solubility relation curves (Figure 29). The point of intersection defines the pH with the maximum solubility of both forms as:

$$pH_{max} = pK_a + \log\left(\frac{S_B}{S_{Ion}}\right).$$

At pH 5.0, a solubility of 175.00 mg/mL was obtained with an ionized fraction of 99.99%, from which the solubility of the ionized form can be derived. Similarly, the solubility of the free base

at $\text{pH} > \text{pH}_{\text{max}}$ was determined in accordance with the presented ionization level. Hence, a pH_{max} of 6.76 was calculated for propranolol in the formulation medium under the presence of 15% cosolvents, implying that propranolol hydrochloride represents the precipitate at $\text{pH} < \text{pH}_{\text{max}}$ and the free propranolol base represents the precipitate at $\text{pH} > \text{pH}_{\text{max}}$. While the addition of cosolvents in the formulations increases total solubility, different solubilities of propranolol in aqueous buffer systems or water were described (range: 23.05 to 251.52 mg/mL) [Rekhi et al., 1995; Wang et al., 2010], which can also be attributed to variations in experimental conduct.

Accordingly, based on thermodynamic solubility being a significant parameter in the preclinical phase, the maximum solubility at a pH of 6.76—which decreases rapidly with increasing proportion of the unionized fraction—has to be considered for subsequent permeability studies.

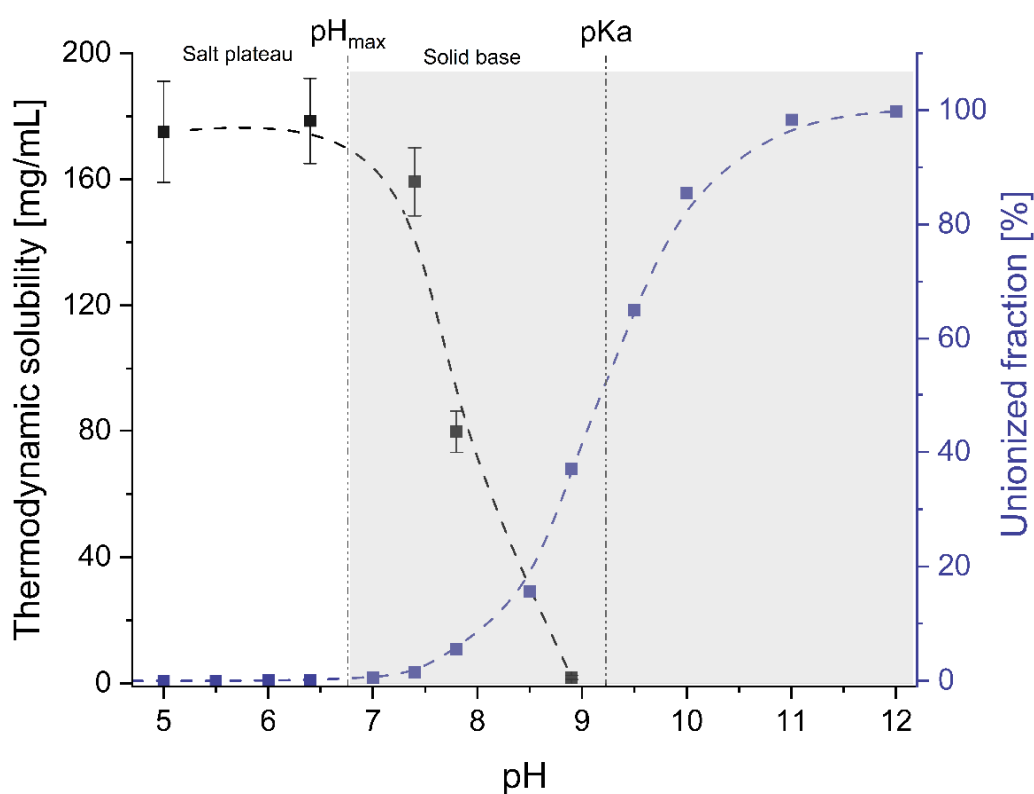


Figure 29: Impact of pH on the relationship between the thermodynamic solubility and the unionized fraction of propranolol in the liquid formulations (mean \pm SEM; $n = 2$). The pH_{max} , pK_a (dotted lines), and pH range for the solid base (gray background) are highlighted. pH_{max} : pH of maximum solubility, pK_a : negative decimal logarithm of the acid dissociation constant.

6.3.3. Impact of formulation pH on oromucosal permeability

After characterizing the pH-dependent solubility, the effect of pH on the permeability of propranolol was investigated using two alternative approaches to animal testing (*ex vivo* and *in vitro*). Appendix 9 – 12 present examples of the different runs within a permeation study of propranolol hydrochloride formulations.

Ex vivo studies

Figure 30 visualizes the pH-dependent permeation profiles of propranolol through porcine esophageal mucosa, as Q_t . The permeation of propranolol was significantly improved (12.71 to 447.03 $\mu\text{g}/\text{cm}^2$) by increasing the pH stepwise from 5.0 to 7.4. However, at pH 8.0, a countertrend decreased permeation was observed (220.62 vs. 447.03 $\mu\text{g}/\text{cm}^2$), with a remarkably high standard deviation. This finding was attributed to the time-dependent formation of an unstable suspension in the donor chamber at pH 8.0, where the subsequently flocculated and floating drug was not available for permeation, resulting in decreased and variable permeability data. The abrupt decrease in permeability at pH values above 7.4 was consistent with findings of Wang et al. [Wang et al., 2010]. According to the pH-partition theory, increasing the proportion of the unionized drug while raising the pH is expected to increase permeability for weak monobasic substances such as propranolol with a pK_a of 9.23 [Schoenwald and Huang, 1983; Schürmann and Turner, 1978; Shore et al., 1957]. The results were in line with previous *ex vivo* studies of pH-dependent oromucosal permeability by Wang et al., reporting the highest permeability of propranolol at pH 7.4, despite differences in the solubilities, which were determined as being potentially related to the utilized medium and methodology [Wang et al., 2010].

Although the pH_{max} was calculated at 6.76, the permeability improved with an increase in the unionized form beyond the pH_{max} . This can be explained by the direct dependence of the permeation rate on the proportion of dissolved unionized propranolol, which increases at higher pH (7.4); however, solubility was not exceeded by the applied dosage of 12.1 mg/mL. Hence, the correlation of the determined permeability coefficients with the calculated fractions of unionized drug confirm this relationship with R^2 of 0.997 for pH 5.0 to 7.4 (Figure 30, inlay). Moreover, the significantly increasing permeation with a higher proportion of unionized API indicated a preference of propranolol for the transcellular diffusion pathway, whereas the protonated form passes through the paracellular diffusion pathway. In addition to the permeation results at pH 8.0, drug precipitation was observed in the freshly prepared pH 9.0 formulation. Thus, the formulation at pH 9.0 was not included in the permeation experiments due to insufficient solubility (congruent with the results from section 6.3.2).

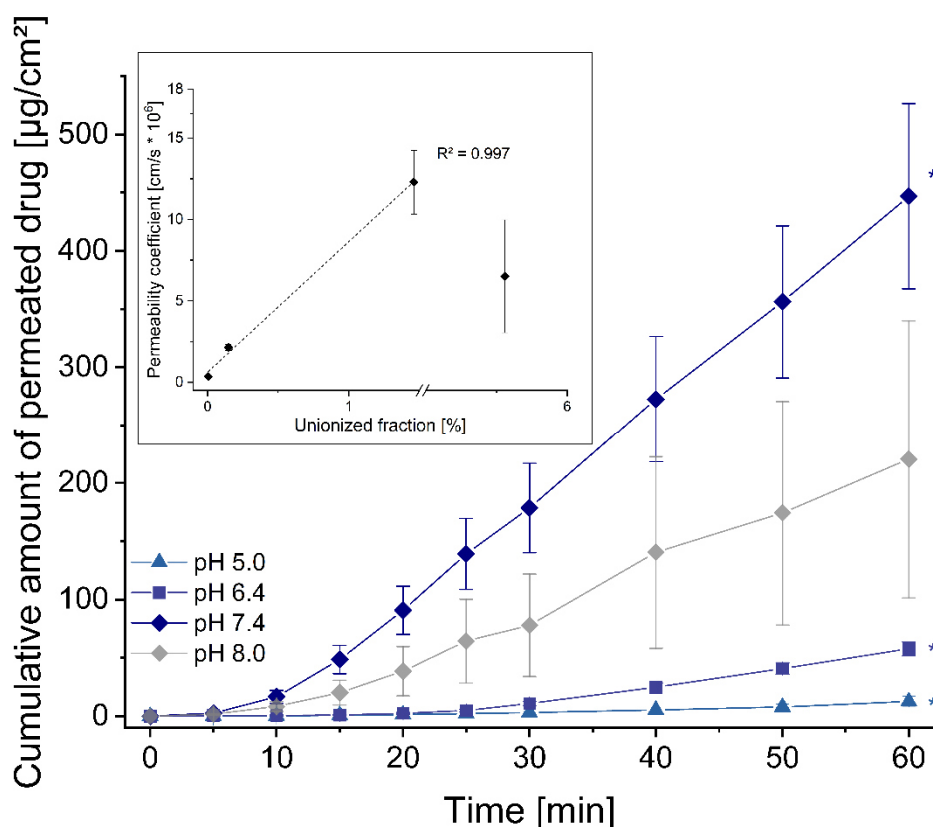


Figure 30: Impact of pH on *ex vivo* permeability of propranolol as cumulative amount of permeated drug per cm² for the respective formulation (mean ± SEM; n ≥ 5). Inlay: correlation of the obtained permeability coefficients (mean ± SEM) with the unionized fractions of propranolol. *R*²: coefficient of determination, *: *p* < 0.05 (unpaired *t*-test).

In vitro studies

By applying artificial Permeapad® Barriers, cumulated propranolol levels between 344.86 and 445.86 µg/cm² were measured, corresponding to the maximum permeation obtained by the *ex vivo* approach. Figure 31 shows the permeation profiles of the single formulations with graphically higher slopes and lower standard deviations when compared to the *ex vivo* experiments. Only minor differences were registered between the formulations at pH 5.0 with the lowest and at pH 6.4 with the highest permeability ($10.92 \cdot 10^{-6}$ vs. $14.68 \cdot 10^{-6}$ cm/s) under the *in vitro* approach. Remarkably, no decreased permeation compared to the *ex vivo* approach was shown at pH 8.0. Since the pH value of 8.0 is above the determined pH_{max} of 6.76, the flocculated and precipitated species in the formulation was the free base. The *ex vivo* results revealed that the amount of available unionized drug is essential for increasing the permeation rate. However, permeation through artificial membranes proved to be insensitive to the proportion of unionized propranolol; thus, no major effects were observed at the applied concentration of 41 mM of propranolol hydrochloride.

In contrast to the pH-partition theory, no continuous improvement of permeability was achieved by increasing pH. Thus, no linear correlation was obtained between the permeability coefficients and the unionized percentage of propranolol ($R^2 = 0.021$). Table 13 summarizes the permeability results for both approaches.

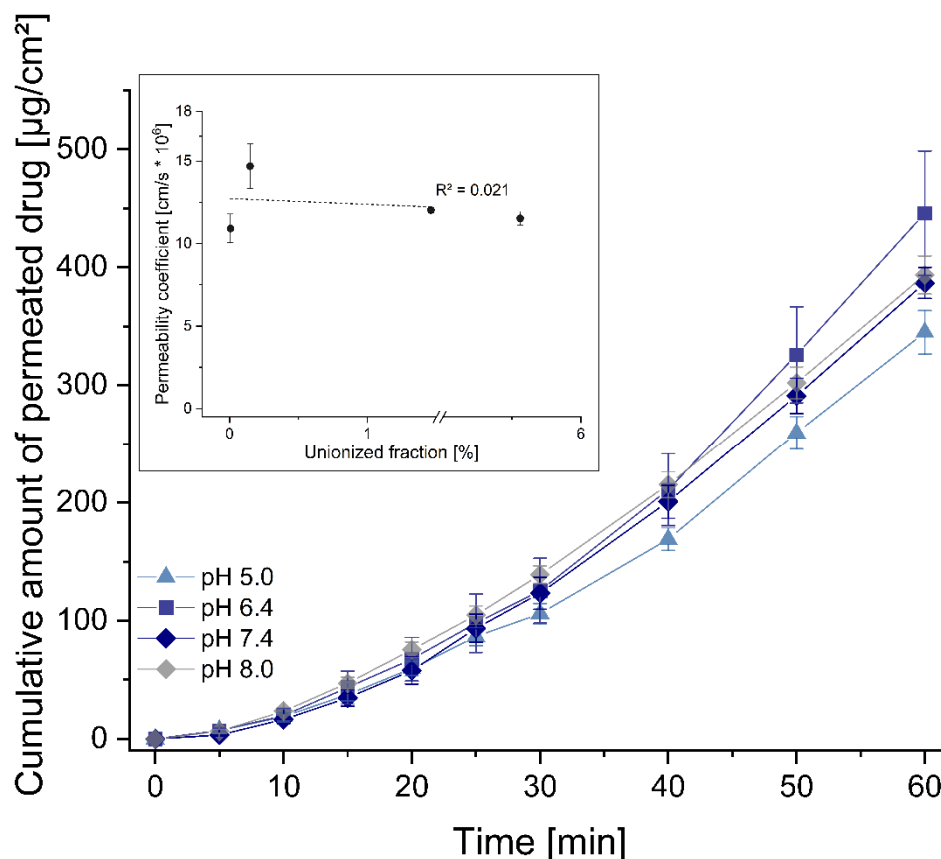


Figure 31: Impact of pH on *in vitro* permeability of propranolol as cumulative amount of permeated drug per cm² for the respective formulation (mean \pm SEM; $n \geq 3$). Inlay: correlation of the obtained permeability coefficients (mean \pm SEM) with the unionized fractions of propranolol. R^2 : coefficient of determination, $p < 0.05$ (unpaired *t*-test).

Permeapad® consisted of phosphatidylcholine (S-100) inserted between support layers to mimic biomembrane properties [Berben et al., 2018]. To date, the focus of Permeapad® use has tended to be on intestinal prediction, with limited studies on oromucosal applications [Berben et al., 2018]. Thereby, its applicability in drug profiling as well as within lipolysis-permeation studies has been presented [Jacobsen et al., 2020]. Regarding pH-dependent oromucosal permeability, Bibi et al. showed a strong correlation between permeation and pH for metoprolol [Bibi et al., 2016]. However, the use of Permeapad® in the preformulation of cyclobenzaprine also resulted in no proportionality between pH and permeability [Majid et al., 2021c]. Moreover, pH-related permeability was also not transferable to the structurally-related (beta receptor blocker) but more lipophilic drug propranolol. The permeability coefficients for propranolol were expected to be higher compared to metoprolol using Permeapad®, regarding

their physicochemical properties (i.e., $\log P_{OW}$, polar surface area) and previous *ex vivo* studies [Amores et al., 2014]. Presumably, by artificially depicting a single lipid bilayer, the influence of the degree of ionization on permeability is not adequately detected—especially in relation to the observed permeability with fully ionized drug in this setup. Further explanations could be found in the different study designs, since the lack of standardization in *ex vivo* and *in vitro* studies limits comparability. Overall, the results from using porcine mucosa instead of artificial barriers in a standardized and automated process were consistent with the expected increase in permeation according to several studies, which conforms to pH-partition theory.

Table 13: Summary of permeability results for each sublingual formulation from *ex vivo* and *in vitro* studies.

Formulation pH (n)	Cumulative amount after 60 min Mean \pm SEM [$\mu\text{g}/\text{cm}^2$]	Permeability coefficient Mean \pm SEM [$\times 10^6 \text{ cm/s}$]
<i>Ex vivo</i> permeability		
5.0 (5)	12.71 \pm 4.75	0.34 \pm 0.08
6.4 (6)	57.78 \pm 5.91	2.15 \pm 0.20
7.4 (5)	447.03 \pm 79.52	12.29 \pm 1.96
8.0 (5)	220.62 \pm 119.28	6.51 \pm 3.47
<i>In vitro</i> permeability		
5.0 (4)	344.86 \pm 18.42	10.92 \pm 0.87
6.4 (4)	445.86 \pm 52.83	14.68 \pm 1.35
7.4 (4)	386.78 \pm 13.13	12.03 \pm 0.17
8.0 (3)	393.57 \pm 16.22	11.54 \pm 0.40

n: amount of experiments, SEM: standard error of the mean

6.3.4. Ex vivo – in vitro – in vivo correlation

Through *in vivo* studies, Dali et al. demonstrated the improved sublingually absorption of propranolol with increased formulation pH. Thus, AUC levels from 335 ng*min/mL at pH 5.0 to 670 ng*min/mL at pH 7.4 were reported [Dali et al., 2006]. Since the formulation with a pH of 9.0 exceeds the physiological pH range of the oral cavity (6.28 to 7.34) [Aframian et al., 2006] and insufficient solubility within permeation studies (section 6.3.2) was observed, the corresponding formulation was excluded from the approach presented here.

The parameters of obtained propranolol permeability (P_{app} , Q_t , J_{SS}) from *ex vivo* and *in vitro* studies were each compared to the corresponding reported *in vivo* parameters (AUC, C_{max}) (Figure 32).

Ex vivo – in vivo correlation

By the direct comparison of the *ex vivo* P_{app} and AUC, a good R^2 of 0.989 was calculated for the different liquid formulations. Dali et al. considered a time period up to 20 minutes in the calculation of their AUC levels to demonstrate oromucosal absorption exclusively (without swallowing). Also, this correlation (the cumulative amount of drug permeated after 20 minutes (Q_{20min}) vs. $AUC_{0-20min}$) exhibited an R^2 of 0.945. C_{max} was considered another pharmacokinetic parameter, and a linear relationship ($R^2 = 0.860$) was obtained with the J_{SS} of the corresponding *ex vivo* study. This demonstrates the relationship between the highest plasma concentrations after sublingual administration of the formulations and the J_{SS} as a characteristic for the amount of pH-dependent diffusion rate. Moreover, a point-to-point correlation of $Q_{0-20min}$ with $AUC_{0-20min}$ revealed good correlations (between 0.993 and 1.000) for the formulations at a pH 5.0, 6.4, and 7.4 (Figure 33). The best fit was achieved by exponential regression as the simplest model. The physiological-clinical adaptation of the model allows for a point-to-point relation for sublingual formulations within a realistic short-term application (20 minutes) instead of the commonly used (but artificial) permeation studies that are performed over many hours.

In vitro – in vivo correlation

In the case of the *in vitro* permeation approach (artificial membrane), no meaningful relationships were observed between the permeability values of P_{app} , Q_{20min} , and J_{SS} and the pharmacokinetic parameters AUC and C_{max} with an $R^2 \leq 0.185$.

Consistent with the results from section 6.3.3 regarding the linear relationship of permeability and the proportion of unionized propranolol, the *ex vivo* approach showed a good correlation to *in vivo* data. Standardization and physiological optimization of the permeation model using esophageal mucosa as a surrogate barrier enabled the pH-dependent estimation of

pharmacokinetic parameters, while considering current experimental limitations (i.e., physiological-clinical relevance, controlled study design, and routine capability).

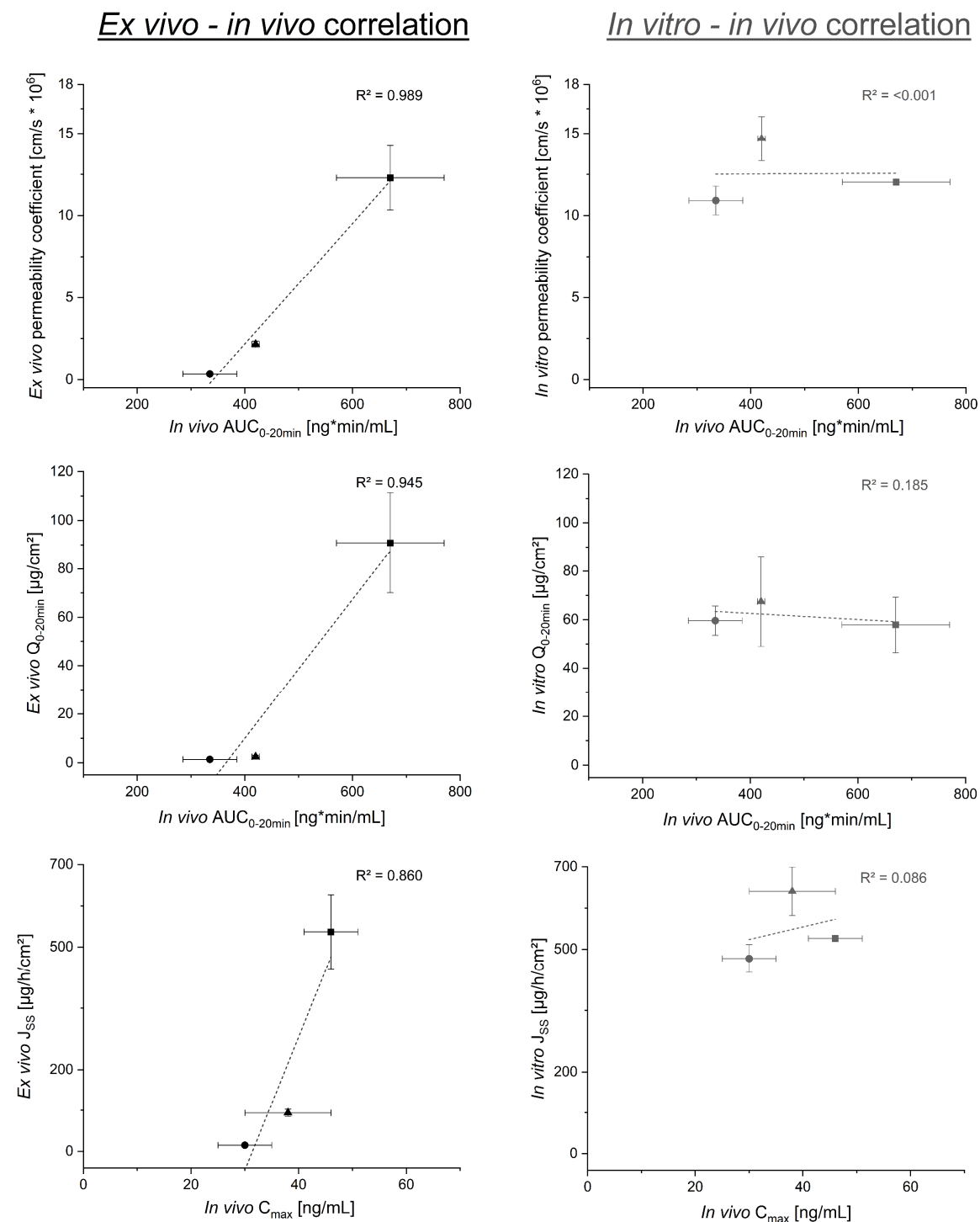


Figure 32: Multiple *ex vivo/in vitro* – *in vivo* correlation of obtained propranolol permeability with pharmacokinetic animal data [Dali et al., 2006]. The symbols represent the respective formulation at pH 5.0 (circle), 6.4 (triangle) and 7.4 (square). *AUC*: area under the curve, *C_{max}*: maximum plasma concentration, *J_{SS}*: steady-state flux, *Q_t*: cumulative amount of permeated drug per cm^2 , *R²*: coefficient of determination.

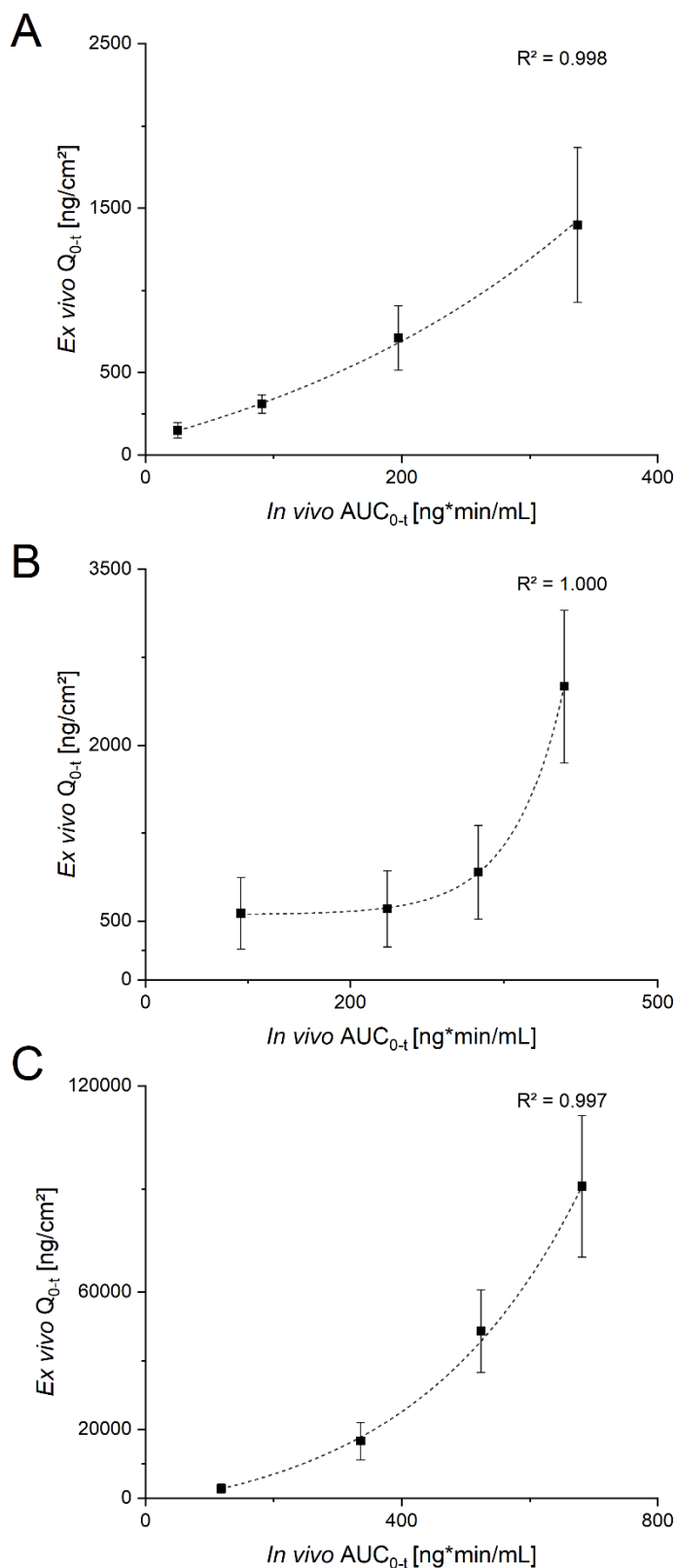


Figure 33: *Ex vivo* – *in vivo* point-to-point correlation for the respective propranolol formulations at pH 5.0 (A), 6.4 (B) and 7.4 (C) at equal time frames. *AUC*: area under the curve, *Q_t*: cumulative amount of permeated drug per cm², *R²*: coefficient of determination, *t* = 5; 10; 15; 20 minutes, respectively.

Following previous studies demonstrating the suitability of esophageal mucosa as a surrogate for buccal permeability, this study extends this with transferability to sublingual absorption using propranolol [Diaz Del Consuelo et al., 2005c; Telò et al., 2016]. Furthermore, the presented outcomes enrich the limited data available on permeability-based IVIVC for oromucosal delivery, as indicated by only 2% of all IVIVC currently submitted to the FDA were buccal formulations [Suarez-Sharp et al., 2016].

Approximately two-thirds of the drugs are chemical substances with acidic and/or basic properties [Charifson and Walters, 2014], which implies that microenvironmental pH is directly involved in the extent of solubility and drug absorption through the galenical formulation and site of administration. Therefore, pH holds a meaningful position in formulation development with regard to optimizing and controlling the systemic uptake of a drug. The pH-dependent permeability of the standardized *ex vivo* model was linear to *in vivo* results using porcine esophagi (a waste product of slaughter). The successful IVIVC confirms the standardized *ex vivo* model as a viable alternative to animal testing for the assessment of oromucosal pharmaceuticals in preclinical development. Our findings indicate that the model presented here results in comparable outcomes to costly *in vivo* experiments. The results provide a further step toward the reduction of animal testing and its targeted application in line with the 3Rs principle. Therefore, further *in vivo* correlations with drugs covering various physicochemical properties are required.

The artificial *in vitro* results showed no correlation to the *in vivo* studies. The influence of the medium was not sufficiently detectable due to the high baseline permeability of the ionized species. Thus, transferability of pH-dependent permeation to the stratified squamous epithelium of the oral cavity was not observed in our studies. Nevertheless, the artificial membrane seems to be appropriate for the biomimesis of the single-layered columnar epithelium of the intestine for profiling substances regarding their permeability [Berben et al., 2018]. The comparative correlation using cell-based *in vitro* studies such as the conventional TR146 cell line as well as recent human tissue models (EpiOral™) as a counterpart to the artificial membranes represents a perspective to be addressed in further studies to additionally complement the obtained results.

Following the successful development, validation, and application of this proof of concept in drug preformulation and formulation development, a good *in vivo* correlation for sublingual propranolol was achieved. In addition to standardization and regulatory adaptations, this brings us closer to enabling its routine implementation and thereby significantly reducing reliance on animal testing. In perspective, extended studies with different compounds and conditions can support the development of *in silico* approaches using reliable experimental data for future pharmacokinetic *in human* prediction.

6.4. Conclusion

Ex vivo and *in vitro* studies on oromucosal permeability were extensively evaluated regarding their pH-dependent predictivity for propranolol [Majid et al., 2021b]. Thereby, the standardized *ex vivo* model using esophageal mucosa as a surrogate barrier provided a good relationship between permeability and physicochemical properties. In a multiple level C analysis, a good correlation to sublingual *in vivo* data on liquid propranolol formulations was attained for the *ex vivo* studies, thereby facilitating the potential reduction and targeted use of animal studies. Due to the successfully performed *in vivo* correlation, the permeability model appears suitable for further implementation in preclinical drug development.

7. Overall conclusion and perspective

In summary, this thesis presents an innovative and distinctive tissue-based *ex vivo* permeation model for implementation in the preclinical development of oromucosal drugs. It is characterized by standardized, automated, and controlled processes to ensure reliable routine application and physiologically and clinically representative study design. To prove the applicability and meaningfulness of the developed model, the oromucosal permeability of cyclobenzaprine was comprehensively characterized for the first time during a preformulation study, followed by use in formulation development up to *in vivo* correlations regarding sublingual absorption (Figure 34). Within preformulation, it was feasible to identify substantially impacting factors and achieve enhanced permeation by adapting the microenvironment at the site of administration.

Thus, based on preformulation results, the model was used to guide the formulation development of sublingual cyclobenzaprine tablets in cooperation with a pharmaceutical company. Permeation was enhanced by a factor of 4.68 via the model-led formulation development considering the integration of the coherent processes of disintegration, dissolution permeation, and metabolism into the physiologically aligned and standardized set-up. Hence, the effectiveness of the permeation model for successful establishment in the purposive formulation development of clinically beneficial oromucosal drugs was demonstrated.

The linear relationship between the obtained permeability and the physicochemical properties of the further model drug propranolol ($R^2 = 0.997$) highlighted the model transferability. To demonstrate the pharmacokinetic predictability of the model, a successful multiple level C correlation was obtained for the *ex vivo* permeation results to *in vivo* sublingual data of various liquid propranolol formulations. Here, the *ex vivo* model was superior in its predictivity for the microenvironmental related permeation of both cyclobenzaprine and propranolol, to the use of novel artificial membranes with biomimetic characteristics. The physiological-clinical relevance of the model obtained good point-to-point correlations of cumulative permeation and *in vivo* AUC over a realistic short-term application (≤ 20 minutes) with $R^2 \geq 0.995$.

Successful model development and application in stages of preclinical drug development, as well as the *in vivo* predictivity of the presented permeation model, enabled the effective support of developing oromucosal drugs while avoiding high costs, effort, and animal testing. Applications for new drug candidates, screening of excipients, permeation enhancers and dosage forms can now be routinely implemented, while formulations in statistical experimental study designs can be reliably and systematically evaluated. Here, the permeation model

facilitates the examination of the final intraoral dosage form by encompassing the multiple processes of disintegration, dissolution, solubility, permeation, and absorption.

Based on cyclobenzaprine, the drug repurposing process toward a beneficial new indication was presented. Frequently reported side effects impacting patient adherence can be reduced by oromucosal administration. The non-relevant formation of active metabolites along with feasible dose reduction by comprehensive characterization as well as the achieved improvement of cyclobenzaprine permeation induce higher patient tolerability and acceptability. Attention to the development of cyclobenzaprine for further indications such as PTSD has been supported by presenting deep insights into its transmucosal permeation. The powerful application of this model to cyclobenzaprine supports the reconsideration of known drugs for new indications and therapeutic customization while circumventing previous pharmacokinetic difficulties by reducing the rate of side effects. Thus, the clinical advantages of oromucosal administration will be fully exploited. Furthermore, an increasing ability to adapt the use of medication to specific patient populations is feasible. For the elderly and children, as well as patients with difficulties in peroral and invasive administration, the establishment of oromucosal administration as a patient-oriented alternative is being advanced. Additionally, in the treatment of acute cases, administration via the oral mucosa is a clinically convenient alternative due to its rapid systemic availability.

By moving from successful and useful applications to small molecules, this work opens the door to extending the model toward promising therapeutic peptides. Peptide drugs are becoming increasingly important in drug therapy, as reflected by the steadily increasing number of new approvals. Due to their physicochemical properties, parenteral administration currently presents the main route of administration. So even using oromucosal absorption as an alternative presents a challenge due to limited permeability. Nevertheless, the development of new approaches to improve absorption can be systematically investigated and evaluated by extending the model and monitoring relevant physiological processes for sufficient peptide availability such as oromucosal metabolism by LC-MS/MS. As a result, a progressive and meaningful development can lead to a broader use of this future important substance class by increasing patient acceptance and the feasibility of self-administration.

Within the research and development according to the 3R principle, models of varying applicability and complexity have been developed. Nevertheless, relatively few made the transition to broad and effective establishment, for example in pharmaceutical development. To achieve this significant step, further studies are required to reduce the systematic and widespread use of animal testing. The standardized permeation model offers this potential via proven applicability in the regulatory environment, suitability for routine use, and predictivity for *in vivo* absorption. Its prior use in assessing the preclinical development process, which would

otherwise occur in *in vivo* studies, allows for the reduction of animal experiments to a more focused and specific conduct.

Additionally, the systematic acquisition and incorporation of numerous drug permeabilities enables the development and establishment of reliable *in silico* approaches, leading to accurate pharmacokinetic *in human* modeling and estimations. Such a large pool of uniform and comparably measured permeation data for further drugs, an equivalent to the biopharmaceutical classification system for oromucosal drugs can be established, to facilitate simplified development as well as approval processes while encouraging accessibility for patients. The well-known biopharmaceutical classification system classifies drugs regarding their solubility and intestinal permeability and provides the estimation of their bioavailability and pharmacokinetic properties. For example, depending on the classification of a drug, additional bioequivalence studies in the approval process (biowaivers) may not be required. Such systems are also conceivable for the oral cavity using reliable models for determining solubility and permeability, which would reduce cost and effort and substantially increase the amount of available oromucosal drugs. Simultaneously, model predictivity enables the reduction of costs, time and resources by the more targeted and focused conduct of *in vivo* studies due to broad predictive screening within several development stages. By combining the coherent processes of disintegration, dissolution permeation and metabolism the systematic selection of the optimal formulation composition and dosage form is feasible, which enable the reduction of API by reaching comparable systemic exposure. In addition to the clinical benefits, together with the reduction of animal studies, more cost-efficient development will be possible in contrast to the focus on heterogeneous complex formulation strategies. The widespread usage may initiate the regulatory recognition, integration and regulation of standardized *ex vivo* permeation studies for oromucosal in equivalence to cell-based studies in peroral drug development.

Notably, this model is not exclusively limited to the oral cavity. Its application can be transferred to additional mucosal routes for drug delivery, such as the nasal route. Thus, the advantages in terms of the development of new therapeutic approaches, patient orientation, resources, and ethics can be potentiated. In particular, the non-invasive nasal administration of vaccines is in focus and offers an opportunity to rapidly achieve high vaccination coverage rates especially in the excessive spread of infectious diseases.

Overall, the presented *ex vivo* permeation model overcomes the limitations of current *in vitro* and *ex vivo* permeation studies and paves the way from academic-investigative to broad pharmaceutical-regulatory application. It also offers scientific advantages by providing a platform to evaluate innovative aspects of oromucosal drug delivery, ethically it can contribute

to a substantial reduction of animal studies, and clinically it can target the therapy of specific patient populations as well as support new therapeutic administration strategies.

Implementation of standardized and physiologically relevant *ex vivo* permeation studies in preclinical drug development

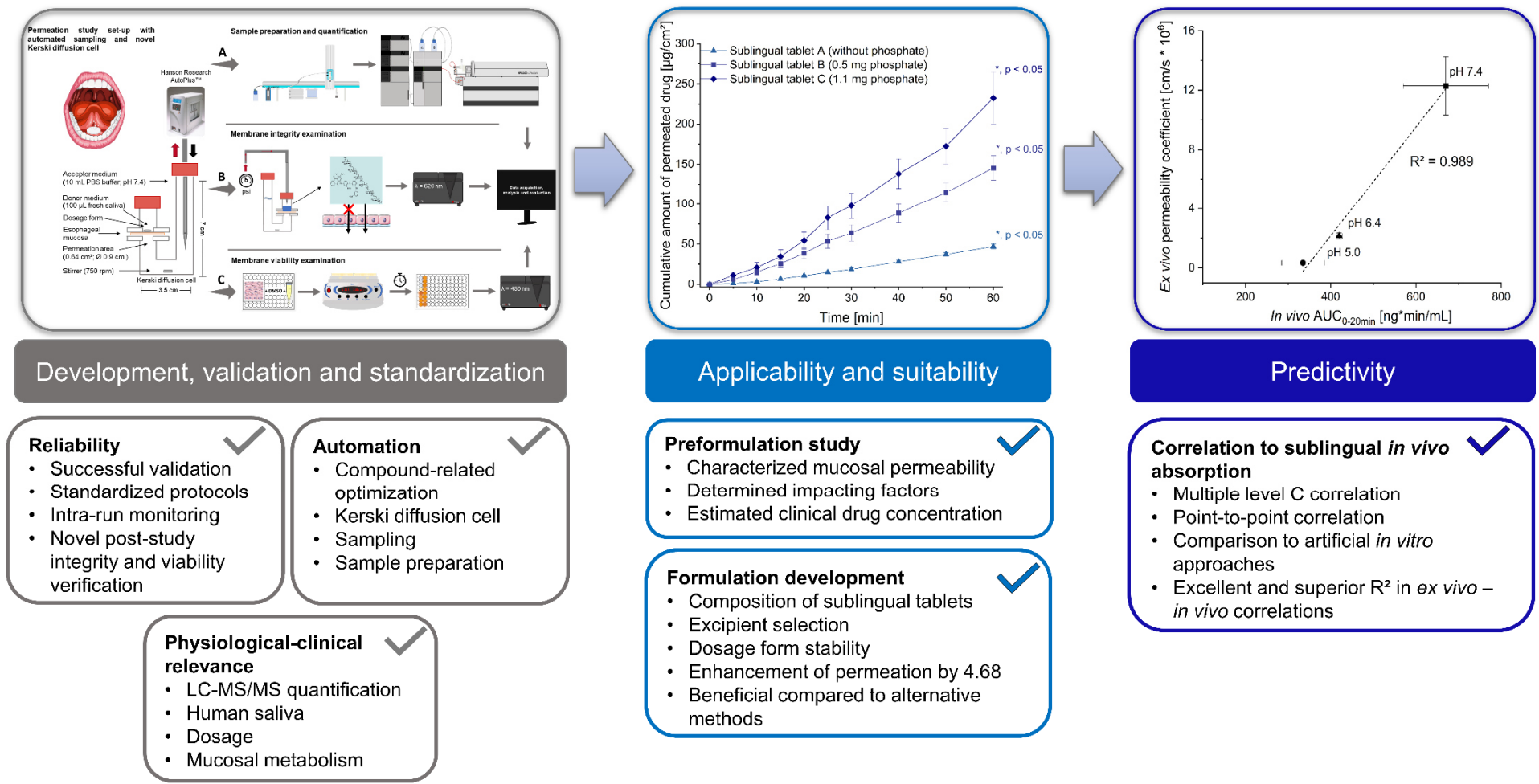


Figure 34: Overview of the conducted development steps and purposive applications of the standardized tissue-based *ex vivo* permeation studies to demonstrate their suitability and establishment for preclinical development of oromucosal drugs.

8. Funding

Parts of this work regarding the oromucosal permeation of cyclobenzaprine were founded by Hexal AG, Industriestrasse 25, 83607 Holzkirchen, Germany.

Conference participation on Euroanalysis XX was supported by the Heine Research Academies.

9. References

- Acarturk, C., McGrath, M., Roberts, B., Ilkkursun, Z., Cuijpers, P., Sijbrandij, M., Sondorp, E., Ventevogel, P., McKee, M., Fuhr, D.C.**, 2021. Prevalence and predictors of common mental disorders among Syrian refugees in Istanbul, Turkey: a cross-sectional study. *Social Psychiatry and Psychiatric Epidemiology* 56, 475–484. <https://doi.org/10.1007/s00127-020-01941-6>.
- Aframian, D.J., Davidowitz, T., Benoliel, R.**, 2006. The distribution of oral mucosal pH values in healthy saliva secretors. *Oral Diseases* 12, 420–423. <https://doi.org/10.1111/j.1601-0825.2005.01217.x>.
- Ajavon, A.D., Taft, D.R.**, 2010. Pharmacokinetics/ADME of Small Molecules, in: Rogge, M.C., Taft, D.R. (Eds.), *Preclinical Drug Development*, 2nd ed. Informa Healthcare, pp. 83–128.
- AlAli, A.S., Aldawsari, M.F., Alalaiwe, A., Almutairy, B.K., Al-Shdefat, R., Walbi, I.A., Fayed, M.H.**, 2021. Exploitation of Design-of-Experiment Approach for Design and Optimization of Fast-Disintegrating Tablets for Sublingual Delivery of Sildenafil Citrate with Enhanced Bioavailability Using Fluid-Bed Granulation Technique. *Pharmaceutics* 13, 870. <https://doi.org/10.3390/pharmaceutics13060870>.
- Ali, J., Bong Lee, J., Gittings, S., Iachelini, A., Bennett, J., Cram, A., Garnett, M., Roberts, C.J., Gershkovich, P.**, 2021. Development and optimisation of simulated salivary fluid for biorelevant oral cavity dissolution. *European Journal of Pharmaceutics and Biopharmaceutics* 160, 125–133. <https://doi.org/10.1016/j.ejpb.2021.01.017>.
- American Psychiatric Association**, 2013. *Diagnostic and statistical manual of mental disorders: DSM-5*, 5th ed. American Psychiatric Publishing.
- Amores, S., Lauroba, J., Calpena, A., Colom, H., Gimeno, A., Domenech, J.**, 2014. A comparative ex vivo drug permeation study of beta-blockers through porcine buccal mucosa. *International Journal of Pharmaceutics* 468, 50–54. <https://doi.org/10.1016/j.ijpharm.2014.03.050>.
- Araújo, J.S.M. de, Volpato, M.C., Muniz, B.V., Xavier, G.G.A., Martinelli, C.C.M., Lopez, R.F.V., Groppo, F.C., Franz-Montan, M.**, 2021. Resistivity Technique for the Evaluation of the Integrity of Buccal and Esophageal Epithelium Mucosa for In Vitro Permeation Studies: Swine Buccal and Esophageal Mucosa Barrier Models. *Pharmaceutics* 13, 643. <https://doi.org/10.3390/pharmaceutics13050643>.

- Assmus, F.**, 2015. Artificial Tissue Binding Models: Development and Comparative Evaluation of High -Throughput Lipophilicity Assays and their Use for PET Tracer Optimization. Doctoral thesis.
- Baka, E., Comer, J.E.A., Takács-Novák, K.**, 2008. Study of equilibrium solubility measurement by saturation shake-flask method using hydrochlorothiazide as model compound. *Journal of Pharmaceutical and Biomedical Analysis* 46, 335–341. <https://doi.org/10.1016/j.jpba.2007.10.030>.
- Bebarta, V.S., Maddry, J., Borys, D.J., Morgan, D.L.**, 2011. Incidence of tricyclic antidepressant-like complications after cyclobenzaprine overdose. *The American Journal of Emergency Medicine* 29, 645–649. <https://doi.org/10.1016/j.ajem.2010.01.014>.
- Berben, P., Bauer-Brandl, A., Brandl, M., Faller, B., Flaten, G.E., Jacobsen, A.-C., Brouwers, J., Augustijns, P.**, 2018. Drug permeability profiling using cell-free permeation tools: Overview and applications. *European Journal of Pharmaceutical Sciences* 119, 219–233. <https://doi.org/10.1016/j.ejps.2018.04.016>.
- Bestha, D., Soliman, L., Blankenship, K., Rachal, J.**, 2018. The Walking Wounded: Emerging Treatments for PTSD. *Current Psychiatry Reports* 20, 94. <https://doi.org/10.1007/s11920-018-0941-8>.
- Bibi, H.A., Holm, R., Bauer-Brandl, A.**, 2016. Use of Permeapad® for prediction of buccal absorption: A comparison to in vitro, ex vivo and in vivo method. *European Journal of Pharmaceutical Sciences* 93, 399–404. <https://doi.org/10.1016/j.ejps.2016.08.041>.
- Blackmore, R., Boyle, J.A., Fazel, M., Ranasinha, S., Gray, K.M., Fitzgerald, G., Misso, M., Gibson-Helm, M.**, 2020. The prevalence of mental illness in refugees and asylum seekers: A systematic review and meta-analysis. *Public Library of Science Medicine* 17, e1003337. <https://doi.org/10.1371/journal.pmed.1003337>.
- Boateng, J., Okeke, O.**, 2019. Evaluation of Clay-Functionalized Wafers and Films for Nicotine Replacement Therapy via Buccal Mucosa. *Pharmaceutics* 11, 104. <https://doi.org/10.3390/pharmaceutics11030104>.
- Bradley, L.A.**, 2009. Pathophysiology of fibromyalgia. *The American Journal of Medicine* 122, 22-30. <https://doi.org/10.1016/j.amjmed.2009.09.008>.
- Brandl, M., Bauer-Brandl, A.**, 2019. Oromucosal drug delivery: Trends in in-vitro biopharmaceutical assessment of new chemical entities and formulations. *European Journal of Pharmaceutical Sciences* 128, 112–117. <https://doi.org/10.1016/j.ejps.2018.11.031>.

- Brayden, D.J., Stuetgen, V.**, 2021. Sodium glycodeoxycholate and sodium deoxycholate as epithelial permeation enhancers: in vitro and ex vivo intestinal and buccal bioassays. *European Journal of Pharmaceutical Sciences* 159, 105737. <https://doi.org/10.1016/j.ejps.2021.105737>.
- Brownlow, J.A., Miller, K.E., Gehrman, P.R.**, 2020. Treatment of Sleep Comorbidities in Posttraumatic Stress Disorder. *Current Treatment Options in Psychiatry* 7, 301–316. <https://doi.org/10.1007/s40501-020-00222-y>.
- Cabrera-Pérez, M.Á., Sanz, M.B., Sanjuan, V.M., González-Álvarez, M., Álvarez, I.G.**, 2016. Importance and applications of cell- and tissue-based in vitro models for drug permeability screening in early stages of drug development, in: Sarmiento, B. (Ed.), *Concepts and models for drug permeability studies: Cell and tissue based In vitro culture models*. Elsevier Ltd, pp. 3–29.
- Caon, T., Simões, C.M.O.**, 2011. Effect of freezing and type of mucosa on ex vivo drug permeability parameters. *AAPS PharmSciTech* 12, 587–592. <https://doi.org/10.1208/s12249-011-9621-2>.
- Castro, P., Madureira, R., Sarmiento, B., Pintado, M.**, 2016. Tissue-based in vitro and ex vivo models for buccal permeability studies, in: Sarmiento, B. (Ed.), *Concepts and models for drug permeability studies: Cell and tissue based In vitro culture models*. Elsevier Ltd, pp. 189–202.
- Çelebi, C.R., Yörükan, S.**, 1999. Physiology of the Oral Cavity, in: Lotti, T.M., Parish, L.C., Rogers, R.S. (Eds.), *Oral Diseases*. Springer, pp. 7–14.
- Charifson, P.S., Walters, W.P.**, 2014. Acidic and basic drugs in medicinal chemistry: a perspective. *Journal of Medicinal Chemistry* 57, 9701–9717. <https://doi.org/10.1021/jm501000a>.
- Chou, R., Peterson, K., Helfand, M.**, 2004. Comparative efficacy and safety of skeletal muscle relaxants for spasticity and musculoskeletal conditions: a systematic review. *Journal of Pain and Symptom Management* 28, 140–175. <https://doi.org/10.1016/j.jpainsymman.2004.05.002>.
- Cimolai, N.**, 2009. Cyclobenzaprine: a new look at an old pharmacological agent. *Expert Review of Clinical Pharmacology* 2, 255–263. <https://doi.org/10.1586/ecp.09.5>.
- Close, C., Kouvonen, A., Bosqui, T., Patel, K., O'Reilly, D., Donnelly, M.**, 2016. The mental health and wellbeing of first generation migrants: a systematic-narrative review of reviews. *Globalization and Health* 12, 47. <https://doi.org/10.1186/s12992-016-0187-3>.

- Collins, L.M., Dawes, C.**, 1987. The surface area of the adult human mouth and thickness of the salivary film covering the teeth and oral mucosa. *Journal of Dental Research* 66, 1300–1302. <https://doi.org/10.1177/00220345870660080201>.
- Cruchley, A.T., Bergmeier, L.A.**, 2018. Structure and Functions of the Oral Mucosa, in: Bergmeier, L.A. (Ed.), *Oral Mucosa in Health and Disease: A Concise Handbook*. Springer International Publishing, pp. 1–18.
- Dahan, A., Miller, J.M.**, 2012. The solubility-permeability interplay and its implications in formulation design and development for poorly soluble drugs. *The AAPS Journal* 14, 244–251. <https://doi.org/10.1208/s12248-012-9337-6>.
- Dali, M.M., Moench, P.A., Mathias, N.R., Stetsko, P.I., Heran, C.L., Smith, R.L.**, 2006. A rabbit model for sublingual drug delivery: comparison with human pharmacokinetic studies of propranolol, verapamil and captopril. *Journal of Pharmaceutical Sciences* 95, 37–44. <https://doi.org/10.1002/jps.20312>.
- Daugherty, B., Monti, N.C., Panzeri, V., Marelli, R., Magnocavallo, E., Reiner, G., Lederman, S.**, 2016. Rapid Sublingual Absorption of Cyclobenzaprine (CBP) with Basifying Agents: Prospect for Bedtime Treatment of Fibromyalgia Syndrome (FM). American Society for Clinical Pharmacology and Therapeutics (ASCPT) Annual Meeting 2016, 154–155.
- Daugherty, B., Sullivan, G.M., Gershell, L., Lederman, S.**, 2015. Serotonin Receptor Profiles of Bedtime Pharmacotherapies Targeting Posttraumatic Stress Disorder (PTSD). *Biological Psychiatry* 70th Annual Scientific Convention and Meeting, 2015, Toronto, Canada.
- Davidson, J.**, 2015. Vintage treatments for PTSD: a reconsideration of tricyclic drugs. *Journal of Psychopharmacology* 29, 264–269. <https://doi.org/10.1177/0269881114565143>.
- Davis, D., Ayman D.**, 1928. Sublingual absorption of drugs: Morphine. *Archives of Internal Medicine* 41, 231. <https://doi.org/10.1001/archinte.1928.00130140093005>.
- Delvadia, P.R., Barr, W.H., Karnes, H.T.**, 2012. A biorelevant in vitro release/permeation system for oral transmucosal dosage forms. *International Journal of Pharmaceutics* 430, 104–113. <https://doi.org/10.1016/j.ijpharm.2012.03.050>.
- Di Cagno, M., Bibi, H.A., Bauer-Brandl, A.**, 2015. New biomimetic barrier Permeapad™ for efficient investigation of passive permeability of drugs. *European Journal of Pharmaceutical Sciences* 73, 29–34. <https://doi.org/10.1016/j.ejps.2015.03.019>.
- Diaz Del Consuelo, I., Falson, F., Guy, R.H., Jacques, Y.**, 2005a. Transport of fentanyl through pig buccal and esophageal epithelia in vitro: influence of concentration and vehicle

- pH. *Pharmaceutical Research* 22, 1525–1529. <https://doi.org/10.1007/s11095-005-6020-y>.
- Diaz Del Consuelo, I., Jacques, Y., Pizzolato, G.-P., Guy, R.H., Falson, F.,** 2005b. Comparison of the lipid composition of porcine buccal and esophageal permeability barriers. *Archives of Oral Biology* 50, 981–987. <https://doi.org/10.1016/j.archoralbio.2005.04.008>.
- Diaz Del Consuelo, I., Pizzolato, G.-P., Falson, F., Guy, R.H., Jacques, Y.,** 2005c. Evaluation of Pig Esophageal Mucosa as a Permeability Barrier Model for Buccal Tissue. *Journal of Pharmaceutical Sciences* 94, 2777–2788. <https://doi.org/10.1002/jps.20409>.
- Dutheil, F., Mondillon, L., Navel, V.,** 2021. PTSD as the second tsunami of the SARS-Cov-2 pandemic. *Psychological Medicine* 51, 1773–1774. <https://doi.org/10.1017/S0033291720001336>.
- Esim, O., Savaser, A., Ozkan, C.K., Bayrak, Z., Tas, C., Ozkan, Y.,** 2018. Effect of polymer type on characteristics of buccal tablets using factorial design. *Saudi Pharmaceutical Journal* 26, 53–63. <https://doi.org/10.1016/j.jsps.2017.10.013>.
- European Medicines Agency,** 2012. Guideline Bioanalytical method validation, EMEA/CHMP/EWP/192217/2009.
- European Medicines Agency,** 2014. Guideline on the quality of transdermal patches, EMA/CHMP/QWP/608924/2014.
- European Medicines Agency,** 2016. Guideline on the principles of regulatory acceptance of 3Rs (replacement, reduction, refinement) testing approaches, EMA/CHMP/CVMP/JEG-3Rs/450091/2012.
- European Medicines Agency,** 2018a. Draft guideline on quality and equivalence of topical products, CHMP/QWP/708282/2018.
- European Medicines Agency,** 2018b. Reflection paper providing an overview of the current regulatory testing requirements for medicinal products for human use and opportunities for implementation of the 3Rs.
- Freedman, L.P., Gibson, M.C.,** 2015. The impact of preclinical irreproducibility on drug development. *Clinical Pharmacology & Therapeutics* 97, 16–18. <https://doi.org/10.1002/cpt.9>.
- Gao, X., Bhattacharya, S., Chan, W.K., Jasti, B.R., Upadrashta, B., Li, X.,** 2014. Expression of P-glycoprotein and CYP3A4 along the porcine oral-gastrointestinal tract: implications on

- oral mucosal drug delivery. *Drug Development and Industrial Pharmacy* 40, 599–603. <https://doi.org/10.3109/03639045.2014.884118>.
- Gayrard, V., Lacroix, M.Z., Collet, S.H., Viguié, C., Bousquet-Melou, A., Toutain, P.-L., Picard-Hagen, N.**, 2013. High bioavailability of bisphenol A from sublingual exposure. *Environmental Health Perspectives* 121, 951–956. <https://doi.org/10.1289/ehp.1206339>.
- Gilhotra, R.M., Ikram, M., Srivastava, S., Gilhotra, N.**, 2014. A clinical perspective on mucoadhesive buccal drug delivery systems. *Journal of Biomedical Research* 28, 81–97. <https://doi.org/10.7555/JBR.27.20120136>.
- Gimeno, A., Calpena, A.C., Sanz, R., Mallandrich, M., Peraire, C., Clares, B.**, 2014. Transbuccal delivery of doxepin: studies on permeation and histological investigation. *International Journal of Pharmaceutics* 477, 650–654. <https://doi.org/10.1016/j.ijpharm.2014.10.060>.
- Goel, A.N., Long, J.L.**, 2019. The Oral Cavity, in: Chhetri, D.K., Dewan, K. (Eds.), *Dysphagia Evaluation and Management in Otolaryngology*. Elsevier, pp. 5–12.
- Goyal, A.K., Singh, R., Chauhan, G., Rath, G.**, 2018. Non-invasive systemic drug delivery through mucosal routes. *Artificial Cells, Nanomedicine, and Biotechnology* 46, 539–551. <https://doi.org/10.1080/21691401.2018.1463230>.
- Guina, J., Nahhas, R.W., Sutton, P., Farnsworth, S.**, 2018. The Influence of Trauma Type and Timing on PTSD Symptoms. *Journal of Nervous & Mental Disease* 206, 72–76. <https://doi.org/10.1097/NMD.0000000000000730>.
- Holm, R., Meng-Lund, E., Andersen, M.B., Jespersen, M.L., Karlsson, J.-J., Garmer, M., Jørgensen, E.B., Jacobsen, J.**, 2013. In vitro, ex vivo and in vivo examination of buccal absorption of metoprolol with varying pH in TR146 cell culture, porcine buccal mucosa and Göttingen minipigs. *European Journal of Pharmaceutical Sciences* 49, 117–124. <https://doi.org/10.1016/j.ejps.2013.02.024>.
- Hua, S.**, 2019. Advances in Nanoparticulate Drug Delivery Approaches for Sublingual and Buccal Administration. *Frontiers in Pharmacology* 10, 1328. <https://doi.org/10.3389/fphar.2019.01328>.
- Hucker, H.B., Stauffer, S.C., Albert, K.S., Lei, B.W.**, 1977. Plasma levels and bioavailability of cyclobenzaprine in human subjects. *Journal of Clinical Pharmacology* 17, 719–727. <https://doi.org/10.1002/j.1552-4604.1977.tb01547.x>.
- Hughes, M., Ghosh, T.**, 2015. Pharmaceuticals for Oral Mucosal Drug Delivery: Regulatory Considerations, in: Rathbone, M.J., Şenel, S., Pather, I. (Eds.), *Oral mucosal drug delivery and therapy*. Springer, pp. 247–274.

- Humphrey, S.P., Williamson, R.T.**, 2001. A review of saliva: normal composition, flow, and function. *The Journal of Prosthetic Dentistry* 85, 162–169. <https://doi.org/10.1067/mpr.2001.113778>.
- Imbert, D., Cullander, C.**, 1999. Buccal mucosa in vitro experiments. *Journal of Controlled Release* 58, 39–50. [https://doi.org/10.1016/S0168-3659\(98\)00143-6](https://doi.org/10.1016/S0168-3659(98)00143-6).
- International Council for Harmonisation of Technical Requirements for Pharmaceuticals for Human Use**, 2005. ICH Harmonised Tripartite Guideline Validation of Analytical Procedures: Text and Methodology Q2(R1).
- International Council for Harmonisation of Technical Requirements for Pharmaceuticals for Human Use**, 2008. ICH Harmonised Tripartite Guideline Pharmaceutical Quality System Q10.
- International Council for Harmonisation of Technical Requirements for Pharmaceuticals for Human Use**, 2009. ICH Harmonised Tripartite Guideline Pharmaceutical Development Q8(R2).
- Itin, C., Barasch, D., Domb, A.J., Hoffman, A.**, 2020. Prolonged oral transmucosal delivery of highly lipophilic drug cannabidiol. *International Journal of Pharmaceutics* 581, 119276. <https://doi.org/10.1016/j.ijpharm.2020.119276>.
- Jacob, S., Nair, A.B., Boddu, S.H.S., Gorain, B., Sreeharsha, N., Shah, J.**, 2021. An Updated Overview of the Emerging Role of Patch and Film-Based Buccal Delivery Systems. *Pharmaceutics* 13, 1206. <https://doi.org/10.3390/pharmaceutics13081206>.
- Jacobsen, A.-C., Nielsen, S., Brandl, M., Bauer-Brandl, A.**, 2020. Drug Permeability Profiling Using the Novel Permeapad® 96-Well Plate. *Pharmaceutical Research* 37, 93. <https://doi.org/10.1007/s11095-020-02807-x>.
- Jacobsen, J., Nielsen, E.B., Brøndum-Nielsen, K., Christensen, M.E., Olin, H.B., Tommerup, N., Rassing, M.R.**, 1999. Filter-grown TR146 cells as an in vitro model of human buccal epithelial permeability. *European Journal of Oral Sciences* 107, 138–146.
- Jacobsen, J., van Deurs, B., Pedersen, M., Rassing, M.R.**, 1995. TR146 cells grown on filters as a model for human buccal epithelium: I. Morphology, growth, barrier properties, and permeability. *International Journal of Pharmaceutics* 125, 165–184. [https://doi.org/10.1016/0378-5173\(95\)00109-V](https://doi.org/10.1016/0378-5173(95)00109-V).
- Janiri, D., Carfi, A., Kotzalidis, G.D., Bernabei, R., Landi, F., Sani, G.**, 2021. Posttraumatic Stress Disorder in Patients After Severe COVID-19 Infection. *Journal of the American Medical Association Psychiatry* 78, 567–569. <https://doi.org/10.1001/jamapsychiatry.2021.0109>.

- Johnston, T.P.**, 2015. Anatomy and Physiology of the Oral Mucosa, in: Rathbone, M.J., Şenel, S., Pather, I. (Eds.), Oral mucosal drug delivery and therapy. Springer, pp. 1–15.
- Junginger, H.E., Hoogstraate, J.A., Verhoef, J.C.**, 1999. Recent advances in buccal drug delivery and absorption — in vitro and in vivo studies. *Journal of Controlled Release* 62, 149–159. [https://doi.org/10.1016/S0168-3659\(99\)00032-2](https://doi.org/10.1016/S0168-3659(99)00032-2).
- Kalia, V., Garg, T., Rath, G., Goyal, A.K.**, 2016. Development and evaluation of a sublingual film of the antiemetic granisetron hydrochloride. *Artificial Cells, Nanomedicine, and Biotechnology* 44, 842–846. <https://doi.org/10.3109/21691401.2014.984303>.
- Katz, M., Barr, M.**, 1955. A study of sublingual absorption. I. Several factors influencing the rate of adsorption. *Journal of the American Pharmaceutical Association* 44, 419–423. <https://doi.org/10.1002/jps.3030440710>.
- Kerski, S., Rathsack, W., Stodt, G.**, 2020. DE202015004165U1 - Permeation cell with isofill chamber. <https://patents.google.com/patent/DE202015004165U1/en> (accessed 26 August 2021).
- Klausner, M., Handa, Y., Aizawa, S.**, 2021. In vitro three-dimensional organotypic culture models of the oral mucosa. *In Vitro Cellular & Developmental Biology - Animal* 57, 148–159.
- Koenen, K.C., Ratanatharathorn, A., Ng, L., McLaughlin, K.A., Bromet, E.J., Stein, D.J., Karam, E.G., Meron Ruscio, A., Benjet, C., Scott, K., Atwoli, L., Petukhova, M., Lim, C.C.W., Aguilar-Gaxiola, S., Al-Hamzawi, A., Alonso, J., Bunting, B., Ciutan, M., Girolamo, G.D., Degenhardt, L., Gureje, O., Haro, J.M., Huang, Y., Kawakami, N., Lee, S., Navarro-Mateu, F., Pennell, B.-E., Piazza, M., Sampson, N., Have, M.T., Torres, Y., Viana, M.C., Williams, D., Xavier, M., Kessler, R.C.**, 2017. Posttraumatic stress disorder in the World Mental Health Surveys. *Psychological Medicine* 47, 2260–2274. <https://doi.org/10.1017/S0033291717000708>.
- Kokate, A., Li, X., Jasti, B.**, 2008. HPLC detection of marker compounds during buccal permeation enhancement studies. *Journal of Pharmaceutical and Biomedical Analysis* 47, 190–194. <https://doi.org/10.1016/j.jpba.2007.12.020>.
- Kolli, C.S., Pather, I.**, 2015. Characterization Methods for Oral Mucosal Drug Delivery, in: Rathbone, M.J., Şenel, S., Pather, I. (Eds.), Oral mucosal drug delivery and therapy. Springer, pp. 125–148.
- Koradia, H., Chaudhari, K.**, 2018. Formulation of unidirectional buccal tablet of Mirtazapine: An in vitro and ex vivo evaluation. *Journal of Drug Delivery Science and Technology* 43, 233–242. <https://doi.org/10.1016/j.jddst.2017.10.012>.

- Koranne, S., Govindarajan, R., Suryanarayanan, R.,** 2017. Investigation of Spatial Heterogeneity of Salt Disproportionation in Tablets by Synchrotron X-ray Diffractometry. *Molecular Pharmaceutics* 14, 1133–1144. <https://doi.org/10.1021/acs.molpharmaceut.6b01052>.
- Kottke, D., Majid, H., Breitzkreutz, J., Burckhardt, B.B.,** 2020. Development and evaluation of mucoadhesive buccal dosage forms of lidocaine hydrochloride by ex-vivo permeation studies. *International Journal of Pharmaceutics* 581, 119293. <https://doi.org/10.1016/j.ijpharm.2020.119293>.
- Kragelund, C., Hansen, C., Torpet, L.A., Nauntofte, B., Brøsen, K., Pedersen, A.M.L., Buchwald, C., Therkildsen, M.H., Reibel, J.,** 2008. Expression of two drug-metabolizing cytochrome P450-enzymes in human salivary glands. *Oral Diseases* 14, 533–540. <https://doi.org/10.1111/j.1601-0825.2007.01415.x>.
- Krampe, R., Visser, J.C., Frijlink, H.W., Breitzkreutz, J., Woerdenbag, H.J., Preis, M.,** 2016. Oromucosal film preparations: points to consider for patient centricity and manufacturing processes. *Expert Opinion on Drug Delivery* 13, 493–506. <https://doi.org/10.1517/17425247.2016.1118048>.
- Krystal, J.H., Davis, L.L., Neylan, T.C., A Raskind, M., Schnurr, P.P., Stein, M.B., Vessicchio, J., Shiner, B., Gleason, T.C., Huang, G.D.,** 2017. It Is Time to Address the Crisis in the Pharmacotherapy of Posttraumatic Stress Disorder: A Consensus Statement of the PTSD Psychopharmacology Working Group. *Biological Psychiatry* 82, e51-e59. <https://doi.org/10.1016/j.biopsych.2017.03.007>.
- Kulkarni, U., Mahalingam, R., Pather, I., Li, X., Jasti, B.,** 2010. Porcine buccal mucosa as in vitro model: effect of biological and experimental variables. *Journal of Pharmaceutical Sciences* 99, 1265–1277. <https://doi.org/10.1002/jps.21907>.
- Kulkarni, U., Mahalingam, R., Pather, S.I., Li, X., Jasti, B.,** 2009. Porcine buccal mucosa as an in vitro model: relative contribution of epithelium and connective tissue as permeability barriers. *Journal of Pharmaceutical Sciences* 98, 471–483. <https://doi.org/10.1002/jps.21436>.
- Lam, J.K.W., Cheung, C.C.K., Chow, M.Y.T., Harrop, E., Lapwood, S., Barclay, S.I.G., Wong, I.C.K.,** 2020. Transmucosal drug administration as an alternative route in palliative and end-of-life care during the COVID-19 pandemic. *Advanced Drug Delivery Reviews* 160, 234–243. <https://doi.org/10.1016/j.addr.2020.10.018>.
- Lawson, K.,** 2020. Sleep Dysfunction in Fibromyalgia and Therapeutic Approach Options. *OBM Neurobiology* 4, 1–16. <https://doi.org/10.21926/obm.neurobiol.2001049>.

- Lee, J., Lee, S.K., Choi, Y.W., Lww, S.K.**, 2002. The effect of storage conditions on the permeability of porcine buccal mucosa. *Archives of Pharmacal Research* 25, 546–549. <https://doi.org/10.1007/BF02976616>.
- Lesch, C.A., Squier, C.A., Cruchley, A., Williams, D.M., Speight, P.**, 1989. The permeability of human oral mucosa and skin to water. *Journal of Dental Research* 68, 1345–1349. <https://doi.org/10.1177/00220345890680091101>.
- Li, Y., Scherer, N., Felix, L., Kuper, H.**, 2021. Prevalence of depression, anxiety and post-traumatic stress disorder in health care workers during the COVID-19 pandemic: A systematic review and meta-analysis. *Public Library of Science One* 16, e0246454. <https://doi.org/10.1371/journal.pone.0246454>.
- Liu, Y., Zhao, D., Zhao, Z.**, 2014. Study of degradation mechanisms of cyclobenzaprine by LC-MS/MS. *Analytical Methods* 6, 2320–2330. <https://doi.org/10.1039/C3AY41409D>.
- Lu, Y., Kim, S., Park, K.**, 2011. In vitro-in vivo correlation: perspectives on model development. *International Journal of Pharmaceutics* 418, 142–148. <https://doi.org/10.1016/j.ijpharm.2011.01.010>.
- Lundqvist, T., Bredenberg, S.**, 2013. Pharmaceutical development, in: Hill, R.G., Rang, H.P. (Eds.), *Drug discovery and development :technology and transition*, 2nd ed. Churchill Livingstone Elsevier, pp. 227–238.
- Majid, H., Bartel, A., Burckhardt, B.B.**, 2021a. Development, validation and standardization of oromucosal ex-vivo permeation studies for implementation in quality-controlled environments. *Journal of Pharmaceutical and Biomedical Analysis* 194, 113769. <https://doi.org/10.1016/j.jpba.2020.113769>.
- Majid, H., Bartel, A., Burckhardt, B.B.**, 2021b. Predictivity of Standardized and Controlled Permeation Studies: Ex vivo – In vitro – In vivo Correlation for Sublingual Absorption of Propranolol. *European Journal of Pharmaceutics and Biopharmaceutics* 169, 12–19. <https://doi.org/10.1016/j.ejpb.2021.09.002>.
- Majid, H., Puzik, A., Maier, T., Eberhard, D., Bartel, A., Mueller, H.-C., Burckhardt, B.B.**, 2021c. Exploring the transmucosal permeability of cyclobenzaprine: A comparative preformulation by standardized and controlled ex vivo and in vitro permeation studies. *International Journal of Pharmaceutics* 601, 120574. <https://doi.org/10.1016/j.ijpharm.2021.120574>.
- Majid, H., Puzik, A., Maier, T., Merk, R., Bartel, A., Mueller, H.-C., Burckhardt, B.**, 2021d. Formulation development of sublingual cyclobenzaprine tablets empowered by

- standardized and physiologically relevant ex vivo permeation studies. *Pharmaceutics* 13, 1409. <https://doi.org/10.3390/pharmaceutics13091409>.
- Marxen, E., Mosgaard, M.D., Pedersen, A.M.L., Jacobsen, J.**, 2017. Mucin dispersions as a model for the oromucosal mucus layer in in vitro and ex vivo buccal permeability studies of small molecules. *European Journal of Pharmaceutics and Biopharmaceutics* 121, 121–128. <https://doi.org/10.1016/j.ejpb.2017.09.016>.
- McLenon, J., Rogers, M.A.M.**, 2019. The fear of needles: A systematic review and meta-analysis. *Journal of Advanced Nursing* 75, 30–42. <https://doi.org/10.1111/jan.13818>.
- Meng-Lund, E., Jacobsen, J., Andersen, M.B., Jespersen, M.L., Karlsson, J.-J., Garmer, M., Jørgensen, E.B., Holm, R.**, 2014. Conscious and anaesthetised Göttingen mini-pigs as an in-vivo model for buccal absorption - pH-dependent absorption of metoprolol from bioadhesive tablets. *Drug Development and Industrial Pharmacy* 40, 604–610. <https://doi.org/10.3109/03639045.2014.884119>.
- Mestres, J., Seifert, S.A., Oprea, T.I.**, 2011. Linking pharmacology to clinical reports: cyclobenzaprine and its possible association with serotonin syndrome. *Clinical Pharmacology & Therapeutics* 90, 662–665. <https://doi.org/10.1038/clpt.2011.177>.
- Moldofsky, H., Harris, H.W., Archambault, W.T., Kwang, T., Lederman, S.**, 2011. Effects of bedtime very low dose cyclobenzaprine on symptoms and sleep physiology in patients with fibromyalgia syndrome: a double-blind randomized placebo-controlled study. *The Journal of Rheumatology* 38, 2653–2663. <https://doi.org/10.3899/jrheum.110194>.
- Moniri, N., Senatorov, I., Cheshmehkani, A., Karmokar, P., Singh, K.**, 2021. The skeletal muscle relaxer cyclobenzaprine is a potent non-competitive histamine H1 receptor antagonist. *The FASEB Journal* 35. <https://doi.org/10.1096/fasebj.2021.35.S1.02020>.
- Montero-Padilla, S., Velaga, S., Morales, J.O.**, 2017. Buccal Dosage Forms: General Considerations for Pediatric Patients. *AAPS PharmSciTech* 18, 273–282. <https://doi.org/10.1208/s12249-016-0567-2>.
- Morales, J.O., Brayden, D.J.**, 2017. Buccal delivery of small molecules and biologics: of mucoadhesive polymers, films, and nanoparticles. *Current Opinion in Pharmacology* 36, 22–28. <https://doi.org/10.1016/j.coph.2017.07.011>.
- National Center for Biotechnology Information**, 2021a. PubChem Compound Summary for CID 2519, Caffeine. <https://pubchem.ncbi.nlm.nih.gov/compound/2519#section=Chemical-and-Physical-Properties> (accessed 27 August 2021).

- National Center for Biotechnology Information**, 2021b. PubChem Compound Summary for CID 2895, Cyclobenzaprine. <https://pubchem.ncbi.nlm.nih.gov/compound/2895> (accessed 27 August 2021).
- National Center for Biotechnology Information**, 2021c. PubChem Compound Summary for CID 4173, Metronidazole. <https://pubchem.ncbi.nlm.nih.gov/compound/4173> (accessed 27 August 2021).
- National Center for Biotechnology Information**, 2021d. PubChem Compound Summary for CID 896, Melatonin. <https://pubchem.ncbi.nlm.nih.gov/compound/896> (accessed 27 August 2021).
- National Institute for Health and Care Excellence**, 2018. Post-traumatic stress disorder: NICE Guideline. <https://www.nice.org.uk/guidance/ng116/resources/posttraumatic-stress-disorder-pdf-66141601777861> (accessed 27 August 2021).
- Naumova, E.A., Dierkes, T., Sprang, J., Arnold, W.H.**, 2013. The oral mucosal surface and blood vessels. *Head & Face Medicine* 9, 8. <https://doi.org/10.1186/1746-160X-9-8>.
- Nicolazzo, J.A., Finnin, B.C.**, 2008. In Vivo and In Vitro Models for Assessing Drug Absorption Across the Buccal Mucosa, in: Kim, K.-J., Ehrhardt, C. (Eds.), *Drug Absorption Studies: In Situ, In Vitro and In Silico Models*, VII, 1st ed. Springer-Verlag, pp. 89–111.
- Nielsen, H.M., Rassing, M.R.**, 2000. TR146 cells grown on filters as a model of human buccal epithelium: IV. Permeability of water, mannitol, testosterone and β -adrenoceptor antagonists. Comparison to human, monkey and porcine buccal mucosa. *International Journal of Pharmaceutics* 194, 155–167. [https://doi.org/10.1016/S0378-5173\(99\)00368-3](https://doi.org/10.1016/S0378-5173(99)00368-3).
- Nielsen, H.M., Rassing, M.R.**, 2002. Nicotine permeability across the buccal TR146 cell culture model and porcine buccal mucosa in vitro: effect of pH and concentration. *European Journal of Pharmaceutical Sciences* 16, 151–157. [https://doi.org/10.1016/S0928-0987\(02\)00083-0](https://doi.org/10.1016/S0928-0987(02)00083-0).
- Obradovic, T., Hidalgo, I.J.**, 2008. In Vitro Models for Investigations of Buccal Drug Permeation and Metabolism, in: Kim, K.-J., Ehrhardt, C. (Eds.), *Drug Absorption Studies: In Situ, In Vitro and In Silico Models*, VII, 1st ed. Springer-Verlag, pp. 167–181.
- Palem, C.R., Dudhipala, N.R., Battu, S.K., Repka, M.A., Rao Yamsani, M.**, 2016. Development, optimization and in vivo characterization of domperidone-controlled release hot-melt-extruded films for buccal delivery. *Drug Development and Industrial Pharmacy* 42, 473–484. <https://doi.org/10.3109/03639045.2015.1104346>.
- Patel, M.A., Luthra, S., Shamblin, S.L., Arora, K.K., Krzyzaniak, J.F., Taylor, L.S.**, 2018. Effect of excipient properties, water activity, and water content on the disproportionation of

- a pharmaceutical salt. *International Journal of Pharmaceutics* 546, 226–234. <https://doi.org/10.1016/j.ijpharm.2018.05.035>.
- Patel, V.F., Liu, F., Brown, M.B.**, 2012. Modeling the oral cavity: in vitro and in vivo evaluations of buccal drug delivery systems. *Journal of Controlled Release* 161, 746–756. <https://doi.org/10.1016/j.jconrel.2012.05.026>.
- Pather, S.I., Rathbone, M.J., Şenel, S.**, 2008. Current status and the future of buccal drug delivery systems. *Expert Opinion on Drug Delivery* 5, 531–542. <https://doi.org/10.1517/17425247.5.5.531>.
- Pinto, S., Pintado, M.E., Sarmiento, B.**, 2020. In vivo, ex vivo and in vitro assessment of buccal permeation of drugs from delivery systems. *Expert Opinion on Drug Delivery* 17, 33–48. <https://doi.org/10.1080/17425247.2020.1699913>.
- Radhakrishnan, C., Sefidani Forough, A., Cichero, J.A.Y., Smyth, H.E., Raidhan, A., Nissen, L.M., Steadman, K.J.**, 2021. A Difficult Pill to Swallow: An Investigation of the Factors Associated with Medication Swallowing Difficulties. *Patient Preference and Adherence* 15, 29–40. <https://doi.org/10.2147/PPA.S277238>.
- Rane, S.S., Moe, D.**, 2015. Tablets and Other Solid Dosage Forms for Systemic Oral Mucosal Drug Delivery, in: Rathbone, M.J., Şenel, S., Pather, I. (Eds.), *Oral mucosal drug delivery and therapy*. Springer, pp. 169–205.
- Rathbone, M.J., Pather, I., Şenel, S.**, 2015a. Overview of Oral Mucosal Delivery, in: Rathbone, M.J., Şenel, S., Pather, I. (Eds.), *Oral mucosal drug delivery and therapy*. Springer, pp. 17–29.
- Rathbone, M.J., Şenel, S., Pather, I.**, 2015b. Design and Development of Systemic Oral Mucosal Drug Delivery Systems, in: Rathbone, M.J., Şenel, S., Pather, I. (Eds.), *Oral mucosal drug delivery and therapy*. Springer, pp. 149–167.
- Reinhard, M.A., Seifert, J., Greiner, T., Toto, S., Bleich, S., Grohmann, R.**, 2021. Pharmacotherapy of 1,044 inpatients with posttraumatic stress disorder: current status and trends in German-speaking countries. *European Archives of Psychiatry and Clinical Neuroscience* 271, 1065–1076. <https://doi.org/10.1007/s00406-020-01223-x>.
- Rekhi, G.S., Porter, S.C., Jambhekar, S.S.**, 1995. Factors Affecting the Release of Propranolol Hydrochloride from Beads Coated with Aqueous Polymeric Dispersions. *Drug Development and Industrial Pharmacy* 21, 709–729. <https://doi.org/10.3109/03639049509048136>.

- Roblegg, E., Fröhlich, E., Meindl, C., Teubl, B., Zaversky, M., Zimmer, A.,** 2012. Evaluation of a physiological in vitro system to study the transport of nanoparticles through the buccal mucosa. *Nanotoxicology* 6, 399–413. <https://doi.org/10.3109/17435390.2011.580863>.
- Rohatgi, A.,** Pacifica, California, USA. WebPlotDigitizer, USA.
- Rossi, S., Sandri, G., Caramella, C.M.,** 2005. Buccal drug delivery: A challenge already won? *Drug Discovery Today-Technologies* 2, 59–65. <https://doi.org/10.1016/j.ddtec.2005.05.018>.
- Russell, W.M.S., Burch, R.L.,** 1992. The principles of humane experimental technique. Universities Federation For Animal Welfare.
- Russell W. M. S., Burch R. L.,** 1959. The principles of humane experimental technique. Methuen.
- Sandri, G., Ruggeri, M., Rossi, S., Bonferoni, M.C., Vigani, B., Ferrari, F.,** 2020. (Trans)buccal drug delivery, in: João Pedro Martins, Hélder A. Santos (Ed.), *Nanotechnology for Oral Drug Delivery*. Elsevier, pp. 225–250.
- Sántha, M.,** 2020. Biologia futura: animal testing in drug development—the past, the present and the future. *Biologia Futura* 71, 443–452. <https://doi.org/10.1007/s42977-020-00050-4>.
- Sarmento, B. (Ed.), 2016. Concepts and models for drug permeability studies: Cell and tissue based In vitro culture models. Elsevier Ltd.
- Sartori, S.B., Singewald, N.,** 2019. Novel pharmacological targets in drug development for the treatment of anxiety and anxiety-related disorders. *Pharmacology & Therapeutics* 204, 107402. <https://doi.org/10.1016/j.pharmthera.2019.107402>.
- Sattar, M., Hadgraft, J., Lane, M.E.,** 2015. Preparation, characterization and buccal permeation of naratriptan. *International Journal of Pharmaceutics* 493, 146–151. <https://doi.org/10.1016/j.ijpharm.2015.07.035>.
- Sattar, M., Sayed, O.M., Lane, M.E.,** 2014. Oral transmucosal drug delivery--current status and future prospects. *International Journal of Pharmaceutics* 471, 498–506. <https://doi.org/10.1016/j.ijpharm.2014.05.043>.
- Schiele, J.T., Quinzler, R., Klimm, H.-D., Pruszydlo, M.G., Haefeli, W.E.,** 2013. Difficulties swallowing solid oral dosage forms in a general practice population: prevalence, causes, and relationship to dosage forms. *European Journal of Clinical Pharmacology* 69, 937–948. <https://doi.org/10.1007/s00228-012-1417-0>.

- Schoenwald, R.D., Huang, H.S.**, 1983. Corneal penetration behavior of beta-blocking agents I: Physiochemical factors. *Journal of Pharmaceutical Sciences* 72, 1266–1272. <https://doi.org/10.1002/jps.2600721108>.
- Schürmann, W., Turner, P.**, 1978. A membrane model of the human oral mucosa as derived from buccal absorption performance and physicochemical properties of the beta-blocking drugs atenolol and propranolol. *The Journal of Pharmacy and Pharmacology* 30, 137–147. <https://doi.org/10.1111/j.2042-7158.1978.tb13185.x>.
- Şenel, S., Rathbone, M.J., Cansız, M., Pather, I.**, 2012. Recent developments in buccal and sublingual delivery systems. *Expert Opinion on Drug Delivery* 9, 615–628. <https://doi.org/10.1517/17425247.2012.676040>.
- Shah, S.M., Jain, A.S., Kaushik, R., Nagarsenker, M.S., Nerurkar, M.J.**, 2014. Preclinical formulations: insight, strategies, and practical considerations. *AAPS PharmSciTech* 15, 1307–1323. <https://doi.org/10.1208/s12249-014-0156-1>.
- Shore, P.A., Brodie, B.B., Hogben, C.A.M.**, 1959. On the mechanism of intestinal absorption of drugs. *The Journal of Pharmacology and Experimental Therapeutics* 125, 275–282.
- Shore, P.A., Brodie, B.B., HOGBEN, C.A.**, 1957. The gastric secretion of drugs: a pH partition hypothesis. *The Journal of Pharmacology and Experimental Therapeutics* 119, 361–369.
- Shrestha, N., Araújo, F., Sarmiento, B., Hirvonen, J., Santos, H.A.**, 2016. 3.1 - Cell-based in vitro models for buccal permeability studies, in: Sarmiento, B. (Ed.), *Concepts and models for drug permeability studies: Cell and tissue based In vitro culture models*. Elsevier Ltd, pp. 31–40.
- Siegel, I.A., Gordon, H.P.**, 1985. Effects of surfactants on the permeability of canine oral mucosa in vitro. *Toxicology Letters* 26, 153–158. [https://doi.org/10.1016/0378-4274\(85\)90160-2](https://doi.org/10.1016/0378-4274(85)90160-2).
- Smart, J.D.**, 2004. Lectin-mediated drug delivery in the oral cavity. *Advanced Drug Delivery Reviews* 56, 481–489. <https://doi.org/10.1016/j.addr.2003.10.016>.
- Sohi, H., Ahuja, A., Ahmad, F.J., Khar, R.K.**, 2010. Critical evaluation of permeation enhancers for oral mucosal drug delivery. *Drug Development and Industrial Pharmacy* 36, 254–282. <https://doi.org/10.3109/03639040903117348>.
- Song, Q., Shen, C., Shen, B., Lian, W., Liu, X., Dai, B., Yuan, H.**, 2018. Development of a fast dissolving sublingual film containing meloxicam nanocrystals for enhanced dissolution and earlier absorption. *Journal of Drug Delivery Science and Technology* 43, 243–252. <https://doi.org/10.1016/j.jddst.2017.10.020>.

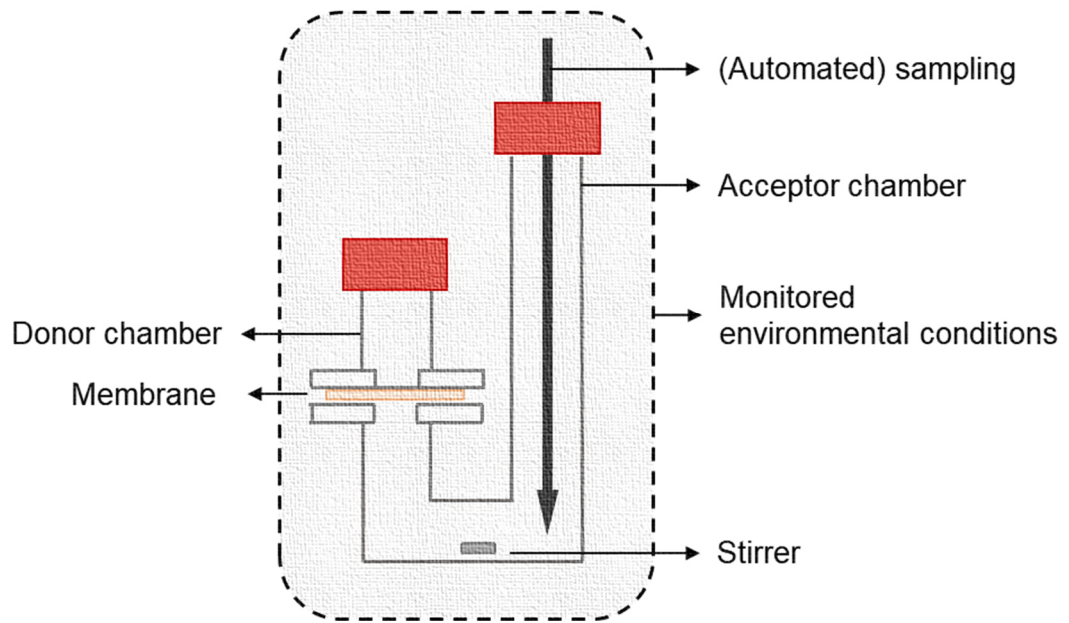
- Spoormaker, V.I., Montgomery, P.**, 2008. Disturbed sleep in post-traumatic stress disorder: secondary symptom or core feature? *Sleep Medicine Reviews* 12, 169–184. <https://doi.org/10.1016/j.smr.2007.08.008>.
- Squier, C.A., Kremer, M.J.**, 2001. Biology of oral mucosa and esophagus. *Journal of the National Cancer Institute Monographs* 29, 7–15. <https://doi.org/10.1093/oxfordjournals.jncimonographs.a003443>.
- Stephenson, G.A., Aburub, A., Woods, T.A.**, 2011. Physical stability of salts of weak bases in the solid-state. *Journal of Pharmaceutical Sciences* 100, 1607–1617. <https://doi.org/10.1002/jps.22405>.
- Suarez-Sharp, S., Li, M., Duan, J., Shah, H., Seo, P.**, 2016. Regulatory Experience with In Vivo In Vitro Correlations (IVIVC) in New Drug Applications. *The AAPS journal* 18, 1379–1390. <https://doi.org/10.1208/s12248-016-9966-2>.
- Sullivan, G.M., Gendreau, R.M., Gendreau, J., Peters, P., Peters, A., Engels, J., Daugherty, B.L., Vaughn, B., Weathers, F.W., Lederman, S.**, 2021. Randomized clinical trial of bedtime sublingual cyclobenzaprine (TNX-102 SL) in military-related PTSD and the role of sleep quality in treatment response. *Psychiatry Research* 301, 113974. <https://doi.org/10.1016/j.psychres.2021.113974>.
- Tavakoli-Saberi, M.R., Audus, K.L.**, 1989. Cultured buccal epithelium: an in vitro model derived from the hamster pouch for studying drug transport and metabolism. *Pharmaceutical Research* 6, 160–166. <https://doi.org/10.1023/A:1015988727757>.
- Taylor, K., Alvarez, L.R.**, 2019. An Estimate of the Number of Animals Used for Scientific Purposes Worldwide in 2015. *Alternatives to Laboratory Animals* 47, 196–213. <https://doi.org/10.1177/0261192919899853>.
- Telò, I., Tratta, E., Guasconi, B., Nicoli, S., Pescina, S., Govoni, P., Santi, P., Padula, C.**, 2016. In-vitro characterization of buccal iontophoresis: the case of sumatriptan succinate. *International Journal of Pharmaceutics* 506, 420–428. <https://doi.org/10.1016/j.ijpharm.2016.04.054>.
- The United States Pharmacopeia**, 2019. Revision Bulletin Cyclobenzaprine Hydrochloride. *Chemical Medicines Monographs* 4. https://www.uspnf.com/sites/default/files/usp_pdf/EN/USPNF/revisions/cyclobenzaprine-hcl-rb-notice-20191227.pdf (accessed 8 July 2021).
- Tian, Y., Orlu, M., Woerdenbag, H.J., Scarpa, M., Kiefer, O., Kottke, D., Sjöholm, E., Öblom, H., Sandler, N., Hinrichs, W.L.J., Frijlink, H.W., Breitkreutz, J., Visser, J.C.**,

2019. Oromucosal films: from patient centricity to production by printing techniques. *Expert Opinion on Drug Delivery* 16, 981–993. <https://doi.org/10.1080/17425247.2019.1652595>.
- Tofferi, J.K., Jackson, J.L., O'Malley, P.G.**, 2004. Treatment of fibromyalgia with cyclobenzaprine: A meta-analysis. *Arthritis Care & Research* 51, 9–13. <https://doi.org/10.1002/art.20076>.
- Tricklebank, M.D., Robbins, T.W., Simmons, C., Wong, E.H.F.**, 2021. Time to re-engage psychiatric drug discovery by strengthening confidence in preclinical psychopharmacology. *Psychopharmacology* 238, 1417–1436. <https://doi.org/10.1007/s00213-021-05787-x>.
- Tsagogiorgas, C., Theisinger, S., Holm, P., Thiel, M., Quintel, M., Holm, R.**, 2013. Buccal absorption of propofol when dosed in 1-perfluorobutylpentane to anaesthetised and conscious Wistar rats and Göttingen mini-pigs. *European Journal of Pharmaceutics and Biopharmaceutics* 85, 1310–1316. <https://doi.org/10.1016/j.ejpb.2013.06.013>.
- U.S. Department of Health and Human Services Food and Drug Administration**, 2018. *Bioanalytical Method Validation Guidance for Industry*.
- van Eyk, A.D., van der Bijl, P.**, 2006. Comparative permeability of fresh and frozen/thawed porcine buccal mucosa towards various chemical markers. *Journal of the South African Dental Association* 61, 200–203.
- Volpe, D.A.**, 2010. Application of method suitability for drug permeability classification. *The AAPS Journal* 12, 670–678. <https://doi.org/10.1208/s12248-010-9227-8>.
- Wang, R.W., Liu, L., Cheng, H.**, 1996. Identification of human liver cytochrome P450 isoforms involved in the in vitro metabolism of cyclobenzaprine. *Drug Metabolism and Disposition* 24, 786–791.
- Wang, S., Zuo, A., Guo, J.**, 2020. Types and evaluation of in vitro penetration models for buccal mucosal delivery. *Journal of Drug Delivery Science and Technology* 61, 102122. <https://doi.org/10.1016/j.jddst.2020.102122>.
- Wang, Y., Zuo, Z., Chen, X., Tomlinson, B., Chow, M.S.S.**, 2010. Improving sublingual delivery of weak base compounds using pH(max) concept: application to propranolol. *European Journal of Pharmaceutical Sciences* 39, 272–278. <https://doi.org/10.1016/j.ejps.2009.12.011>.
- Wang, Z., Chow, M.S.**, 2014. Overview and appraisal of the current concept and technologies for improvement of sublingual drug delivery. *Therapeutic Delivery* 5, 807–816. <https://doi.org/10.4155/tde.14.50>.

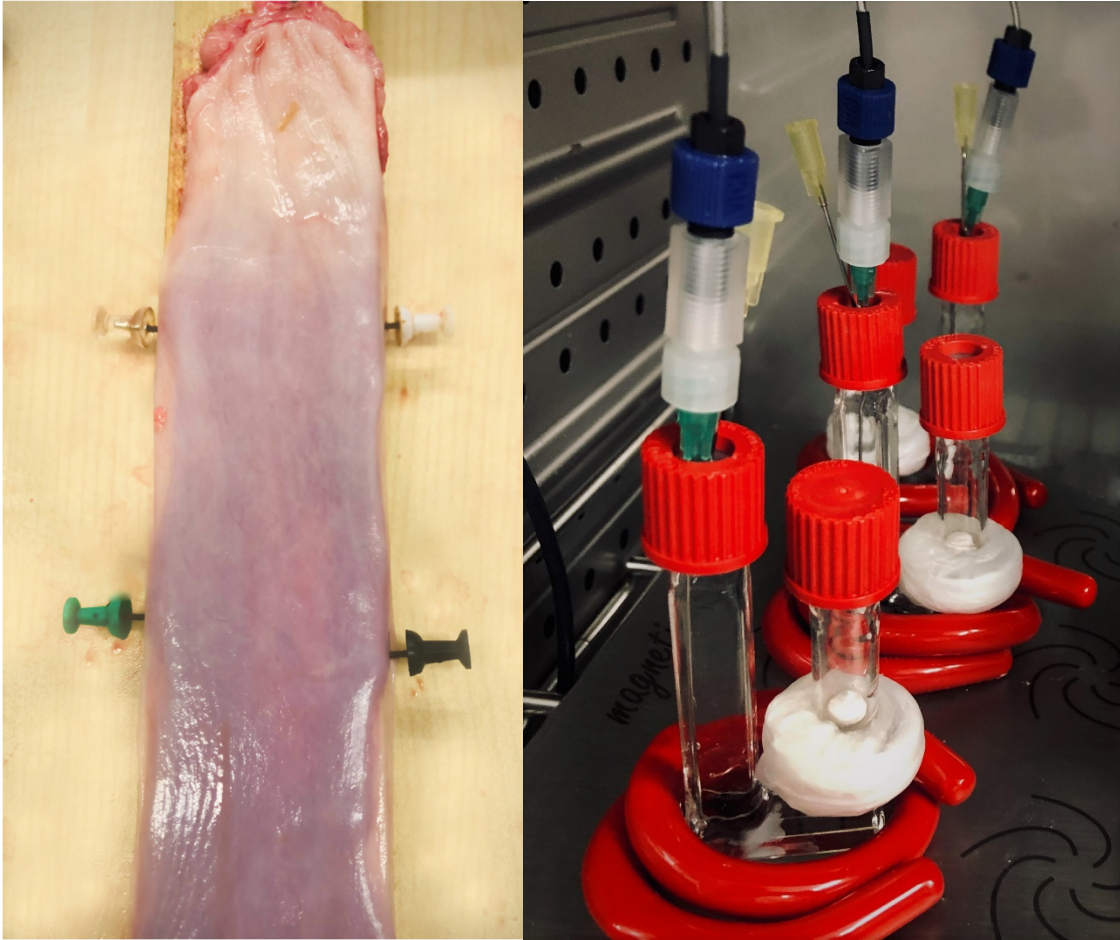
- Wertz, P.W.**, 2021. Roles of Lipids in the Permeability Barriers of Skin and Oral Mucosa. *International Journal of Molecular Sciences* 22, 5229. <https://doi.org/10.3390/ijms22105229>.
- Winchell, G.A., King, J.D., Chavez-Eng, C.M., Constanzer, M.L., Korn, S.H.**, 2002. Cyclobenzaprine pharmacokinetics, including the effects of age, gender, and hepatic insufficiency. *Journal of Clinical Pharmacology* 42, 61–69. <https://doi.org/10.1177/0091270002042001007>.
- Yasuhara, H., Dujovne, C.A., Ueda, I.**, 1979. Relationship between surface activity and toxicity to Chang liver cultures of tricyclic antidepressants. *Pharmacology* 18, 95–102. <https://doi.org/10.1159/000137236>.
- Yu, J.**, 2014. Cyclobenzaprine, in: Lee, P.W. (Ed.), *Handbook of metabolic pathways of xenobiotics*. Wiley, pp. 1–5.
- Zane, P., Gieschen, H., Kersten, E., Mathias, N., Ollier, C., Johansson, P., van den Bergh, A., van Hemelryck, S., Reichel, A., Rotgeri, A., Schäfer, K., Müllertz, A., Langguth, P.**, 2019. In vivo models and decision trees for formulation development in early drug development: A review of current practices and recommendations for biopharmaceutical development. *European Journal of Pharmaceutics and Biopharmaceutics* 142, 222–231. <https://doi.org/10.1016/j.ejpb.2019.06.010>.
- Zhang, H., Zhang, J., Streisand, J.B.**, 2002. Oral mucosal drug delivery: clinical pharmacokinetics and therapeutic applications. *Clinical Pharmacokinetics* 41, 661–680. <https://doi.org/10.2165/00003088-200241090-00003>.

10. Appendix

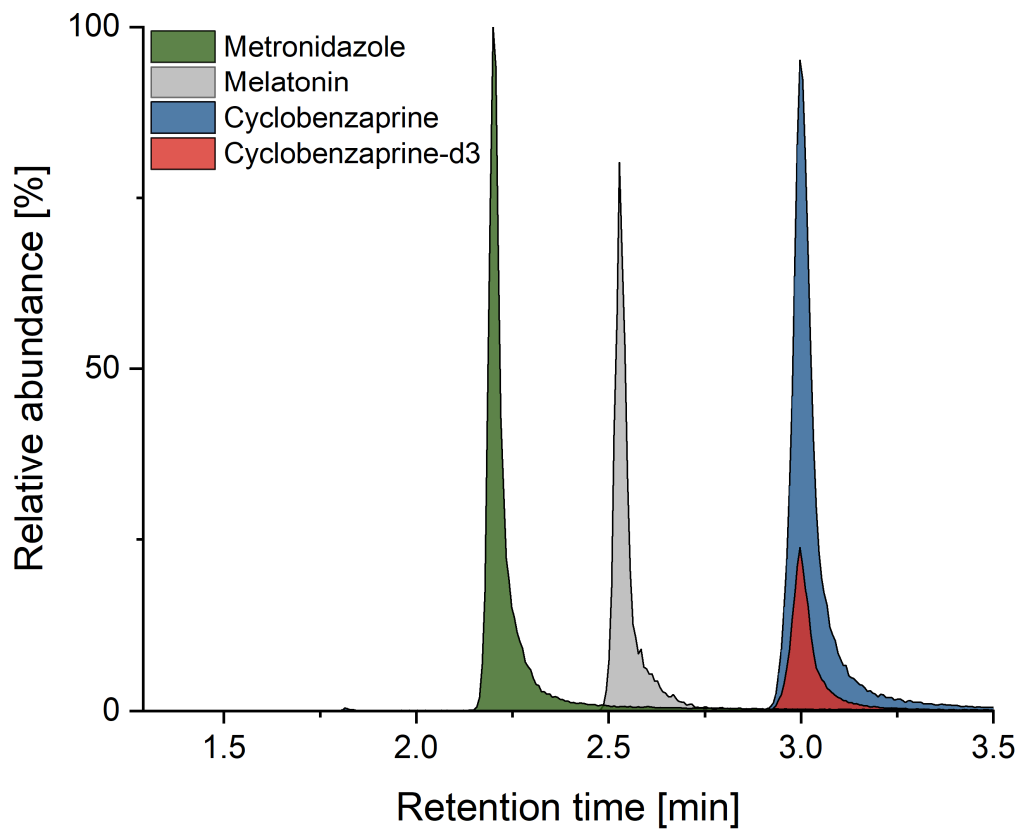
Appendix 1: Schematic illustration of the Kerski diffusion cell	142
Appendix 2: Porcine esophagus (left) before preparation of mucosal tissue and Kerski diffusion cells during permeation study using sublingual tablets.	143
Appendix 3: LC-MS/MS chromatogram of metronidazole (380.96 ng/mL), melatonin (380.96 ng/mL), cyclobenzaprine (190.48 ng/mL) and cyclobenzaprine-d3 .	144
Appendix 4: Exemplary run of accuracy and precision of cyclobenzaprine hydrochloride	145
Appendix 5: Exemplary run of accuracy and precision of desmethyl cyclobenzaprine hydrochloride.....	147
Appendix 6: Exemplary run of accuracy and precision of cyclobenzaprine N-oxide.....	149
Appendix 7: TOF-MS scan of cyclobenzaprine and cyclobenzaprine N-oxide	151
Appendix 8: Product ion scan (TOF-MS/MS) of cyclobenzaprine N-oxide	152
Appendix 9: Exemplary run of performance qualification for absorption reader within a permeation study of propranolol hydrochloride.	153
Appendix 10: Exemplary run of LC-MS/MS quantification within a permeation study of propranolol hydrochloride.	154
Appendix 11: Exemplary run of membrane integrity within a permeation study of propranolol hydrochloride.	158
Appendix 12: Exemplary run of membrane viability within a permeation study of propranolol hydrochloride.	159



Appendix 1: Schematic illustration of the Kerski diffusion cell.



Appendix 2: Porcine esophagus (left) before preparation of mucosal tissue and Kerski diffusion cells during permeation study using sublingual tablets.



Appendix 3: LC-MS/MS chromatogram of metronidazole (380.96 ng/mL), melatonin (380.96 ng/mL), cyclobenzaprine (190.48 ng/mL) and cyclobenzaprine-d3.

Appendix 4: Exemplary run of accuracy and precision of cyclobenzaprine hydrochloride.

Sample	Sample type	NomConc. [ng/mL]	Area ratio	Used	Modified	CalConc. [ng/mL]	Accuracy [%]
Blank.1	Blank	n.a.	n.a.	-	-	n.a.	n.a.
Blank.2	Blank	n.a.	n.a.	-	-	n.a.	n.a.
Zero.1	-	n.a.	0.03	-	-	0.17	n.a.
Zero.2	-	n.a.	0.03	-	-	0.15	n.a.
K11.1	STD	0.92	0.30	+	-	0.98	106
K11.2	STD	0.92	0.29	+	-	0.94	102
K10.1	STD	1.85	0.54	+	-	1.71	92.3
K10.2	STD	1.85	0.56	+	-	1.78	96.3
K9.1	STD	3.70	1.18	+	-	3.67	99.2
K9.2	STD	3.70	1.17	+	-	3.65	98.7
K8.1	STD	7.40	2.34	+	-	7.22	97.6
K8.2	STD	7.40	2.31	+	-	7.13	96.4
K7.1	STD	14.79	4.59	+	-	14.10	95.4
K7.2	STD	14.79	4.59	+	-	14.08	95.2
K6.1	STD	29.58	9.63	+	-	29.45	99.6
K6.2	STD	29.58	9.53	+	-	29.16	98.6
K5.1	STD	59.17	19.90	+	-	60.50	102
K5.2	STD	59.17	20.10	+	-	61.16	103
K4.1	STD	118.33	40.50	+	-	122.80	104
K4.2	STD	118.33	43.00	+	-	130.20	110
K3.1	STD	236.67	81.50	+	-	244.20	103
K3.2	STD	236.67	79.10	+	-	237.10	100
K2.1	STD	473.33	162.00	+	-	476.80	101
K2.2	STD	473.33	169.00	+	-	495.00	105
K1.1	STD	946.67	324.00	+	-	916.20	96.8
K1.2	STD	946.67	330.00	+	-	931.70	98.4
LLOQ 1	QC	0.92	0.33	+	-	1.06	115
LLOQ 2	QC	0.92	0.30	+	-	0.98	106
LLOQ 3	QC	0.92	0.31	+	-	1.02	111
LLOQ 4	QC	0.92	0.30	+	-	0.99	107
LLOQ 5	QC	0.92	0.29	+	-	0.96	104
LQC 1	QC	3.70	1.09	+	-	3.39	91.8
LQC 2	QC	3.70	1.06	+	-	3.31	89.5

LQC 3	QC	3.70	1.12	+	-	3.49	94.4
LQC 4	QC	3.70	1.15	+	-	3.58	96.7
LQC 5	QC	3.70	1.11	+	-	3.47	93.9
MQC 1	QC	59.17	20.10	+	-	61.31	104
MQC 2	QC	59.17	20.20	+	-	61.50	104
MQC 3	QC	59.17	20.50	+	-	62.55	106
MQC 4	QC	59.17	19.60	+	-	59.58	101
MQC 5	QC	59.17	19.90	+	-	60.57	102
HQC 1	QC	473.33	156.00	+	-	459.70	97.1
HQC 2	QC	473.33	154.00	+	-	453.10	95.7
HQC 3	QC	473.33	164.00	+	-	481.90	102
HQC 4	QC	473.33	172.00	+	-	504.90	107
HQC 5	QC	473.33	157.00	+	-	461.30	97.5

CalConc.: calculated concentration, HQC: high quality control, LLOQ: lower limit of quantification, LQC: low quality control, MQC: middle quality control, n.a.: not applicable, NomCalc.: nominal concentration, QC: quality control, STD: standard

Appendix 5: Exemplary run of accuracy and precision of desmethyl cyclobenzaprine hydrochloride.

Sample	Sample type	NomConc. [ng/mL]	Area ratio	Used	Modified	CalConc. [ng/mL]	Accuracy [%]
Blank.1	Blank	n.a.	n.a.	-	-	n.a.	n.a.
Blank.2	Blank	n.a.	n.a.	-	-	n.a.	n.a.
Zero.1	-	n.a.	0.03	-	-	0.07	n.a.
Zero.2	-	n.a.	0.04	-	-	0.08	n.a.
K11.1	STD	0.93	0.38	+	-	0.91	98.2
K11.2	STD	0.93	0.41	+	-	0.98	106
K10.1	STD	1.86	0.73	+	-	1.76	94.5
K10.2	STD	1.86	0.70	+	-	1.70	91.3
K9.1	STD	3.72	1.61	+	-	3.90	105
K9.2	STD	3.72	1.65	+	-	4.01	108
K8.1	STD	7.44	3.04	+	-	7.38	99.2
K8.2	STD	7.44	3.07	+	-	7.45	100
K7.1	STD	14.88	6.15	+	-	14.93	100
K7.2	STD	14.88	6.04	+	-	14.68	98.7
K6.1	STD	29.76	12.50	+	-	30.28	102
K6.2	STD	29.76	12.40	+	-	30.19	101
K5.1	STD	59.52	24.20	+	-	58.92	99
K5.2	STD	59.52	25.20	+	-	61.28	103
K4.1	STD	119.05	49.50	+	-	121.10	102
K4.2	STD	119.05	50.20	+	-	122.60	103
K3.1	STD	238.10	94.20	+	-	231.70	97.3
K3.2	STD	238.10	88.80	+	-	218.30	91.7
K2.1	STD	476.19	185.00	+	-	459.60	96.5
K2.2	STD	476.19	190.00	+	-	472.40	99.2
K1.1	STD	952.38	372.00	+	-	954.00	100
K1.2	STD	952.38	387.00	+	-	992.30	104
LLOQ 1	QC	0.93	0.44	+	-	1.05	113
LLOQ 2	QC	0.93	0.41	+	-	0.98	105
LLOQ 3	QC	0.93	0.42	+	-	1.02	109
LLOQ 4	QC	0.93	0.42	+	-	1.01	109
LLOQ 5	QC	0.93	0.41	+	-	0.98	105
LQC 1	QC	3.72	1.40	+	-	3.38	90.7

LQC 2	QC	3.72	1.49	+	-	3.61	97.1
LQC 3	QC	3.72	1.44	+	-	3.49	93.9
LQC 4	QC	3.72	1.50	+	-	3.62	97.3
LQC 5	QC	3.72	1.47	+	-	3.56	95.7
MQC 1	QC	59.52	24.70	+	-	60.27	101
MQC 2	QC	59.52	25.00	+	-	60.84	102
MQC 3	QC	59.52	26.00	+	-	63.30	106
MQC 4	QC	59.52	24.20	+	-	58.96	99.1
MQC 5	QC	59.52	24.60	+	-	60.02	101
HQC 1	QC	476.19	179.00	+	-	444.80	93.4
HQC 2	QC	476.19	178.00	+	-	442.00	92.8
HQC 3	QC	476.19	182.00	+	-	453.80	95.3
HQC 4	QC	476.19	195.00	+	-	485.60	102
HQC 5	QC	476.19	185.00	+	-	460.10	96.6

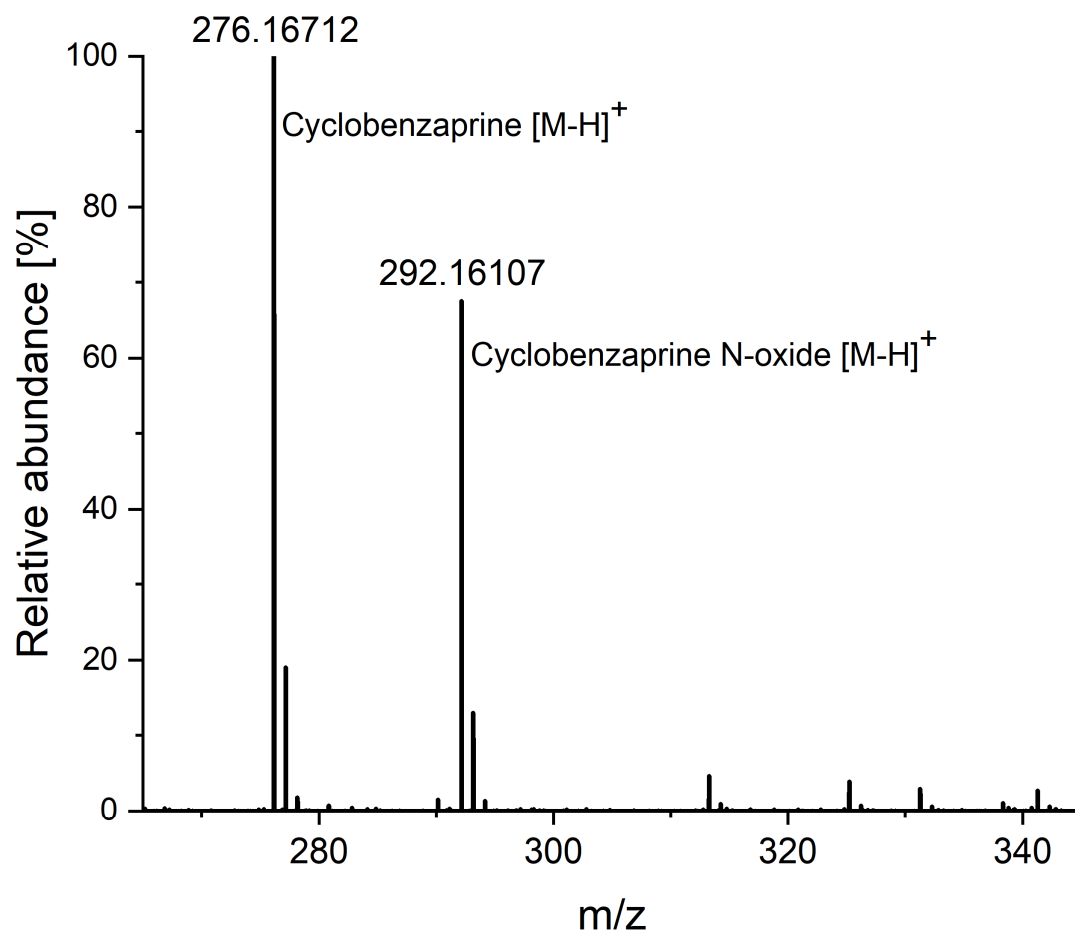
CalConc.: calculated concentration, HQC: high quality control, LLOQ: lower limit of quantification, LQC: low quality control, MQC: middle quality control, n.a.: not applicable, NomCalc.: nominal concentration, QC: quality control, STD: standard

Appendix 6: Exemplary run of accuracy and precision of cyclobenzaprine N-oxide.

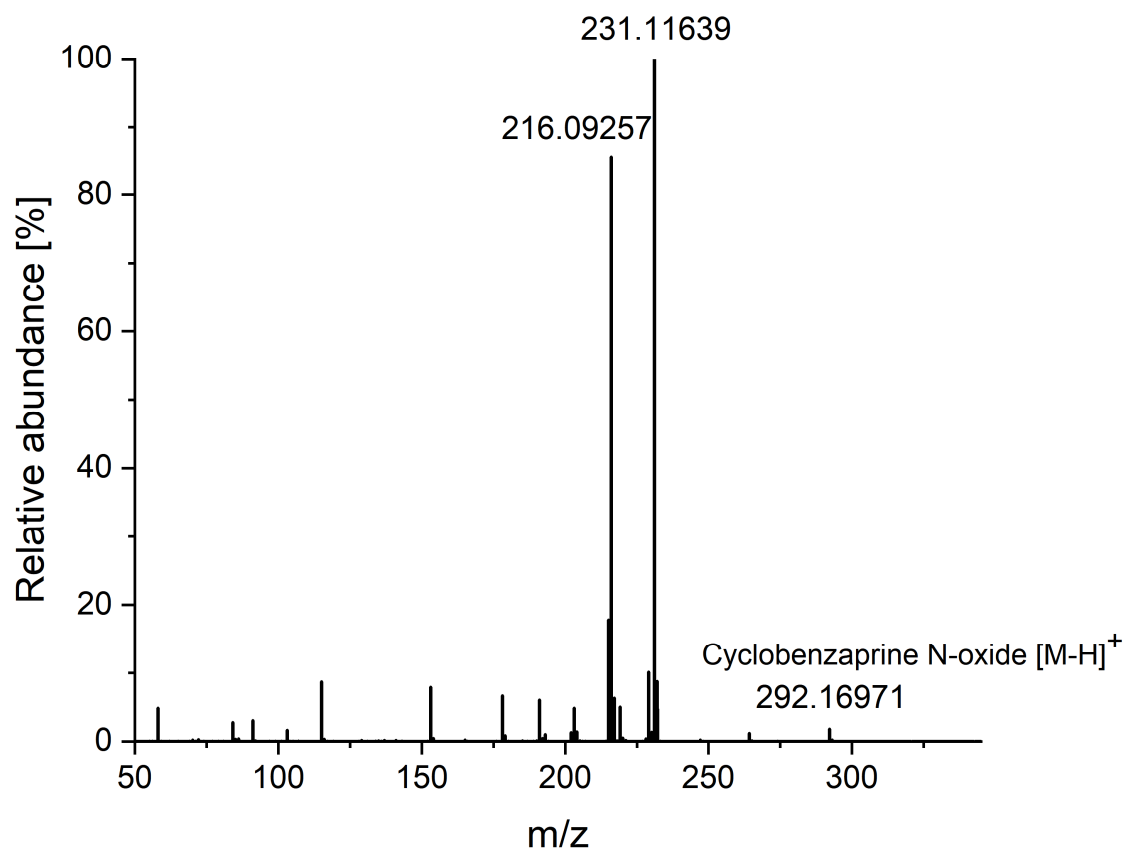
Sample	Sample type	NomConc. [ng/mL]	Area ratio	Used	Modified	CalConc. [ng/mL]	Accuracy [%]
Blank.1	Blank	n.a.	n.a.	-	-	n.a.	n.a.
Blank.2	Blank	n.a.	n.a.	-	-	n.a.	n.a.
Zero.1	-	n.a.	0.02	-	-	< 0	n.a.
Zero.2	-	n.a.	0.02	-	-	< 0	n.a.
K11.1	STD	0.93	0.60	+	-	0.89	95.7
K11.2	STD	0.93	0.62	+	-	0.93	99.6
K10.1	STD	1.86	1.09	+	-	1.77	95.2
K10.2	STD	1.86	1.13	+	-	1.84	99.1
K9.1	STD	3.72	2.37	+	-	4.06	109
K9.2	STD	3.72	2.50	+	-	4.31	116
K8.1	STD	7.44	4.47	+	-	7.84	105
K8.2	STD	7.44	4.46	+	-	7.83	105
K7.1	STD	14.88	8.49	+	-	15.07	101
K7.2	STD	14.88	8.34	+	-	14.80	99.4
K6.1	STD	29.76	17.30	+	-	30.91	104
K6.2	STD	29.76	17.00	+	-	30.48	102
K5.1	STD	59.52	30.70	+	-	55.43	93.1
K5.2	STD	59.52	31.90	+	-	57.51	96.6
K4.1	STD	119.05	61.40	+	-	112.00	94.1
K4.2	STD	119.05	64.60	+	-	117.90	99.1
K3.1	STD	238.10	117.00	+	-	217.50	91.3
K3.2	STD	238.10	113.00	+	-	209.70	88.1
K2.1	STD	476.19	237.00	+	-	456.90	96
K2.2	STD	476.19	243.00	+	-	471.20	98.9
K1.1	STD	952.38	463.00	+	-	981.60	103
K1.2	STD	952.38	483.00	+	-	1034.00	109
LLOQ 1	QC	0.93	0.61	+	-	0.91	98
LLOQ 2	QC	0.93	0.62	+	-	0.92	98.6
LLOQ 3	QC	0.93	0.61	+	-	0.90	97.2
LLOQ 4	QC	0.93	0.61	+	-	0.90	97.2
LLOQ 5	QC	0.93	0.61	+	-	0.90	96.9
LQC 1	QC	3.72	2.11	+	-	3.61	96.9
LQC 2	QC	3.72	2.11	+	-	3.60	96.8

LQC 3	QC	3.72	2.11	+	-	3.59	96.6
LQC 4	QC	3.72	2.07	+	-	3.52	94.6
LQC 5	QC	3.72	2.08	+	-	3.54	95.1
MQC 1	QC	59.52	31.80	+	-	57.29	96.3
MQC 2	QC	59.52	32.30	+	-	58.33	98
MQC 3	QC	59.52	32.90	+	-	59.42	99.8
MQC 4	QC	59.52	31.00	+	-	55.86	93.8
MQC 5	QC	59.52	31.00	+	-	55.96	94
HQC 1	QC	476.2	217.00	+	-	416.50	87.5
HQC 2	QC	476.2	227.00	+	-	436.30	91.6
HQC 3	QC	476.2	226.00	+	-	435.60	91.5
HQC 4	QC	476.2	245.00	+	-	473.60	99.5
HQC 5	QC	476.2	219.00	+	-	420.00	88.2

CalConc.: calculated concentration, HQC: high quality control, LLOQ: lower limit of quantification, LQC: low quality control, MQC: middle quality control, n.a.: not applicable, NomCalc.: nominal concentration, QC: quality control, STD: standard



Appendix 7: TOF-MS scan of cyclobenzaprine and cyclobenzaprine N-oxide.



Appendix 8: Product ion scan (TOF-MS/MS) of cyclobenzaprine N-oxide.

Appendix 9: Exemplary run of performance qualification for absorption reader within a permeation study of propranolol hydrochloride.

Sample	NomConc. [µg/mL]	Optical density	CV [%]
PQ1.1	900.00	3.1374	1.12
PQ1.2	900.00	3.1271	
PQ1.3	900.00	3.1106	
PQ1.4	900.00	3.1301	
PQ1.5	900.00	3.0512	
PQ2.1	450.00	1.7945	0.45
PQ2.2	450.00	1.7867	
PQ2.3	450.00	1.7754	
PQ2.4	450.00	1.7901	
PQ2.5	450.00	1.7785	
PQ3.1	225.00	0.8882	1.02
PQ3.2	225.00	0.8859	
PQ3.3	225.00	0.8910	
PQ3.4	225.00	0.9041	
PQ3.5	225.00	0.8795	
PQ4.1	112.50	0.4534	0.61
PQ4.2	112.50	0.4501	
PQ4.3	112.50	0.4516	
PQ4.4	112.50	0.4504	
PQ4.5	112.50	0.4460	
PQ5.1	56.25	0.2392	0.66
PQ5.2	56.25	0.2404	
PQ5.3	56.25	0.2392	
PQ5.4	56.25	0.2393	
PQ5.5	56.25	0.2362	
PQ6.1	28.13	0.1339	0.68
PQ6.2	28.13	0.1338	
PQ6.3	28.13	0.1335	
PQ6.4	28.13	0.1336	
PQ6.5	28.13	0.1317	

CV: coefficient of variation, NomConc.: nominal concentration, PQ: performance qualification

Appendix 10: Exemplary run of LC-MS/MS quantification within a permeation study of propranolol hydrochloride.

Sample	Sample type	NomConc. [ng/mL]	Area ratio	Used	Modified	CalConc. [ng/mL]	Accuracy [%]
Blank.1	Blank	n.a.	n.a.	-	-	n.a.	n.a.
Blank.2	Blank	n.a.	n.a.	-	-	n.a.	n.a.
Zero.1	-	n.a.	0.002	-	-	< 0	n.a.
Zero.2	-	n.a.	0.003	-	-	< 0	n.a.
SST.1	-	n.a.	1.29	-	-	201.60	n.a.
SST.2	-	n.a.	1.28	-	-	200.30	n.a.
SST.3	-	n.a.	1.31	-	-	205.10	n.a.
SST.4	-	n.a.	1.27	-	-	198.10	n.a.
SST.5	-	n.a.	1.29	-	-	201.90	n.a.
SST.6	-	n.a.	1.27	-	-	198.60	n.a.
K11.1	STD	1.86	0.02	+	-	1.78	95.8
K11.2	STD	1.86	0.02	+	-	1.79	96
K10.1	STD	3.72	0.03	+	-	4.02	108
K10.2	STD	3.72	0.03	+	-	3.93	106
K9.1	STD	7.44	0.05	+	-	7.59	102
K9.2	STD	7.44	0.05	+	-	7.63	103
K8.1	STD	14.88	0.10	+	-	15.45	104
K8.2	STD	14.88	0.10	+	-	15.32	103
K7.1	STD	29.76	0.19	+	-	28.99	97.4
K7.2	STD	29.76	0.19	+	-	28.97	97.3
K6.1	STD	59.52	0.38	+	-	58.79	98.8
K6.2	STD	59.52	0.38	+	-	58.80	98.8
K5.1	STD	119.05	0.74	+	-	115.30	96.9
K5.2	STD	119.05	0.75	+	-	116.80	98.1
K4.1	STD	238.10	1.50	+	-	234.20	98.4
K4.2	STD	238.10	1.52	+	-	237.30	99.7
K3.1	STD	476.19	3.01	+	-	473.20	99.4
K3.2	STD	476.19	3.00	+	-	471.40	99
K2.1	STD	952.38	5.90	+	-	932.50	97.9
K2.2	STD	952.38	5.97	+	-	943.80	99.1
K1.1	STD	1904.76	12.00	+	-	1927.00	101
K1.2	STD	1904.76	12.00	+	-	1932.00	101

LQC 1	QC	7.44	0.05	+	-	7.64	103
LQC 2	QC	7.44	0.05	+	-	7.62	102
QC 1.1 1/10	QC	205.50	1.34	+	-	209.30	102
QC 1.2 1/10	QC	207.30	1.30	+	-	203.00	97.9
QC 1.1	-	n.a.	1.32	-	-	205.50	n.a.
QC 1.2	-	n.a.	1.33	-	-	207.30	n.a.
1 5min 1/10	-	n.a.	0.11	-	-	16.60	n.a.
2 5min 1/10	-	n.a.	0.32	-	-	51.52	n.a.
3 5min 1/10	-	n.a.	0.77	-	-	126.50	n.a.
4 5min 1/10	-	n.a.	0.10	-	-	15.28	n.a.
5 5min 1/10	-	n.a.	0.04	-	-	5.67	n.a.
6 5min 1/10	-	n.a.	0.04	-	-	6.28	n.a.
7 5min 1/10	-	n.a.	0.07	-	-	10.01	n.a.
8 5min 1/10	-	n.a.	0.07	-	-	11.24	n.a.
1 10min 1/10	-	n.a.	0.07	-	-	10.05	n.a.
2 10min 1/10	-	n.a.	0.19	-	-	30.46	n.a.
3 10min 1/10	-	n.a.	0.48	-	-	78.25	n.a.
4 10min 1/10	-	n.a.	0.07	-	-	10.09	n.a.
5 10min 1/10	-	n.a.	0.02	-	-	3.13	n.a.
6 10min 1/10	-	n.a.	0.04	-	-	5.98	n.a.
7 10min 1/10	-	n.a.	0.04	-	-	6.29	n.a.
8 10min 1/10	-	n.a.	0.13	-	-	20.30	n.a.
1 15min 1/10	-	n.a.	0.24	-	-	39.29	n.a.
2 15min 1/10	-	n.a.	0.25	-	-	39.89	n.a.
3 15min 1/10	-	n.a.	0.51	-	-	82.52	n.a.
4 15min 1/10	-	n.a.	0.06	-	-	9.57	n.a.
5 15min 1/10	-	n.a.	0.02	-	-	2.98	n.a.
6 15min 1/10	-	n.a.	0.11	-	-	16.97	n.a.
7 15min 1/10	-	n.a.	0.08	-	-	11.79	n.a.
8 15min 1/10	-	n.a.	0.52	-	-	85.15	n.a.
1 20min 1/10	-	n.a.	1.47	-	-	242.00	n.a.
2 20min 1/10	-	n.a.	0.79	-	-	129.50	n.a.
3 20min 1/10	-	n.a.	0.87	-	-	142.30	n.a.
4 20min 1/10	-	n.a.	1.98	-	-	325.10	n.a.
5 20min 1/10	-	n.a.	0.08	-	-	12.19	n.a.
6 20min 1/10	-	n.a.	0.70	-	-	114.60	n.a.

7 20min 1/10	-	n.a.	0.46	-	-	75.31	n.a.
8 20min 1/10	-	n.a.	3.07	-	-	506.90	n.a.
Z1 25min 1/10	-	n.a.	2.52	-	-	414.80	n.a.
Z2 25min 1/10	-	n.a.	0.81	-	-	131.60	n.a.
Z3 25min 1/10	-	n.a.	1.77	-	-	291.10	n.a.
Z4 25min 1/10	-	n.a.	11.90	-	-	2002.00	n.a.
Z5 25min 1/10	-	n.a.	0.69	-	-	112.90	n.a.
Z6 25min 1/10	-	n.a.	1.40	-	-	229.60	n.a.
Z7 25min 1/10	-	n.a.	0.85	-	-	138.70	n.a.
Z8 25min 1/10	-	n.a.	4.27	-	-	707.10	n.a.
MQC1	QC	119.05	0.75	+	-	116.80	98.2
MQC2	QC	119.05	0.77	+	-	119.70	101
1 30min 1/10	-	n.a.	4.76	-	-	789.00	n.a.
2 30min 1/10	-	n.a.	2.32	-	-	382.20	n.a.
3 30min 1/10	-	n.a.	4.03	-	-	667.10	n.a.
4 30min 1/10	-	n.a.	35.90	-	-	6414.00	n.a.
5 30min 1/10	-	n.a.	2.38	-	-	392.00	n.a.
6 30min 1/10	-	n.a.	2.85	-	-	469.20	n.a.
7 30min 1/10	-	n.a.	1.91	-	-	313.90	n.a.
8 30min 1/10	-	n.a.	7.22	-	-	1202.00	n.a.
1 40min 1/10	-	n.a.	10.20	-	-	1704.00	n.a.
2 40min 1/10	-	n.a.	5.84	-	-	969.60	n.a.
3 40min 1/10	-	n.a.	8.76	-	-	1464.00	n.a.
4 40min 1/10	-	n.a.	56.60	-	-	10790.00	n.a.
5 40min 1/10	-	n.a.	5.13	-	-	850.70	n.a.
6 40min 1/10	-	n.a.	7.13	-	-	1187.00	n.a.
7 40min 1/10	-	n.a.	5.14	-	-	852.70	n.a.
8 40min 1/10	-	n.a.	13.40	-	-	2260.00	n.a.
1 50min 1/10	-	n.a.	14.10	-	-	2393.00	n.a.
2 50min 1/10	-	n.a.	8.17	-	-	1364.00	n.a.
3 50min 1/10	-	n.a.	11.50	-	-	1933.00	n.a.
4 50min 1/10	-	n.a.	63.60	-	-	12420.00	n.a.
5 50min 1/10	-	n.a.	9.69	-	-	1623.00	n.a.
6 50min 1/10	-	n.a.	9.23	-	-	1545.00	n.a.
7 50min 1/10	-	n.a.	6.90	-	-	1149.00	n.a.
8 50min 1/10	-	n.a.	15.40	-	-	2615.00	n.a.

1 60min 1/10	-	n.a.	15.20	-	-	2582.00	n.a.
2 60min 1/10	-	n.a.	9.82	-	-	1646.00	n.a.
3 60min 1/10	-	n.a.	13.00	-	-	2202.00	n.a.
4 60min 1/10	-	n.a.	53.30	-	-	10050.00	n.a.
5 60min 1/10	-	n.a.	13.70	-	-	2325.00	n.a.
6 60min 1/10	-	n.a.	11.20	-	-	1891.00	n.a.
7 60min 1/10	-	n.a.	8.14	-	-	1359.00	n.a.
8 60min 1/10	-	n.a.	17.60	-	-	2999.00	n.a.
HQC 1	QC	952.38	5.82	+	-	920.70	96.7
HQC 2	QC	952.38	5.82	+	-	920.10	96.6
QC 2.1 1/10	QC	226.60	1.43	+	-	222.70	98.3
QC 2.2 1/10	QC	233.00	1.49	+	-	233.50	100
QC 2.1	-	n.a.	1.45	-	-	226.60	n.a.
QC 2.2	-	n.a.	1.49	-	-	233.00	n.a.
SST.7	-	n.a.	1.25	-	-	195.20	n.a.
SST.8	-	n.a.	1.25	-	-	194.70	n.a.

CalConc.: calculated concentration, HQC: high quality control, LLOQ: lower limit of quantification, LQC: low quality control, MQC: middle quality control, n.a.: not applicable, NomCalc.: nominal concentration, QC: quality control, SST: system suitability test, STD: standard

Appendix 11: Exemplary run of membrane integrity within a permeation study of propranolol hydrochloride.

Sample	Optical density	Blank-normalized optical density
Blank.1	0.0283	n.a.
Blank.2	0.0280	n.a.
Blank.3	0.0283	n.a.
Positive control	1.3303	47.1738
Diffusion cell 1	0.0308	1.0922
Diffusion cell 2	0.0319	1.1312
Diffusion cell 3	0.0284	1.0071
Diffusion cell 4	0.0472	1.6738
Diffusion cell 5	0.0283	1.0035
Diffusion cell 6	0.0272	0.9645
Diffusion cell 7	0.0301	1.0674
Diffusion cell 8	0.0501	1.7766

n.a.: not applicable

Appendix 12: Exemplary run of membrane viability within a permeation study of propranolol hydrochloride.

Sample	Optical density	Blank-reduced optical density	Viability [%]
Blank.1	0.0552	n.a.	n.a.
Blank.2	0.0517	n.a.	n.a.
Blank.3	0.0529	n.a.	n.a.
PBS	0.0441	n.a.	n.a.
Negative control	0.0806	0.0273	1.51
Positive control	2.6632	n.a.	n.a.
Diffusion cell 1	1.754	1.7007	94.13
Diffusion cell 2	1.942	1.8887	104.54
Diffusion cell 3	1.8005	1.7472	96.71
Diffusion cell 4	2.1645	2.1112	116.86
Diffusion cell 5	1.8288	1.7755	98.27
Diffusion cell 6	2.0952	2.0419	113.02
Diffusion cell 7	1.9914	1.9381	107.27
Diffusion cell 8	2.0557	2.0024	110.83

n.a.: not applicable, PBS: phosphate-buffered isotonic saline solution

11. Publications of Haidara Majid

Parts of this thesis have already been published in international peer-reviewed journals or were presented at international conferences.

Publications in international peer-reviewed journals:

- I. **Majid, H.**, Bartel, A., Burckhardt, B.B., 2021. Predictivity of Standardized and Controlled Permeation Studies: Ex vivo – In vitro – In vivo Correlation for Sublingual Absorption of Propranolol. *European Journal of Pharmaceutics and Biopharmaceutics* 169, 12–19. <https://doi.org/10.1016/j.ejpb.2021.09.002>.
- II. **Majid, H.**, Puzik, A., Maier, T., Merk, R., Bartel, A., Mueller, H.-C., Burckhardt, B., 2021d. Formulation development of sublingual cyclobenzaprine tablets empowered by standardized and physiologically relevant ex vivo permeation studies. *Pharmaceutics* 13, 1409. <https://doi.org/10.3390/pharmaceutics13091409>.
- III. **Majid, H.**, Puzik, A., Maier, T., Eberhard, D., Bartel, A., Mueller, H.-C., Burckhardt, B.B., 2021. Exploring the transmucosal permeability of cyclobenzaprine: A comparative preformulation by standardized and controlled ex vivo and in vitro permeation studies. *International Journal of Pharmaceutics* 601, 120574. <https://doi.org/10.1016/j.ijpharm.2021.120574>.
- IV. **Majid, H.**, Bartel, A., Burckhardt, B.B., 2021. Development, validation and standardization of oromucosal ex-vivo permeation studies for implementation in quality-controlled environments. *Journal of Pharmaceutical and Biomedical Analysis* 194, 113769. <https://doi.org/10.1016/j.jpba.2020.113769>.
- V. Kottke, D., **Majid, H.**, Breitzkreutz, J., Burckhardt, B.B., 2020. Development and evaluation of mucoadhesive buccal dosage forms of lidocaine hydrochloride by ex-vivo permeation studies. *International Journal of Pharmaceutics* 581, 119293. <https://doi.org/10.1016/j.ijpharm.2020.119293>.

Poster presentations:

- I. **Majid, H.**, Kottke, D., Bartel, A., Burckhardt, B.B., 2019. Development of a Suitable LC-MS/MS Quantification Method as Key Element in Intraoral Ex-vivo Permeation Studies within Pharmaceutical Research. Euroanalysis XX; 2019 September 1-5; Istanbul, Turkey.
- II. Makowski, N., Burdman, I., Ali, M., **Majid, H.**, Farahani, S., Ciplea AM., Bartel, A., Burckhardt, B.B., 2019. P64 Quality assessment for the continuous bioanalysis of aldosterone: application in an European paediatric study. Archives of Disease in Childhood;104:e43-e44. European Society for Developmental Perinatal and Paediatric Pharmacology (ESDPPP) Congress; 2019 May 28-31; Basel, Switzerland.
- III. Feickert, M., Burdman, I., Makowski, N., Ali, M., Farahani, S., **Majid, H.**, Ciplea AM., Bartel, A., Burckhardt, B.B., 2019. P34 Reliable results in continuous bioanalysis of paediatric renin samples-comprehensive quality assessment within clinical studies in children. Archives of Disease in Childhood, e31.1-e31. European Society for Developmental Perinatal and Paediatric Pharmacology (ESDPPP) Congress; 2019 May 28-31; Basel, Switzerland.
- IV. **Majid, H.**, Kottke, D., Bartel, A., Burckhardt, B.B., 2018. Approach of a Physiologically-Based Permeation Model Utilizing LC-MS/MS to Investigate the Safety Potential of Buccal Drug Applications. DPhG Annual Meeting; 2018 October 2-5; Hamburg, Germany.
- V. Kottke, D., **Majid, H.**, Breitzkreutz, J., Burckhardt, B.B., 2018. Ex-vivo Permeation Studies to Facilitate the Development of a Buccal Child-Appropriate Dosage Form by Using Lidocaine Minitablets. Biological Barriers 2018; 2018 August 27-29; Saarbruecken, Germany.

12. Curriculum vitae

Personal details

First name/ Last name	Haidara Majid
Date and place of birth	17.07.1993 in Damascus, Syrian Arab Republic
Address	Universitätsstr. 1, 40225 Düsseldorf, Germany
Telephone	+49 211 8113840
Fax	+49 211 8110741
E-Mail	Haidara.majid@hhu.de
Nationality	German

Professional experience

Since 09/2021	Bayer AG, Monheim am Rhein, Germany Lab Leader
01/2018 – 08/2021	Institute for Clinical Pharmacy and Pharmacotherapy, Heinrich Heine University Düsseldorf, Düsseldorf, Germany Scientific co-worker
03/2020 – 03/2021	Apotheke in Rath, Düsseldorf, Germany Pharmacist
05/2017 – 10/2017	Delfin-Apotheke, Hannover, Germany Pre-registration pharmacist
11/2016 – 04/2017	Berlin-Chemie AG, Berlin, Germany Pre-registration pharmacist

Education

Since 01/2018	Institute for Clinical Pharmacy and Pharmacotherapy, Heinrich Heine University Düsseldorf, Düsseldorf, Germany PhD student
12/2017	Apothekerkammer Niedersachsen, Germany Certification as registered pharmacist
10/2012 – 04/2016	Technische Universität Braunschweig, Braunschweig, Germany Pharmacy studies
06/2012	Gymnasium Lutherschule, Hannover, Germany Allgemeine Hochschulreife (university entrance qualification)